Assessing different aspects of present state and ongoing climate changes at both Adriatic and local scale

Activity 3.1

Deliverable 3.1.1

Delivery date: 31 January 2020

Version 1.0

DELIVERABLE 3.1.1

PROJECT CHANGE WE CARE

https://www.italy-croatia.eu/web/changewecare

Work Package:	WP3
Activity:	3.1
Phase Leader:	Ivica Vilibić
Deliverable:	3.1.1: Report: Assessing different aspects of present state and ongoing climate changes at both Adriatic and local scale. This document will summarise the main results of the physical assessment carried out in this activity, as: (i) Assessment of ongoing trends and variability of different meteo, oceanic and hydrological parameters on the basin-wide level (northern and central Adriatic area) as gained through various observational techniques, (ii) Performance assessment of existing atmospheric, oceanic and coupled climate models and their results for the Adriatic Sea, (iii) Downscaling of climate processes and parameters to the selected case study areas, assessment of variability and trends of meteo, oceanic and hydrological key processes at each site. (iv) Documentation of the site-specific meteo-ocean-hydrological properties, based on campaigns performed on sites, (v) Identification and quantification of key processes that may change the climate setting of the area, including an assessment of their dynamical trends as resulting from the in situ campaigns and regional climate models.

Version:	Draft/Final 1.0	Date:	31 January 2020
Type:	Report		
Availability:	Public		
Responsible Partner:	Institute of Oceanography and Fisheries		
Editor:	Ivica Vilibić		
Contributors:	Ivica Vilibić, Clea Denamiel, Petra Pranić, Iva Tojčić, Hrvoje Mihanović, Davide Bonaldo, Fabio Raicich, Renato Colucci, Angela Pomaro		

CONTENTS

1. FOREWORD

This document has been produced in the framework of the INTERREG Italy – Croatia CHANGE WE CARE Project. CHANGE WE CARE fosters concerted and coordinated climate adaptation actions at transboundary level, tested in specific and representative pilot sites, exploring climate risks faced by coastal and transitional areas contributing to a better understanding of the impact of climate variability and change on water regimes, salt intrusion, tourism, biodiversity and agro-ecosystems affecting the cooperation area. The main goal of the Project is to deliver integrated, ecosystem-based and shared planning options for different problems related to climate change (CC), together with adaptation measures for vulnerable areas, to decision makers and coastal communities. Additional information and updates on the CHANGE WE CARE can be found at https://www.italy-croatia.eu/web/changewecare.

2. INTRODUCTION

The Mediterranean Sea is a temperate sea characterized by high salinities and oligotrophic conditions, surrounded substantially by land, which in turn significantly defines its atmosphere and ocean climate. Its northernmost part, the Adriatic Sea, is exhibiting a substantial influence of the European land processes, for which freshwater load is substantial to the sea, about 1/3 of all Mediterranean load. Therefore, the Adriatic salinity is lower than the Mediterranean salinity. The prevailing currents flow counterclockwise from the Strait of Otranto, along the eastern coast and back to the strait along the western (Italian) coast. The Adriatic Sea is a microtidal basin, with tides ranging from 20 cm in southern to a metre in the northern Adriatic. According to the Köppen climate classification, the upper half of the Adriatic is classified as humid subtropical climate (Cfa), with wetter summers and colder and drier winters, and the southern Adriatic is classified as hot-summer Mediterranean climate (Csa).

This deliverable contains an assessment of present-climate changes in the Adriatic Sea and surrounding regions, affecting atmospheric and oceanic properties and dynamical processes. The first part of the assessment is based on existing literature and knowledge about climate changes in the Adriatic Sea, mostly based on in situ atmosphere, hydrosphere and ocean long-term measurements. The assessment will continue with the analysis of multi-decadal atmosphere-ocean climate model runs, which are available at high resolutions for the area. They are found useful for downscaling of the climate characteristics to the five Pilot Study areas of the CHANGE WE CARE project (Po River delta, Banco di Mula di Muggia, Vransko Lake, Jadro River and Neretva River sites), for which the detailed analysis of climate characteristics, both in ocean and in the

atmosphere, are part of the deliverable. Such an assessment will allow for proper assessment of climate drivers and pressures in the Adriatic Sea and at all Pilot Sites, allowing for proper future management in light of foreseen climate changes.

3. ASSESSMENT OF THE ADRIATIC METEO-OCEAN PROCESSES

3.1. State-of-the-art

3.1.1. Trends and variability of atmospheric variables and processes

By analyzing long-term meteorological stations in the coastal Adriatic and inland (Branković et al., 2010; Toreti and Desiato, 2008) (Figs. 1 and 2), one can detect several characteristics: (i) there is a strong interannual and decadal variability in air temperature, and (ii) the trends in air temperature are becoming larger when being computed over a recent period. Increase of mean annual air temperature continued and is amplified by the beginning of the 21st century, when 5 and 6 warmest years during the whole measuring period were recorded in stations Crikvenica and Hvar. The annual temperature trend was as high as +0.35 ^{o}C over decade at Hvar to 0.75 ^{o}C over decade at Crikvenica, being the largest during summer and autumn. Two periods can be found regarding trends: a weakly decreasing trend in 1960s and 1970 and strongly increasing trend after 1980. Such trends are the result of the multidecadal variability induced by Atlantic Multidecadal Oscillation (AMO) that affect the whole Mediterranean Sea (Knight et al., 2006).

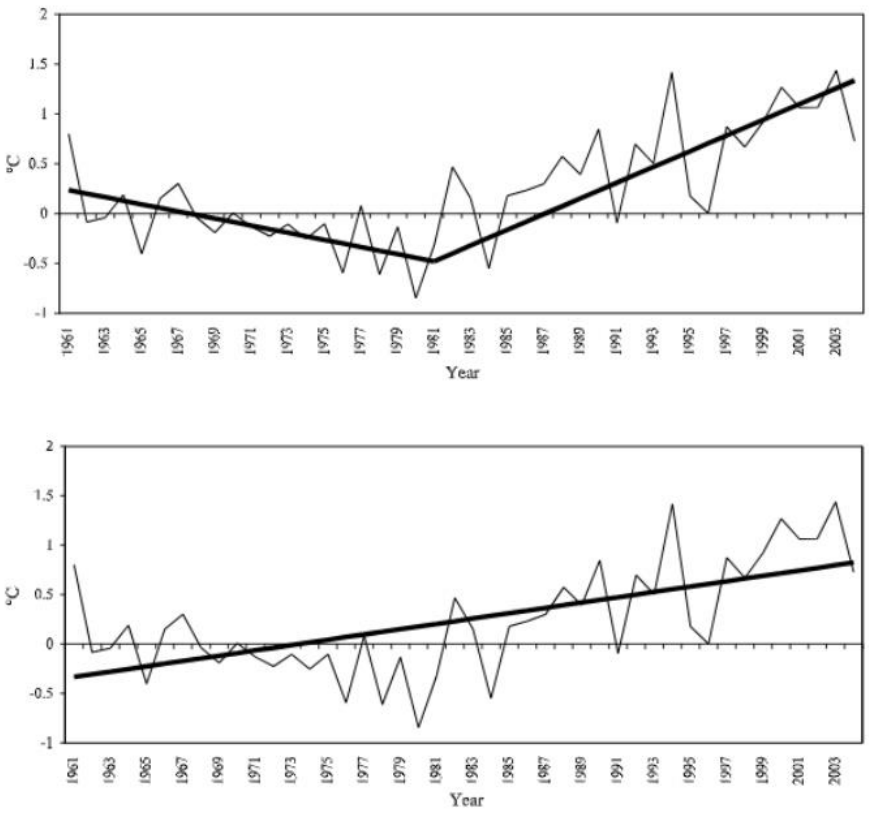

Figure 1. Air temperature anomalies and trends over Italy estimated by linear and piecewise models. Source: Toreti and Desiato (2008).

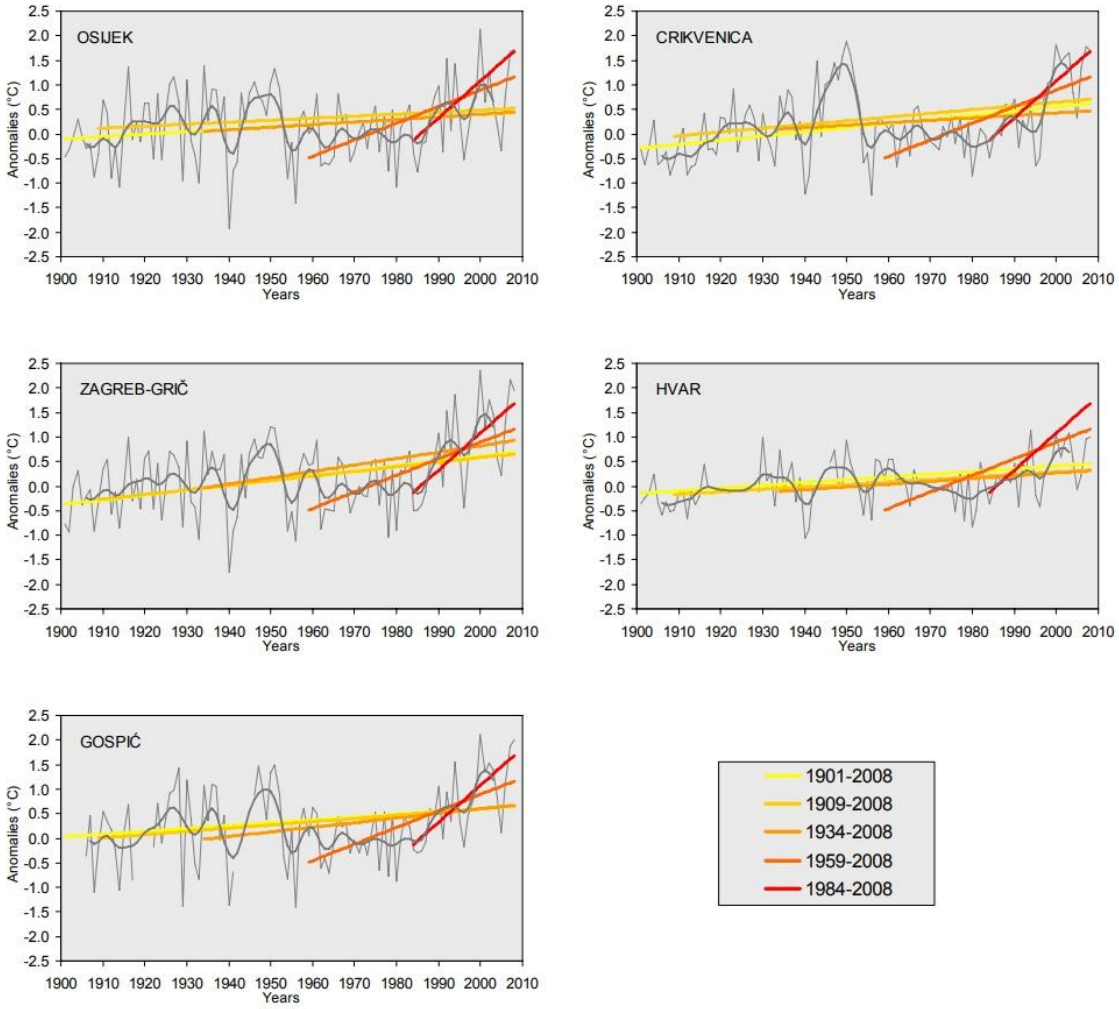

Figure 2. Time series for the mean annual air temperature related 11-year binomial moving averages, and trends for 108-, 100-, 75-, 50- and 25-year period for long-term stations in Croatia. Unit is anomalies (°C) with respect to 1961-1990 average. Source: Branković et al. (2010).

Precipitation in the coastal eastern Adriatic area has been recorded with a negative trend (Fig. 3), from -1.8% over 10 years in Crikvenica to -1.2 years over 10 years in Hvar. The trend is largely defined by a climate shift observed in 1940s, when several periods with less precipitation occurred. In the area of northern Adriatic (Crikvenica) decrease in all seasonal precipitation amounts has been observed, mostly expressed during summer (-2.7% in 10 years), then in spring (-2.2% in 10 years) and winter (-1.8% in 10 years). On Dalmatian islands (Hvar) decrease in annual precipitation amounts is a result of decline in winter (-2.9% in 10 years) and spring (-2.0% in 10 years) precipitation amounts.

Change in precipitation regime patterns can be also indicated by tendency in frequency and intensity of precipitation extremes defined by number of days in which the precipitation amount Rd exceeds defined thresholds (dry days, wet days and very wet days). Dry days are defined as days in which Rd<1.0 mm, wet days have Rd ≥ 75th percentile and very wet days Rd ≥ 95th percentile of daily amounts, determined by the sample of all precipitation days (Rd≥1.0 mm) within standard reference period 1961-1990. In the period 1901-2008 there was statistically significant increase of annual number of dry days in the coastal Adriatic (Fig. 4), while mostly negative trend of wet days significant in the northern Adriatic (Crikvenica).

Trends over the whole Adriatic basin (Fig. 5) indicate the decrease in precipitation in the most of the basin and in particular over the northern Italy (Philandras et al., 2011), particularly relevant for the rainy season (October-March). The decrease is slightly lower over the Dinarides. This reanalysis fits well to the long-term observations in the area.

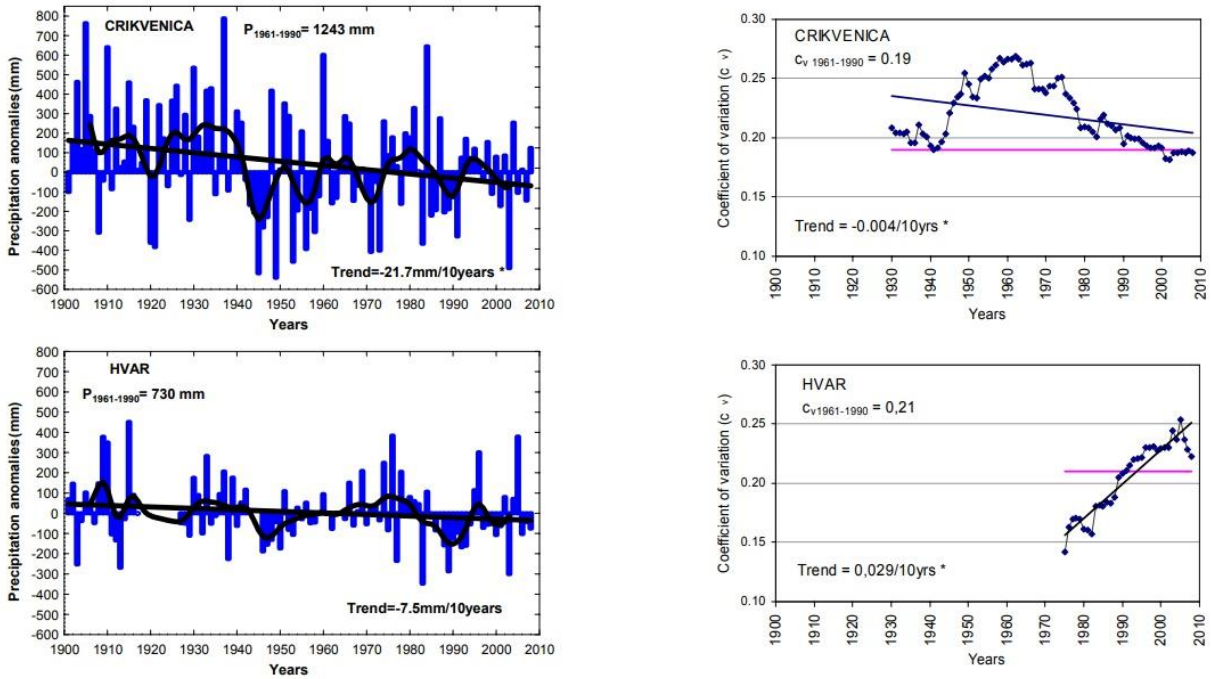

Figure 3. Time series for the annual precipitation amounts, related 11-year binomial moving averages and trends (left, unit is anomalies (mm) with respect to 1961-1990 average). Time series for the coefficients of variation for 30-year periods with one year shift and trends (right). (- trends significant at the 5% level). Period: 1901-2008. Source: Branković et al. (2010).*

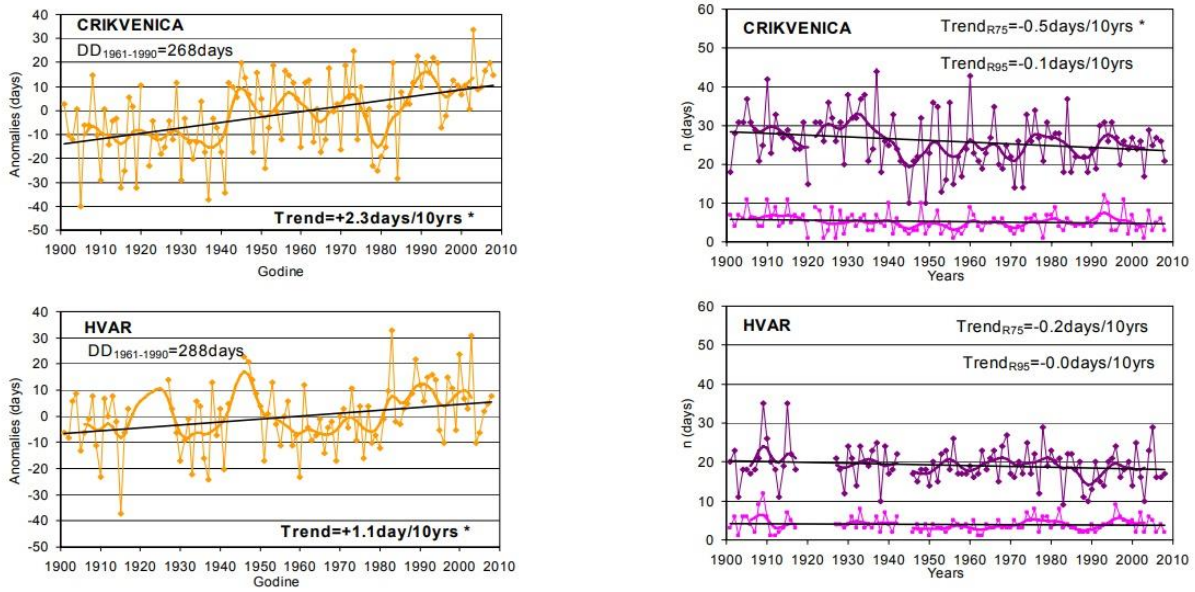

Figure 4. Time series for the number of dry days (left), unit is anomalies (days) with respect to 1961-1990 average. On the right time series for the number of moderate wet days (Rd>R75% - above) and very wet days (Rd>R95% - below), related 11-year binomial moving averages and trends (- trends significant at the 5% level). Period: 1901-2008. Source: Branković et al. (2010).*

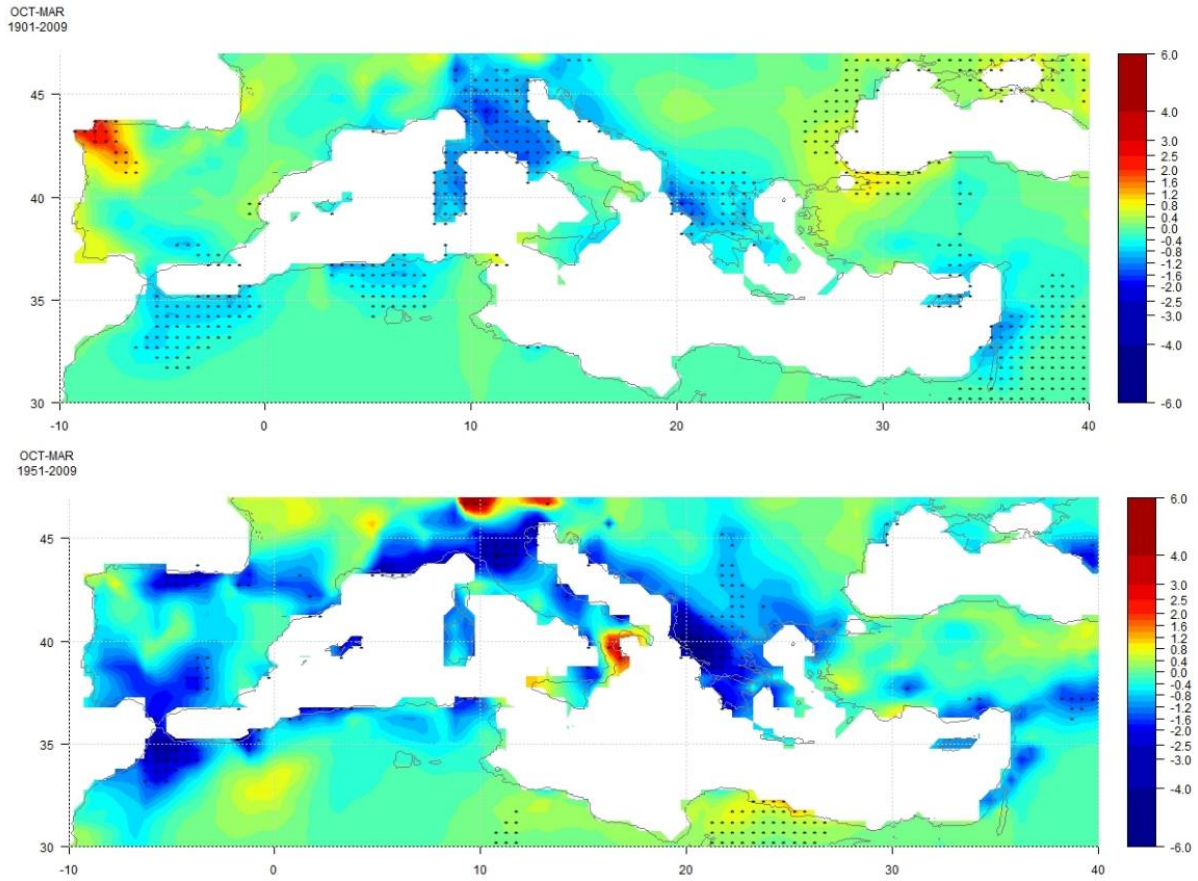

Figure 5. Spatial distribution of precipitation trends for the rain season (October–March) concerning gridded datasets (CRU TS 3.1), for 1901–2009 (upper graph) and 1951–2009 (lower graph). Source: Philandras et al. (2011).

3.1.2. Trends and variability of oceanic variables and processes

Ocean temperature in the Adriatic Sea is decreasing from the entrance, where defined by an inflow of warmer Eastern Mediterranean waters, to the northern Adriatic influenced by severe winter outbreaks and generally losing more energy than in the southern Adriatic. The along-Adriatic surface temperature (Fig. 6) is reflecting during winter (JFM) lowest temperatures (>10 ^{o}C) in the northern Adriatic, while being higher in the southern Adriatic (close to 14 ^{o}C). The temperatures in the rest of a year doesn't reflect such a strong gradient, yet being lower in the coastal eastern Adriatic, where lot of freshwater load is coming through submarine springs and lower rate of energy gain is occurring.

Surface salinity in the Adriatic Sea (Fig. 7) is mainly driven by large freshwater load in the northern Adriatic, ranging from 38.5 in the southern Adriatic to less than 36.0 off the Po River delta.

Long-term trends of temperature, salinity and dissolved oxygen (Fig. 8) are indicating a weakening of the Adriatic thermohaline circulation, i.e. lower water mass exchange between the Adriatic and the Ionian Seas. For that reason, the temperature trends are negative in intermediate layer, while salinity has the largest trends in coastal regions due to decreasing of freshwater load in time. Further, dissolved oxygen trend is indicating less ventilation of deep Adriatic waters, i.e. lower rates of dense water generation during wintertime in the northern Adriatic. As a consequence, deep pelagic and benthic organisms can be affected by these changes, especially in the biodiversity of niches such as found in the nearby Jabuka Pit, which serves as a collector for dense water from the northern Adriatic Sea.

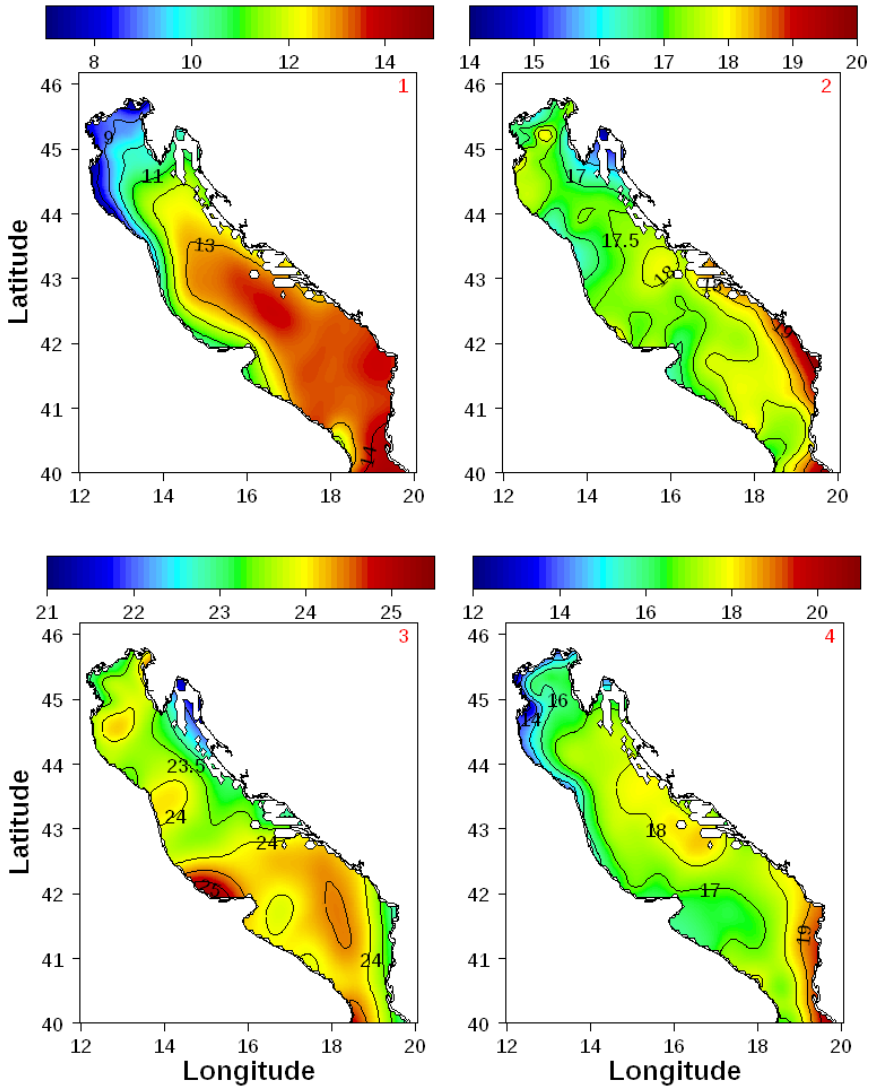

Figure 6. Surface ocean temperature in the Adriatic Sea during winter (JFM, top left), spring (top, right), summer (bottom, left) and autumn (bottom, right) as computed from centennial Adriatic in situ measurements. Source: Lipizer et al. (2014).

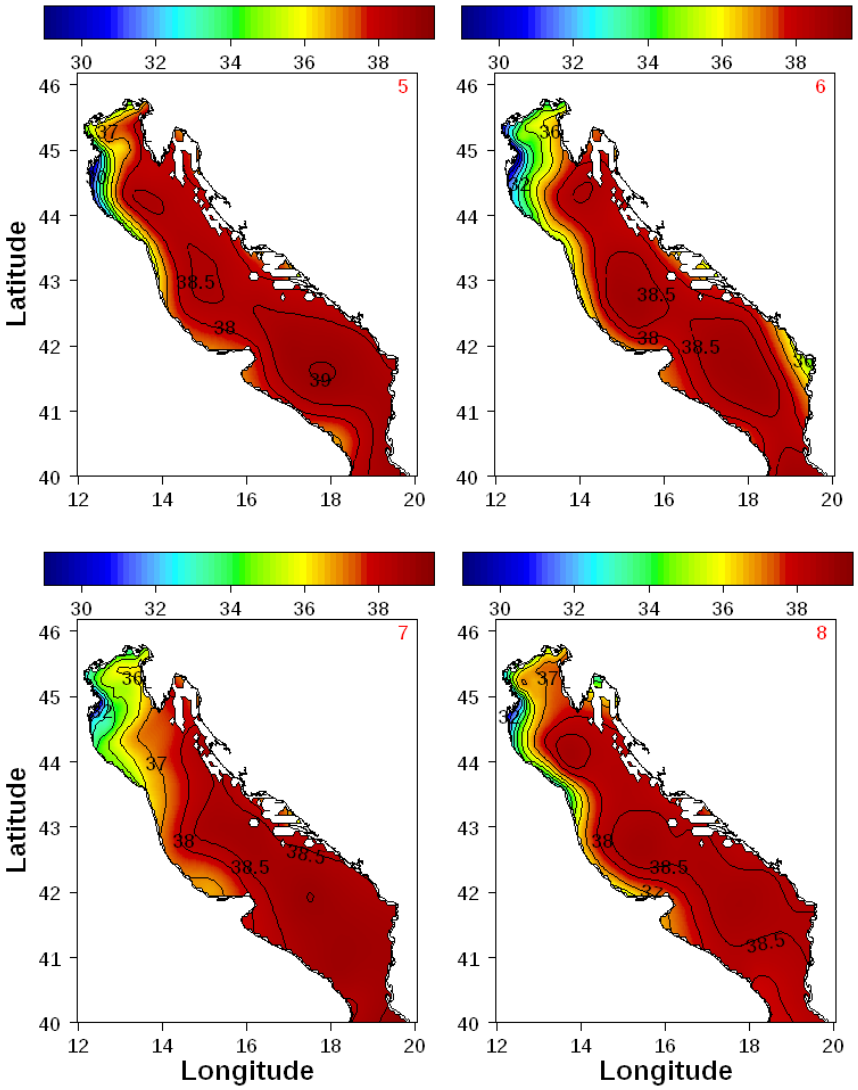

Figure 7. Surface salinity in the Adriatic Sea during winter (JFM, top left), spring (top, right), summer (bottom, left) and autumn (bottom, right) as computed from centennial Adriatic in situ measurements. Source: Lipizer et al. (2014).

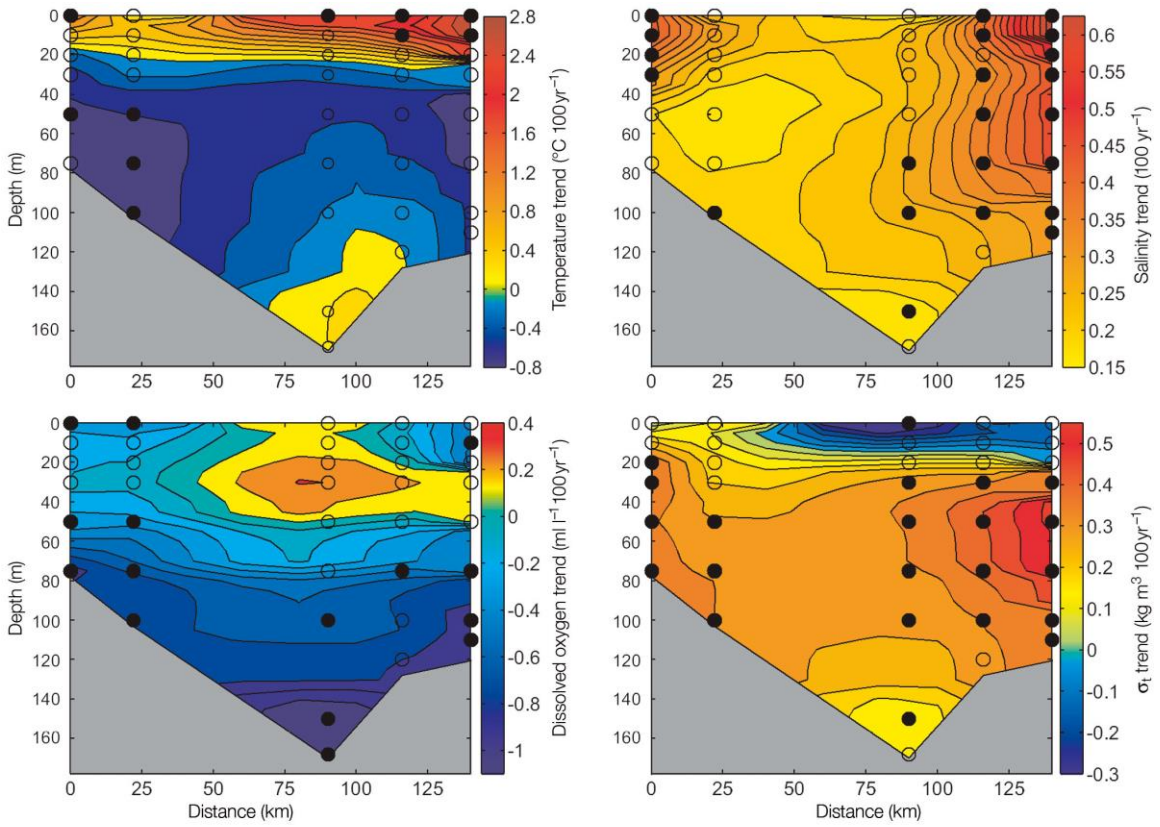

Figure 8. Trends in ocean temperature, salinity dissolved oxygen and density as computed from the Palagruža Sill data (1952-2010). Source: Vilibić et al. (2013).

Concerning the ocean chemistry of the Adriatic Sea, the most relevant issue is a decrease in dissolved oxygen content in deep Adriatic layers due to weakening of the Adriatic thermohaline circulation (Fig. 9). Such a decrease might have a substantial influence to the benthic organisms, including also in coastal regions. On top of that, large interannual and decadal variability may be noticed, peaking in the 1990s during the Eastern Mediterranean transient (Klein et al., 1999). Nutrients were much higher during that period, as waters mainly come to the Adriatic from the Western Mediterranean which have higher nutrient content. Such a change also reflected in N:P ratio, reducing limitation in phosphorus known to dominate in the Eastern Mediterranean (Krom et al., 1991). According to climate projections, such events will become more frequently in the future climate.

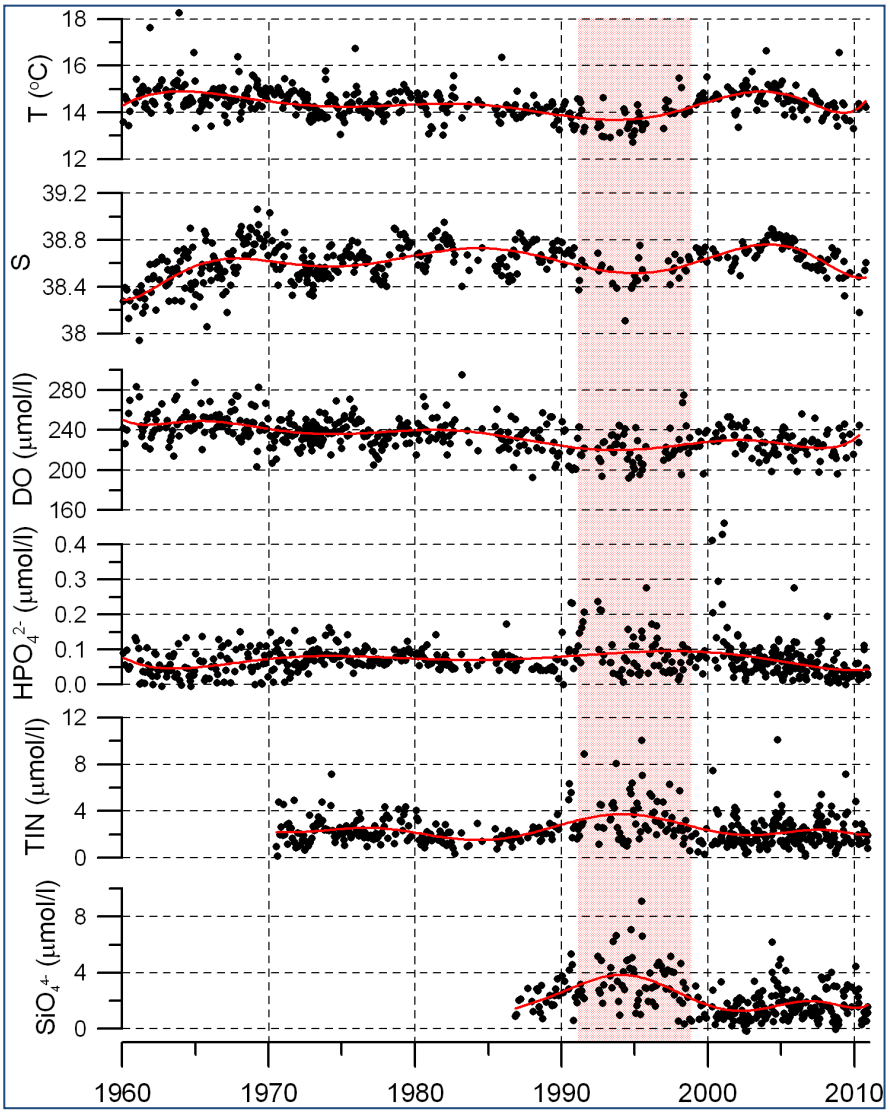

Figure 9. Temperature, salinity, dissolved oxygen and nutrient concentrations measured at the bottom of the Stončica station. Source: Vilibić et al. (2012).

Sea level rise in the Adriatic Sea is reflecting the overall changes in the Adriatic current and thermohaline regimes. The rise is found to accelerate (Figs. 10 and 11) in all coasts of the Adriatic, what is also projected in the future. Currently, sea level trends are at rates of approximately 45-55 cm per century, what are several times higher than these accounting the last 100 years.

Such acceleration in sea level rise rates are reflected in number of floods that are documented in the Adriatic Sea, in particular in its northernmost part like Venice (Fig. 12). However, the floods

are recorded in a great number of coastal cities and low lands, including World Heritage sites along the eastern Adriatic coast (Fig. 13).

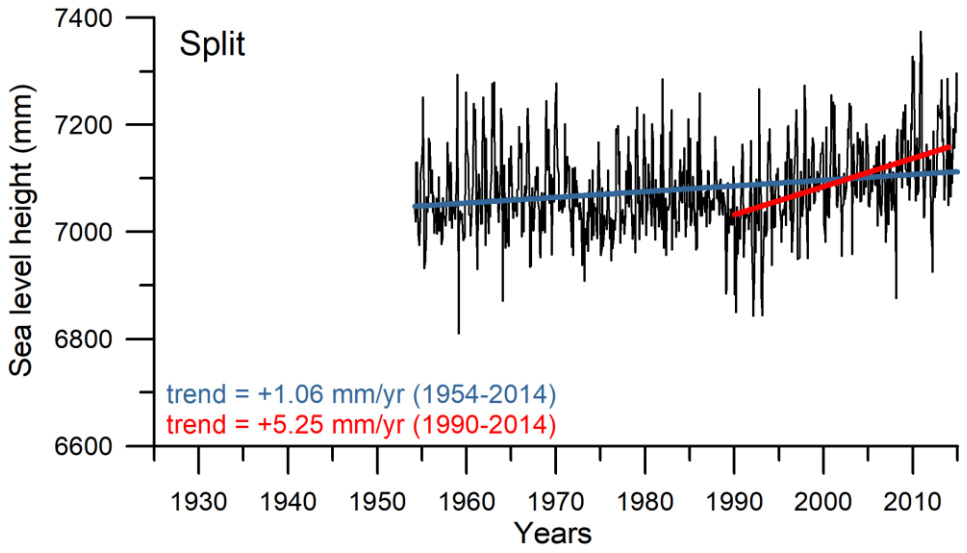

Figure 10. Monthly sea level data and sea level trends at tide gauge Split.

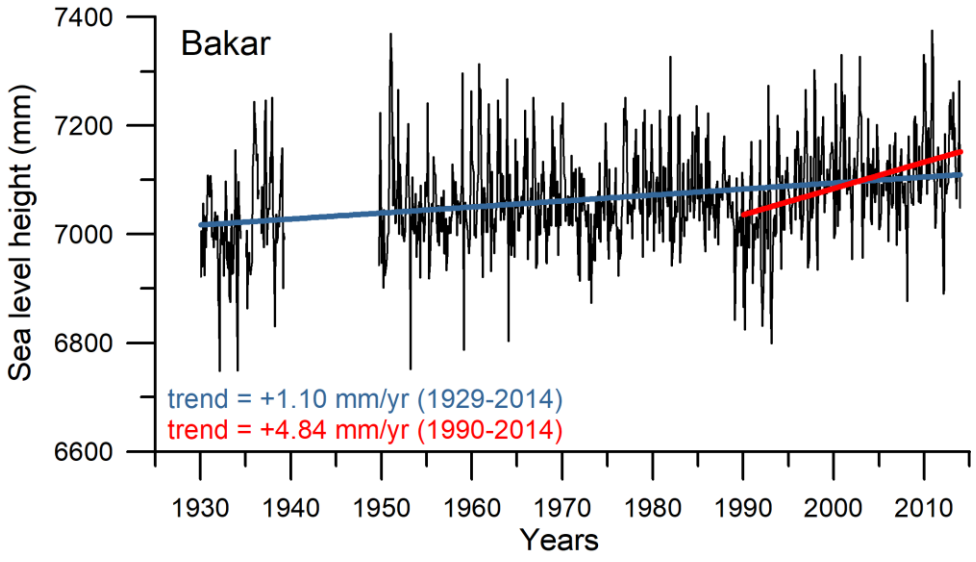

Figure 11. Monthly sea level data and sea level trends at tide gauge Bakar.

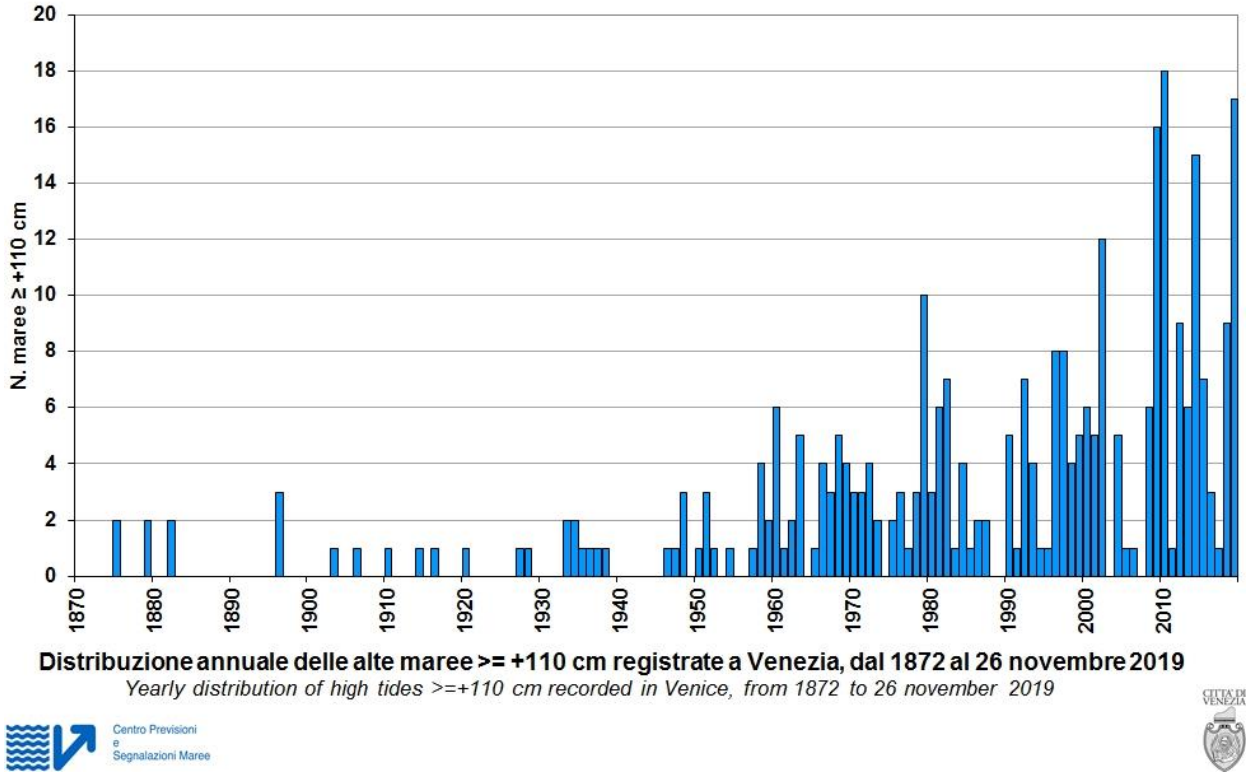

Figure 12. Number of extreme sea level heights (>110 cm) measured in Venice since 1872. Source: https://www.comune.venezia.it/it/content/distribuzione-annuale-delle-alte-maree-110-cm

Figure 13. The flood of the city of Šibenik in December 2019.

3.1.3. Trends and variability of hydrological variables

The precipitation decrease is reflected in a decrease of the freshwater load to the Adriatic Sea (Fig. 14), which is also important as bringing nutrients to the coastal regions. The decrease is particularly relevant after 1970s as the largest Adriatic river, the Po River, is considered. The rest of the Adriatic rivers show a general decrease (about 30%) in recent decades, in comparison with the discharges before the 1980s.

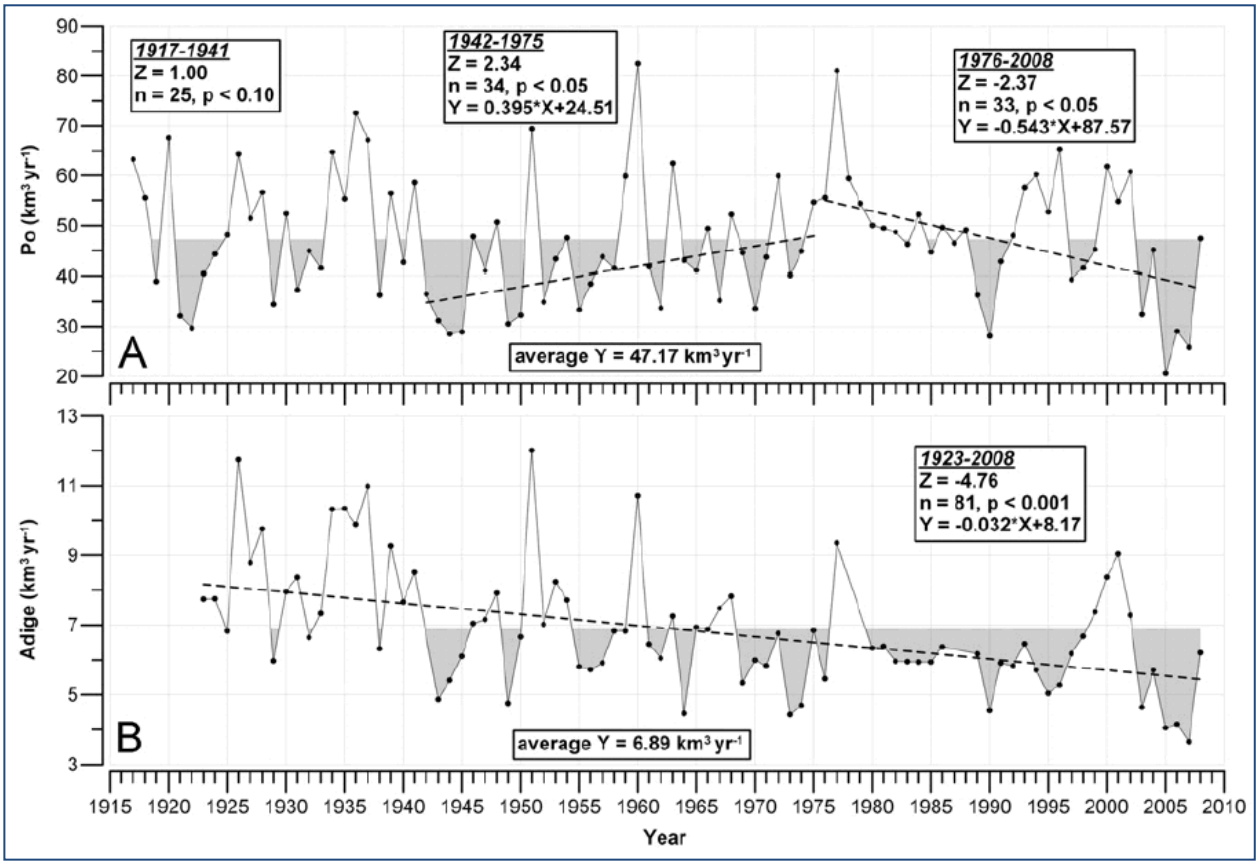

Figure 14. Annual average discharges of two largest northern Adriatic rivers, Po and Adige. Source: Cozzi and Giani (2011).

3.2. Trends and variability coming from selected long-term observations

3.2.1. CNR-ISMAR at Trieste

- ***Description of the station***

Atmospheric Pressure (AP) and Sea-Level Pressure (SLP) @CNR-ISMAR Trieste. The AP was measured at CNR-ISMAR in Trieste by means of barographs, periodically calibrated by comparison to the direct readings from a Fortin mercury barometer. Until mid-1970s AP was measured in millimeters (0.1 mm accuracy), while hectopascal was adopted afterwards (0.1 hPa accuracy). Data come from analogue instruments until 31/01/2000 and from digital ones afterwards.

The instruments were located at the following heights above mean sea level:

- 01/01/1921-19/07/1944: 7.8 m, Istituto Geofisico/Talassografico building;
- 19/07/1944-22/08/1950: 11.0 m, via Corsica, approximately 500 m from Istituto Talassografico;
- 22/08/1950-31/01/2000: 8.7 m, Istituto Talassografico building;
- 01/02/2000-31/12/2018: 11.0 m, Istituto Talassografico garden.

Sea-level pressure (SLP) was obtained by reducing the original measurements to mean sea level by means of Eq. 10 in Eckholm (1905).

Air Temperature (AT) @CNR-ISMAR Trieste. Temperature was originally measured at CNR-ISMAR in Trieste by using traditional weekly thermographs with accuracy of ±0.5°C working in parallel together with an alcohol-in-glass thermometer and a mercury-in-glass thermometer having accuracy of ±0.1°C. This procedure was the best used to calibrate the thermographs data and set temperature extremes in a chosen time interval (generally 24 hours). Starting from the late 1980s data sampling was 60 s and every hour temperature extremes (minimum and maximum) in the interval were digitally recorded and archived. The instrumentation was installed in the same Stevenson Screen located in the garden of the Institute at 11 m a.s.l. since 1921.

Wind Data (WIND) @CNR-ISMAR Venezia. The two available dataset of wind data recorded at the CNR-ISMAR "Acqua Alta" oceanographic research tower, located in the Northern Adriatic Sea, in 16 meters of depth, 15 km off the coast of the Venice lagoon (GPS coordinates 45° 18' 51.288'' N, 12° 30' 29.694'' E) consist in:

- 36 years dataset, staring in 1983 and continuing nowadays, with the help of Centro Previsioni e Segnalazioni Maree of the Municipality of Venice. Wind data have been collected by Micros-Siap t033 TDV and t031 TVV installed at 16 m above the sea level until 2017 then the sensors have been raised to 20 m
- 12 years dataset, starting in 2008 and continuing nowadays, with a Davis Vantage Pro meteostation. Its wind sensor has been installed at 18 m above the sea level until 2017 then the sensor has been raised to 21 m

Precipitation (PREC) @CNR-ISMAR Trieste. PREC was recorded at CNR-ISMAR in Trieste by tilting bucket rain gauge transducers, having a 200, 500 and 1000 cm^2 funnel area and conversion constant of 0.2 mm impulse-1. Solid precipitation (snow) measurements were possible thanks to a heating system directly built on the rain gauge. Data recorded were periodically controlled by a manual rain gauge having the same funnel area and working in parallel.

The location of the rain gauges was the following:

- Since 1921: Roof of Istituto Geofisico, Talassografico - rain gauge 200 cm^2;
- Between 1944 and 1992: Garden of Istituto Talassografico close to the Stevenson Screen - rain gauge 200 cm^2;
- Between 1992 and 2018: Garden of Istituto Talassografico - rain gauge 1000 cm^2;
- Between 2007 and 2018: Garden of Istituto Talassografico - rain gauge 500 cm^2.

Sea Temperature (ST) @CNR-ISMAR Trieste. Near-surface ST was observed daily with well thermometers or automated recording thermographs until 2008, but in 1986 digital records also became available. The complete description of the data sets, observation sites and instruments

can be found in Raicich and Colucci (2019a); the data are available in Raicich and Colucci (2019b). Although data are available since 1899, we only take into account the time series from 1946 onwards, that does not exhibit gaps.

Sea Level (SL) @CNR-ISMAR Trieste. Relative SL heights were measured at the Molo Sartorio tide-gauge station (n. 340 of GLOSS core network) by means of the following tide gauges: a N. 605 manufactured by Fuess until 29/10/1984, a Büsum by OTT from 4/8/1966 onwards, both of which are analogue instruments, and a digital Thalimedes by OTT from 12/1/2001 onwards.

The hourly data and related metadata are available in Raicich (2019).

- ***Analysis***

The time series of the annual means (SLP and AT) and totals (PR) are displayed in Figure 15. Superimposed are the 10-year running means.

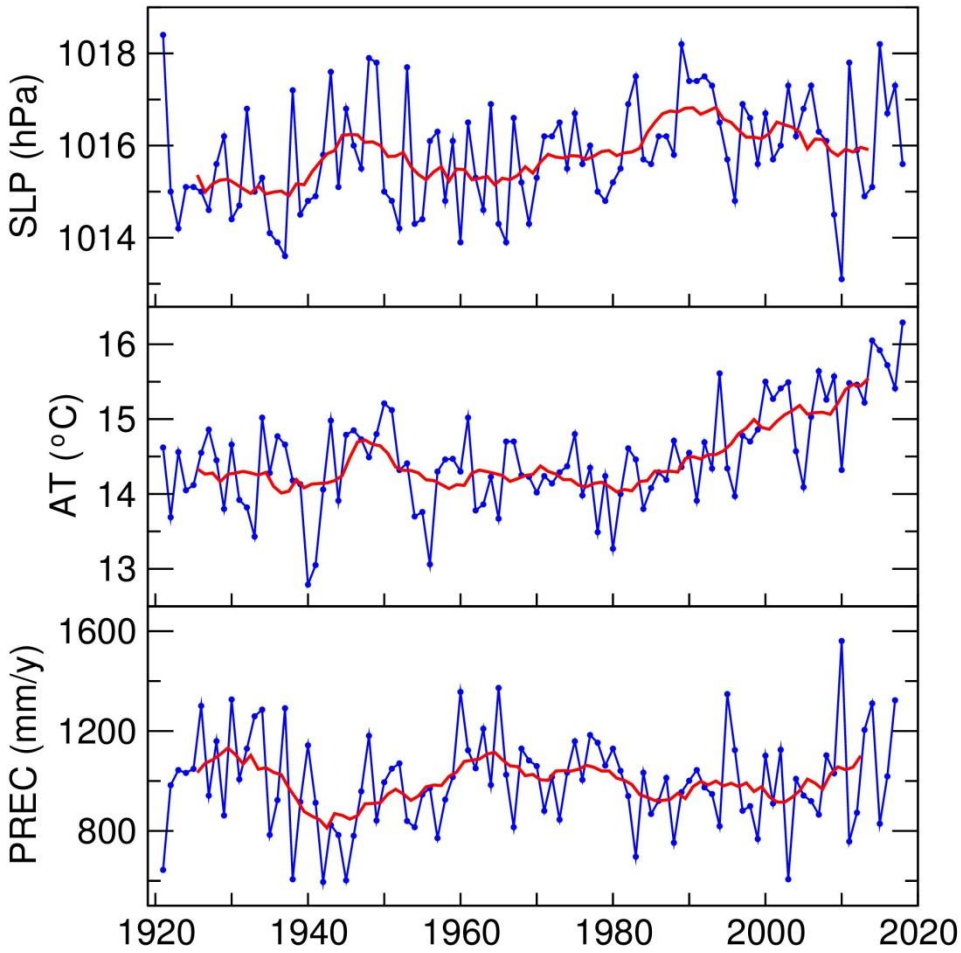

Figure 15. Blue curves represent the times series of annual mean SLP (upper panel) and AT (middle panel), and annual total PR (lower panel) @CNR-ISMAR Trieste. Red curves are the 10-y running means.

SLP is mainly characterized by multi-decadal fluctuations. Interannual variability significantly reduced around 1970, when a relatively high SLP regime started. During the last decade higher interannual variability seemed to occur again.

The variability of AT is dominated by the increasing trend that began in the early 1980's, coherent with the ongoing global atmospheric warming. The related slope change of the time series makes the estimate of a long-term trend essentially useless.

Decadal fluctuations of PR can be observed approximately in counter-phase to those of SLP, while there is no clear long-term tendency.

In 16 we present a selection of mean annual cycles computed for 30-year periods. The periods 1931-1960 and 1961-1990 represent two examples of the 'past' climate, while the cycles computed from the latest available 30 years (up to 2018 for SLP and AT and 2017 for PREC) represent the 'present' climate.

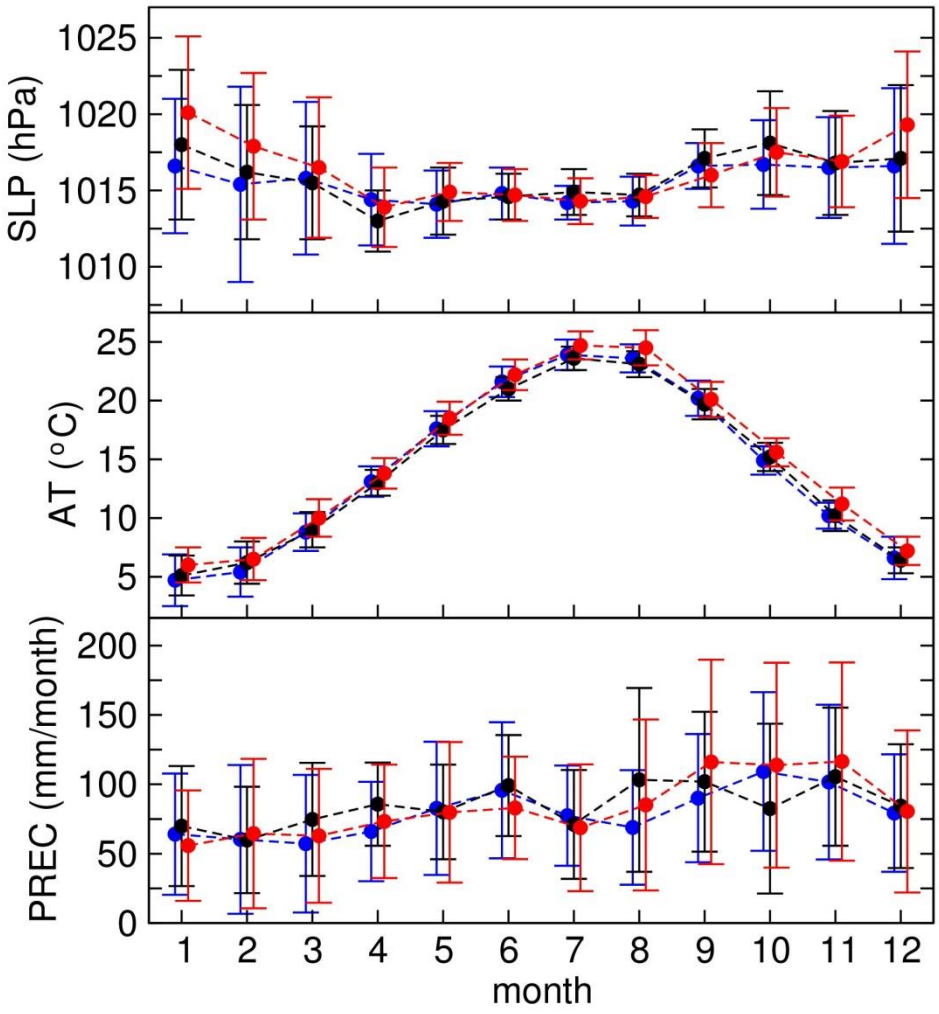

Figure 16. Annual cycles of SLP (upper panel), AT (middle panel) and PR (lower panel) @CNR-ISMAR Trieste. Blue symbols refer to the 1931-1960 period, black symbols to 1961-1990 and red to 1989-2018 (for SLP and AT) and 1988-2017 (for PR). Error bars represent ±1 STD.

Mean values are affected by large variability, represented by the error bars (±1 STD from the mean). Nevertheless, it is possible to recognize some relevant changes that occurred in the annual cycles during the last 30 years, namely a SLP increase in winter (December through February), up about 2 hPa, and a general AT increase, more marked in late spring and summer.

As for the near-surface temperature, its behavior is strongly affected by that of AT, with an increasing trend since the early 1980's. As in the case of AT, a long-term trend estimate has little or no meaning.

As ST data start in 1939, we only show the mean annual cycles for 1961-1990 and 1986-2015 (Fig. 17, upper panel). The most evident recent changes are represented by a general warming, more pronounced in summer and late autumn.

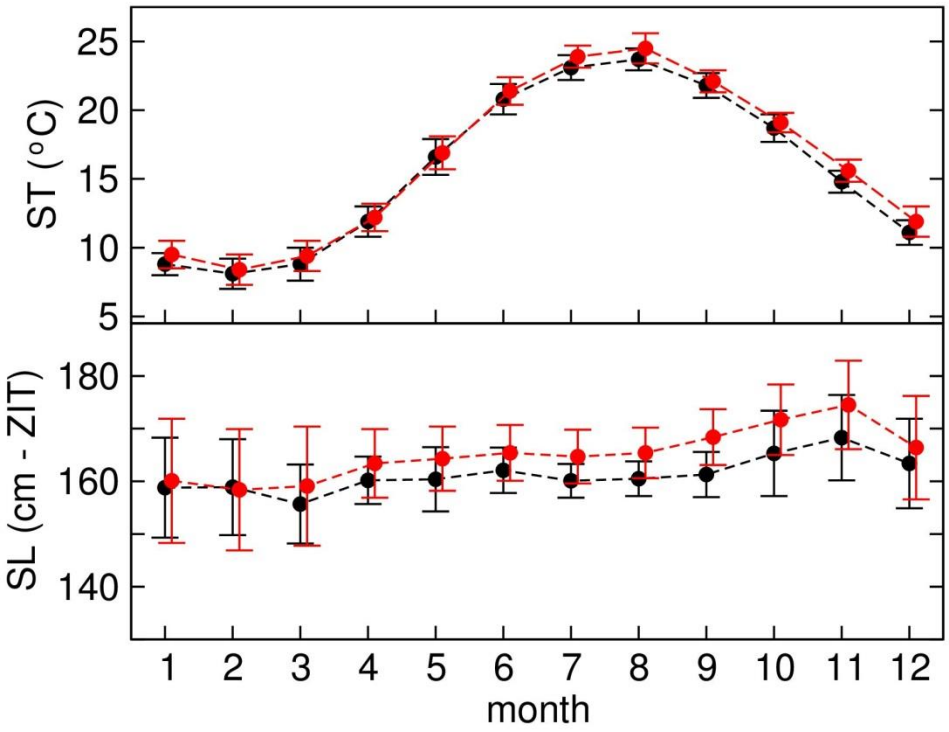

Figure 17. Annual cycles of ST (upper panel) and SL (lower panel) @CNR-ISMAR Trieste. Black symbols refer to the 1961-1990 period and red symbols to 1989-2015 (for ST) and 1986-2018 (for SL). Error bars represent ±1 STD from the mean. Symbols are staggered for better visibility.

The time series of the annual means and related 10-year running means are shown in Figs. 18 and 19. The well-known mean sea level (MSL) rise is apparent, with mean secular trend of about 1.3 mm/y. The time series reflects the typical behavior of SL observed in the Mediterranean Sea, characterized by an overall rise, except for a period of stability between 1960 and 1993 (Tsimplis and Baker, 2000; Zerbini et al., 2017).

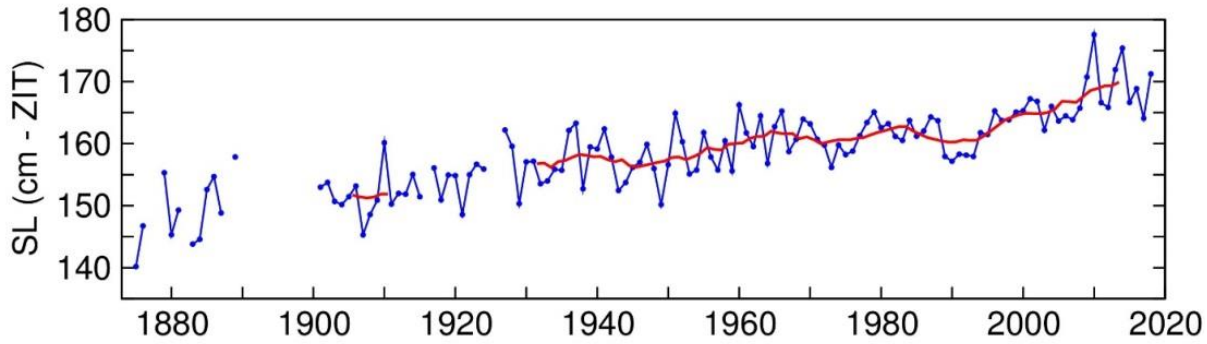

Figure 18. Time series of annual mean SL (blue curve) and related 10-y running mean (red curve) @CNR-ISMAR Trieste. SL is measured relative to the tide gauge datum (ZIT).

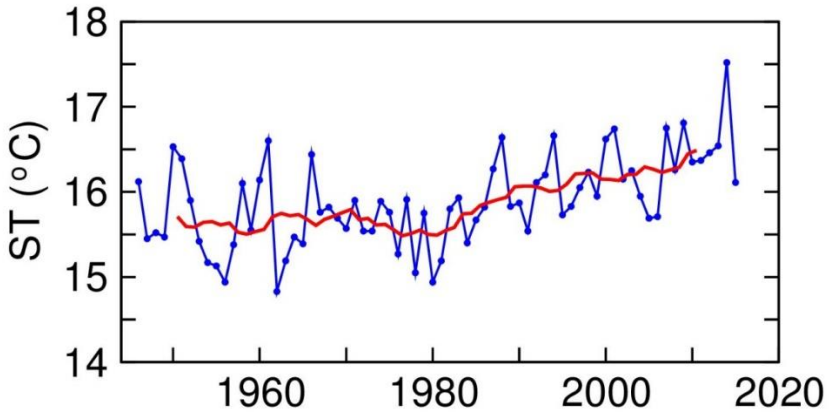

Figure 19. Time series of annual mean ST (blue curve) and related 10-y running mean (red curve) @CNR-ISMAR Trieste.

Also in this case two mean annual cycles are presented, namely for 1961-1990 and 1989-2018 (Fig. 17, upper panel). The general increase related to the MSL rise is apparent in all months except for January and February. This behavior is mainly connected with larger inverted barometer effect caused by higher AP (see below).

3.2.2. CNR-ISMAR at Venice

- ***Description of the station and the dataset***

Wind Data (WIND) @CNR-ISMAR Venezia. The two available dataset of wind data recorded at the CNR-ISMAR "Acqua Alta" oceanographic research tower, located in the Northern Adriatic Sea, in 16 meters of depth, 15 km off the coast of the Venice lagoon (GPS coordinates 45° 18' 51.288'' N, 12° 30' 29.694'' E) consist in:

- 36 years dataset, staring in 1983 and continuing nowadays, with the help of Centro Previsioni e Segnalazioni Maree of the Municipality of Venice. Wind data have been collected by Micros-Siap t033 TDV and t031 TVV installed at 16 m above the sea level until 2017 then the sensors have been raised to 20 m
- 12 years dataset, starting in 2008 and continuing nowadays, with a Davis Vantage Pro meteostation. Its wind sensor has been installed at 18 m above the sea level until 2017 then the sensor has been raised to 21 m.

Wave Data (WAVE) @CNR-ISMAR Venezia. The dataset consists of 39 years of directional wave time series recorded since 1979 at the CNR-ISMAR "Acqua Alta" oceanographic research tower, located in the Northern Adriatic Sea, in 16 meters of depth, 15 km off the coast of the Venice lagoon (Fig. 1, GPS coordinates 45° 18' 51.288'' N, 12° 30' 29.694'' E). The tower is managed by the Institute of Marine Sciences of the National Research Council of Italy and is still in fully working order. A thorough upgrade of the structure has been recently completed, allowing the continuation of the described time series and further implementation of new wave measuring instruments.

Different wave gauges have been used since the start of the measurements, progressively upgraded and repositioned during maintenance operations. The recorded wave data have been thoroughly verified and corrected where necessary and published Open-Data on the repository PANGAEA (Pomaro et al., 2018) (https://doi.org/10.1594/PANGAEA.885361) as documented in Pomaro et al., 2019.

The tower was installed in March 1970 and dedicated special purpose wave measurement campaigns started in 1971. However, only in early 1979 regular automatic wave measurements

were started. During the years, in response to the steadily growing use of the structure for meteorological, oceanographic, biological and chemical measurements, the tower has gone through various modifications and expansions, until the present configuration.

Nowadays, the wave measurements continue on a regular basis, with the aim of better characterizing the wave climate in the Northern Adriatic Sea, with specific consideration for the Venice littoral, and of monitoring its long term wave changes.

Since the start of the measurements at the Acqua Alta research tower, the instrumental system has been progressively upgraded and repositioned during maintenance operations, and three different recording periods can be considered. In the first one (1979–1986) two pressure transducers were used. In the central period (1987–2003) the system was upgraded to three pressure transducers. In the third period (2004 to present) the pressure transducers have been replaced by echo sounders.

In addition to this relevant observational dataset, recently published Open Data, a more recent wave time-series, beginning in 2008, has been recorded by means of a Nortek 1 MHz AWAC ADCP. The instrument has been installed on the sea floor (16 m), 50 m off the “Acqua Alta” tower and it delivers data in real time. The sampling strategy is based on measurements done every 30’ with 2048 samples at 2 Hz. Data are processed by the on board by the prolog processor but raw data are recorded as well.

The availability of different data sources allows for inter-comparisons and validation studies, since the high sensitivity of long-term measured dataset to changes through time.

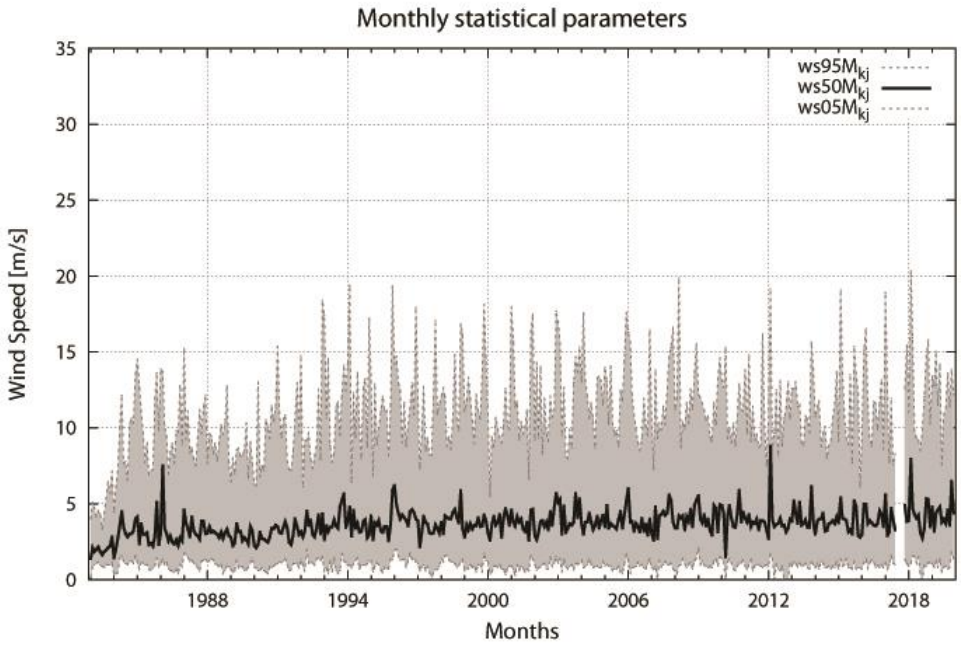

Figure 20. Statistical distribution of the 36-year long wind data set. The 5th, 50th and 95th monthly percentiles (W5M, W50M and W95M) are given.

- ***Analysis***

The extent of the directional wind time series recorded since 1983 at the CNR-ISMAR "Acqua Alta" oceanographic research tower (AAOT) allows to describe the wind climate in the North Adriatic region and to identify trends. The northern part of the Adriatic Sea is characterized by two main wind and correspondingly wave regimes, strongly forced by the regional orography.

The availability of different data sources allows for inter-comparisons and validation studies, since the high sensitivity of long-term measured dataset to changes through time.

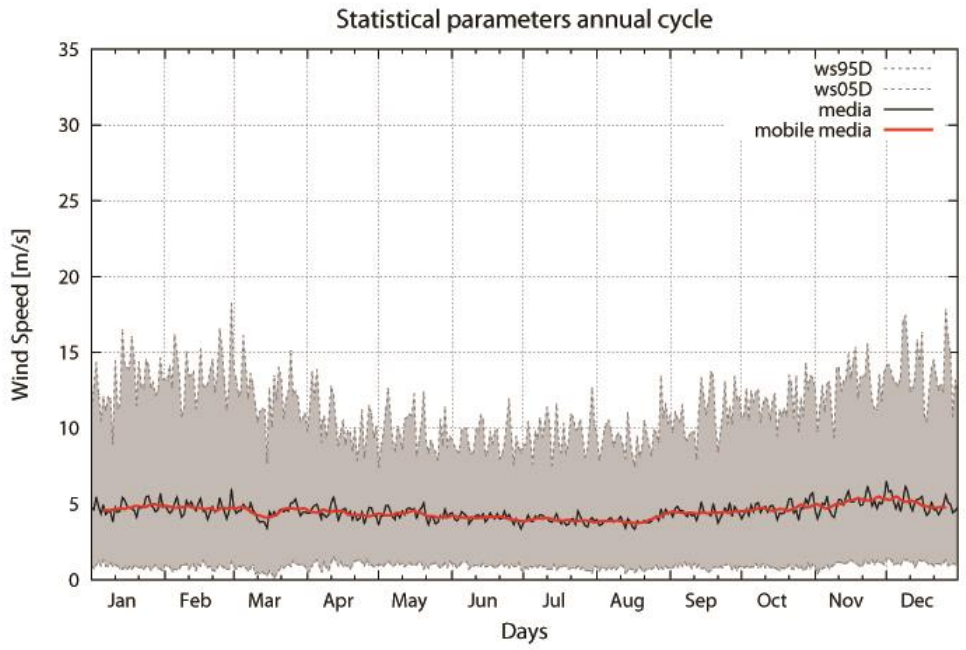

Figure 21. Annual cycle of the 5th, 95th and 99th percentiles (W5D, W95D and W99D) and the mean values. The figure shows values for each calendar day based on the whole 36-year long wind data set. The shaded area marks the 31-day running mean of the daily 5th and 95th percentiles. The white line shows the 31-day running mean value of the daily mean wind speed, the black line on top the one of the 99th percentile.

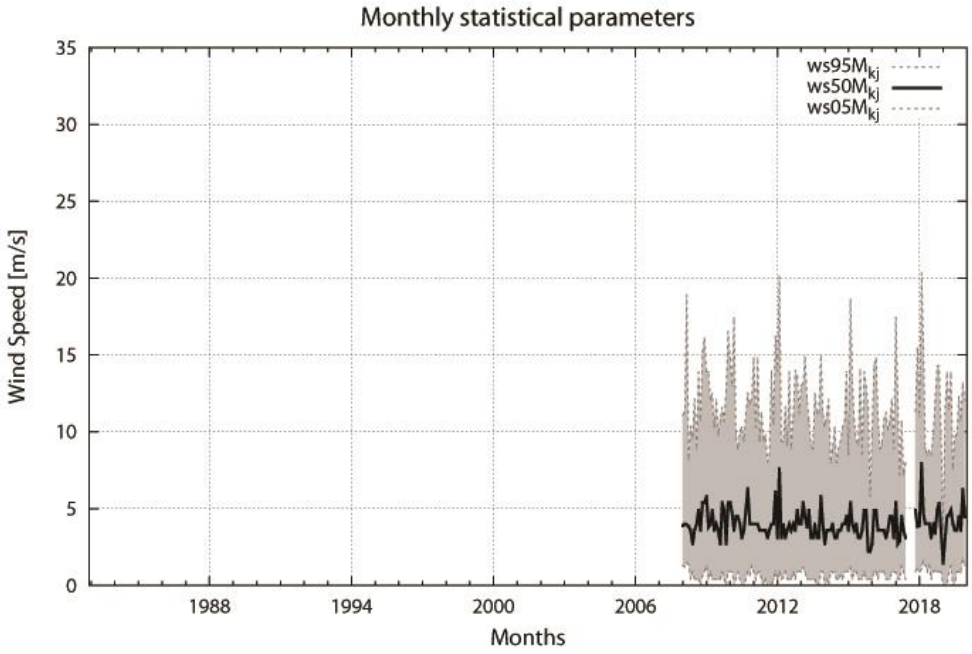

Figure. 22. Statistical distribution of the 12-year long wind data set. The 5th, 50th and 95th monthly percentiles (W5M, W50M and W95M) are given.

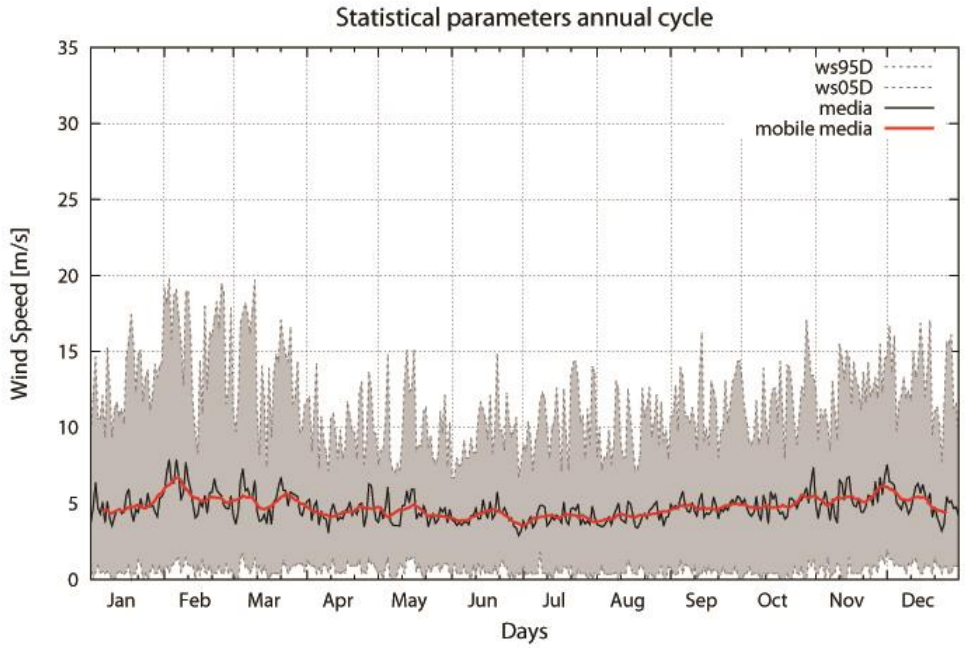

Figure 23. Annual cycle of the 5th, 95th and 99th percentiles (W5D, W95D and W99D) and the mean values. The figure shows values for each calendar day based on the whole 12-year long wind data set. The shaded area marks the 31-day running mean of the daily 5th and 95th percentiles. The white line shows the 31-day running mean value of the daily mean wind speed, the black line on top the one of the 99th percentile.

The extent of the directional wave time series recorded since 1979 at the CNR-ISMAR "Acqua Alta" oceanographic research tower allows to describe the wave climate in the North Adriatic region and to identify trends and links with large scale climate patterns obtained from a single and permanent observational source. The high sensitivity of this particular area to even small variations of large scale meteorological patterns allows to explore possible links of the local wave, hence wind, activity with large-scale north hemisphere circulation or weather regimes.

The two main wind and wave regimes characterizing the northern Adriatic Sea are: the long-fetch south-easterly 'sirocco' and the short-fetch strong north-easterly 'bora' wind generated waves, blowing along the major and minor axis of the basin, respectively. Bora is the most frequent regime, but high waves are mostly associated to sirocco. A clear decrease of the significant wave height 99th percentile is evident, paralleled by a smaller, but distributed along the annual cycle, increase of the 50th and 75th ones. The estimated trend of the frequency of events above a certain threshold confirms an increase of the average storm frequency, with a shift from both the lower and the higher to the central part of the distribution, paralleled by a decrease of the maximum Hs values. In particular, a distributed decrease of the bora significant wave height is recognized. For sirocco the tendency is less pronounced, but with an evident increase of the frequency of the mean values.

Observations show an evident tendency towards a reduction of the wave activity in the Northern Adriatic Sea, in terms of intensity of the events, and a general increase in terms of frequency (50th and 75th characteristic percentiles). The geometry and orography of the basin suggest that this is true for most of the basin. Of the two wind regimes, the decrease of intensity is mainly due to bora (particularly in the upper percentiles), while the increased storminess is associated to sirocco conditions.

Further details are given in the following figures, belonging to the paper by Pomaro et al. (2017).

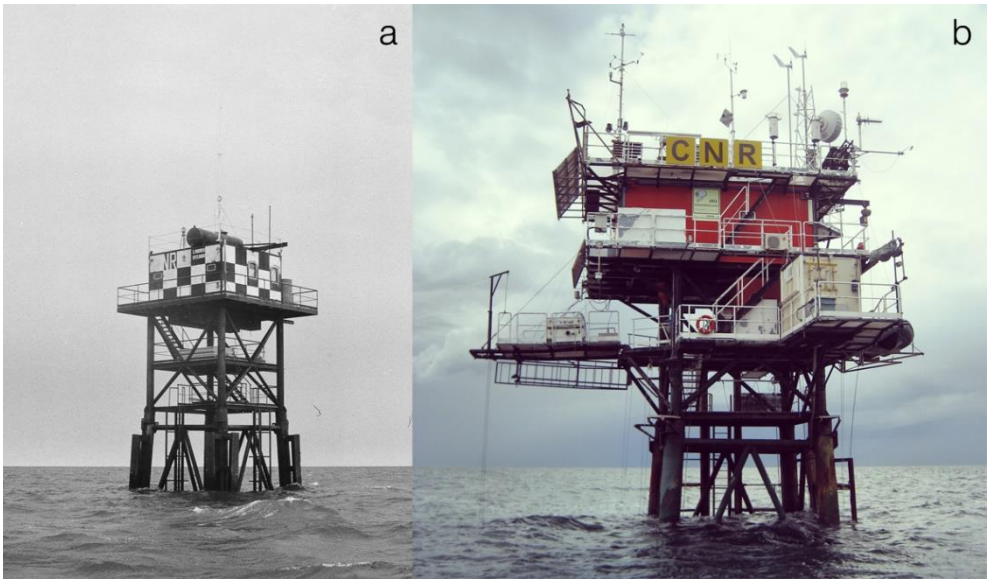

Figure 24. The Acqua Alta oceanographic tower. (a) In 1970, soon after its positioning, and (b) in 2017.

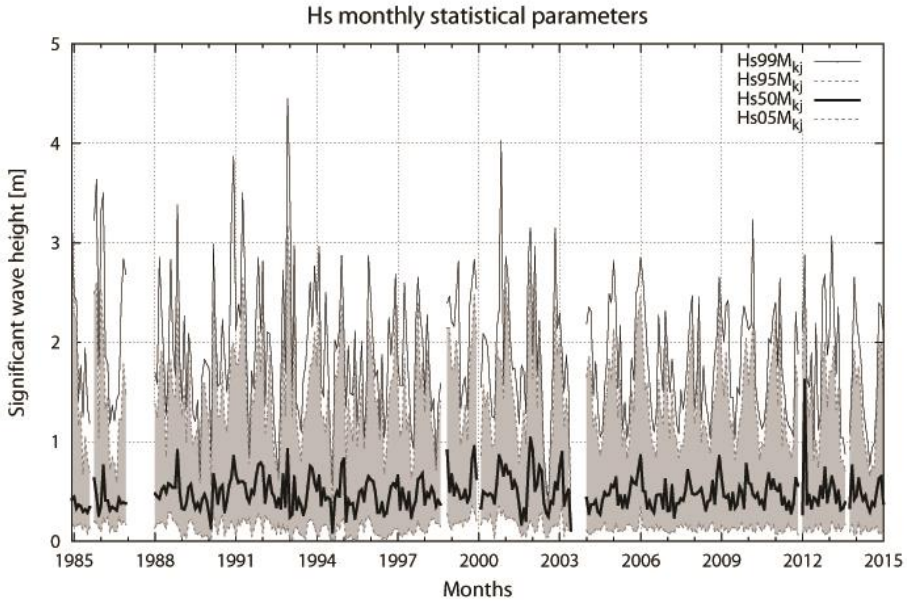

Figure 25. Statistical distribution of the 37-year long significant wave height original data set. The 5th, 50th and 95th monthly percentiles (Hs5M, Hs50M and Hs95M) are given.

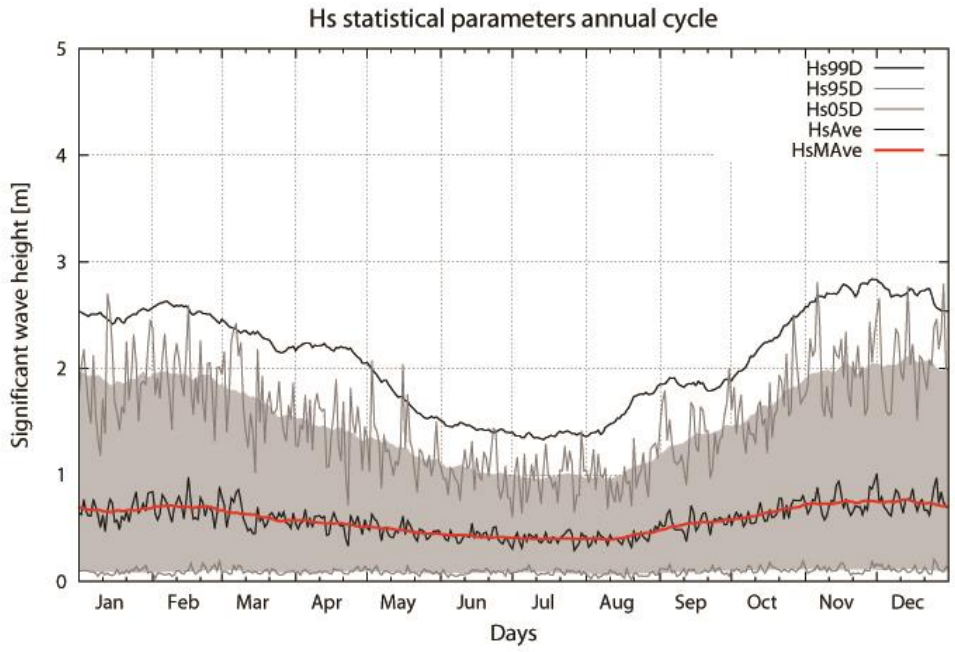

Figure 26. Annual cycle of the 5th, 95th and 99th percentiles (Hs5D, Hs95D and Hs99D) and the mean values. The figure shows values for each calendar day based on the whole 37-year long significant wave height data set. The shaded area marks the 31-day running mean of the daily 5th and 95th percentiles. The white line shows the 31-day running mean value of the daily mean Hs, the black line on top the one of the 99th percentile.

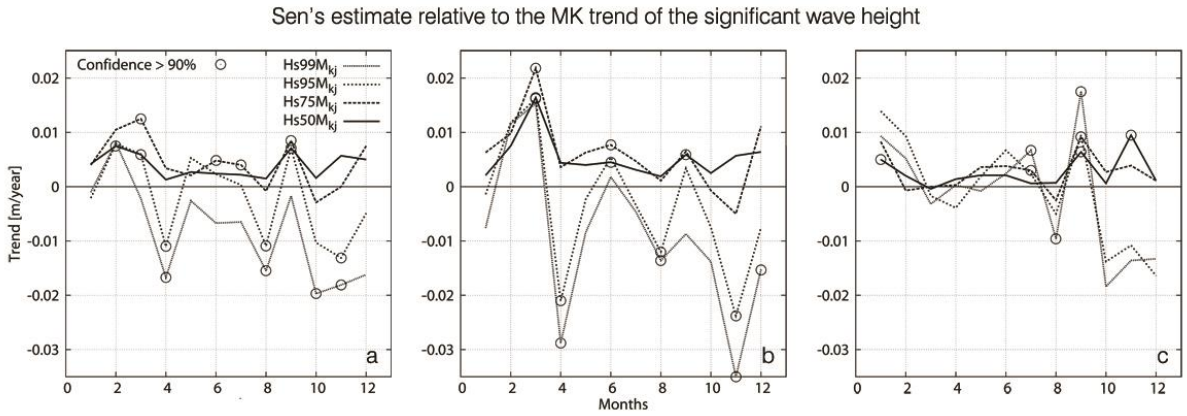

Figure 27. Monthly trends of the 50th, 75th, 95th and 99th Hs percentiles: (a) all regimes, (b) bora regime and (c) sirocco regime. The circles identify trends statistically significant at the 90% confidence level.

More studies are undergoing in order to fully investigate the 12-years long recorded wave dataset, staring in 2008, and make it available for climate studies.

3.3. Trends and variability reproduced by coupled climate models

3.3.1. Description of the ADRISC modelling suite

The Adriatic Sea and Coast (AdriSC) Meteotsunami Forecast is a research product that was developed within the framework of two Croatian research projects: (1) project MESSI (http://www.izor.hr/messi), for reproduction and forecast of the Adriatic meteotsunamis, being a part of a pilot meteotsunami early warning system and (2) project ADIOS (http://www.izor.hr/ADIOS), with an ongoing effort to better understand the interactions between the Ionian and Adriatic Seas over interannual to decadal timescale and their potential effects on the ocean circulation along the Croatian coastline and islands.

Two different AdriSC modules have been developed: (1) a basic module using the COAWST model with WRF (3 km highest resolution) for the atmosphere and ROMS (1 km highest resolution) for the ocean (in blue in the figure) and (2) a dedicated meteotsunami module using

WRF (1.5 km resolution) for the atmosphere and ADCIRC (between 10 m and 5 km) for the ocean (in red in the figure).

The basic module domains are presented in Fig. 30 and are defined as follow: a 15km grid (horizontal size: 140 x 140) for the atmospheric model, approximately covering the central Mediterranean basin, and a nested 3km atmospheric grid (266 x 361) encompassing the entire Adriatic and Ionian Seas; the same 3km grid is used for the ocean model with a nested additional 1km grid (676 x 730) allowing for better representation of the complex geomorphology of the Adriatic Sea and most particularly of the Croatian coast. The vertical discretization of the grids is achieved via terrain-following coordinates: 58 levels refined in the surface layer for the atmosphere (Laprise, 1992) and 35 levels refined near both the sea surface and bottom floor for the ocean (Shchepetkin, 2009). Additionally, the basic module is using a common tidal and river forcing for the ocean grids. Eight tidal constituents (M2, S2, N2, K2, K1, O1, P1, Q1) – extracted from the Mediterranean and Black Seas (2011) 1/30° regional solution of the OSU Tidal Inversion Software (OTIS – Egbert, Bennett, and Foreman,1994; Egbert and Erofeeva, 2002), are imposed on the offshore boundaries of the 3km grid. These constituents are found to satisfactorily reproduce tidal dynamics in a micro-tidal Adriatic Sea (Cushman-Roisin and Naimie, 2002; Janeković and Kuzmić, 2005).

A total of 54 river flows (49 for the 1 km grid) are imposed over at least 6 grid points each (18 grid points for the Po river delta), with river mouths located along the coastline of Greece, Albania and Montenegro, Croatia and Slovenia, Italian peninsula and Sicily. The river flow monthly climatology is based on the RivDis database (Vörösmarty et al., 1996), and studies from Malačič and Petelin (2009), Pano and Avdyli (2002), Pano et al. (2010), Janeković et al. (2014) and Ljubenkov (2015). The interannual variability of the flows is derived from Ludwig et al. (2009).

The basic module of the AdriSC modelling suite is based on a modified version of the Coupled Ocean-Atmosphere-Wave-Sediment-Transport (COAWST V3.3) modelling system developed by Warner et al. (2010), which couples (online) the Regional Ocean Modeling System (ROMS svn 885) (Shchepetkin & McWilliams, 2005, 2009) and the Weather Research and Forecasting (WRF v3.9.1.1) model (Skamarock et al., 2005) via the Model Coupling Toolkit (MCT v2.6.0) (Larson et al., 2005) and the remapping weights computed – between the 15km, 3km and 1km atmospheric and ocean grids, with the Spherical Coordinate Remapping and Interpolation Package (SCRIP).

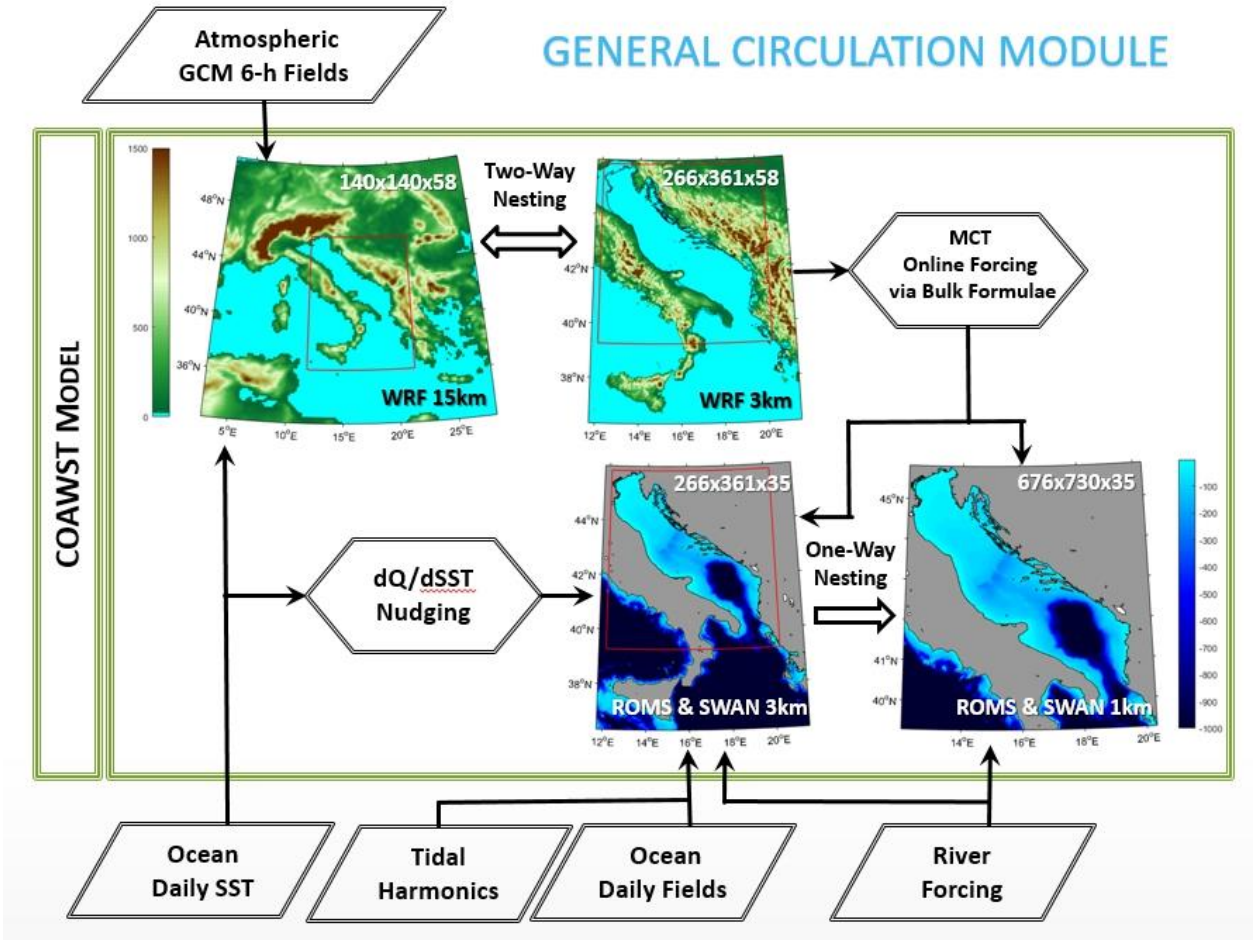

Figure 30. General circulation module of the AdriSC modelling suite, used in the present-climate simulation.

3.3.2. Assessment of atmospheric variables and processes

Mean air temperature at 2 m, wind speed and direction at 10 m and precipitation rate obtained for the whole AdriSC climate simulation (1987-2017) are presented in Figs. 31-33. The temperature shows clearly several characteristics: (i) it is much higher over the sea than over the land, (ii) it is decreasing from north

to south over the sea, (iii) it is strongly affected by the orography and mountains surrounding the Adriatic Sea. For the wind, it can be seen that (i) the bora wind is dominating in the coastal region of the eastern Adriatic with annual averages up to 6 m/s, (ii) the average speed is much lower along the western Adriatic Sea, (iii) it is strongly modulated by the orography. The precipitation rate is (i) maximal in the coastal region of the Adriatic Sea, over the Dinaric Alps, and (ii) minimal in the central open Adriatic,

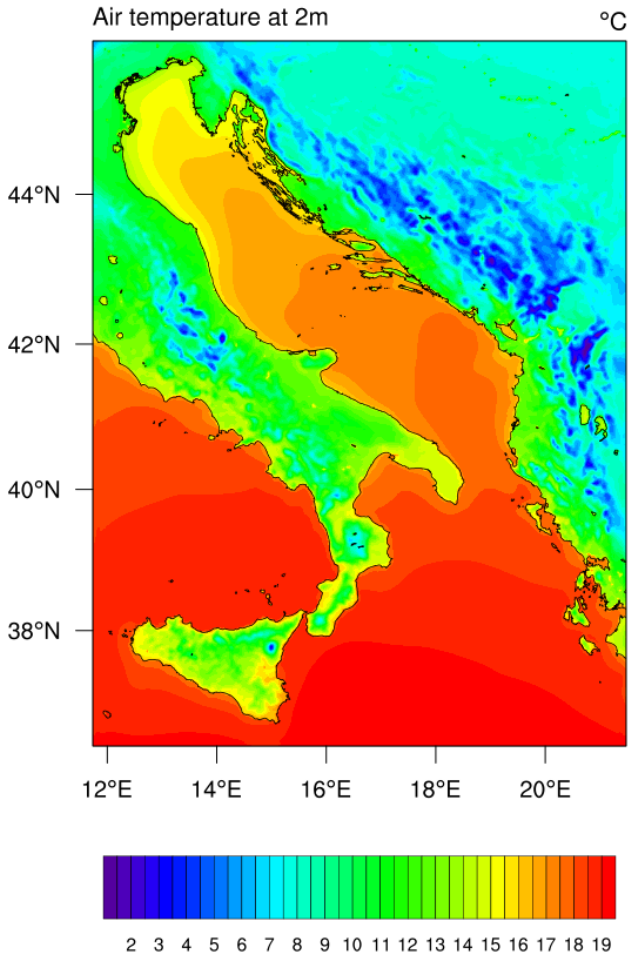

Figure 31. Mean air temperature at 2 m in the period 1987-2017 as simulated by the AdriSC modelling suite.

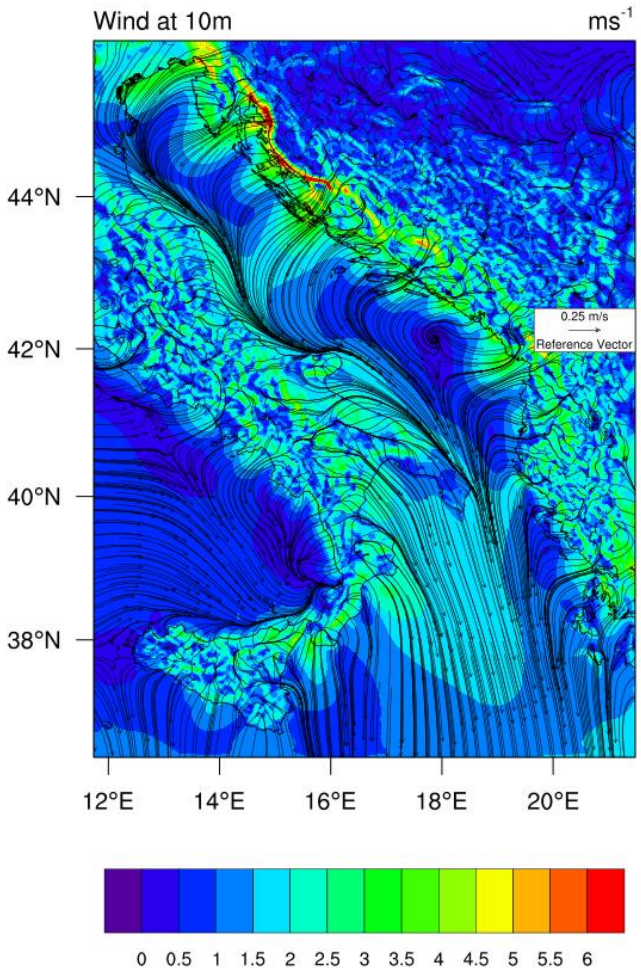

Figure 32. Mean wind speed and direction at 10 m in the period 1987-2017 as simulated by the AdriSC modelling suite.

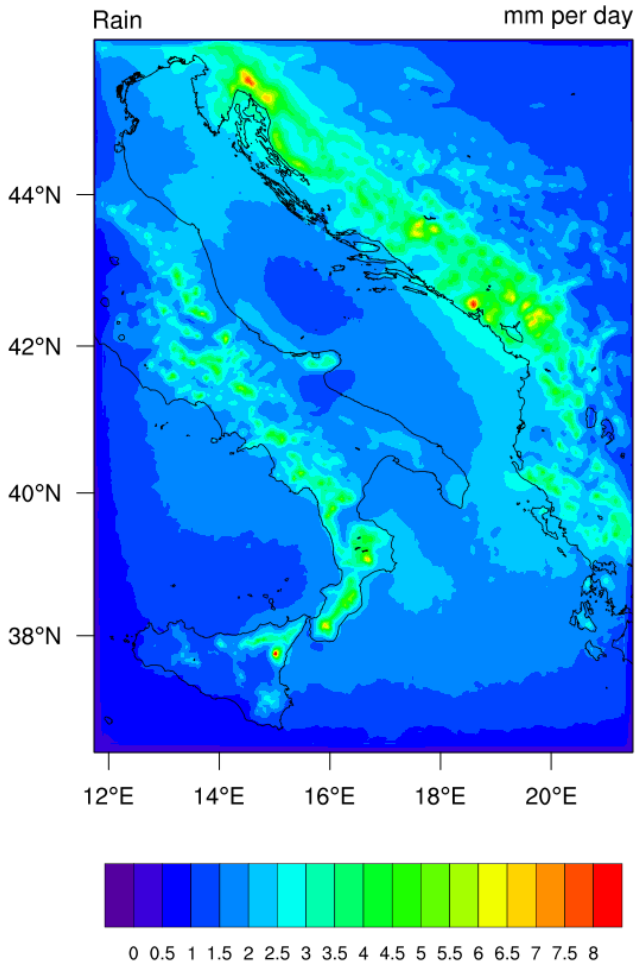

Figure 33. Mean precipitation rate in the period 1987-2017 as simulated by the AdriSC modelling suite.

Linear trends in mean air temperature at 2 m, wind speed and direction at 10 m and precipitation rate obtained for the whole AdriSC climate simulation (1987-2017) are presented in Figs. 34-36. From figures it can be deduced that: (i) air temperature trend is positive over the whole domain, but with much higher rates over the ocean (> 0.25 ^{o}C per decade) and Balkans than Italy and northern parts of Croatia (0.1-0.2 ^{o}C per decade), (ii) wind speed trend is a positive

over the Adriatic and coastal regions, with maximum along the Velebit Channel related to the bora wind, and negative over the highest mountains and continental part of the domain, (iii) precipitation rate trend is positive over the Adriatic and most of Italy, but negative over the Dinaric Alps and the continent.

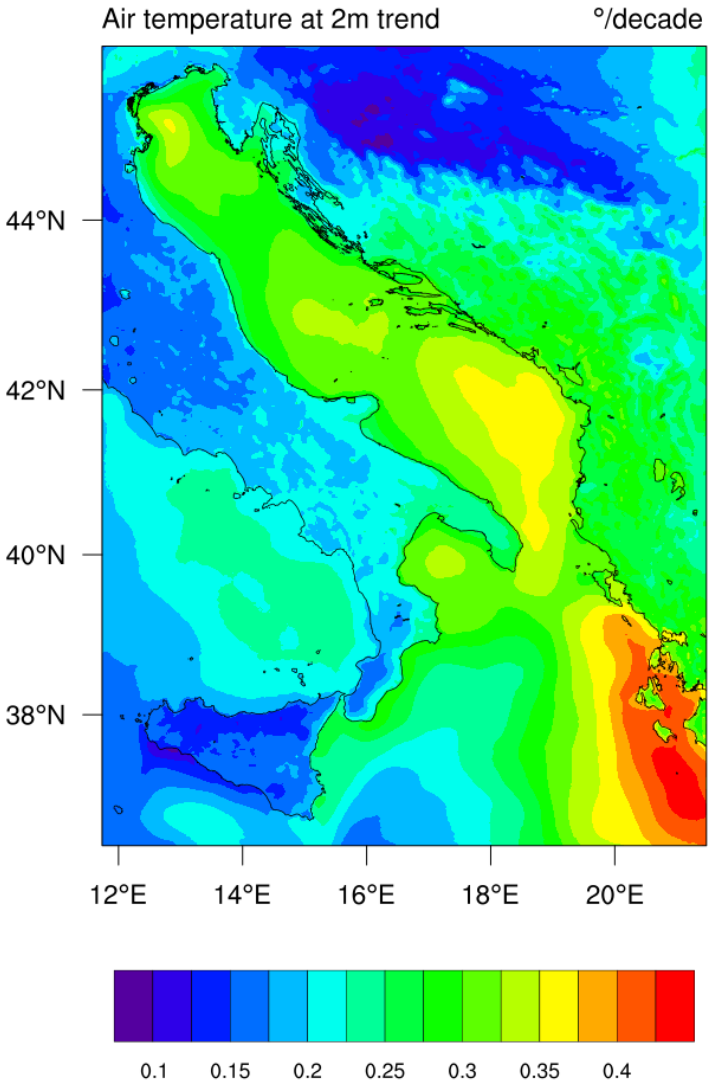

Figure 34. Mean air temperature at 2 m trend in the period 1987-2017 as simulated by the AdriSC modelling suite.

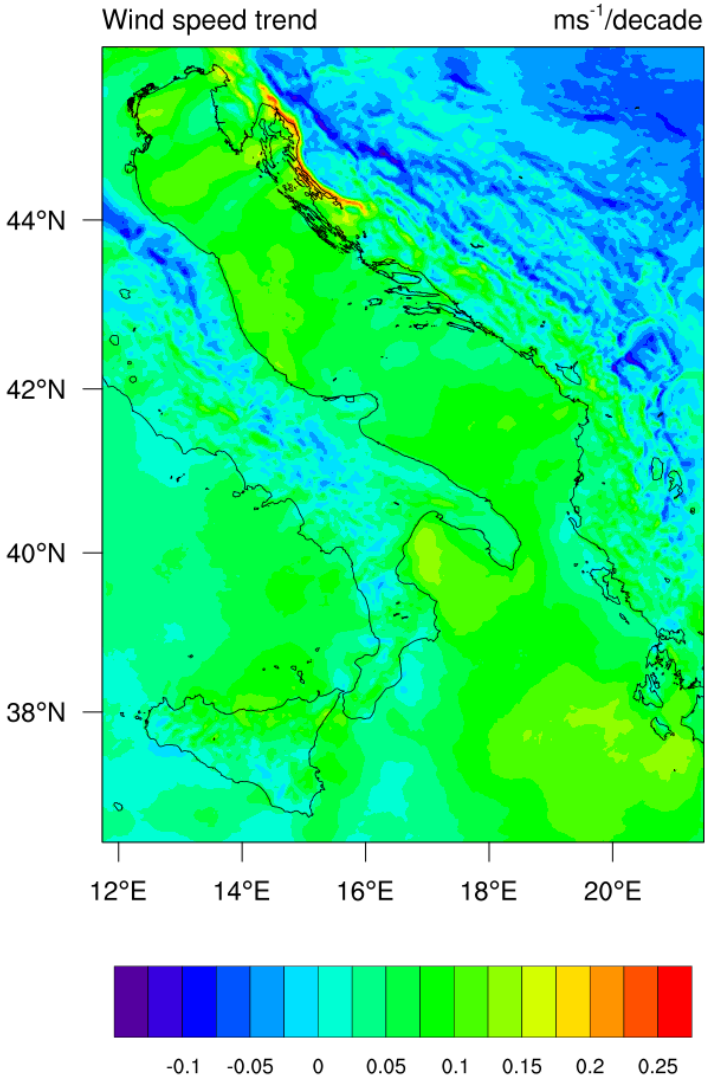

Figure 35. Mean wind speed at 10 m trend in the period 1987-2017 as simulated by the AdriSC modelling suite.

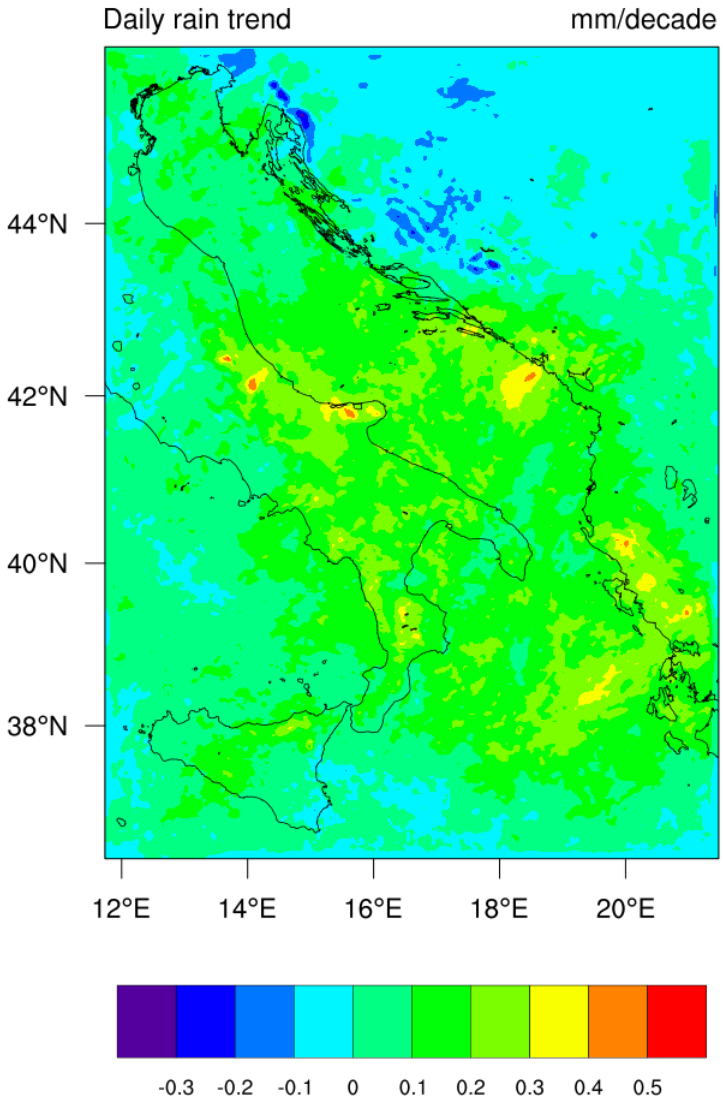

Figure 36. Mean precipitation rate trend in the period 1987-2017 as simulated by the AdriSC modelling suite.

Although positive on the annual scale, air temperature trends resemble a difference between seasons (Figs. 37-40). Winter trends are the largest over the sea and in the northern Ionian Sea, while being a low over the mountainous regions and even negative in central Italy. The spring temperature trends are stronger and positive everywhere, with highest values over the northern Ionian and southern Adriatic Sea. Summer trends are positive and largest over the central and

southern Adriatic Sea, but also over the most of the Dinaric Alps. Autumn trends are of lower rates, being the lowest in the coastal northeastern Adriatic and inland Croatia.

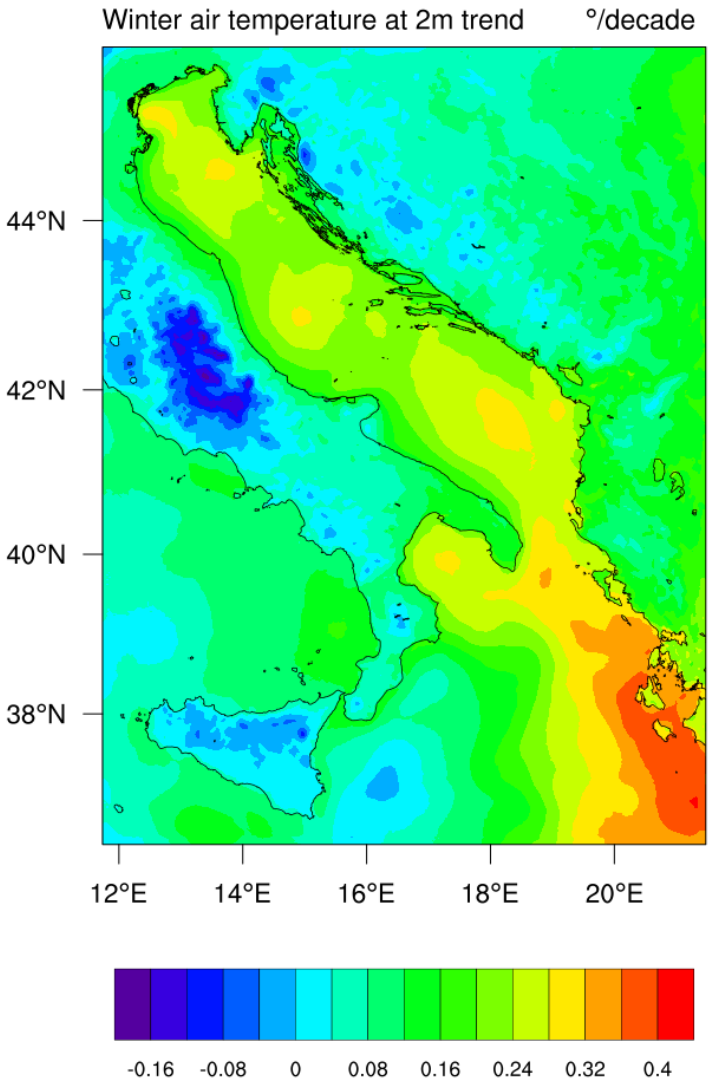

Figure 37. Winter (DJF) air temperature at 2 m trend in the period 1987-2017 as simulated by the AdriSC modelling suite.

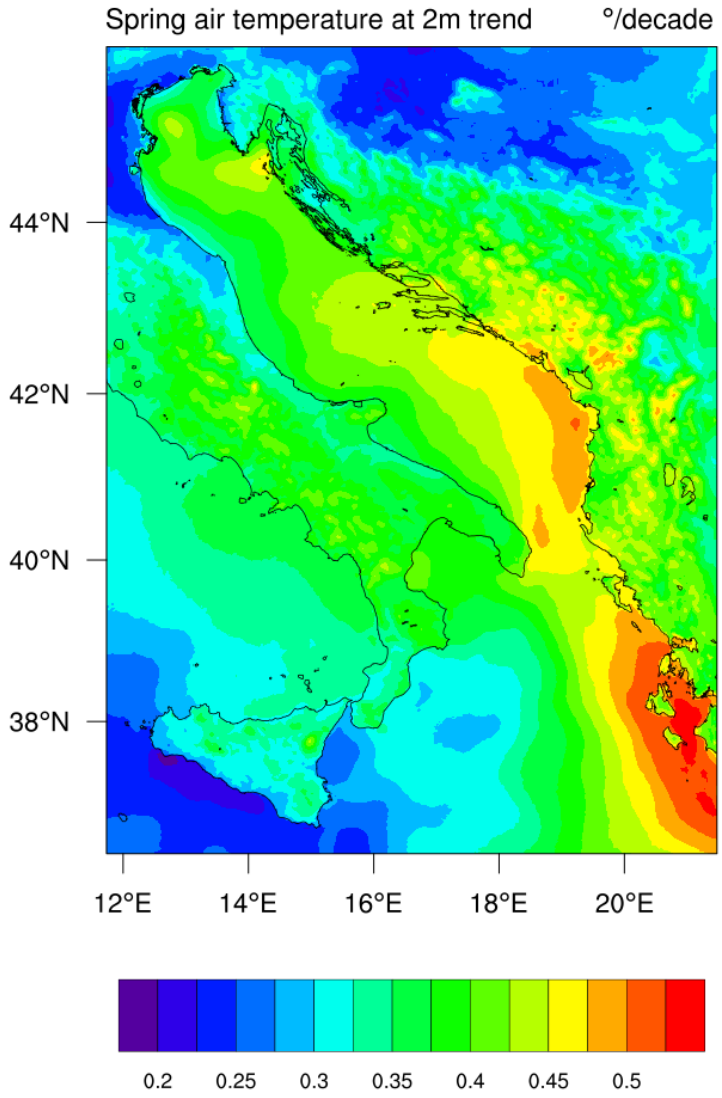

Figure 38. Spring (MAM) air temperature at 2 m trend in the period 1987-2017 as simulated by the AdriSC modelling suite.

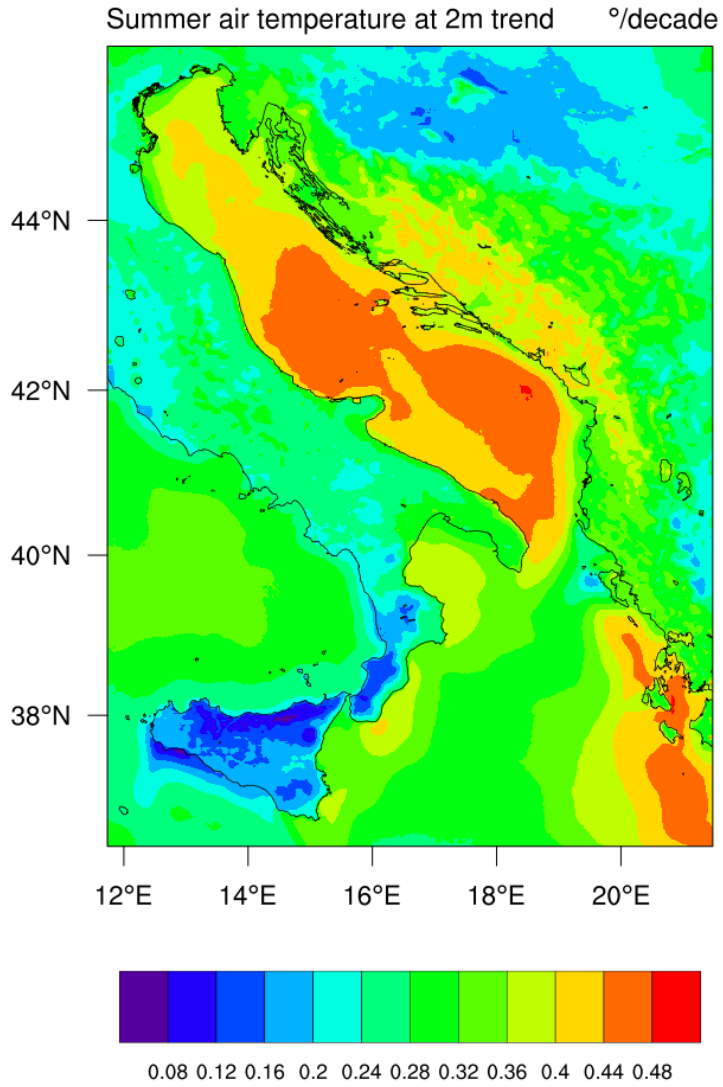

Figure 39. Summer (JJA) air temperature at 2 m trend in the period 1987-2017 as simulated by the AdriSC modelling suite.

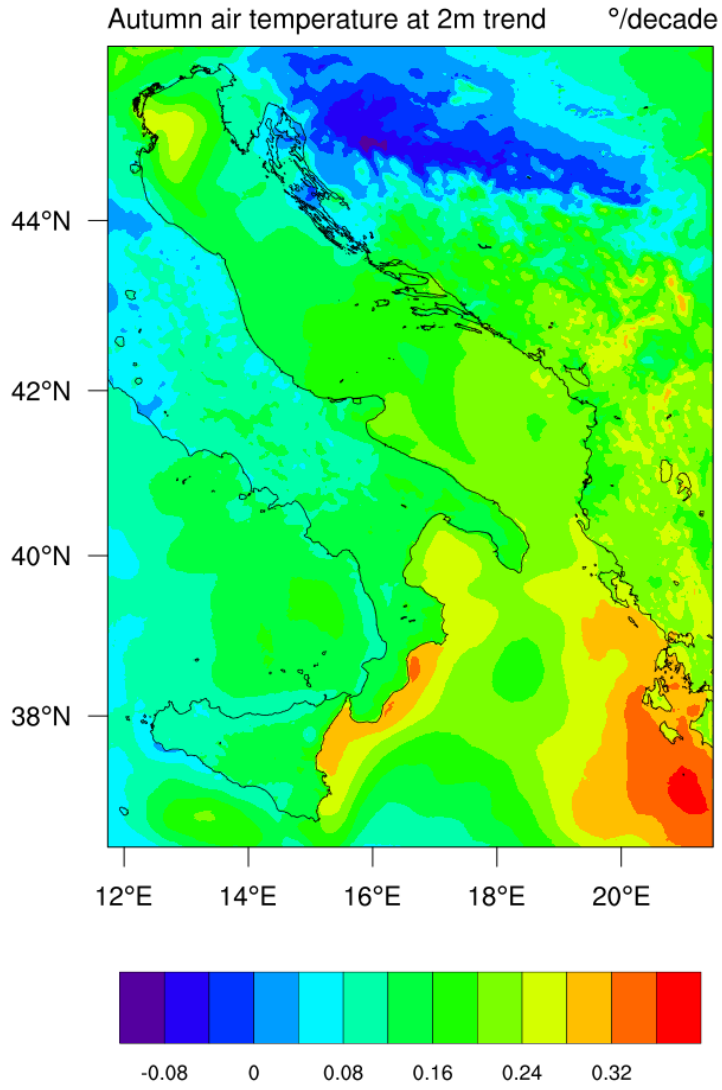

Figure 40. Autumn (SON) air temperature at 2 m trend in the period 1987-2017 as simulated by the AdriSC modelling suite.

The trends in wind speed are generally positive over the domain during the winter (Figs. 41-44), in contrary to the spring ones which are much lower. The only exception is coastal mountains along the eastern Adriatic coastline, where the trends are strongly positive, indicating local strengthening of the bora at places where being generated. Summer trends in wind speed is also

not significant, aside some mountainous region and the northern Ionian Sea. The autumn wind speed is generally negative over the southern part of the domain while positive over the northern Adriatic.

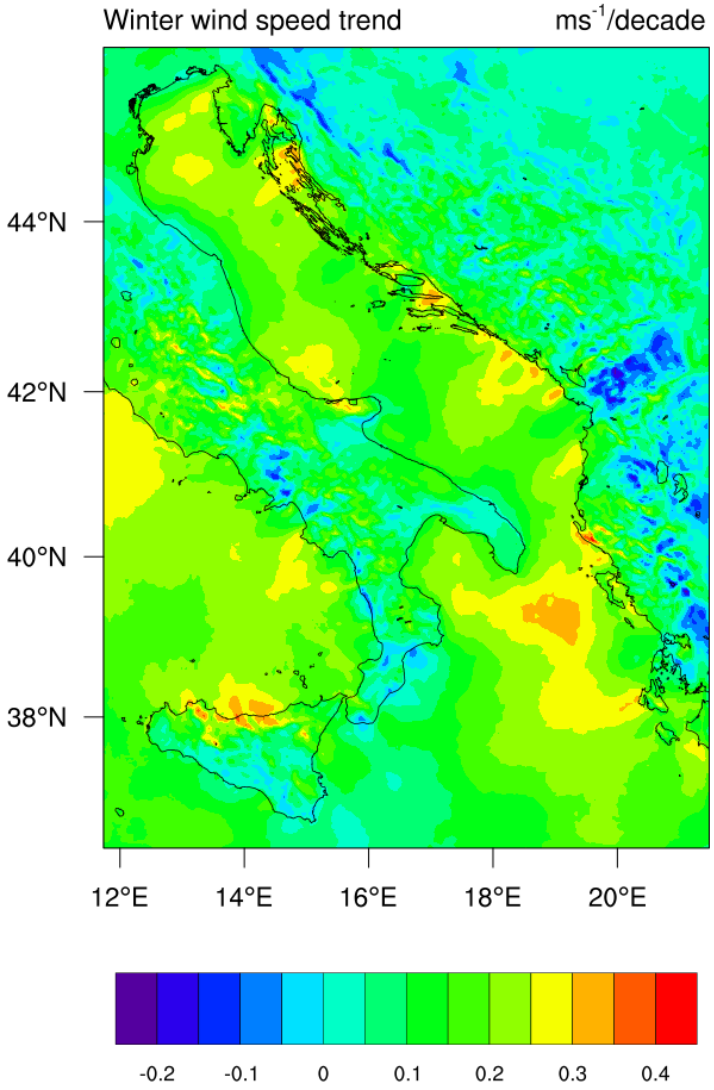

Figure 41. Winter (DJF) wind speed at 10 m trend in the period 1987-2017 as simulated by the AdriSC modelling suite.

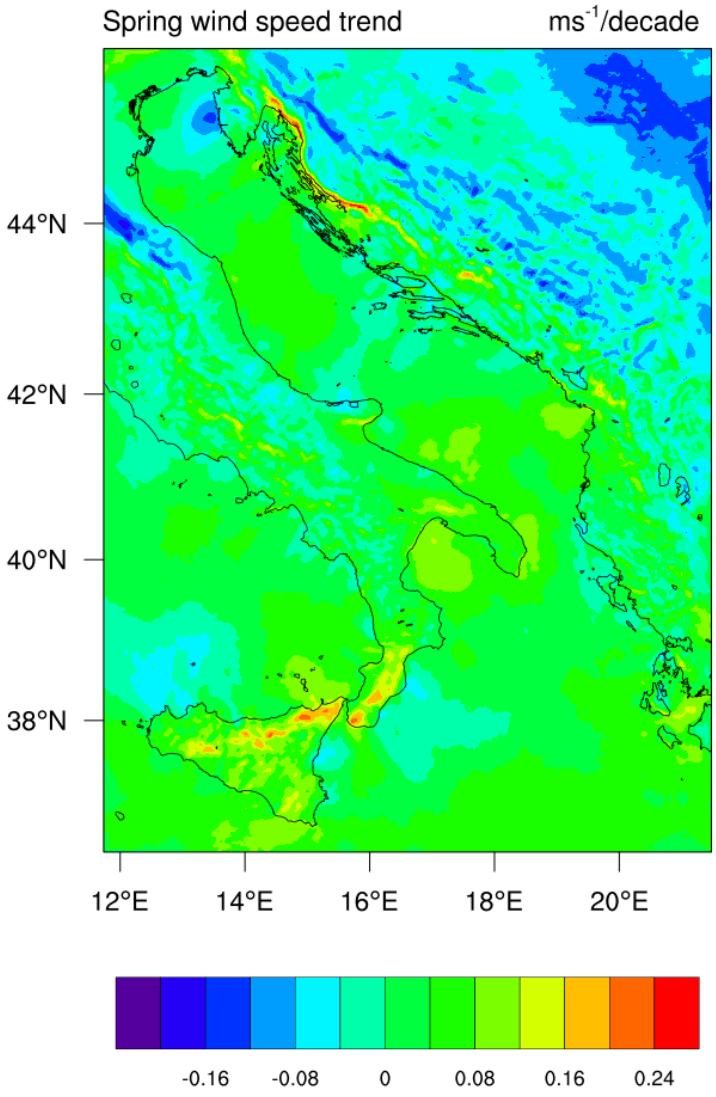

Figure 42. Spring (DJF) wind speed at 10 m trend in the period 1987-2017 as simulated by the AdriSC modelling suite.

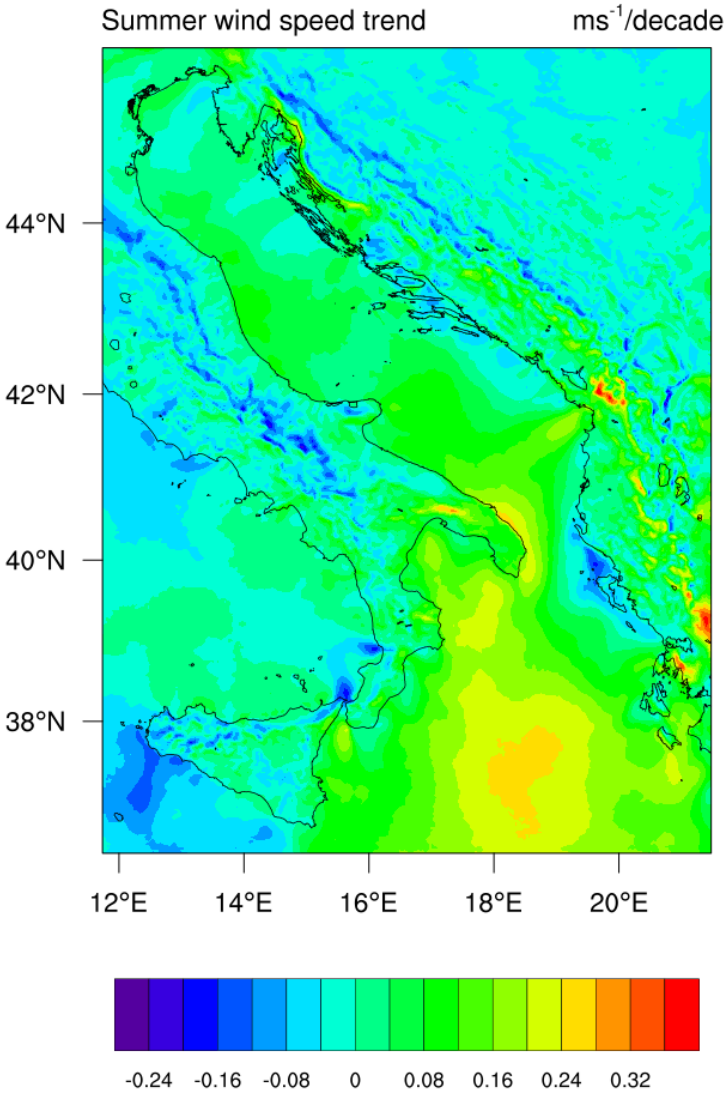

Figure 43. Summer (JJA) wind speed at 10 m trend in the period 1987-2017 as simulated by the AdriSC modelling suite.

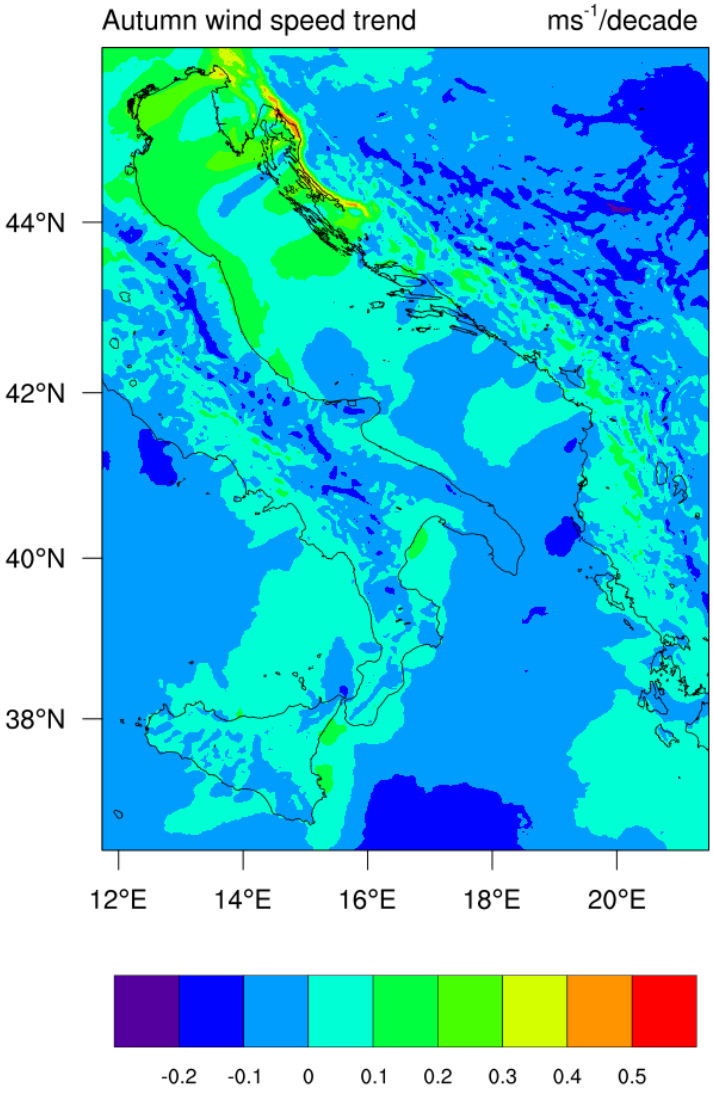

Figure 44. Autumn (SON) wind speed at 10 m trend in the period 1987-2017 as simulated by the AdriSC modelling suite.

For precipitation (Figs. 45-48), the winter trends are mostly positive, being larger in the coastal eastern Adriatic. The positive trends may be found also in spring, while being mostly negative in mountainous regions during summer. The mostly positive precipitation rate trends might be found during autumn.

It seems that all of these trends are affected by decadal oscillations, which can be clearly seen on measurements (Figs. 1-3).

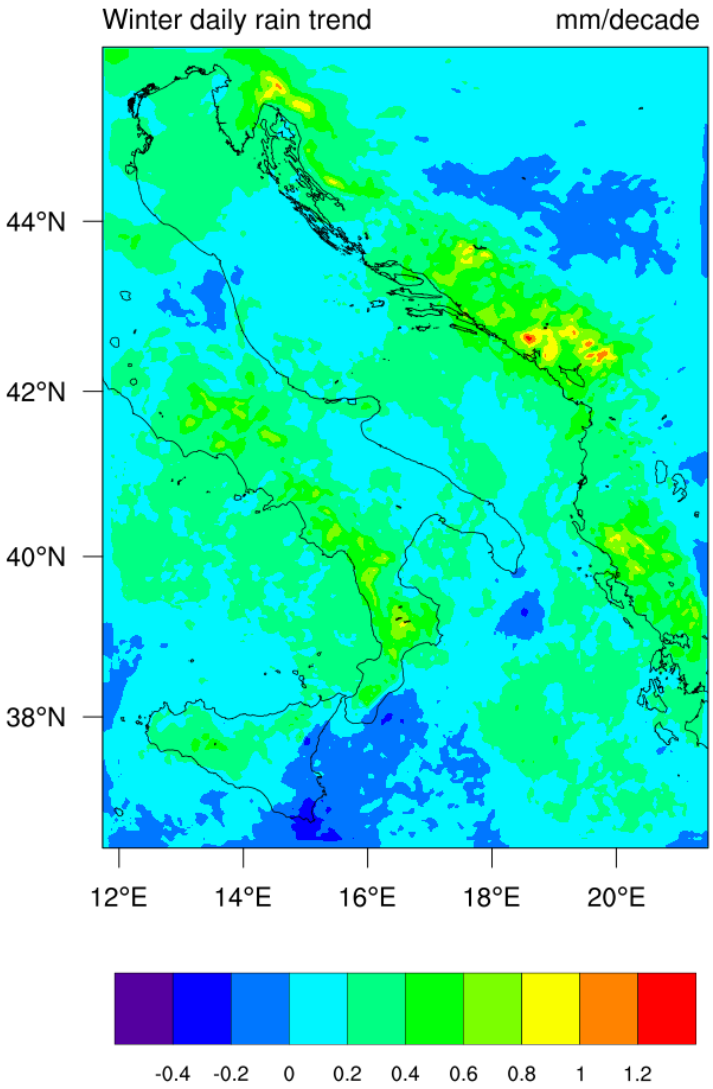

Figure 45. Winter (DJF) precipitation rate trend in the period 1987-2017 as simulated by the AdriSC modelling suite.

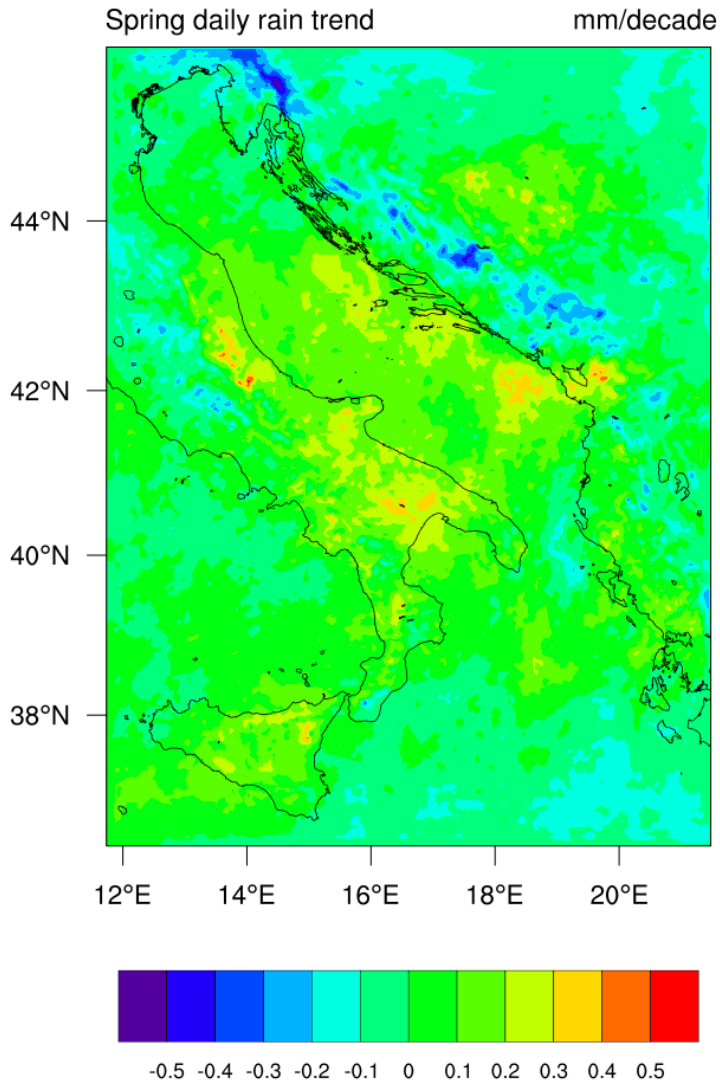

Figure 46. Spring (MAM) precipitation rate trend in the period 1987-2017 as simulated by the AdriSC modelling suite.

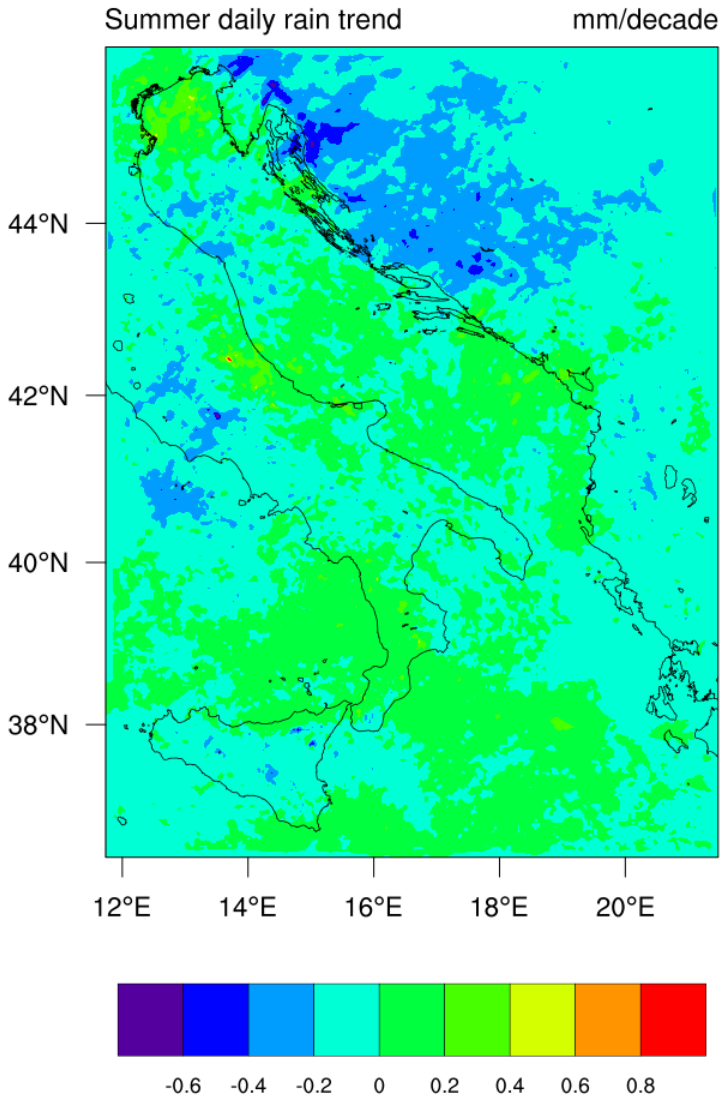

Figure 47. Summer (JJA) precipitation rate trend in the period 1987-2017 as simulated by the AdriSC modelling suite.

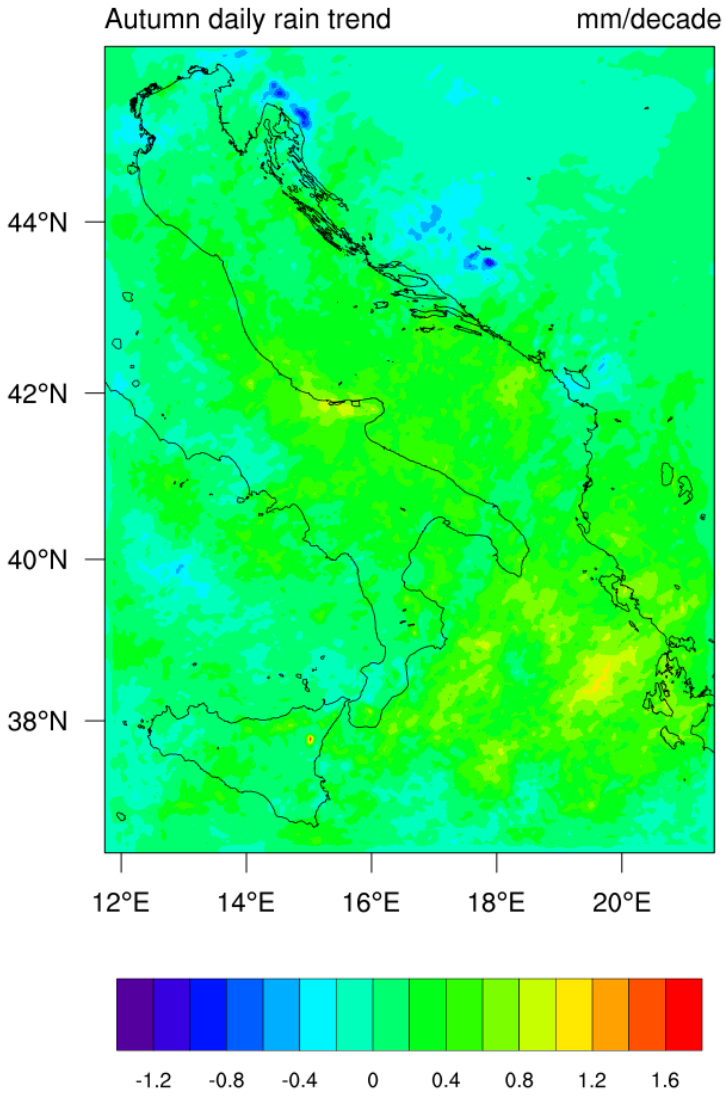

Figure 48. Autumn (SON) precipitation rate trend in the period 1987-2017 as simulated by the AdriSC modelling suite.

3.3.3. Assessment of oceanic variables and processes

For the purpose of the report, ocean temperature, salinity and current speed at different depths and the respective trends will be presented here (Figs. 49-84), plus the sea level trend (Fig. 85).

Mean sea surface temperature is decreasing from the northern Ionian Sea to the northernmost part of the Adriatic. Going deeper, the temperature is decreasing, with minimum values near the Italian shelf and at the Adriatic deepest depressions, which serve as collectors of dense waters (Jabuka Put, South Adriatic Pit). Mean salinity is increasing from the southern to the northern Adriatic, with lowest values downstream of the Po River delta. The current speed is reflecting the features of the Adriatic general circulation, having maximum values at the perimeters of the Southern Adriatic Gyre and Western Coastal Current in surface and perimeters of large gyres and over the shelf in deeper layers.

The trend in temperature is positive in the whole domain, in particular in the southern Adriatic and within the Eastern Adriatic Coastal Current. The temperature trend is lower but positive in the Jabuka Pit, while being strongly positive at the bottom of the South Adriatic Pit. Salinity trends are also positive, with maximum values off the Po River delta, while having the minimum in the centre of the Southern Adriatic Gyre. Current speed trends are generally patchy, but having some coherent structures, like weakening of the Southern Adriatic Gyre, in particular in deeper layers.

Sea level trend is around 1 cm per decade in the most of the Adriatic Sea, except in the Southern Adriatic where it double the value at the perimeter of the Southern Adriatic Gyre.

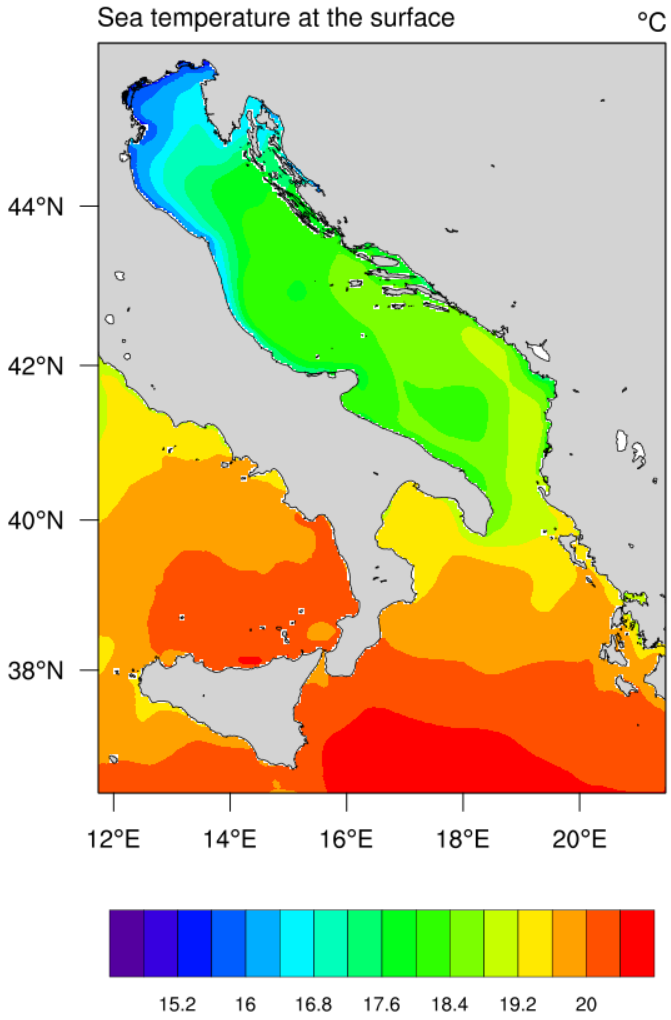

Figure 49. Mean sea surface temperature in the period 1987-2017 as simulated by the AdriSC modelling suite.

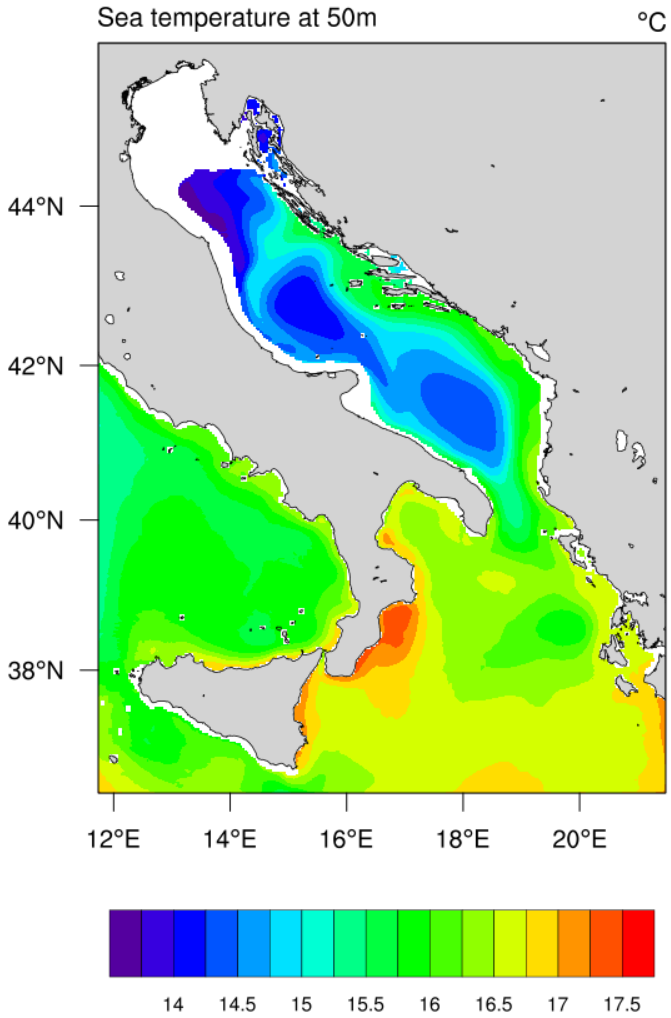

Figure 50. Mean sea temperature at 50 m in the period 1987-2017 as simulated by the AdriSC modelling suite.

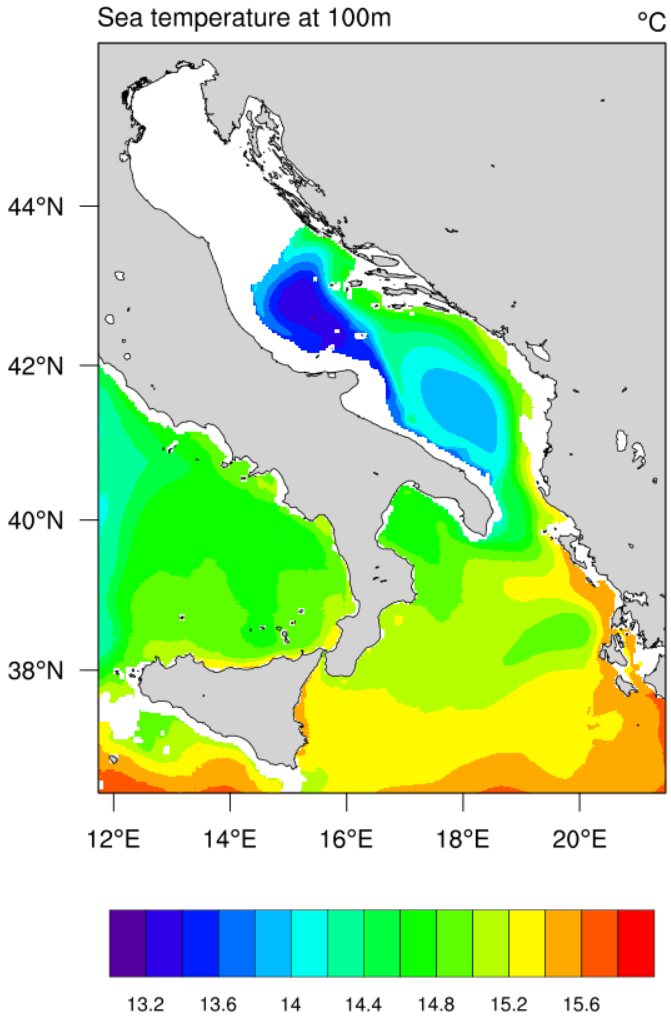

Figure 51. Mean sea temperature at 100 m in the period 1987-2017 as simulated by the AdriSC modelling suite.

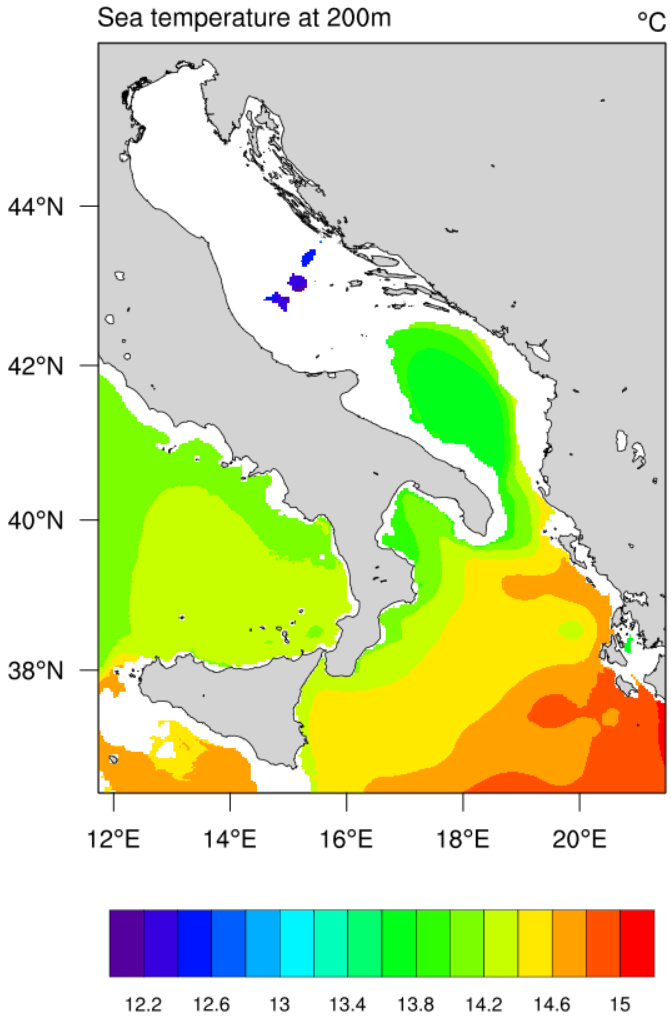

Figure 52. Mean sea temperature at 200 m in the period 1987-2017 as simulated by the AdriSC modelling suite.

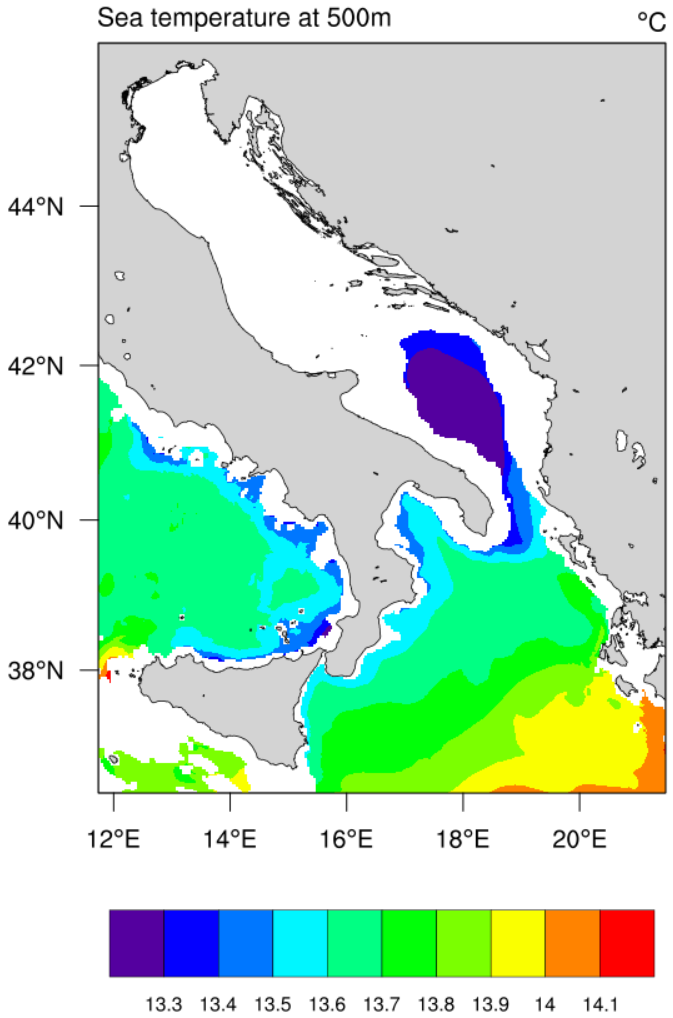

Figure 53. Mean sea temperature at 500 m in the period 1987-2017 as simulated by the AdriSC modelling suite.

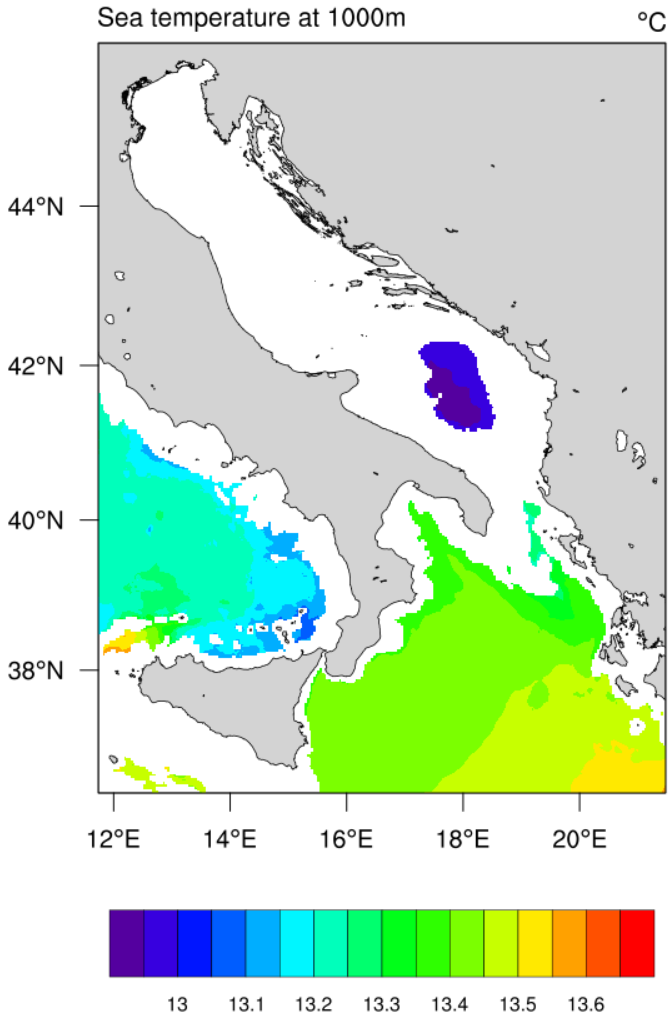

Figure 54. Mean sea temperature at 1000 m in the period 1987-2017 as simulated by the AdriSC modelling suite.

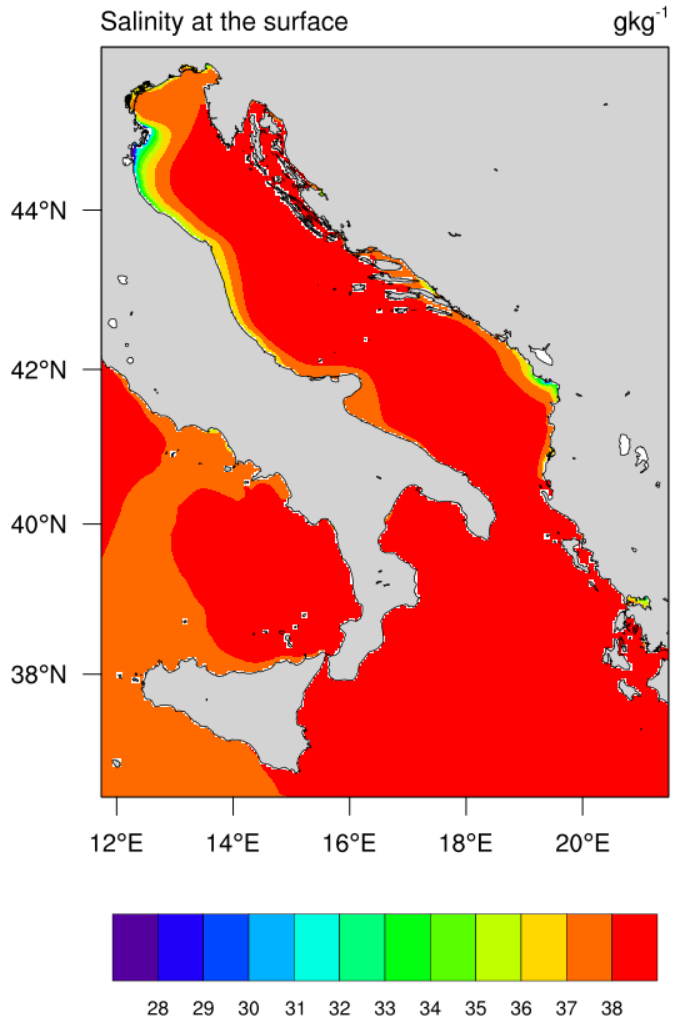

Figure 55. Mean surface salinity in the period 1987-2017 as simulated by the AdriSC modelling suite.

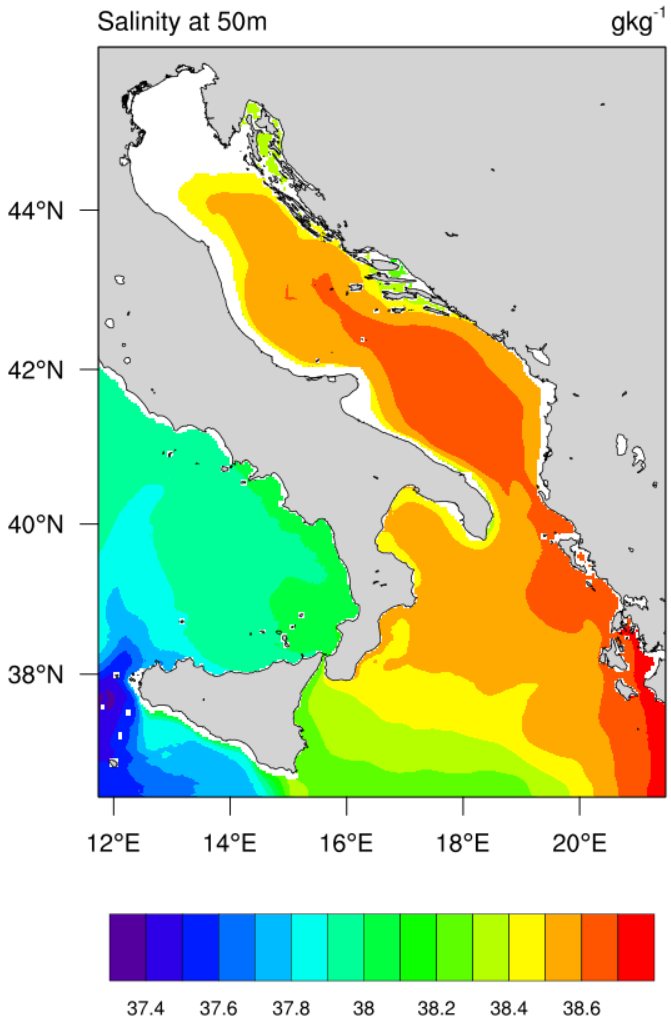

Figure 56. Mean salinity at 50 m in the period 1987-2017 as simulated by the AdriSC modelling suite.

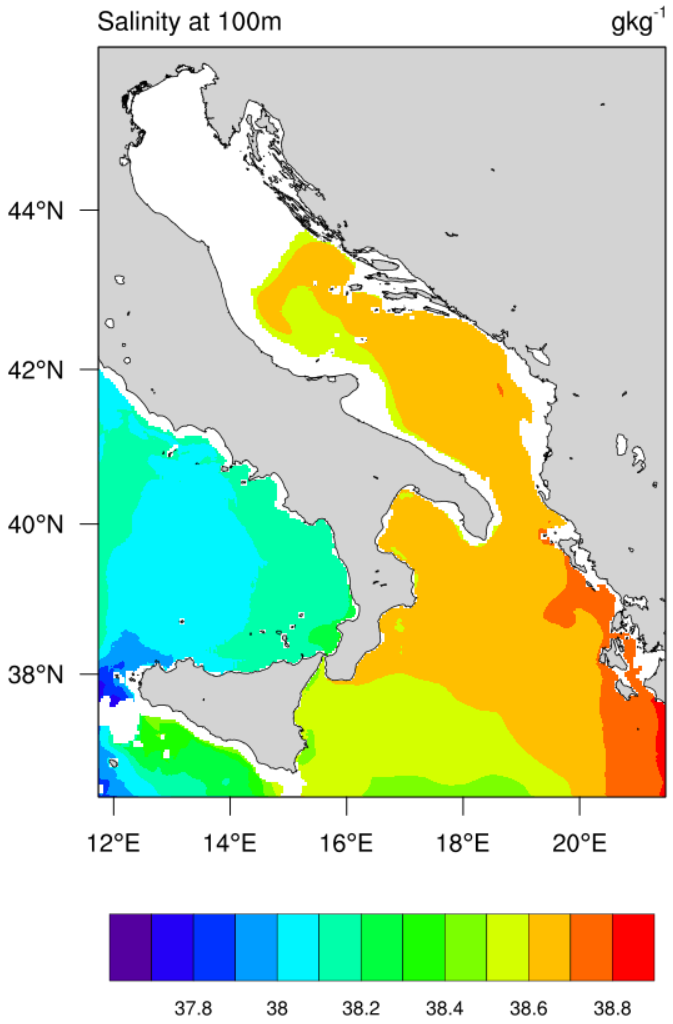

Figure 57. Mean salinity at 100 m in the period 1987-2017 as simulated by the AdriSC modelling suite.

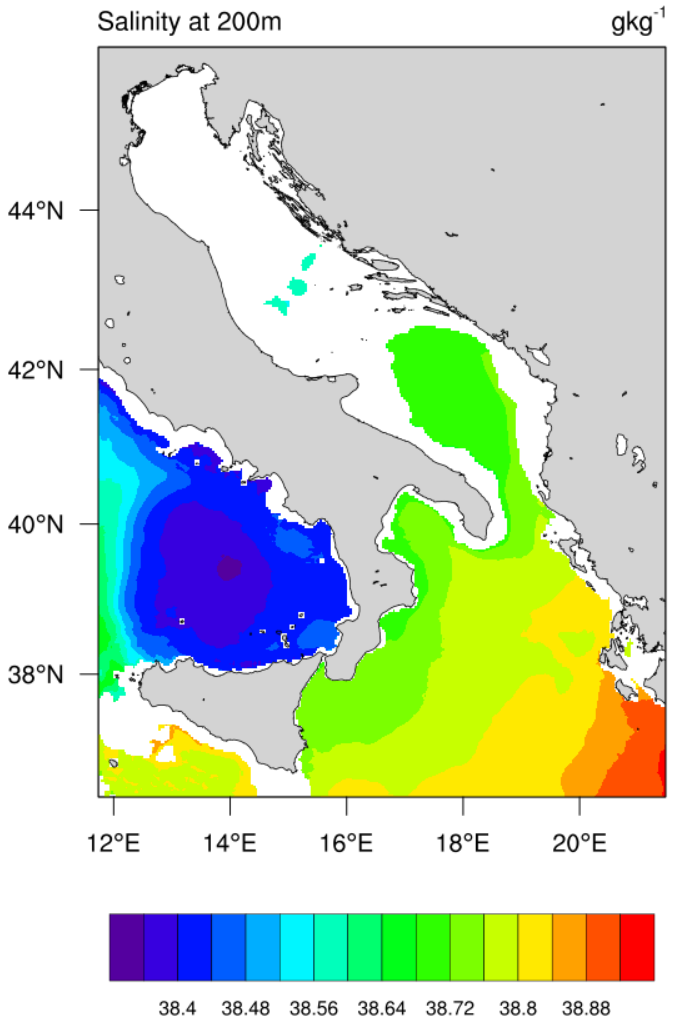

Figure 58. Mean salinity at 200 m in the period 1987-2017 as simulated by the AdriSC modelling suite.

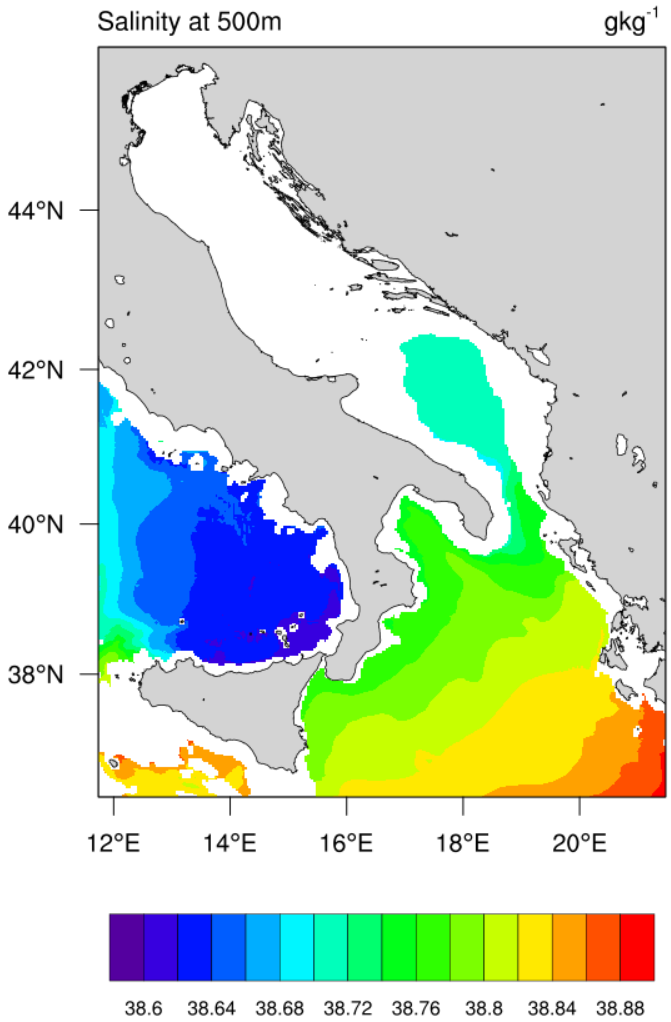

Figure 59. Mean salinity at 500 m in the period 1987-2017 as simulated by the AdriSC modelling suite.

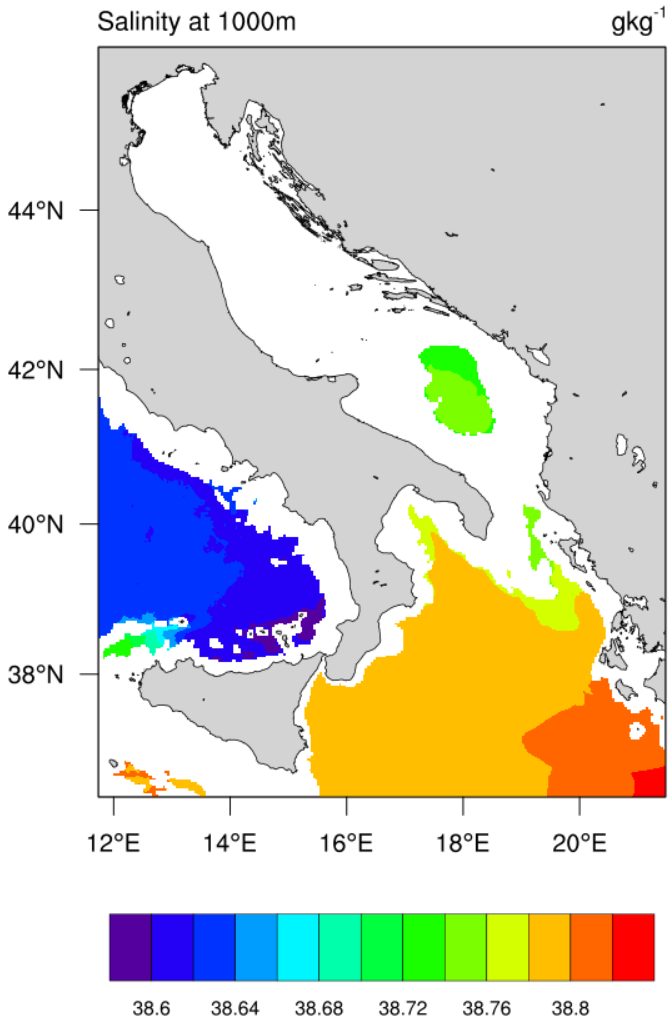

Figure 60. Mean salinity at 1000 m in the period 1987-2017 as simulated by the AdriSC modelling suite.

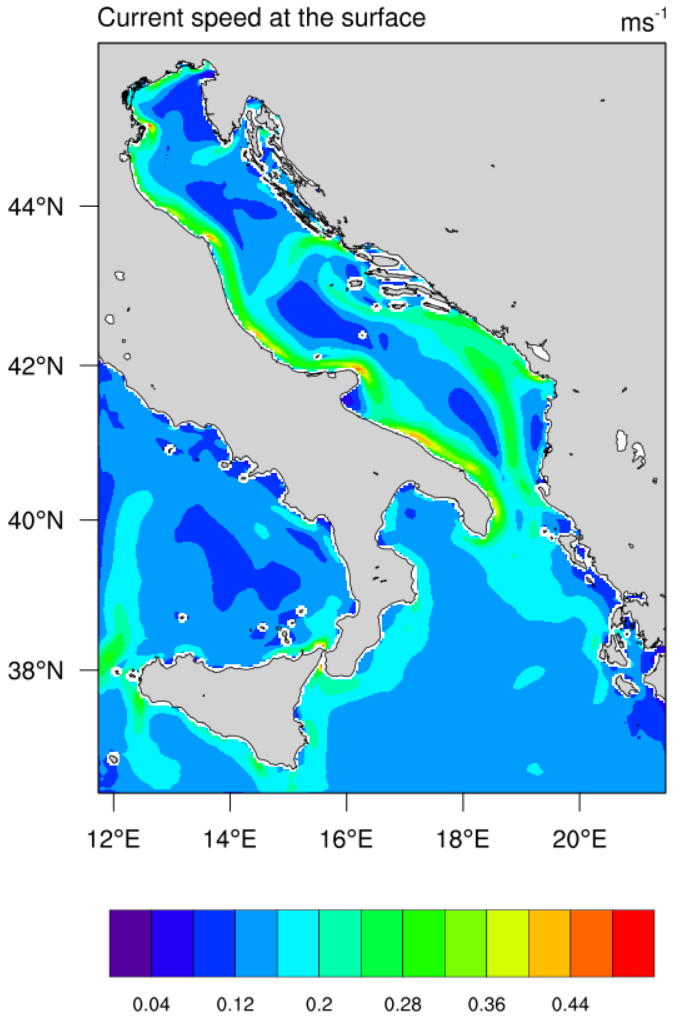

Figure 61. Mean surface current speed in the period 1987-2017 as simulated by the AdriSC modelling suite.

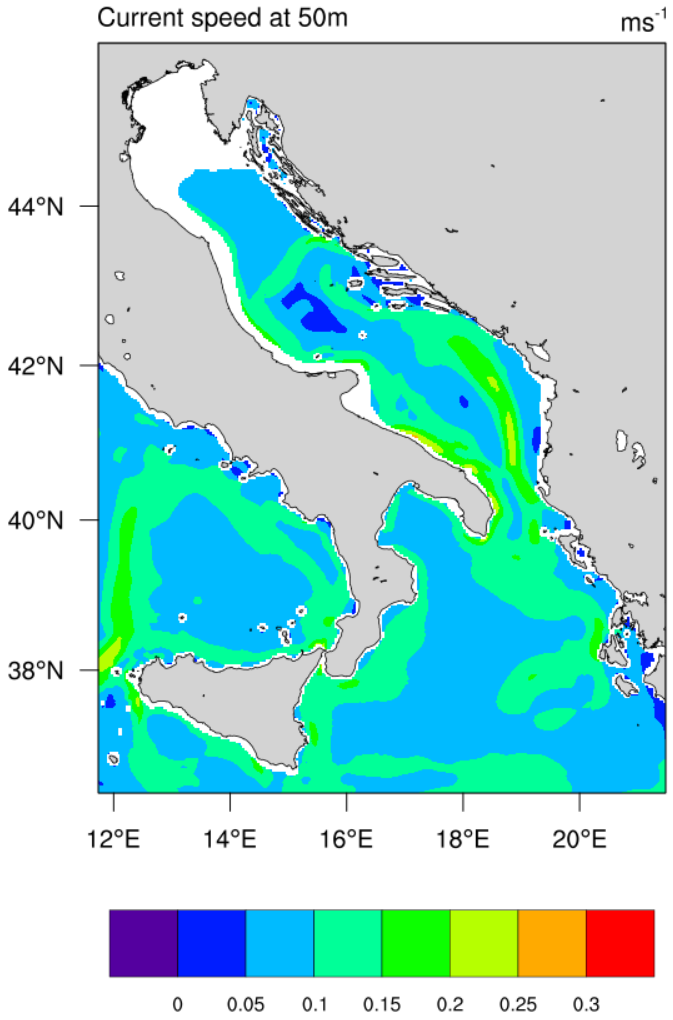

Figure 62. Mean current speed at 50 m in the period 1987-2017 as simulated by the AdriSC modelling suite.

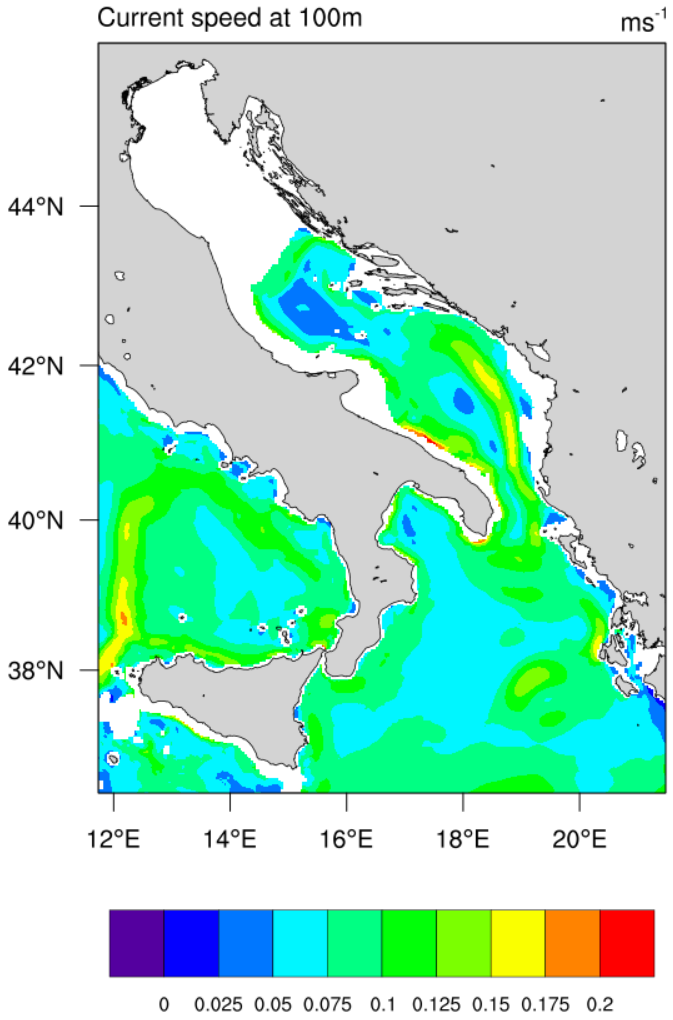

Figure 63. Mean current speed at 100 m in the period 1987-2017 as simulated by the AdriSC modelling suite.

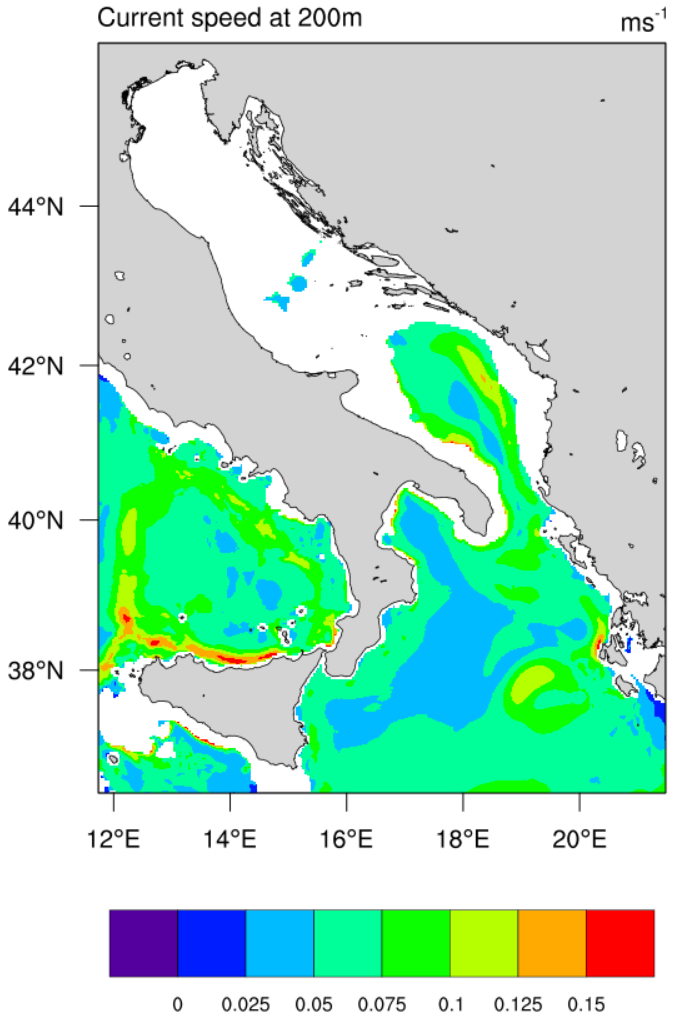

Figure 64. Mean current speed at 200 m in the period 1987-2017 as simulated by the AdriSC modelling suite.

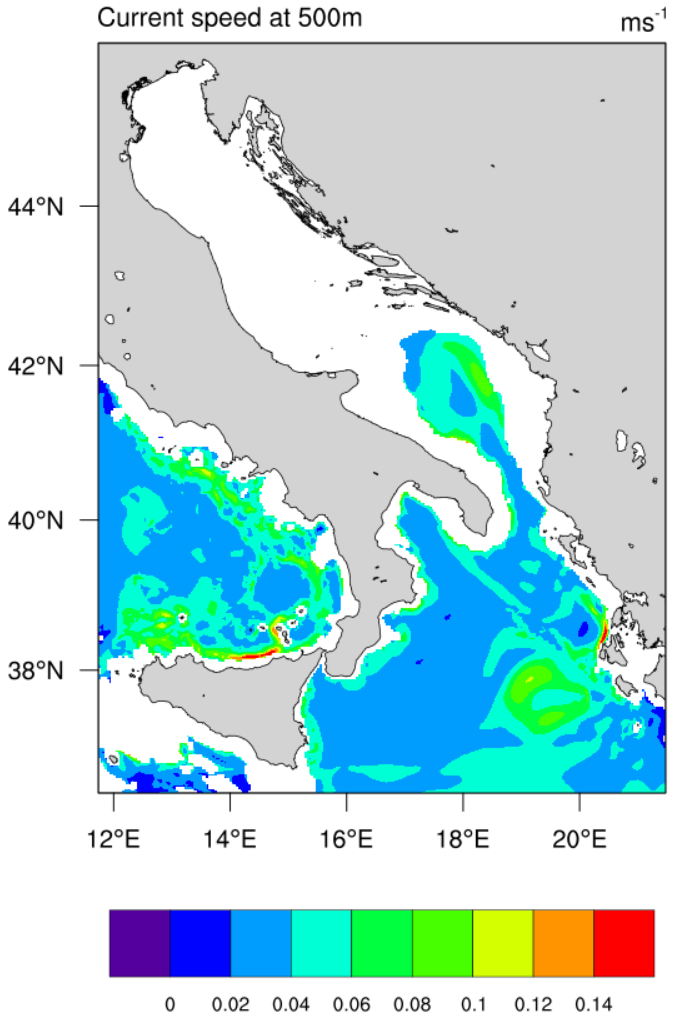

Figure 65. Mean current speed at 500 m in the period 1987-2017 as simulated by the AdriSC modelling suite.

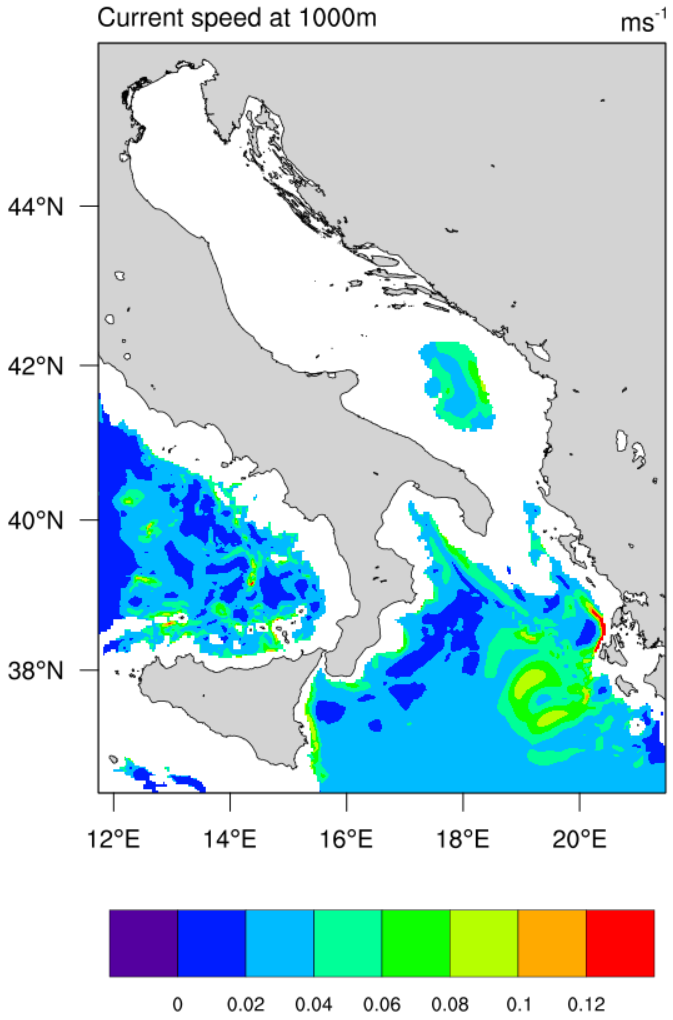

Figure 66. Mean current speed at 1000 m in the period 1987-2017 as simulated by the AdriSC modelling suite.

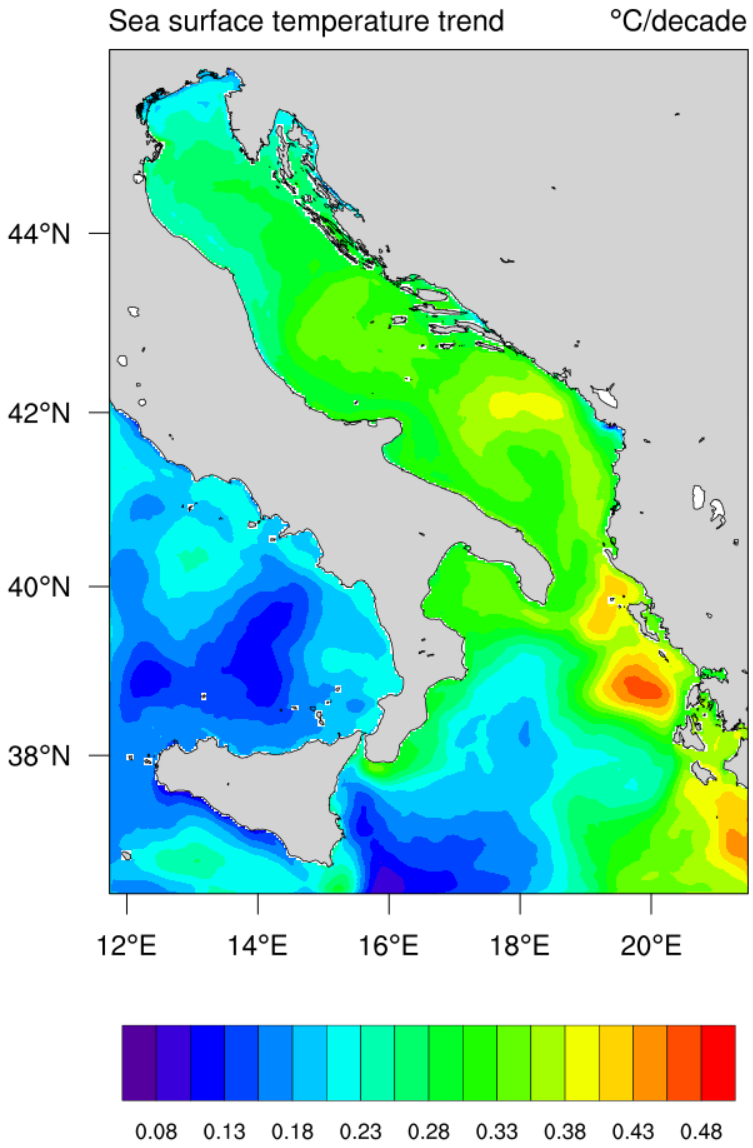

Figure 67. Mean surface temperature trend in the period 1987-2017 as simulated by the AdriSC modelling suite.

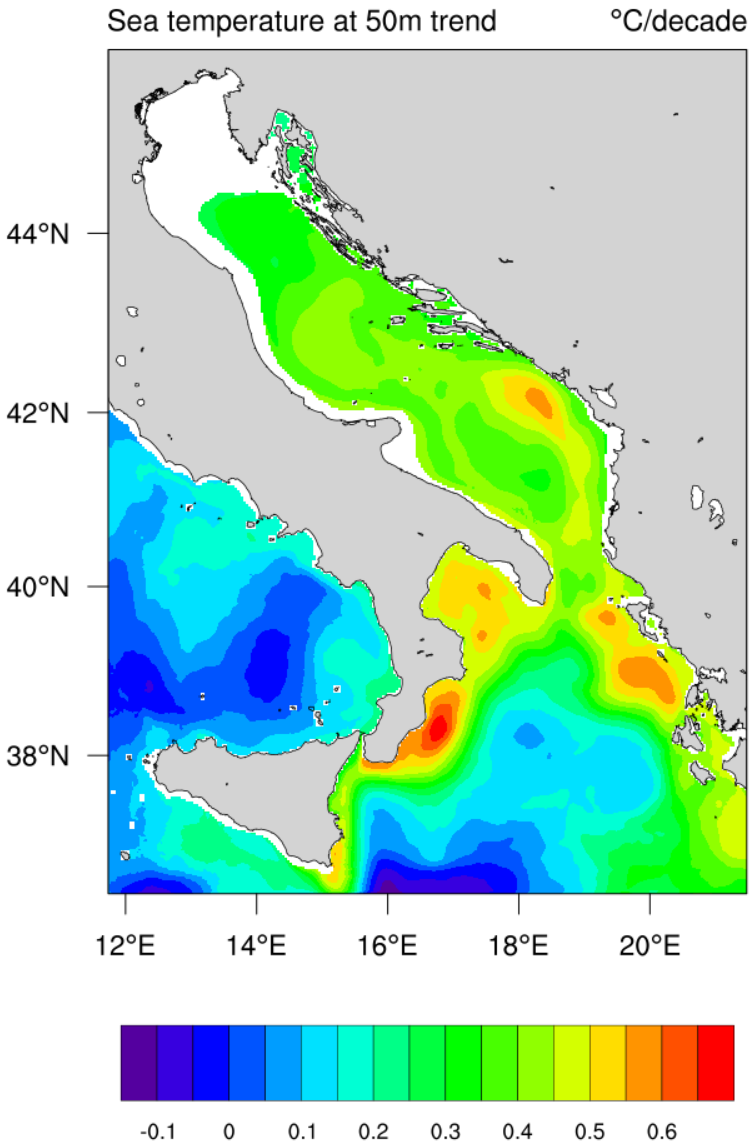

Figure 68. Mean temperature trend at 50 m in the period 1987-2017 as simulated by the AdriSC modelling suite.

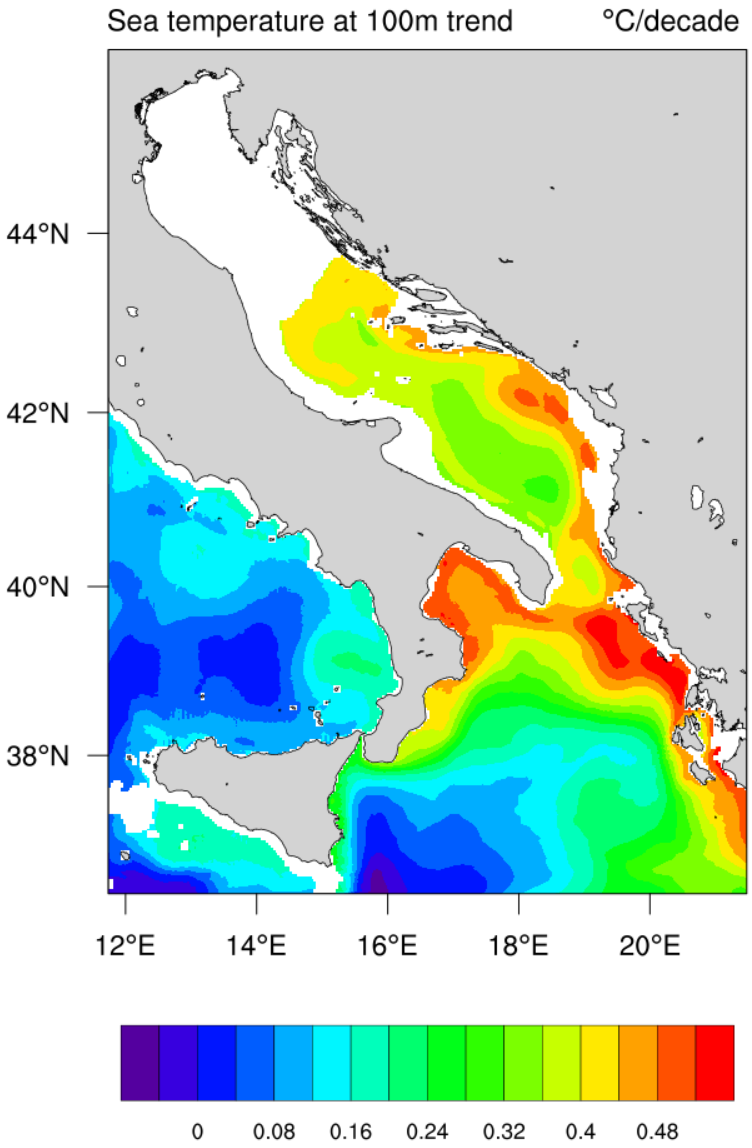

Figure 69. Mean temperature trend at 100 m in the period 1987-2017 as simulated by the AdriSC modelling suite.

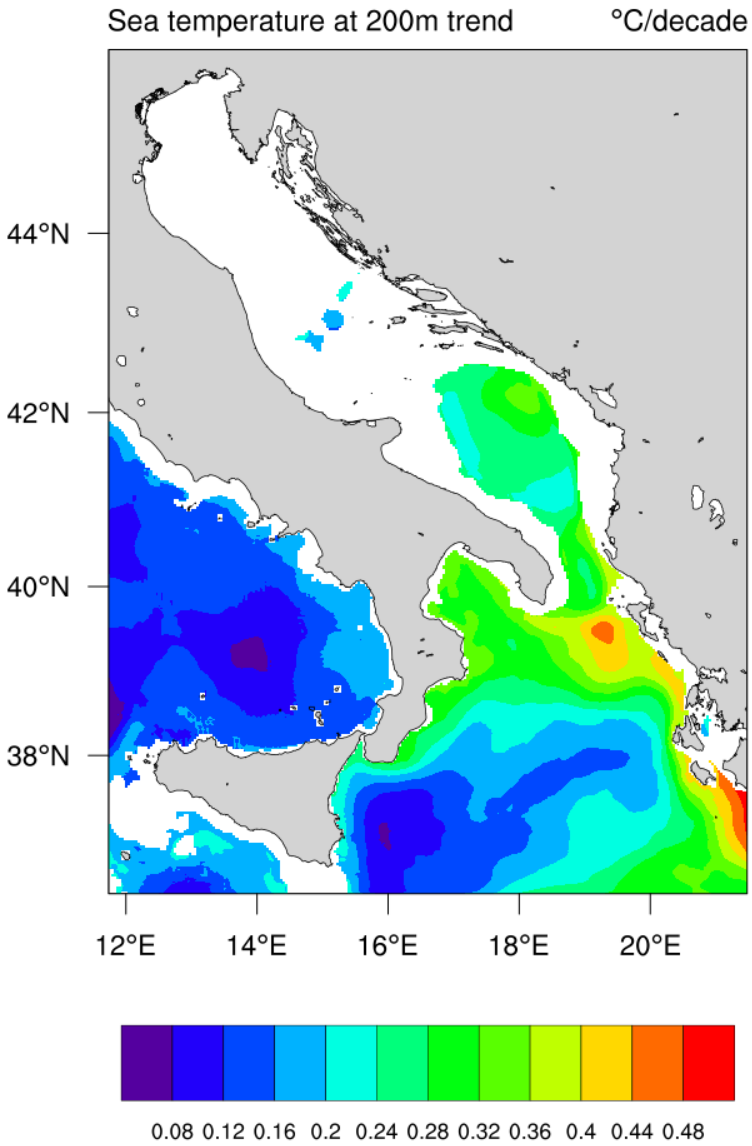

Figure 70. Mean temperature trend at 200 m in the period 1987-2017 as simulated by the AdriSC modelling suite.

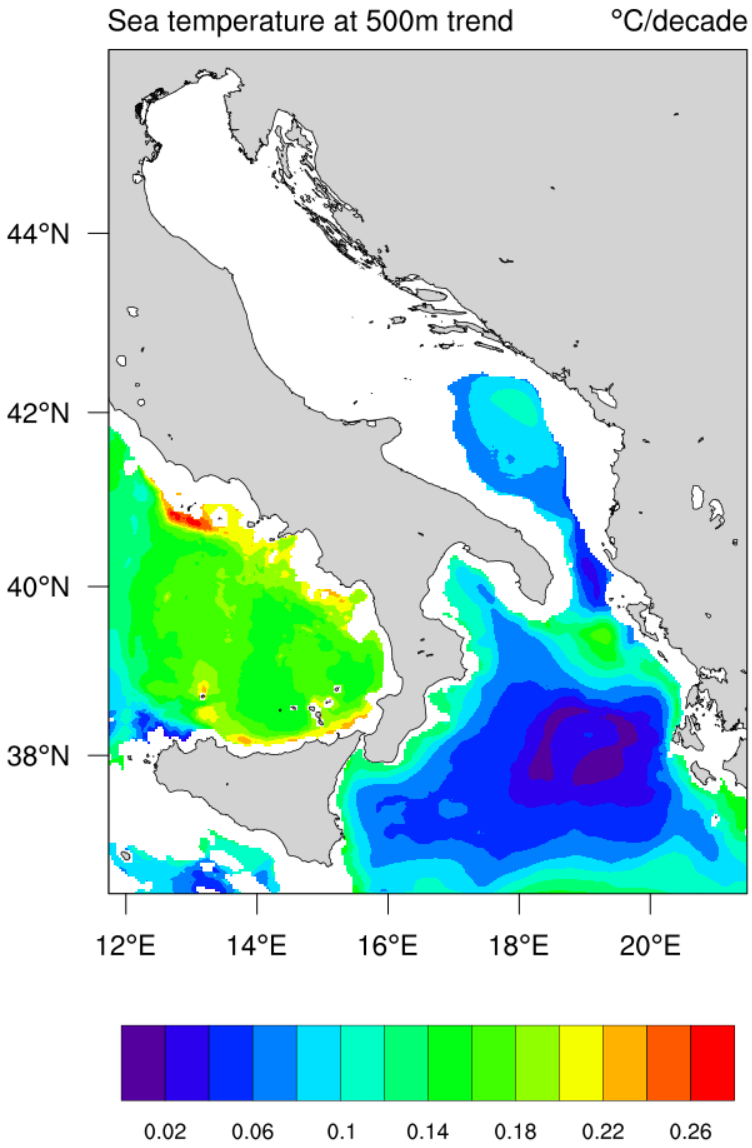

Figure 71. Mean temperature trend at 500 m in the period 1987-2017 as simulated by the AdriSC modelling suite.

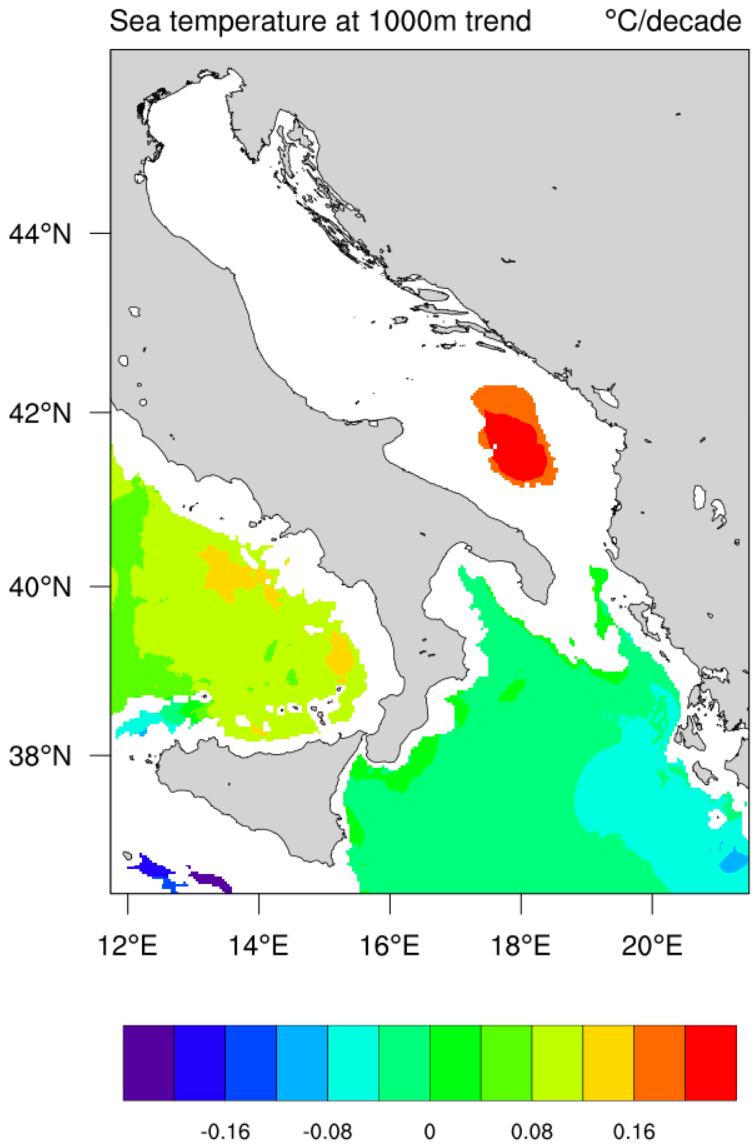

Figure 72. Mean temperature trend at 1000 m in the period 1987-2017 as simulated by the AdriSC modelling suite.

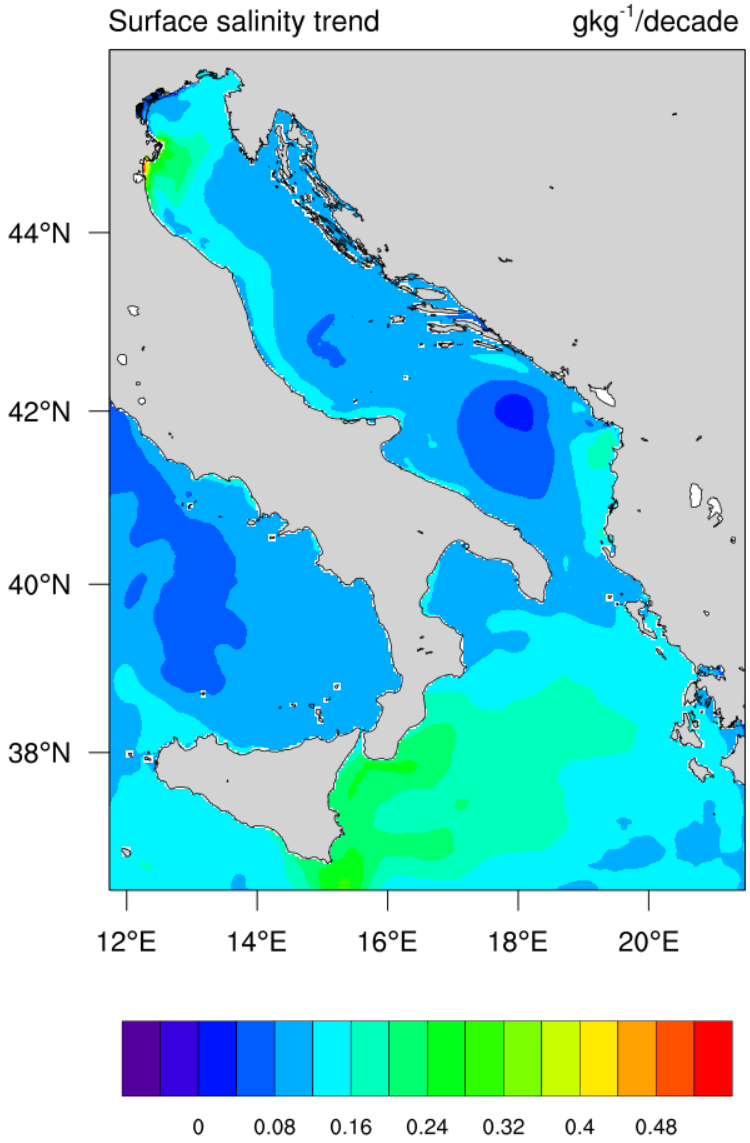

Figure 73. Mean surface salinity trend in the period 1987-2017 as simulated by the AdriSC modelling suite.

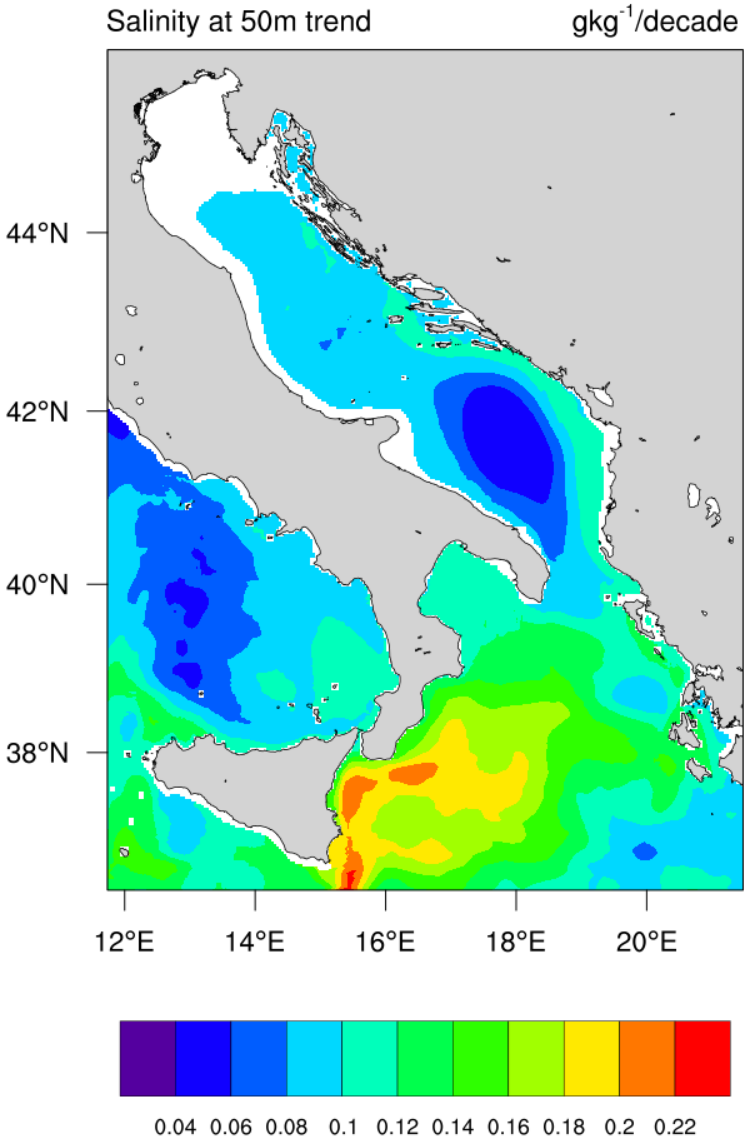

Figure 74. Mean salinity trend at 50 m in the period 1987-2017 as simulated by the AdriSC modelling suite.

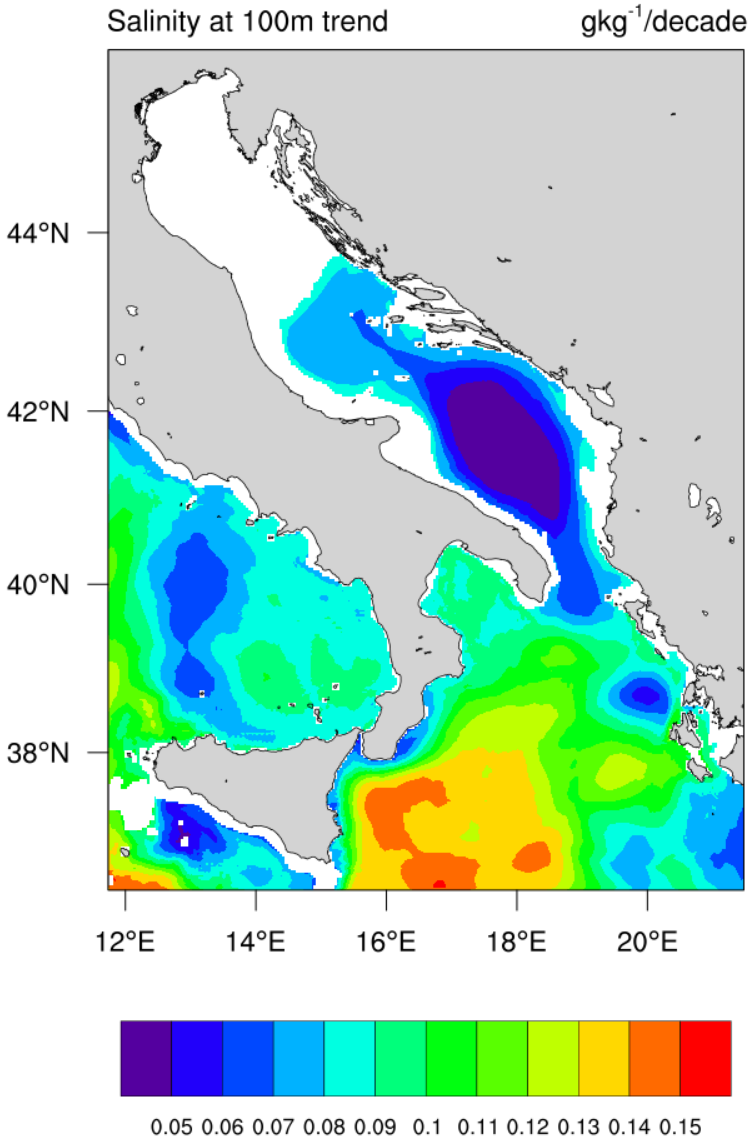

Figure 75. Mean salinity trend at 100 m in the period 1987-2017 as simulated by the AdriSC modelling suite.

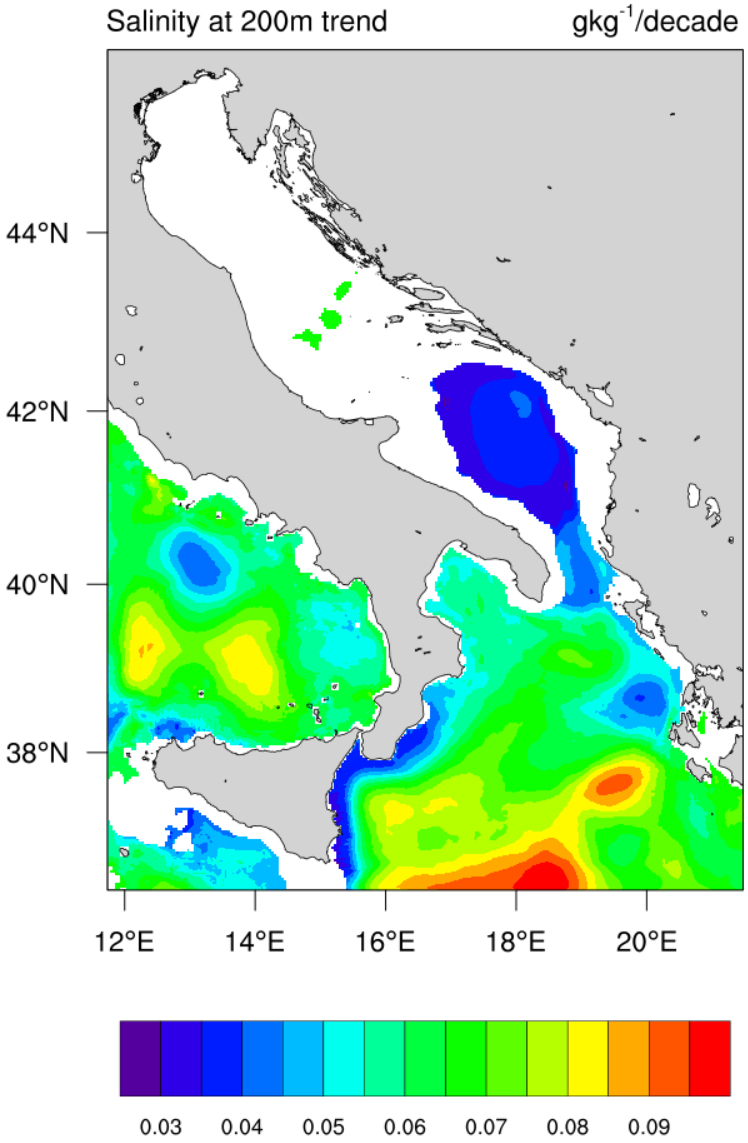

Figure 76. Mean salinity trend at 200 m in the period 1987-2017 as simulated by the AdriSC modelling suite.

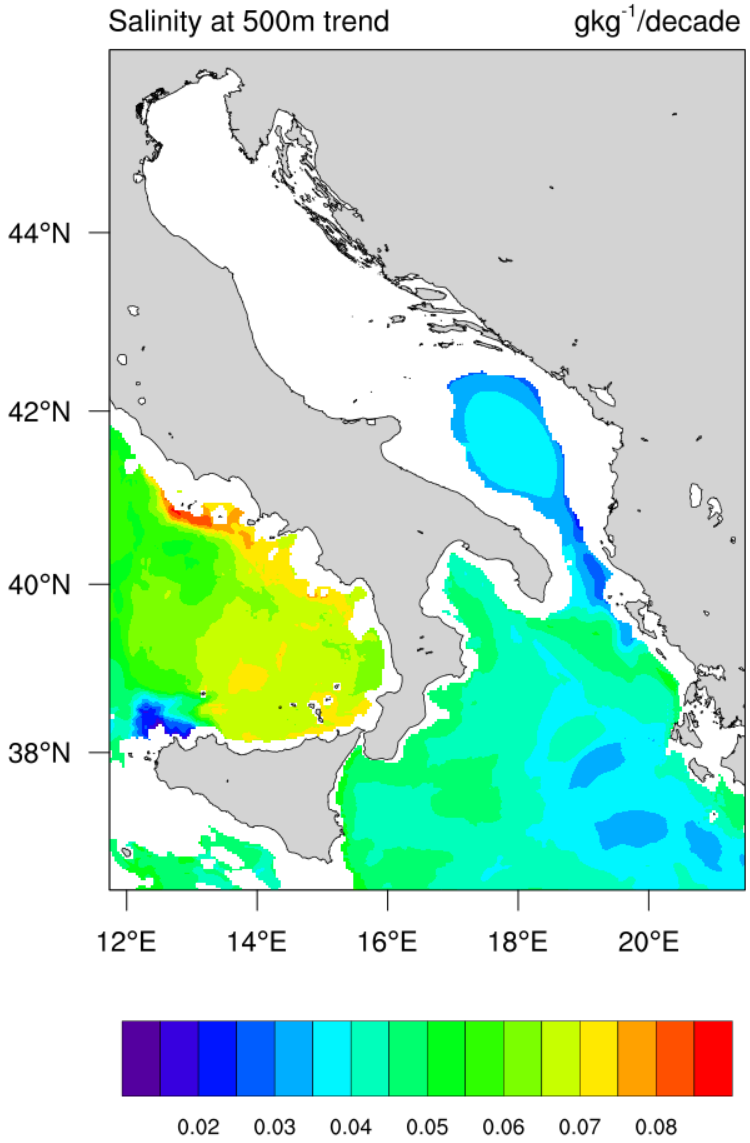

Figure 77. Mean salinity trend at 500 m in the period 1987-2017 as simulated by the AdriSC modelling suite.

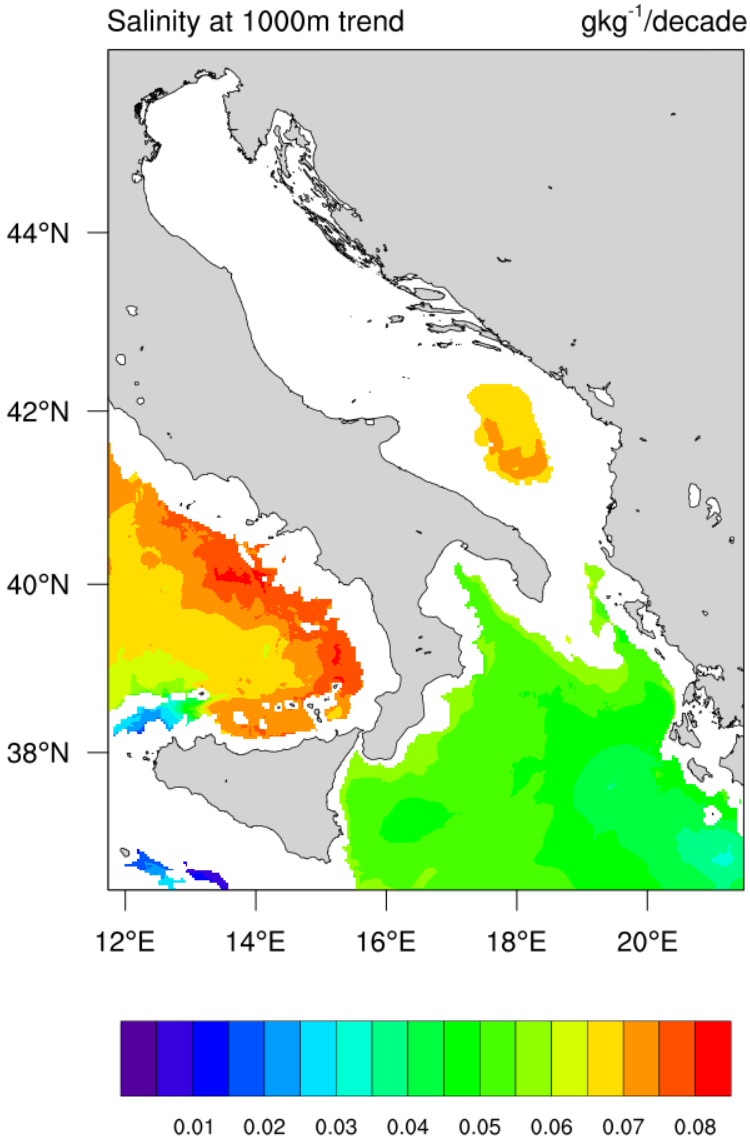

Figure 78. Mean salinity trend at 1000 m in the period 1987-2017 as simulated by the AdriSC modelling suite.

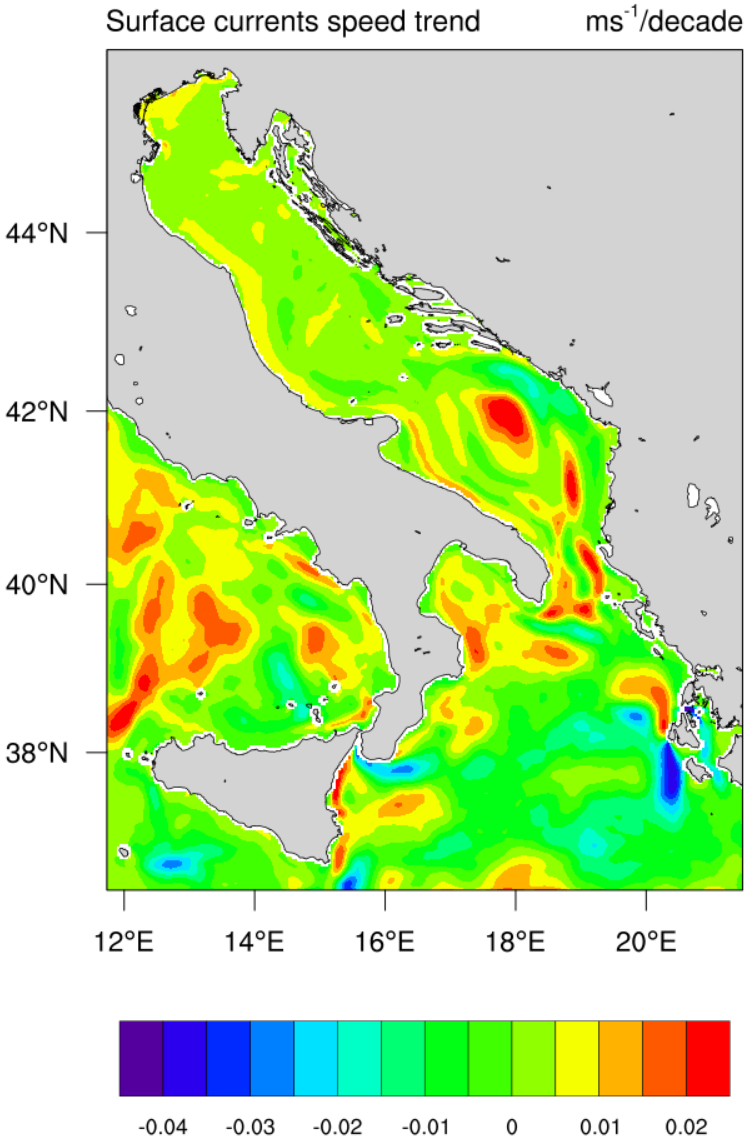

Figure 79. Mean surface current speed trend in the period 1987-2017 as simulated by the AdriSC modelling suite.

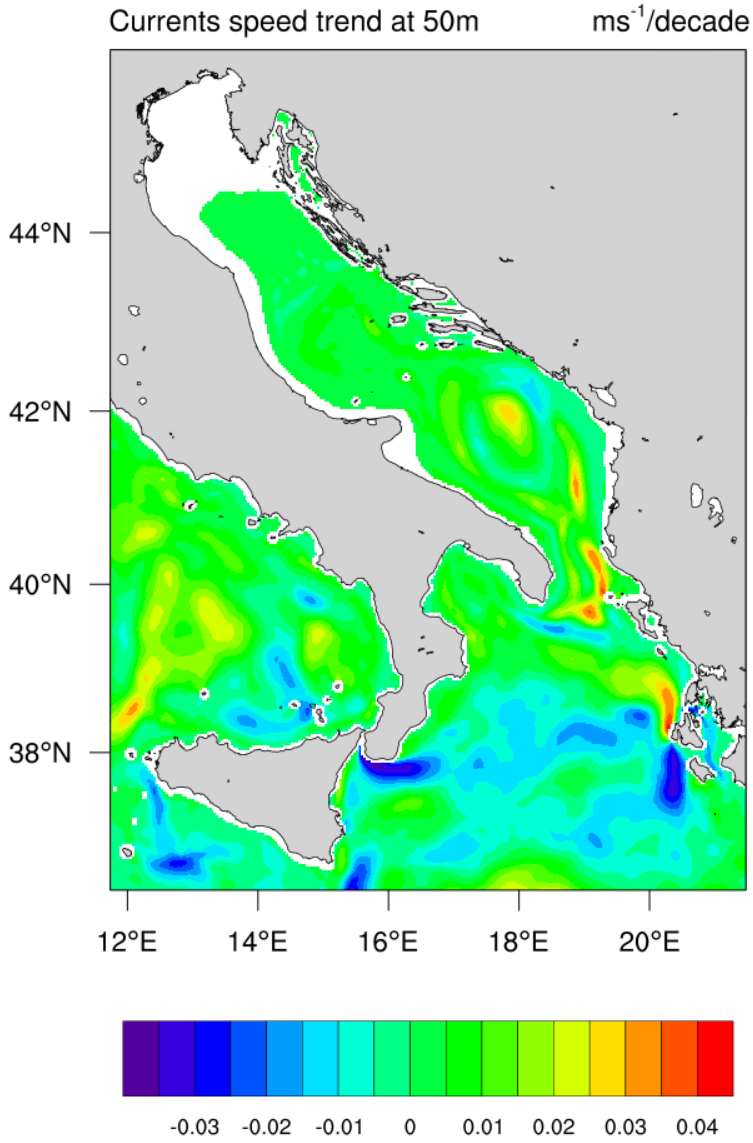

Figure 80. Mean current speed trend at 50 m in the period 1987-2017 as simulated by the AdriSC modelling suite.

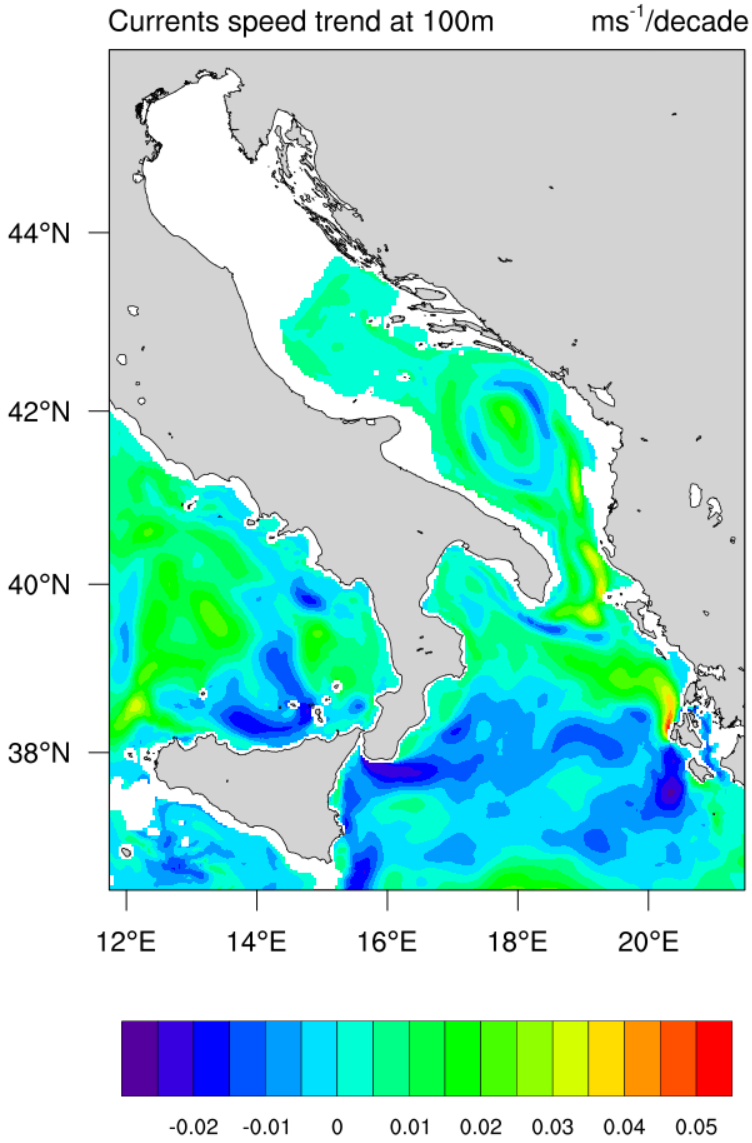

Figure 81. Mean current speed trend at 100 m in the period 1987-2017 as simulated by the AdriSC modelling suite.

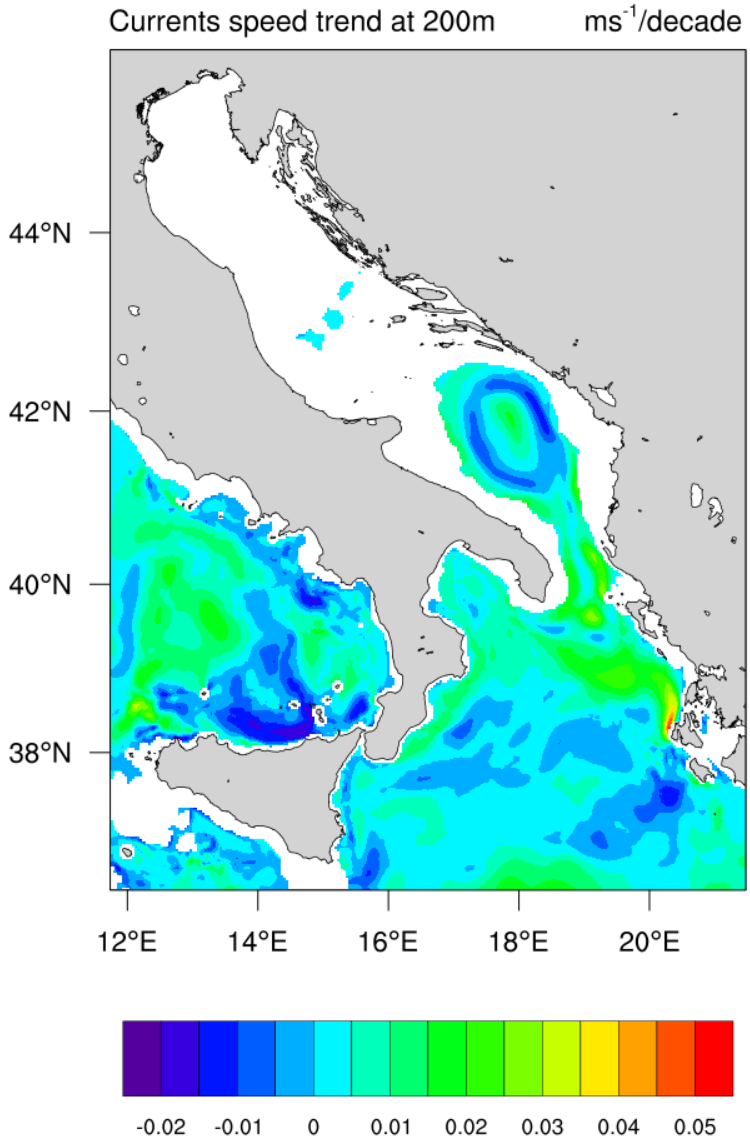

Figure 82. Mean current speed trend at 200 m in the period 1987-2017 as simulated by the AdriSC modelling suite.

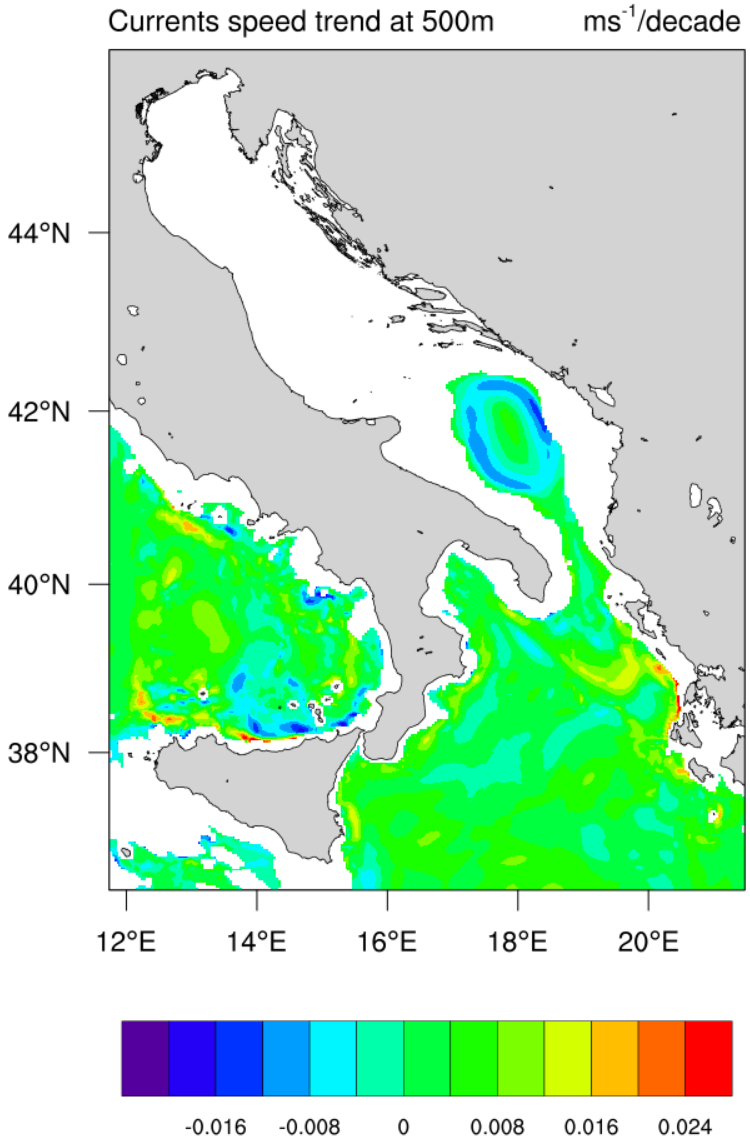

Figure 83. Mean current speed trend at 500 m in the period 1987-2017 as simulated by the AdriSC modelling suite.

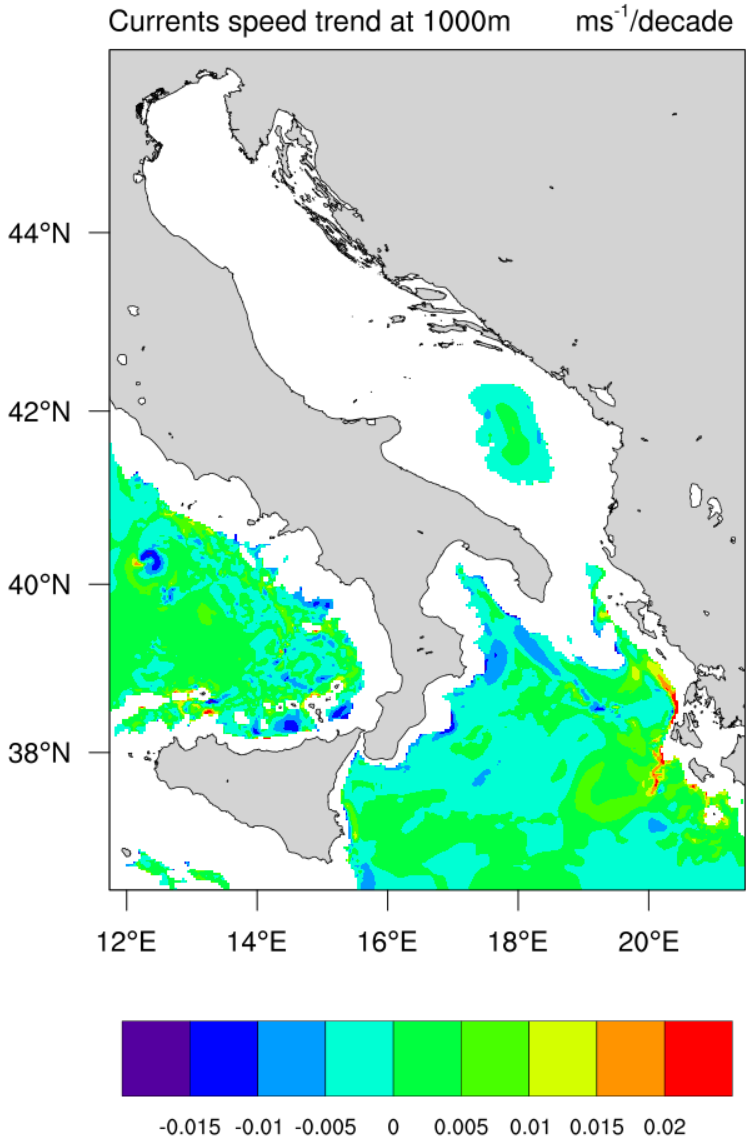

Figure 84. Mean current speed trend at 1000 m in the period 1987-2017 as simulated by the AdriSC modelling suite.

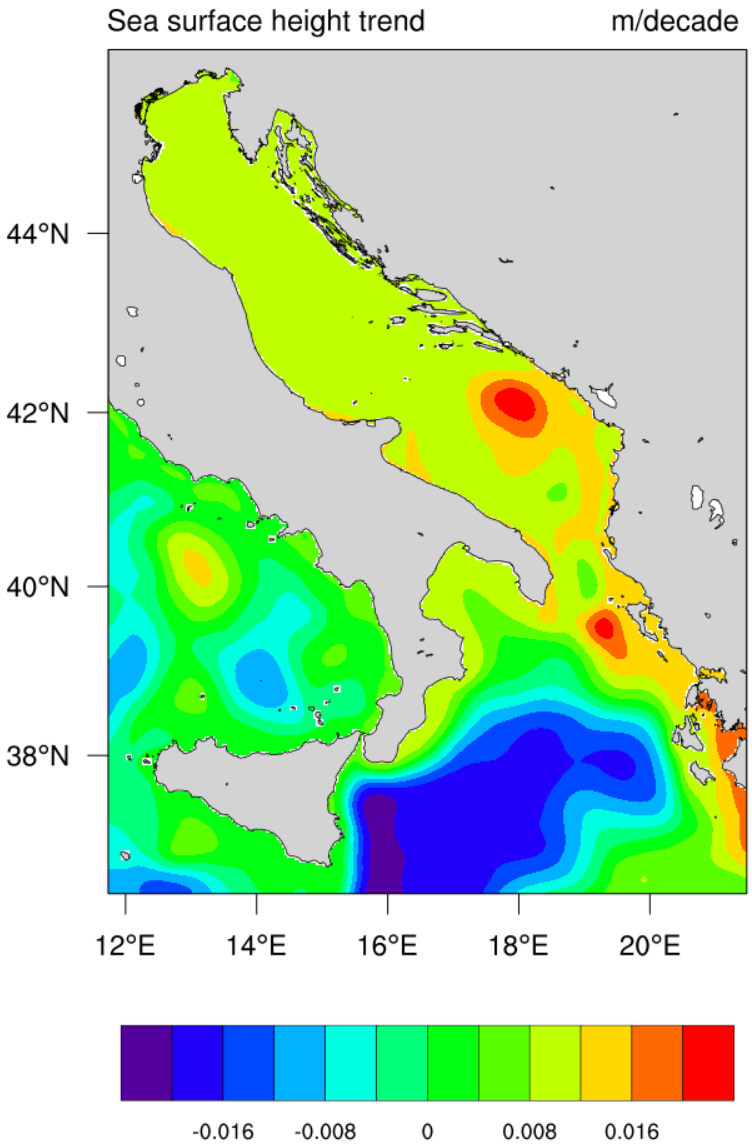

Figure 85. Mean sea surface height trend in the period 1987-2017 as simulated by the AdriSC modelling suite.

3.3.4. Towards a numerical ocean climate projection in a severe climate change scenario

In order to convey the present knowledge of the Adriatic thermohaline and circulation variability into the prediction of future dynamics in response to climate change, a long-term ocean climate modelling effort is currently in progress. This task is part of the upcoming Activity 4.1 (Evolution of key hydrological and physical quantities and energy fluxes) and here briefly described in order to clarify the conceptual link between the information collected in the present assessment and the envisaged projections of future scenarios.

The work in progress consists of a multi-decadal implementation of ROMS (Regional Ocean Modeling System) over the Adriatic Sea, continuously spanning 113 years from 1987 to 2100 and describing the future conditions under the RCP8.5 climate change scenario. The domain is discretized into a structured orthogonal curvilinear grid with horizontal resolution ranging between 2 (in the north-west) and 8 (in the south-east) kilometres, and a vertical discretization into 15 sigma terrain-following levels. Initial conditions have been taken from the 1/16° Mediterranean Forecasting System physical reanalysis provided by the Copernicus Marine Environment Monitoring Service (CMEMS). The atmospheric forcing and the boundary conditions have been obtained from the MED-CORDEX dataset. For the former, 6-hourly fields from the SMHI-RCA4 model (a stand-alone atmosphere simulation for which a preliminary assessment has shown a good capability of capturing the main features of wind climate over the basin) have been interpolated on the model grid, whereas the latter have been prescribed at the south-eastern boundary (Otranto Strait) as monthly temperature and salinity anomaly profiles from the General Circulation Model CMCC-CM.

The analysis of the results will focus on the identification of interannual variability and long-term trends of some key quantities (e.g. sea temperature and salinity, ocean heat content) and processes (e.g. storm surge, dense water production), as well as on ocean climate statistics performed over 30-year periods. In particular, the first period (1987-2016) will be used as a control dataset for model validation, to be carried out against the observational data and model reanalysis presented in this Deliverable, while future periods will be identified in order to address both the scientific challenges and open questions concerning climate change effects in the Adriatic Sea and the information requirements for coastal planning and management purposes.

4. CLIMATE PROCESSES AND VARIABLES AT PILOT SITES

4.1. Po River delta site

4.1.1. Assessment of atmospheric variables and processes

Here the annual time series of temperature at 2 m and precipitation will be analysed, plus the wind rose, extracted for the area of Po River delta site and coming from the AdriSC climate simulation (1987-2017). The analysis accompanies the fields the modelled atmospheric fields described in Section 2.3.

Annual values of temperature at 2 m range from 11 to 13 °C (Fig. 86), where the last value is reached in 2014. Clear temperature trend can be seen in the series, with the rate of approx. 0.2 °C per decade. The warming trend may be seen in all seasons (Fig. 87), with winter mean temperatures ranging between 4 and 7 °C, while summer mean temperatures are ranging from 18 to 20 °C.

The precipitation rate (Fig. 88) is changing between 1 and 3 mm/day, i.e. between 400 and 1100 mm per year. The precipitation rate is maximal during autumn (Fig. 89), when it might reach 6 mm/day, while the minimum precipitation rate is achieved during winter and spring, when it might go down to 0.4 mm/day, or about 40 mm per season.

The wind rose (Fig. 90) denotes the strongest winds from northeast, which are resembling bora conditions and the jet coming from the Golfo di Trieste. However, the most frequency, but weak, winds are blowing from west, along the Po Valley.

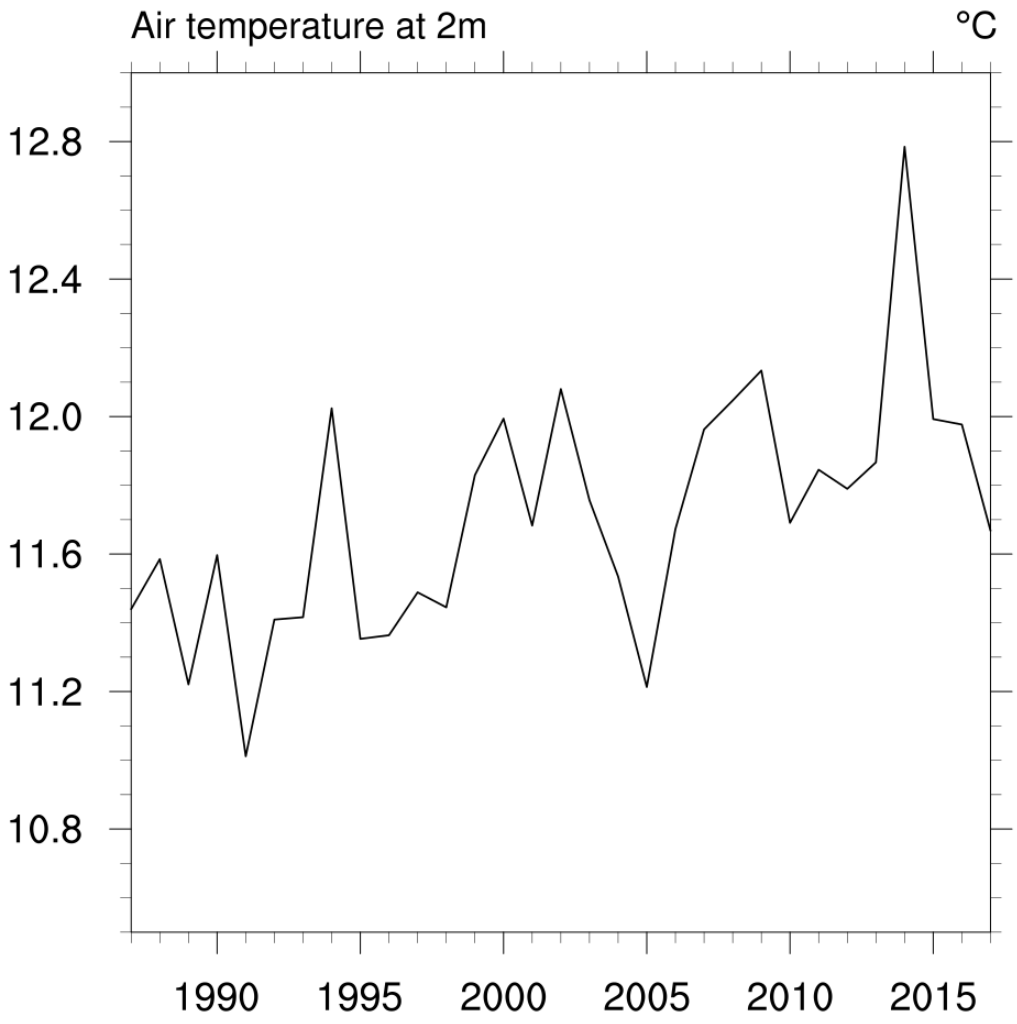

Figure 86. Annual air temperature at 2 m time series in the period 1987-2017 at the Po River delta site as simulated by the AdriSC modelling suite.

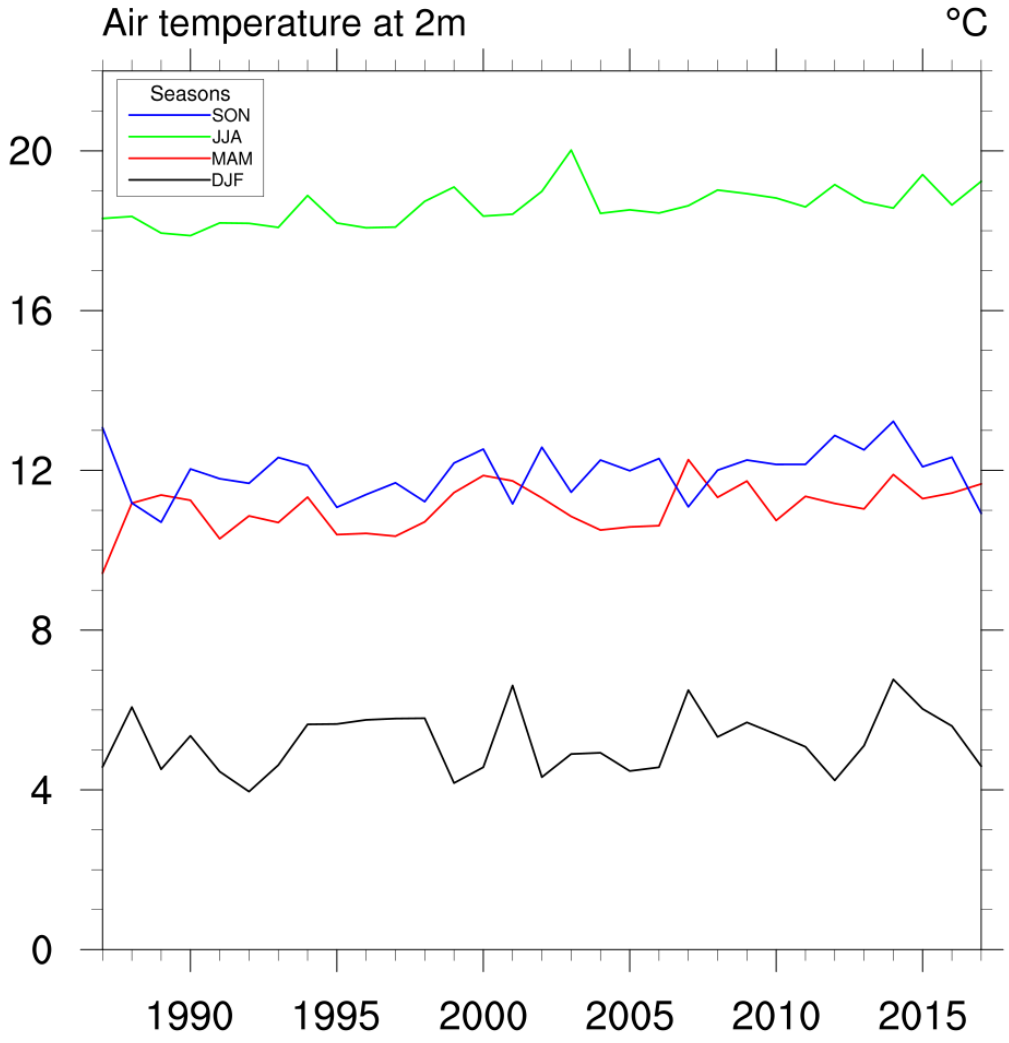

Figure 87. Seasonal air temperature at 2 m time series in the period 1987-2017 at the Po River delta site as simulated by the AdriSC modelling suite.

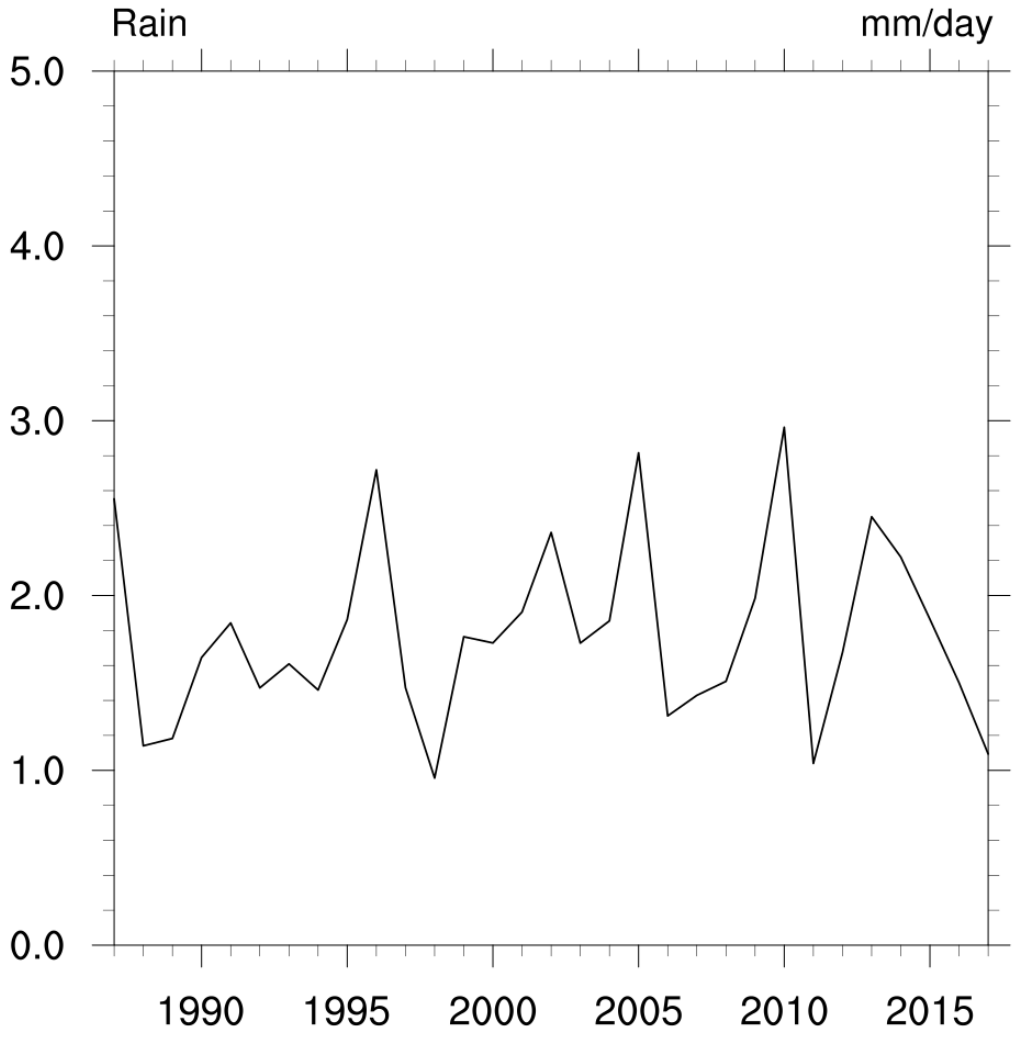

Figure 88. Annual precipitation time series in the period 1987-2017 at the Po River delta site as simulated by the AdriSC modelling suite.

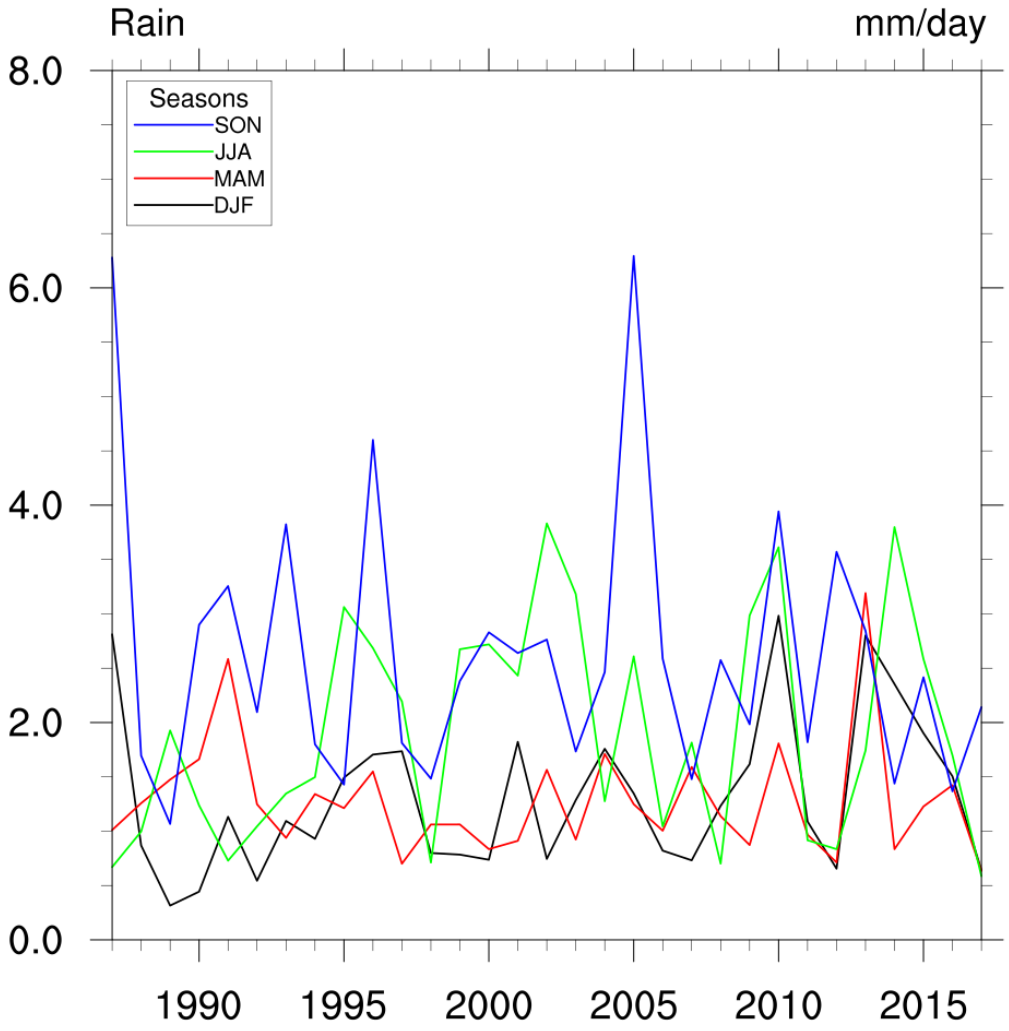

Figure 89. Seasonal precipitation rate time series in the period 1987-2017 at the Po River delta site as simulated by the AdriSC modelling suite.

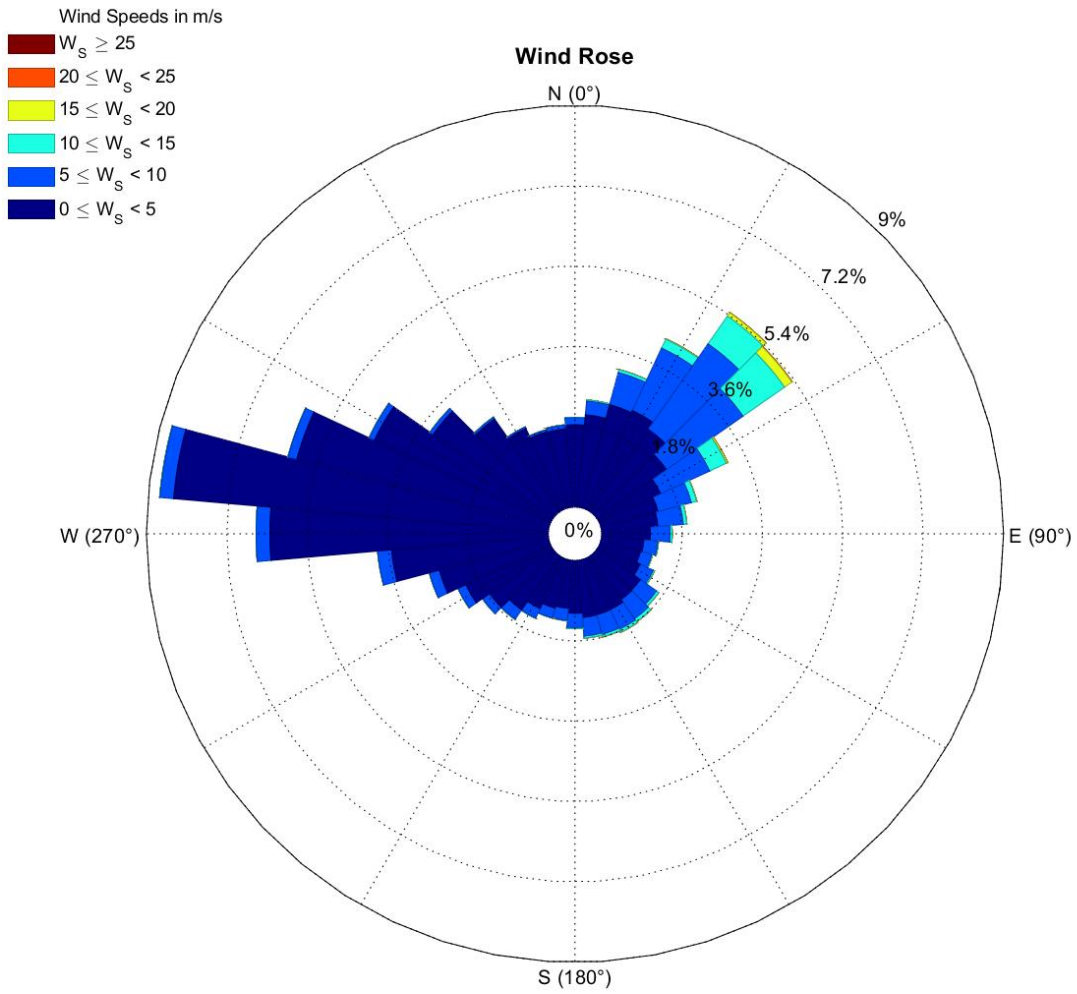

Figure 90. Wind rose at the Po River delta site as simulated by the AdriSC modelling suite (1987-2017).

4.1.2. Assessment of oceanic variables and processes

Off the Po River delta, the mean annual temperature (Fig. 91) has values rising from 15.5 °C at the beginning of the AdriSC simulation to 16-17 °C at the end of the AdriSC simulation. The positive trends are strongest in spring and autumn periods (Fig. 92). Sea surface salinity has strong interannual variability, ranging from 31 to 35, with lowest values in spring and highest in summer and autumn (Figs. 93-94). Sea level constantly rose in the considered period (Fig. 95), yet with quite strong interannual variability.

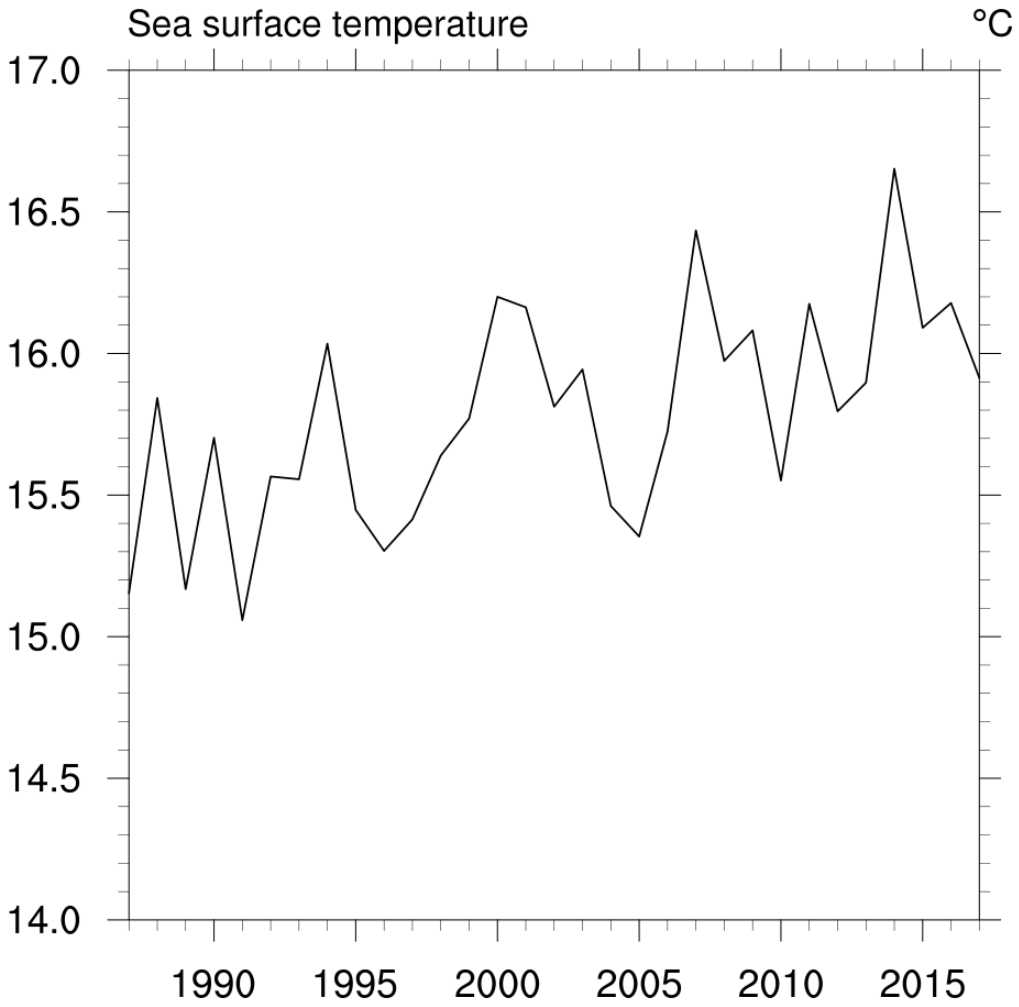

Figure 91. Annual sea surface temperature time series in the period 1987-2017 at the Po River delta site as simulated by the AdriSC modelling suite.

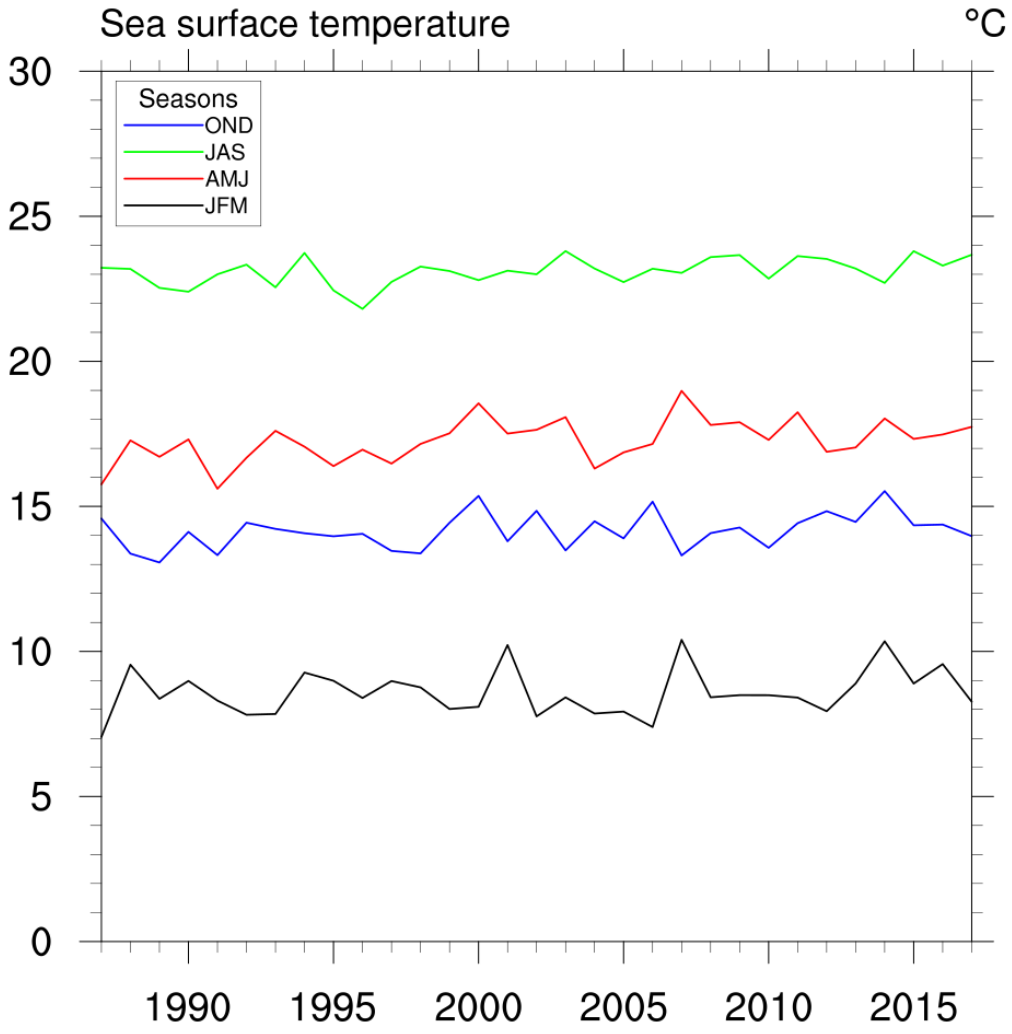

Figure 92. Seasonal sea surface temperature time series in the period 1987-2017 at the Po River delta site as simulated by the AdriSC modelling suite.

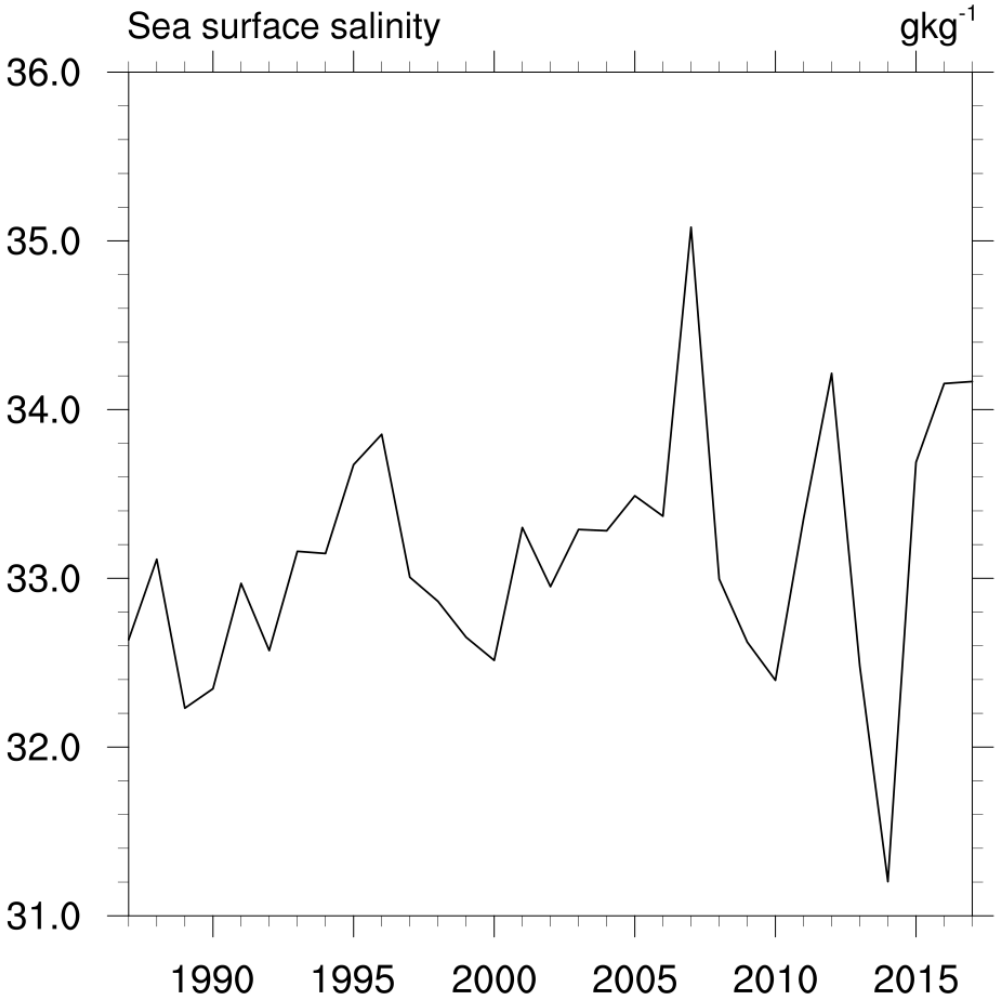

Figure 93. Annual surface salinity time series in the period 1987-2017 at the Po River delta site as simulated by the AdriSC modelling suite.

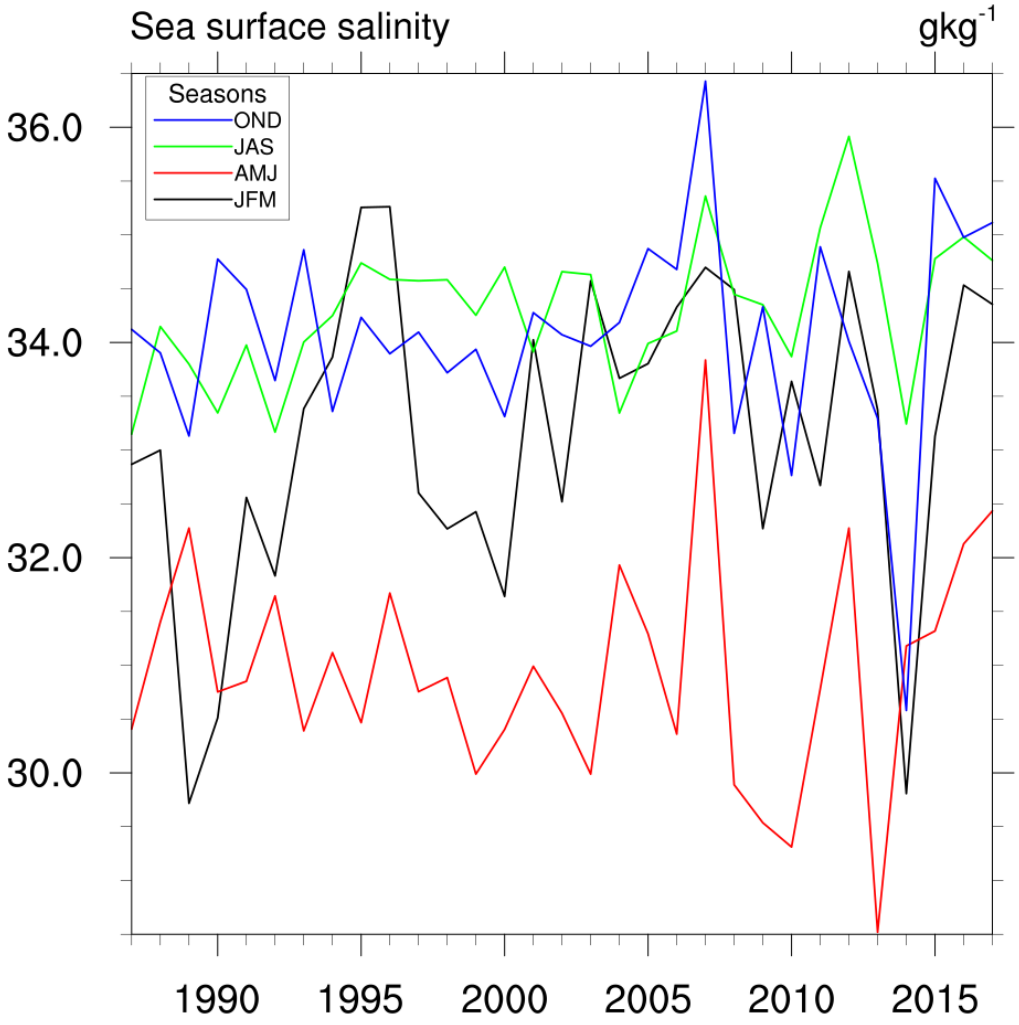

Figure 94. Seasonal surface salinity time series in the period 1987-2017 at the Po River delta site as simulated by the AdriSC modelling suite.

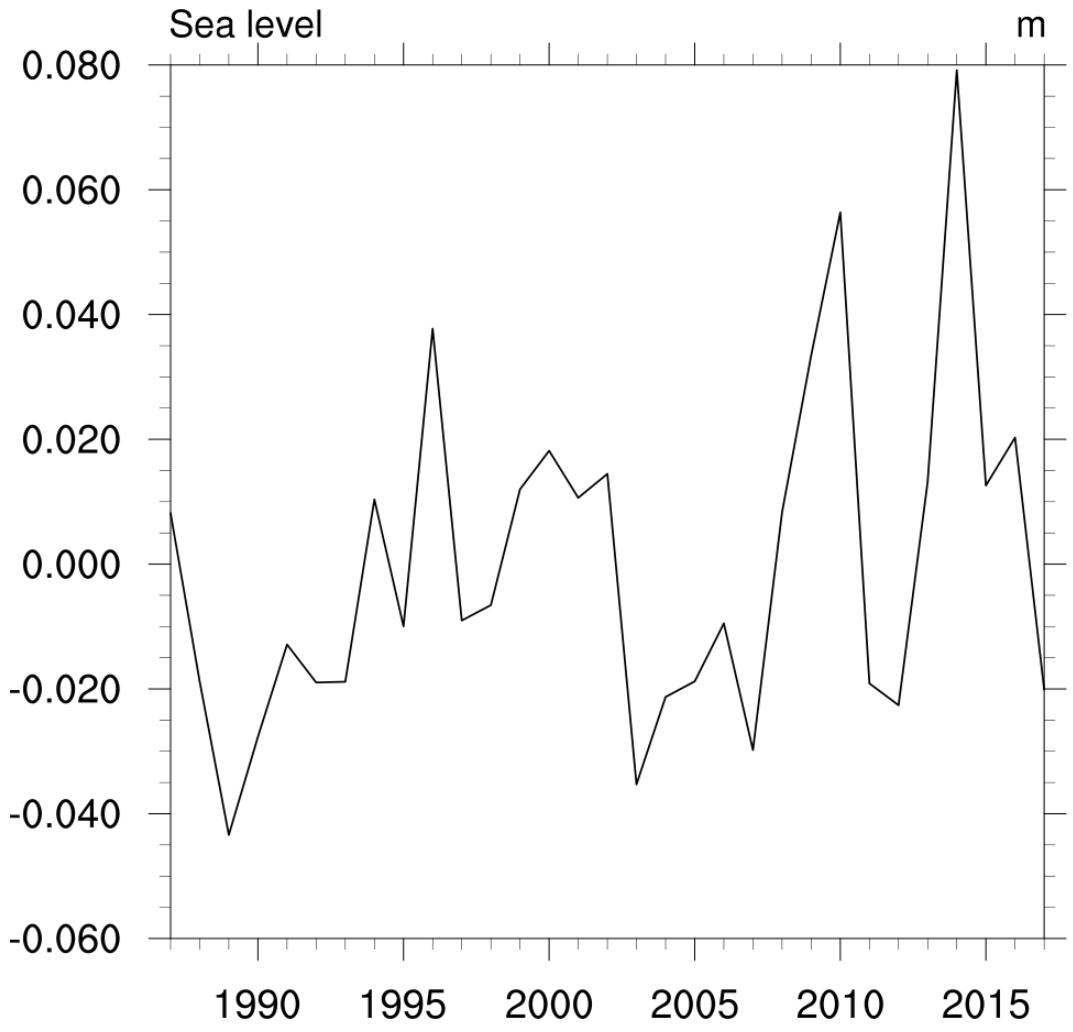

Figure 95. Annual sea surface height time series in the period 1987-2017 at the Po River delta site as simulated by the AdriSC modelling suite.

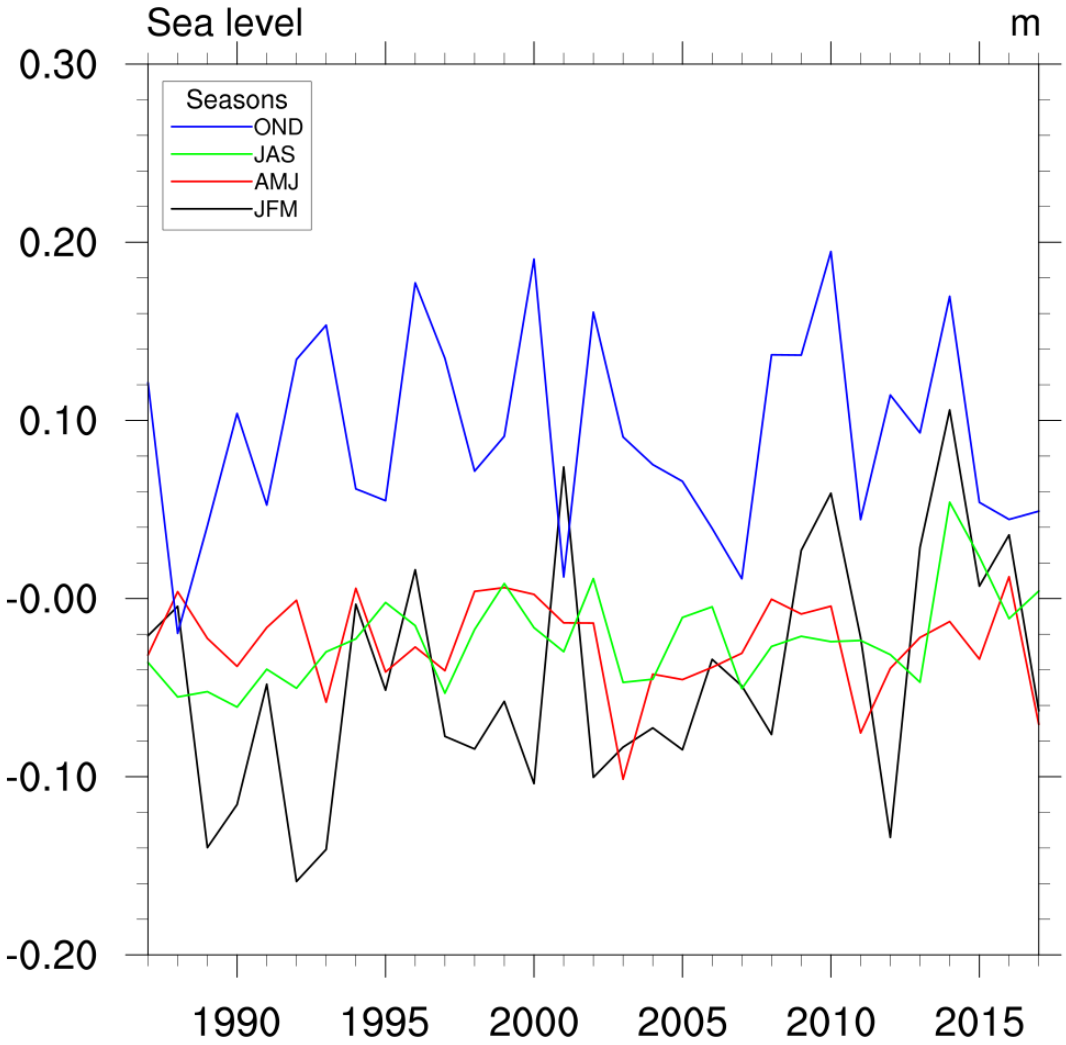

Figure 96. Seasonal sea surface height time series in the period 1987-2017 at the Po River delta site as simulated by the AdriSC modelling suite.

4.2. Banco di Mula di Muggia site

4.2.1. Assessment of atmospheric variables and processes

The Friuli Venezia Giulia Region is characterized by a geographical position and by an orography that significantly affect its meteorology and therefore the climate. The Region is located in the middle latitudes, where the contrast between the polar and tropical air masses is marked: this contrast frequently generates disturbances of the normal state of the atmosphere.

Furthermore, Friuli Venezia Giulia is part of those regions, orographically complex, where the processes of formation of perturbations and their evolution are strongly influenced by the reliefs: specifically, it is the Alpine chain that modulates the atmospheric circulation with effects both on temperatures than on rains.

The Alps prevent the flow of particularly cold air masses from the North and in this sense operate a major mitigating action, especially on minimum winter temperatures. The Alps also constitute a barrier to the humid flows from the South West and South East, which are typical of regional meteorology, causing a significant increase in rainfall, both in terms of quantity and frequency, compared to other areas in northern Italy.

The Adriatic Sea tends to mitigate temperatures: the coastal areas compared to those of the internal plain have higher average temperatures in winter and lower in summer. However, it should be noted that the Upper Adriatic is a relatively shallow basin and this element causes the mass of water to cool down considerably in winter and to heat up considerably in summer. Consequently, the mitigation effects of the winter and summer thermal extremes are contained. On the other hand, the contribution to the increase in rainfall (both summer storms and autumn and spring storms) caused by the transfer of humidity from the sea to the air masses passing through the Adriatic before investing Friuli Venezia Giulia is very important.

- Air Temperature

The average annual temperature for the coastal area of Friuli Venezia Giulia is 14.5° C – 15.5°C (Fig. 97).

Considering the trend of the average monthly temperatures, it is noted how the maximum values are recorded in the months of July and August and the minimum values in February (Figs. 98-100).

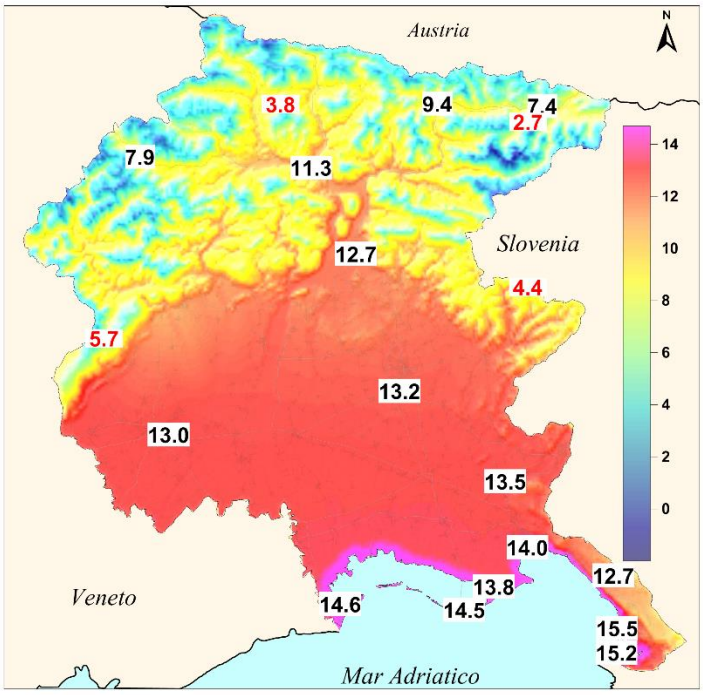

Figure 97. Average annual temperature for Friuli Venezia Giulia (1993-2013). ARPA FVG - OSMER.

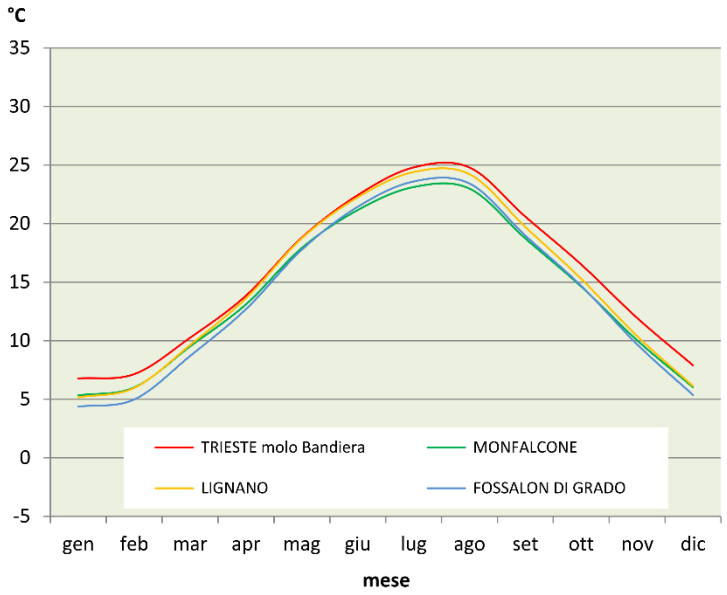

Figure 98. Coastal locations: average monthly temperatures (regional meteorological network data 1991-2010). ARPA FVG - OSMER.

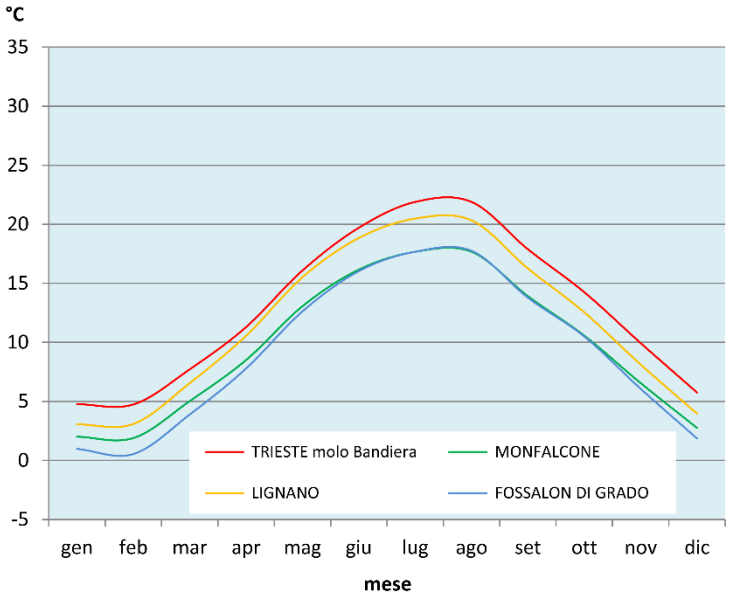

Figure 99. Coastal locations: average monthly minimum temperatures (regional meteorological network data 1991-2010. ARPA FVG - OSMER.

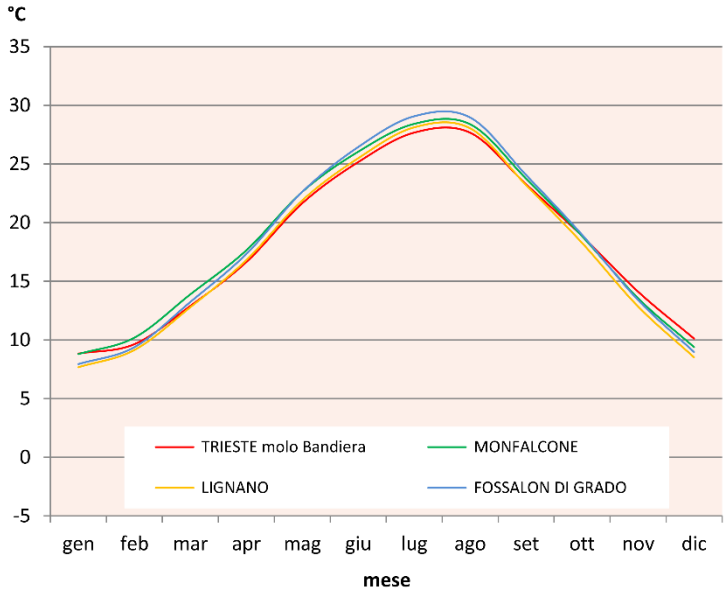

Figure 100. Coastal locations: average maximum monthly temperatures (regional meteorological network data 1991-2010). ARPA FVG - OSMER.

Also in Friuli Venezia Giulia the sea conditions the thermal trend on the coast. However, it is important to know the values that reflect this conditioning: the average annual sea temperature measured in Trieste in twenty years (1995-2014) is around 16 °C, the annual average of the absolute minimum is 7 °C and the annual average of the absolute maximums is 27.5 °C. By contrast, in the plains the annual average of the air temperature is 13.0/13.5 °C, the average of the annual minimums is around -9 °C, while the absolute maximums reach an average of 35/36 °C each year.

It can be noted how the sea mitigates the average daily temperature range: in Trieste the difference between minimum and maximum temperatures in winter is on average 4 °C and in summer 6 °C; in Fossalon these values become 7 and 11 °C, in Palazzolo dello Stella 9 and 13 °C.

The analysis of climatic data collected by the regional network and processed by ARPA FVG - OSMER shows, as a more evident trend, the increase in the average temperature in FVG.

At the annual level, this trend is well represented Fig. 100. In the entire period 1961-2016 the average increase in average temperature was 0.3 ° C every 10 years, with a clear acceleration trend in more recent decades (dotted line in Fig. 101).

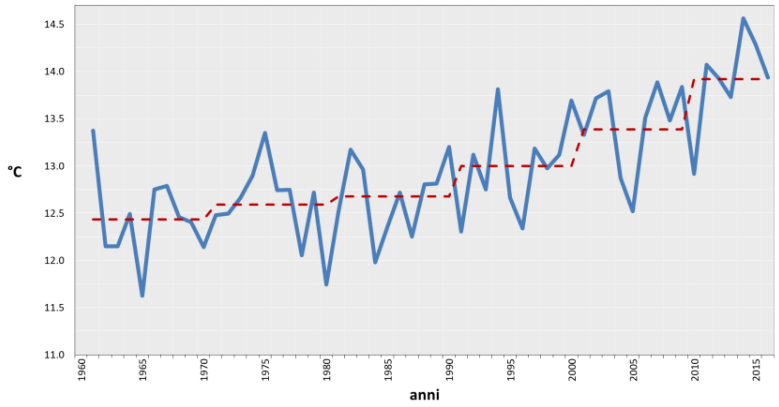

Figure 101. Trend of average annual temperatures in the period 1961-2016 for the Friuli Venezia Giulia plain (continuous blue line). The dotted line represents the trend of average temperatures in the various decades. Processing by ARPA FVG – OSMER.

The seasonal temperatures simulated by the AdriSC climate simulation (1987-2017) at the Banco di Mula di Muggia site indicate a strong variability between years, which might be as high as 3 °C (Fig. X). The least variable season is summer, for which the largest linear trend can be seen. Some years are emerging like warmer-than-usual (e.g. summer of 2003, winter and spring of 2007), while cold anomalies may be detected in others (e.g. winter of 1987, autumn of 2007).

- Rainfall

The nature and origin of the rains, of course, vary during the year: during the late autumn, winter and spring months, the rains are generally linked to the synoptic circulation (large-scale atmospheric circulation - even a few thousand km) and the southern humid flows; during the summer and early autumn months, the contribution to total rainfall of rains of convective origin (showers and

thunderstorms) or in any case linked to dynamics at the mesoscale (a geographical extension from tens of km to a few hundred km) becomes significant or even prevalent.

On the Friuli Venezia Giulia coast, annual rainfall is around 1000 mm. On average, in a decade, in the least rainy year, rainfall accumulations vary from 800 mm in the least rainy areas, to 1000 mm in the karst ones; in the wettest year of the decade, the territorial distribution varies in the same way from 1300 mm to 1500 mm (Fig. 102).

Fig. 103 shows the trend of multi-year average monthly rainfall in 4 stations in the coastal area. In the whole area the least rainy month is February with average rainfall around 55-60 mm; the months where rainfall is most abundant are September, October and November with values around 110-120 mm.

The autumn season is definitely the wettest and the average monthly precipitation data in November vary from 100 mm of the coast to 400 mm of Uccea, place included in the supply basin of the Isonzo River.

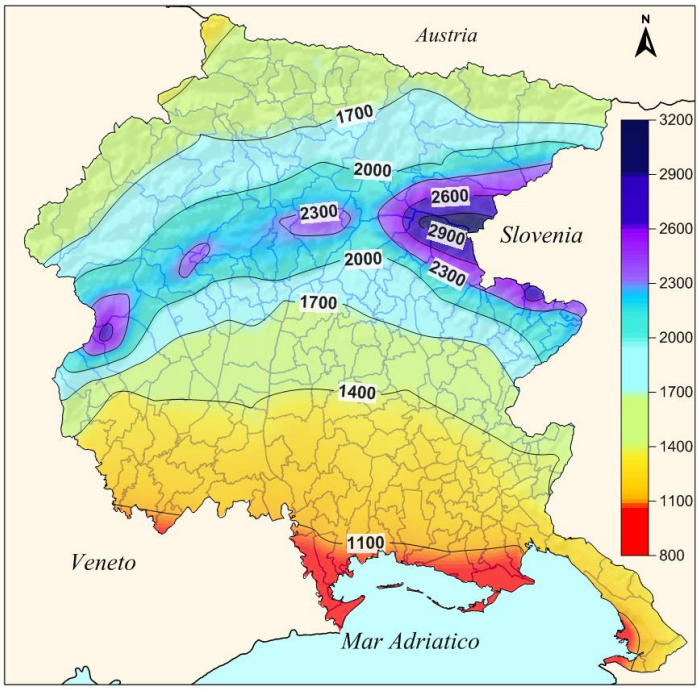

Figure 102. Friuli Venezia Giulia: average annual rainfall (regional meteorological network data 1961-2010). ARPA FVG - OSMER.

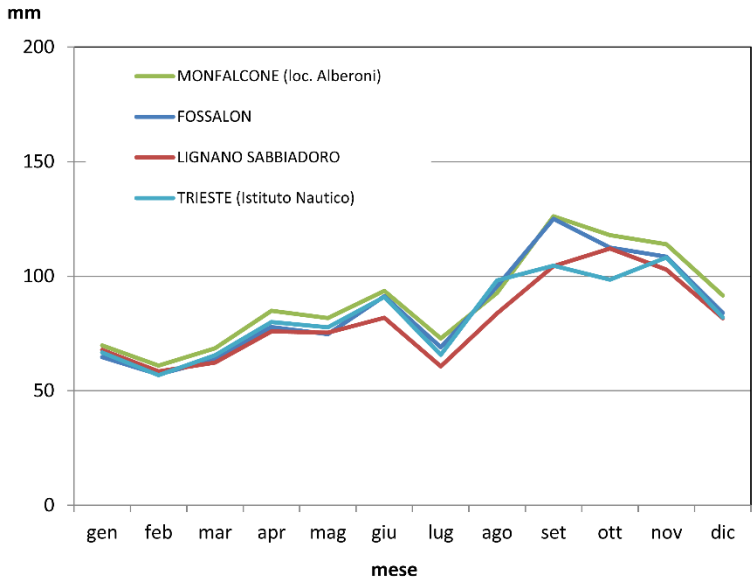

Figure 103. Coastal locations: average monthly rainfall (regional meteorological network data 1961-2010). ARPA FVG - OSMER.

The number of rainy days, i.e. the days when it rains at least 1 mm, in the average annual values varies, from south-west to north-east, going from 85-90 in Lignano to 95-100 in Monfalcone and the karst area of Trieste (Fig. 104).

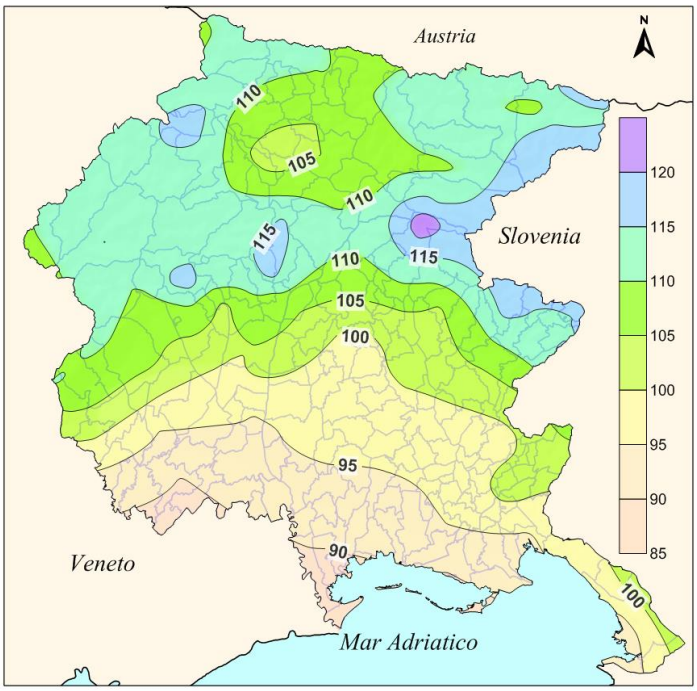

Figure 104. Friuli Venezia Giulia: average annual number of rainy days (regional weather network data 1961-2010). ARPA FVG - OSMER.

The signal of climate change on the rainfall of our region is less clear, also due to the strong interannual variability of this meteorological quantity. If you analyze daily rainfall data for the period 1961-2015, it is noted that over a large part of the region there is a general reduction of rainfall during the spring and summer season which varies from -2 to -4 mm per season. During the autumn and winter seasons there is an increase in rainfall even if the trends are not statistically significant.

- Wind regime

The reconstruction of the local anemological regime was conducted on the basis of the wind data recorded by the ISPRA station in Grado (http://www.ispravenezia.it). ISPRA data were measured on the ground (inside the Marano-Grado lagoon).

The weather station is located at the jetty of the dock on the main channel of the Grado inlet. The registrations from 2000 to 2009 were analysed (excluding 2002, because not available). The

data, scanned every 15 minutes, were transformed into a three-hour series and merged into both direction and intensity classes. The results obtained are summarized in Table 1 and Table 2.

The most frequent winds have speeds between 2 and 4 m / s (breeze regime), while the winds with velocity greater than 8 m / s, correspond to about 4.5% of the total (Table 1).

The direction analysis (Table 2) shows that the most frequent winds are those coming from the 1st quadrant (Bora). Winds from the eastern sector (Levante), southern (Sirocco) and south-western (Libeccio) are less frequent, while winds from the western sector (Ponente and Mistral) are much rarer.

TABELLA 1		
v(m/s)	*n°valori*	*Frequenza%*
0-1	3632	13.81
1-2	5738	21.81
2-4	9251	35.17
4-6	3362	12.78
6-8	1441	5.48
8-10	778	2.96
>10	386	1.47
N/D	1716	6.52

Table 1. Wind speed statistics for Grado station for the period 2000-2009.

TABELLA 2		
Direzione	*n°valori*	*Frequenza%*
N	141	0.54
NNE	1925	7.32
NE	3954	15.03
ENE	3752	14.26
E	1834	6.97
ESE	1579	6.00
SE	1395	5.30
SSE	1828	6.95
S	1840	7.00
SSO	1881	7.15
SO	1550	5.89
OSO	1173	4.46
O	628	2.39
ONO	553	2.10
NO	373	1.42
NNO	182	0.69

Table 2. Wind direction statistics for Grado station for the period 2000-2009.

The wind roses in Figs. 105-106 indicate that the winds from the first quadrant are generally also the most intense. In fact, the Bora wind can blow at speeds even higher than 100 km/h. However, intense winds are also coming from the eastern sector (Levante) and from the south-eastern sector (Sirocco).

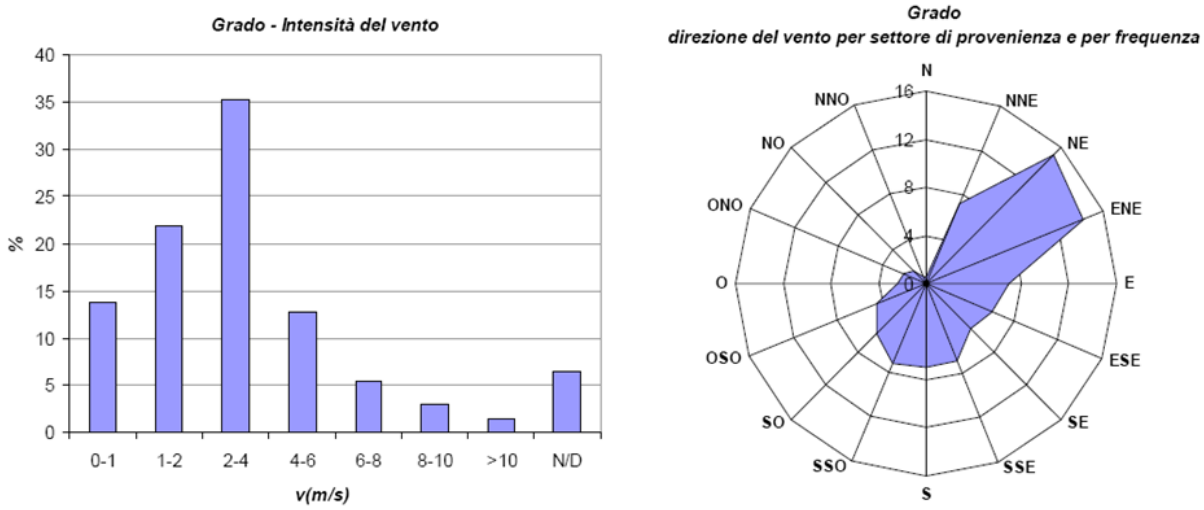

Figure 105. Grado station: occurrence percentages of wind speed and direction. Tri-hourly data 2000-2009.

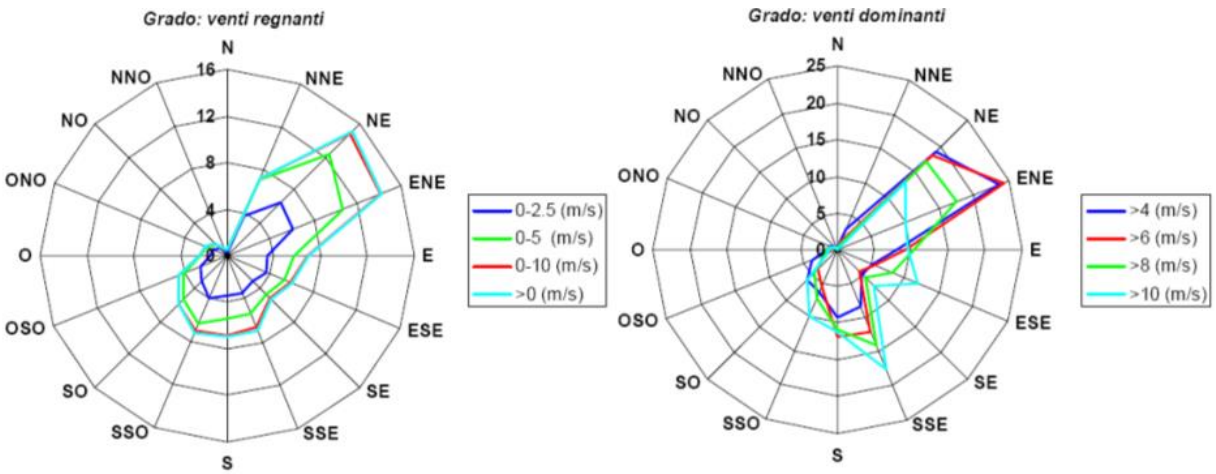

Figure 106. Grado station: most frequent wind rose (links) and dominant wind roses. Tri-hourly data 2000-2009.

The time series of air temperature at 2 m coming from the AdriSC simulation (1987-2017) (Fig. 107) is denoting the interannual variability in temperatures. There were some winters much warmer than the average, like 1988, 2001, 2007 and 2014, of which the latter has been recognized to impact dense water production in the Adriatic Sea (Mihanović et al., 2018). The spring of 2007 was also warmer than usual, contrasting to autumn, which was colder than usual. As an outlier, the summer of 2003 was quite warm, and – in combination of low precipitation, it produced quite anomalous thermohaline properties in the Adriatic Sea (Grbec et al., 2007).

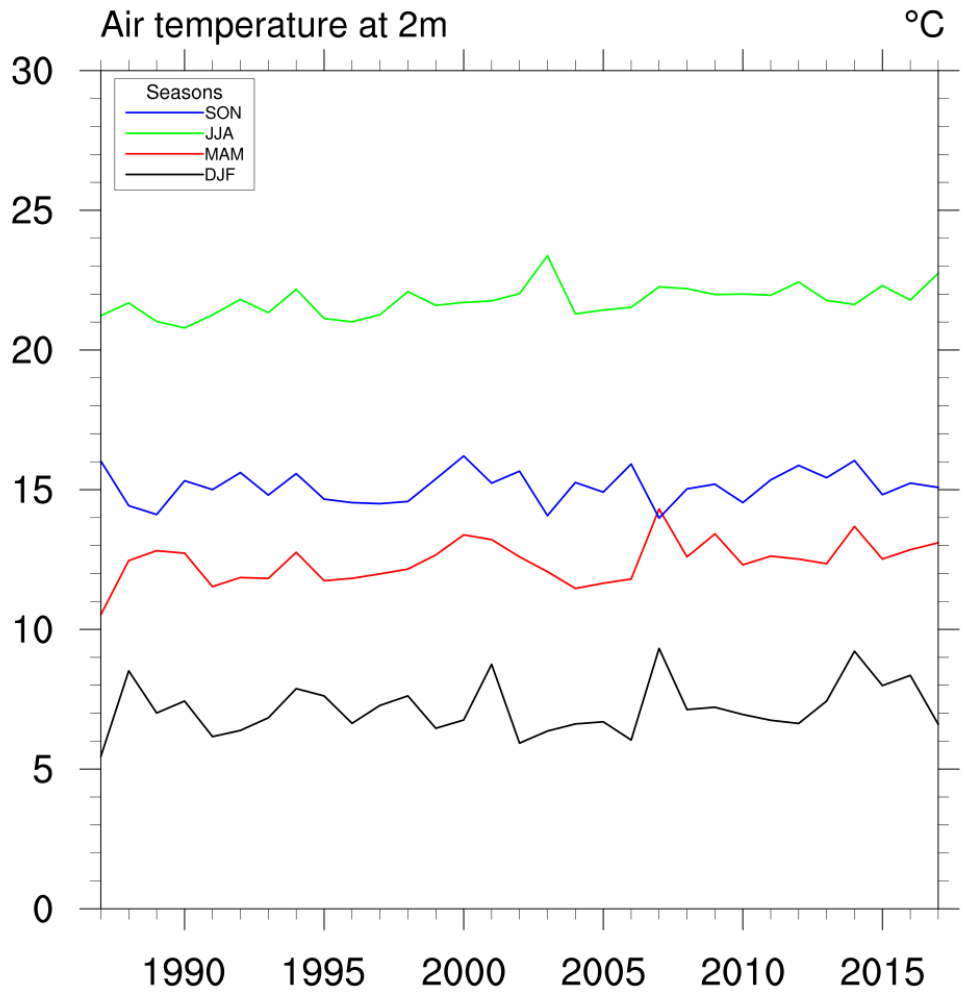

Figure 107. Air temperature at 2 m seasonal time series in the period 1987-2017 at the Banco di Mula di Muggia site as simulated by the AdriSC modelling suite.

Regarding precipitation rate (Fig. 108), the maximum is achieved in autumn (SON), having a minimum between 2002 and 2007. This minimum coincided with minimum in summer (JJA) precipitation rate. The peak in precipitation rate during both winter and summer may be noticed in 2014, when the precipitation reached its maximum in the whole considered period. In conclusion, there might be noticed a great interannual variability in all seasons, which for sure may influence the hydrological budget in the area of the site.

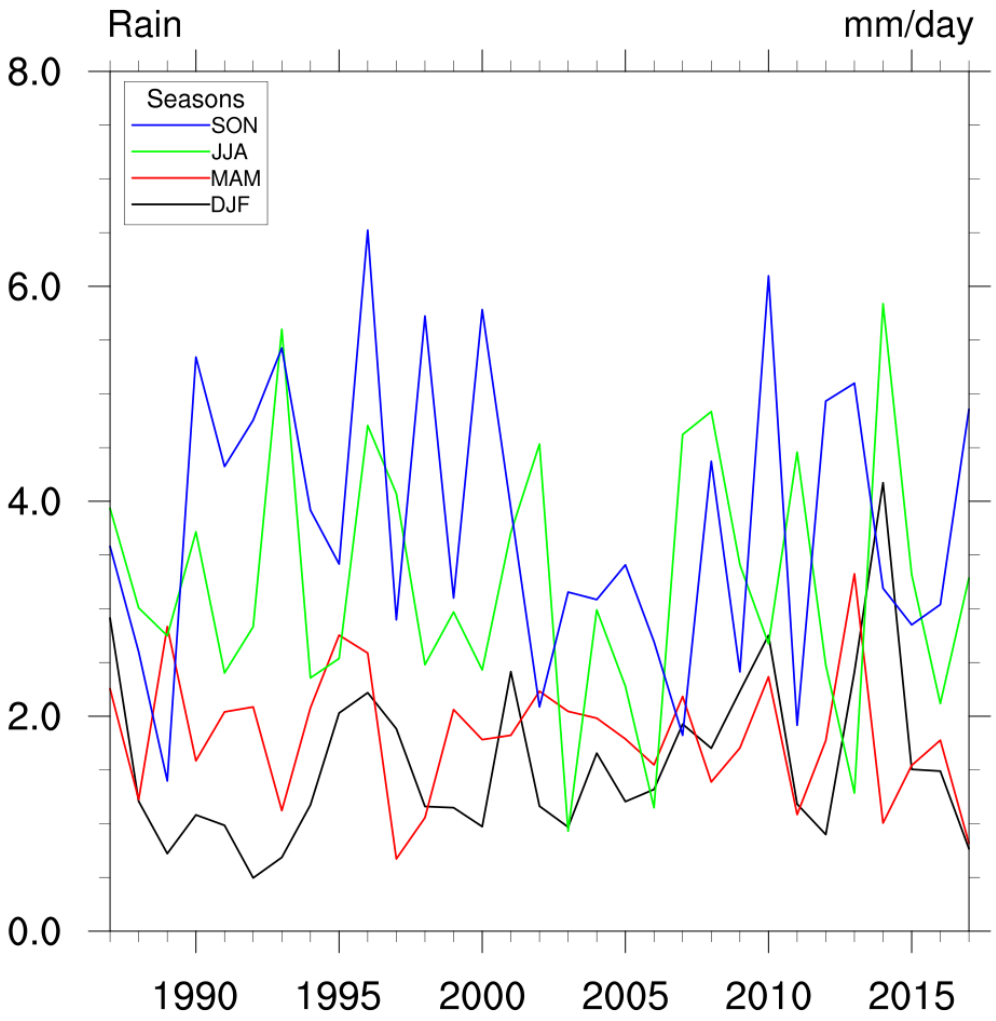

Figure 108. Precipitation rate seasonal time series in the period 1987-2017 at the Banco di Mula di Muggia site as simulated by the AdriSC modelling suite.

Regarding wind climatology at the Banco di Mula di Muggia site coming from the AdriSC climate simulation (Fig. 109), it follows the observations with the most frequent wind coming from NE

(bora). Stronger but not frequent sirocco wind coming from south to southeast can be seen as well. The winds from other directions are not frequent at the site.

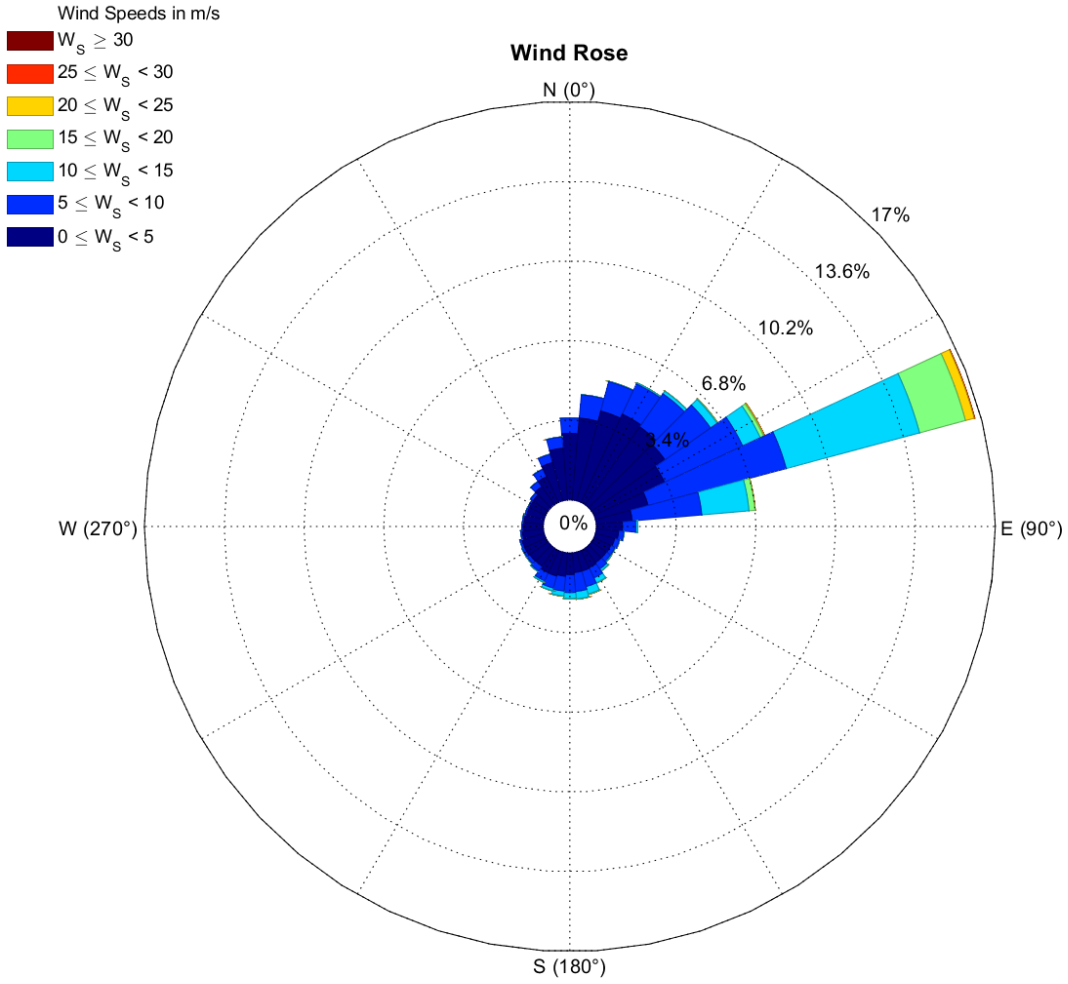

Figure 109. Wind rose at the Banco di Mula di Muggia site as simulated by the AdriSC modelling suite (1987-2017).

4.2.2. Assessment of oceanic variables and processes

Off the Banco di Mula di Muggia site, the mean annual temperature (Fig. 110) has values rising from 15.5 °C at the beginning of the AdriSC simulation to 16-17 °C at the end of the AdriSC simulation. The positive trends are strongest in spring and autumn periods (Fig. 111). Sea surface salinity has strong interannual variability, ranging from 37.5 to 38.1, with lowest values in spring and highest in summer and autumn (Figs. 112-113). Sea level constantly rose in the considered period (Fig. 114), yet with quite strong interannual variability.

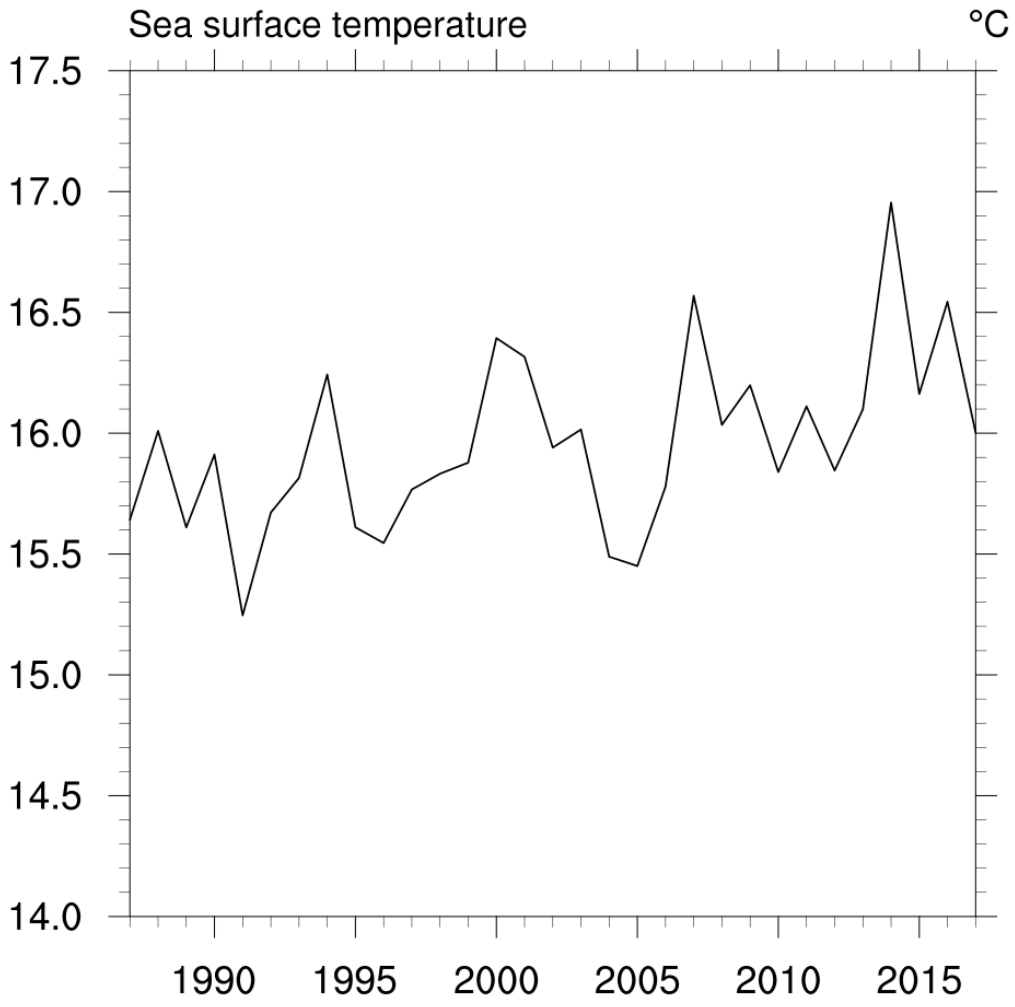

Figure 110. Annual sea surface temperature time series in the period 1987-2017 at the Banco di Mula di Muggia site as simulated by the AdriSC modelling suite.

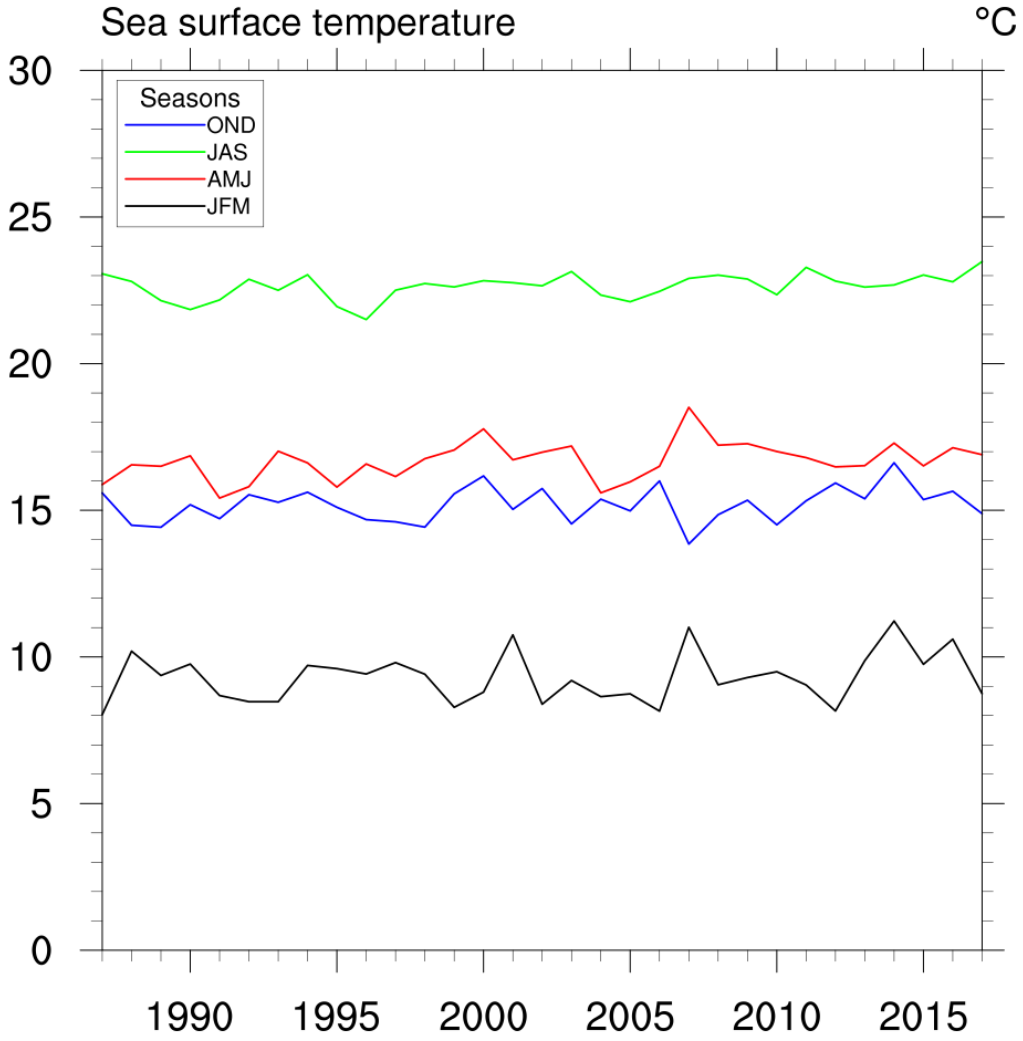

Figure 111. Seasonal sea surface temperature time series in the period 1987-2017 at the Banco di Mula di Muggia site as simulated by the AdriSC modelling suite.

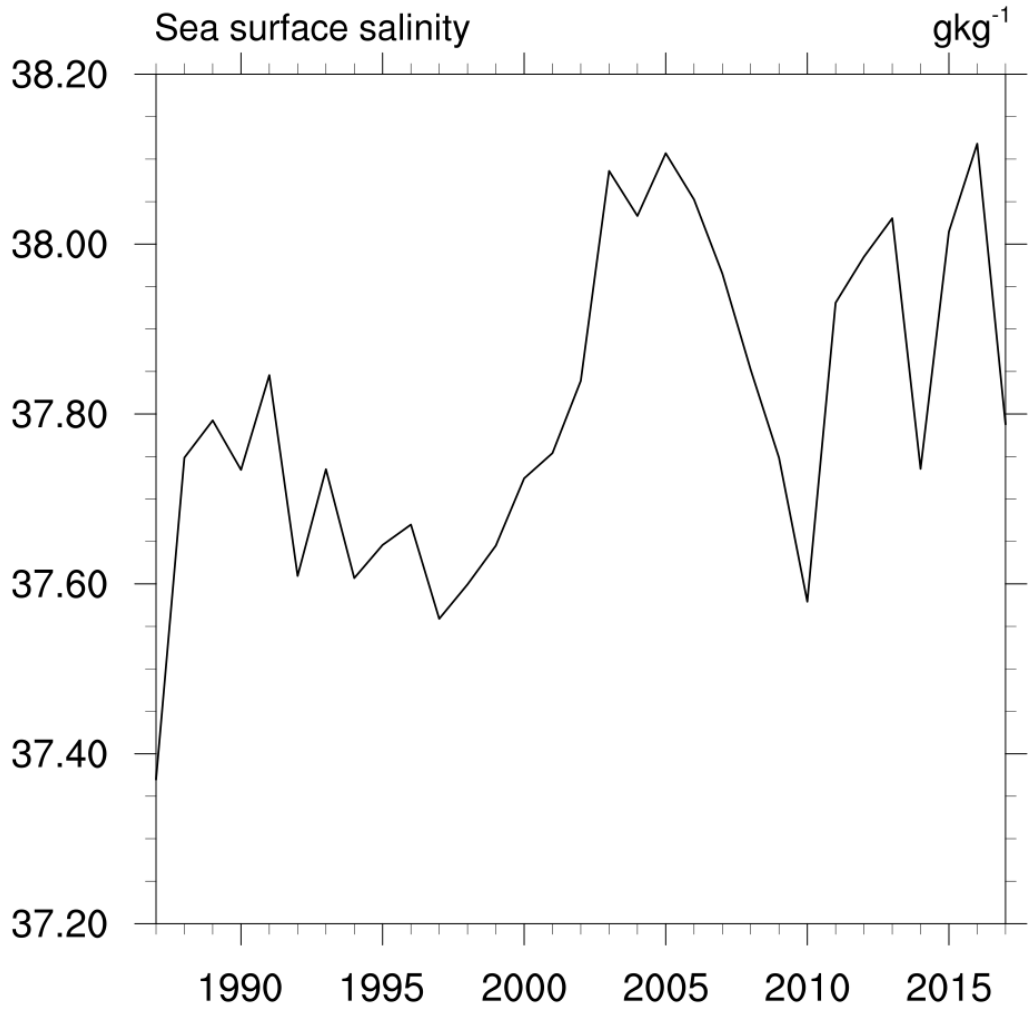

Figure 112. Annual surface salinity time series in the period 1987-2017 at the Banco di Mula di Muggia site as simulated by the AdriSC modelling suite.

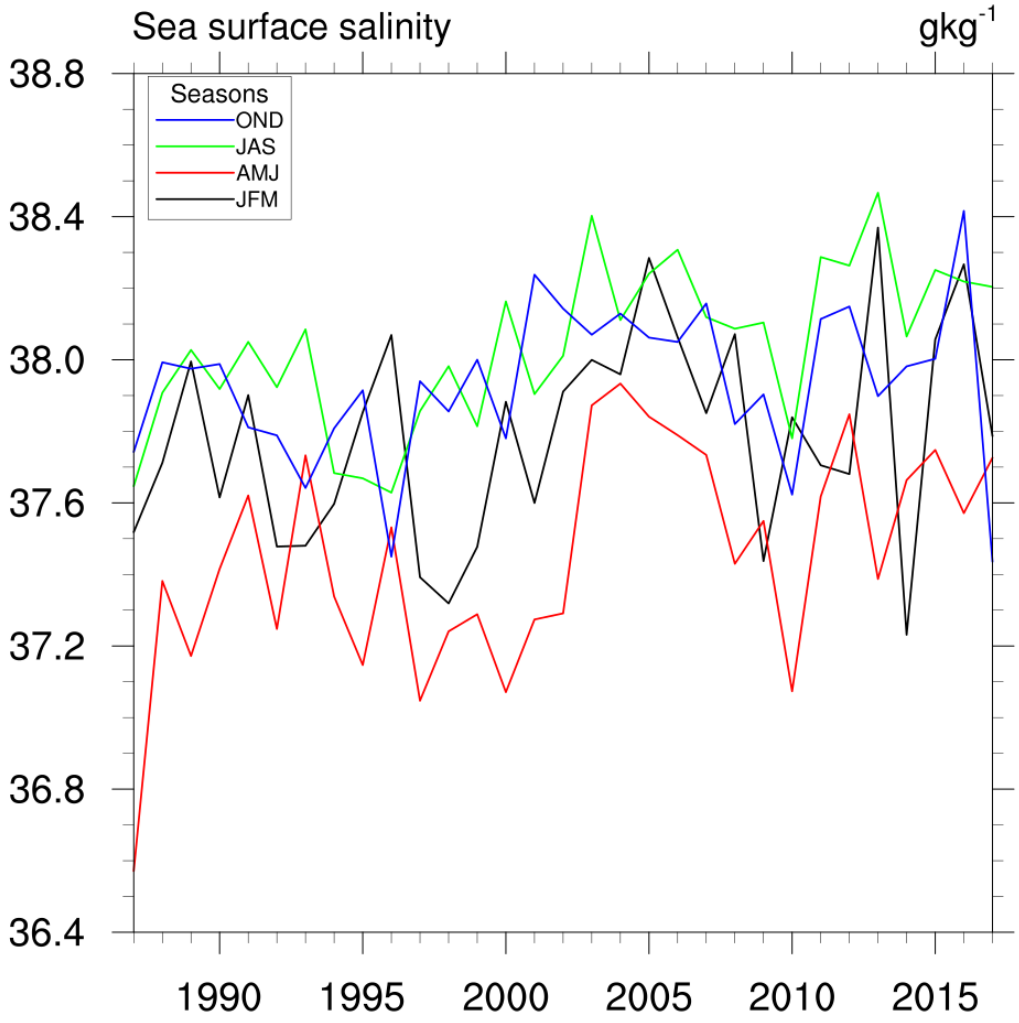

Figure 113. Seasonal surface salinity time series in the period 1987-2017 at the Banco di Mula di Muggia site as simulated by the AdriSC modelling suite.

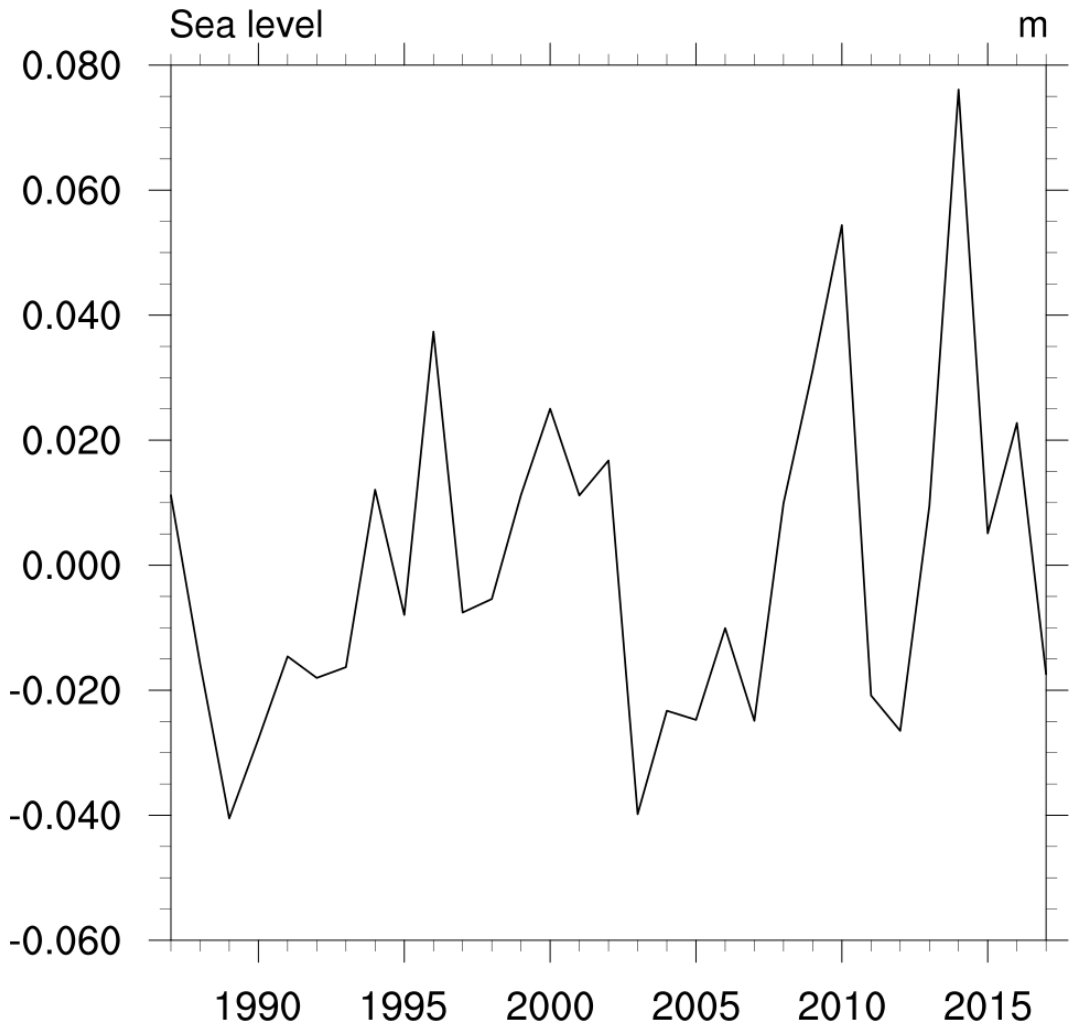

Figure 114. Annual sea surface height time series in the period 1987-2017 at the Banco di Mula di Muggia site as simulated by the AdriSC modelling suite.

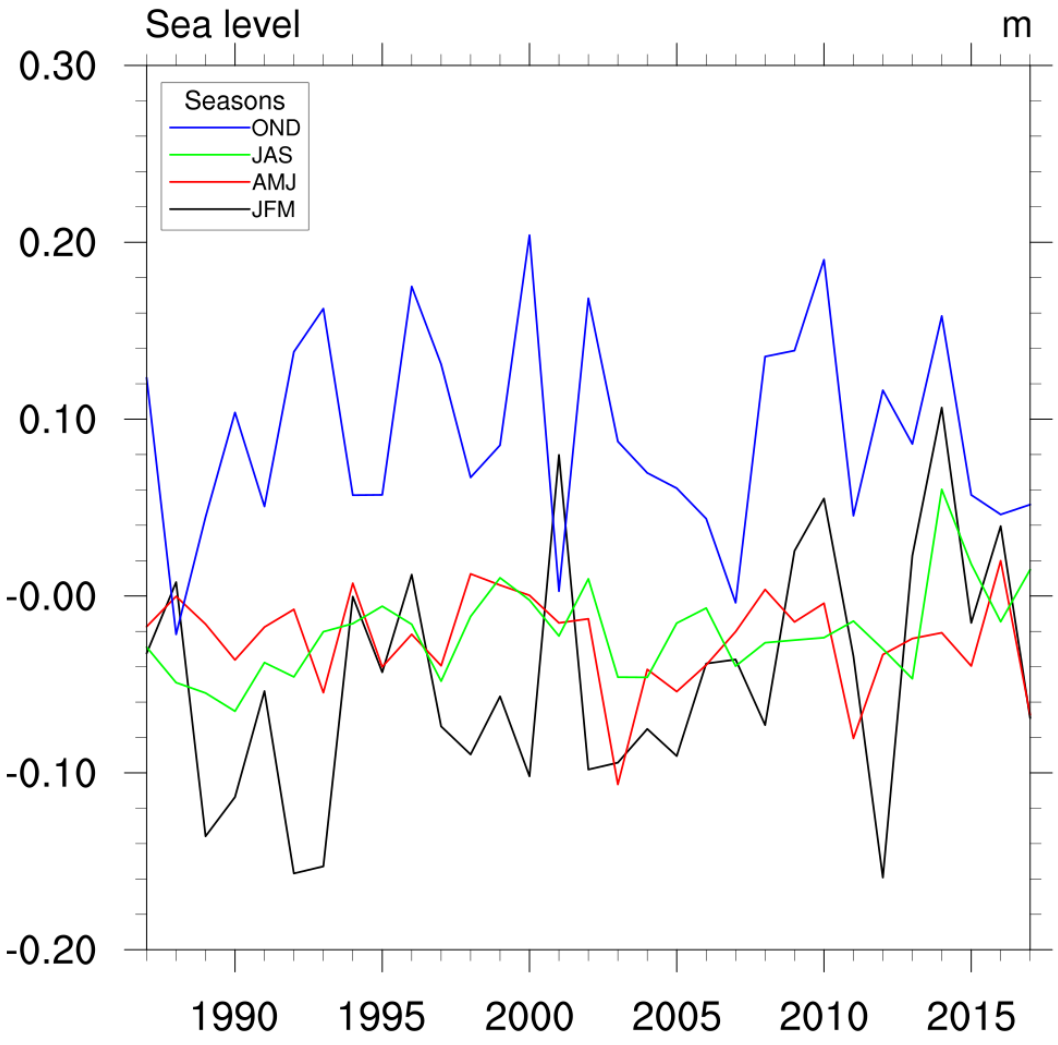

Figure 115. Seasonal sea surface height time series in the period 1987-2017 at the Banco di Mula di Muggia site as simulated by the AdriSC modelling suite.

4.3. Vransko Lake

4.3.1. Assessment of atmospheric variables and processes

Vransko Lake has a typical Mediterranean climate, with mild and rainy winter periods, and dry, hot summers. Köppen classification denotes this type of climate as “Olive tree climate” and its vegetation is characterized by Holm oak forests, marquis and dry grasslands on karst terrain.

Average annual temperature is around 15°C. Warmest months of the year are July and August, with January and February being the coolest. November and December have the highest precipitation, and June and July are the driest months.

Long-term measurements of the temperature trends in the area indicate a warming (Fig. 116), whie the trend in precipitation is negative (Fig. 117). The most of precipitation is measured in November (Fig. 118), while the lowest precipitation is observed in July.

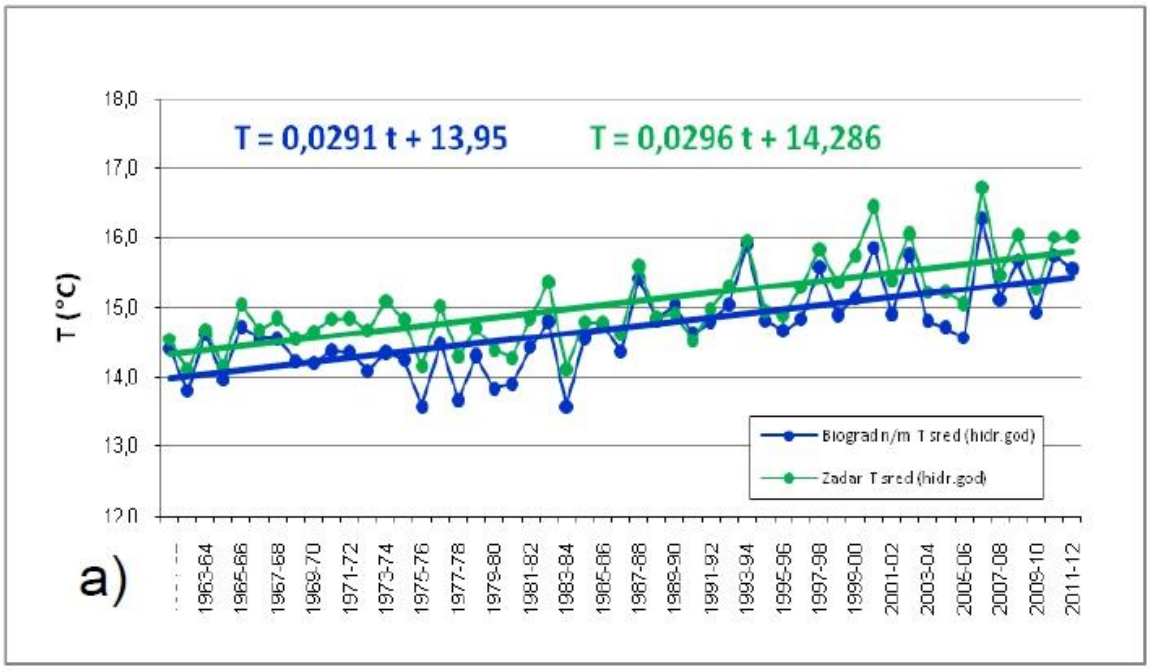

Figure 116. Annual air temperature at 2 m time series in the period 1963-2012 at Biograd and Zadar meteorological stations (after Rubinić, 2014).

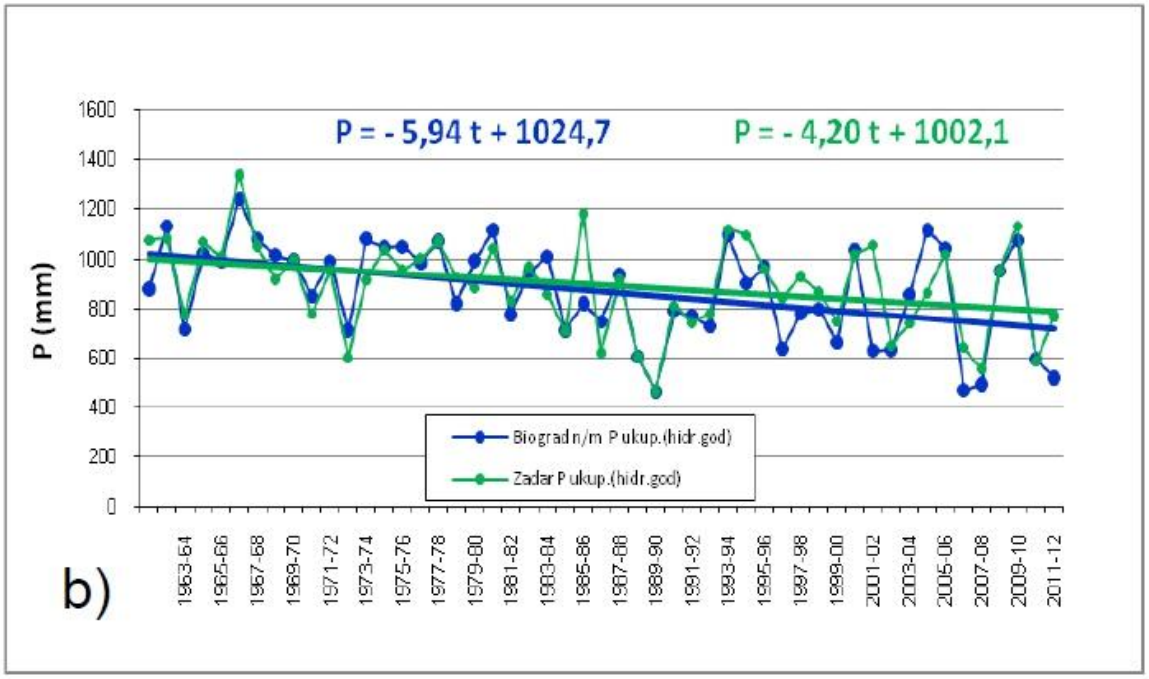

Figure 117. Annual precipitation time series in the period 1963-2012 at Biograd and Zadar meteorological stations (after Rubinić, 2014).

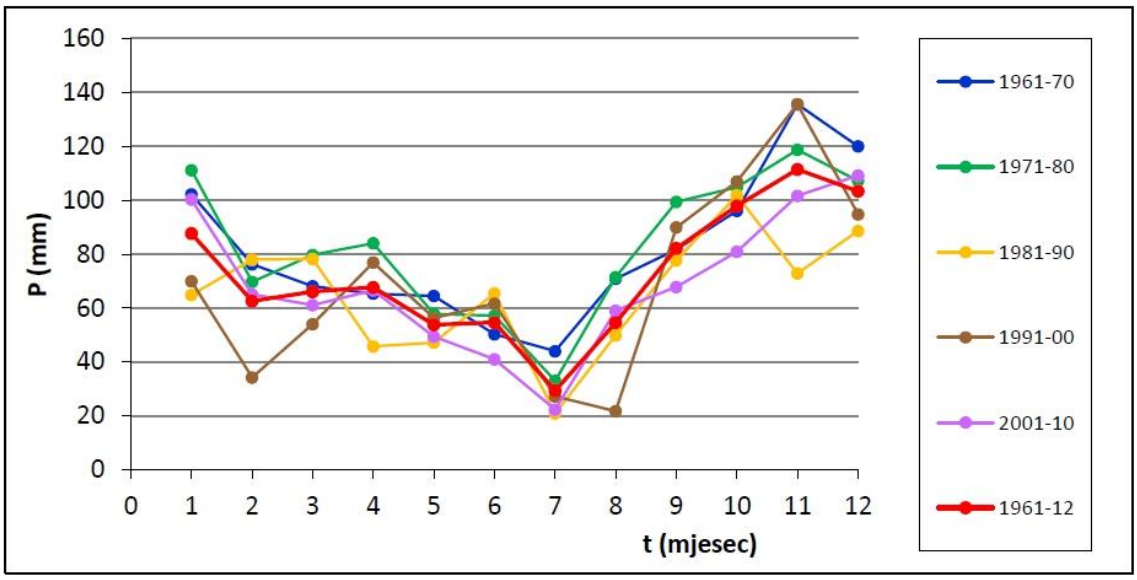

Figure 118 Seasonal changes in precipitation at Biograd meteorological station (after Rubinić, 2014).

Similar temperature and precipitation climatology has been reproduced by the AdriSC climate simulation (1987-2017) (Figs. 119-122). However, one should be aware that the trends differ from measurements, as shorter and newer time interval has been covered by the simulation. Thus, the simulation keeps the temperature trend positive, while the trend in precipitation is here not significant, as the simulation started in a dry period of 1980s.

Wind rose (Fig. 123) show the dominance of north-easterly winds, i.e. of bora wind, both in intensity and frequency, while higher speeds have been reproduced for south-easterly winds, i.e. sirocco.

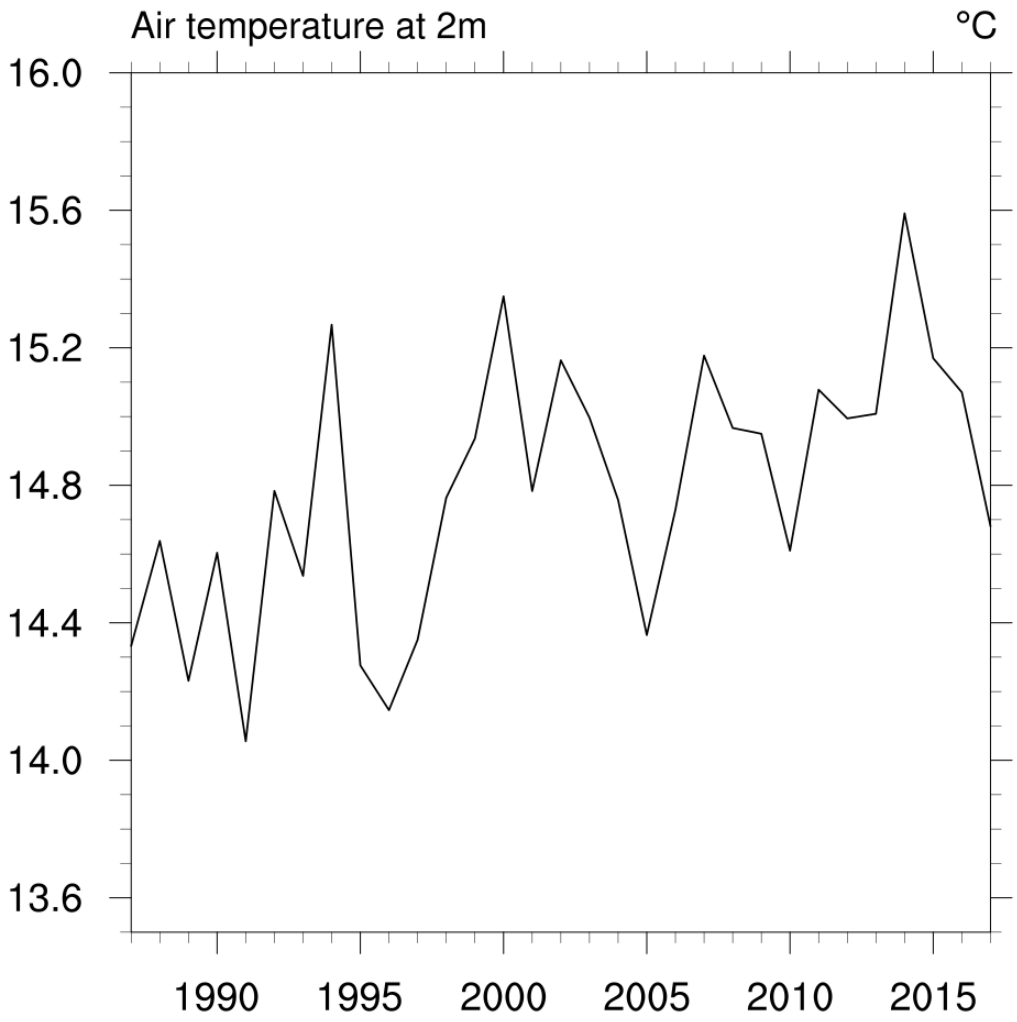

Figure 119. Annual air temperature at 2 m time series in the period 1987-2017 at the Vransko Lake site s simulated by the AdriSC modelling suite.

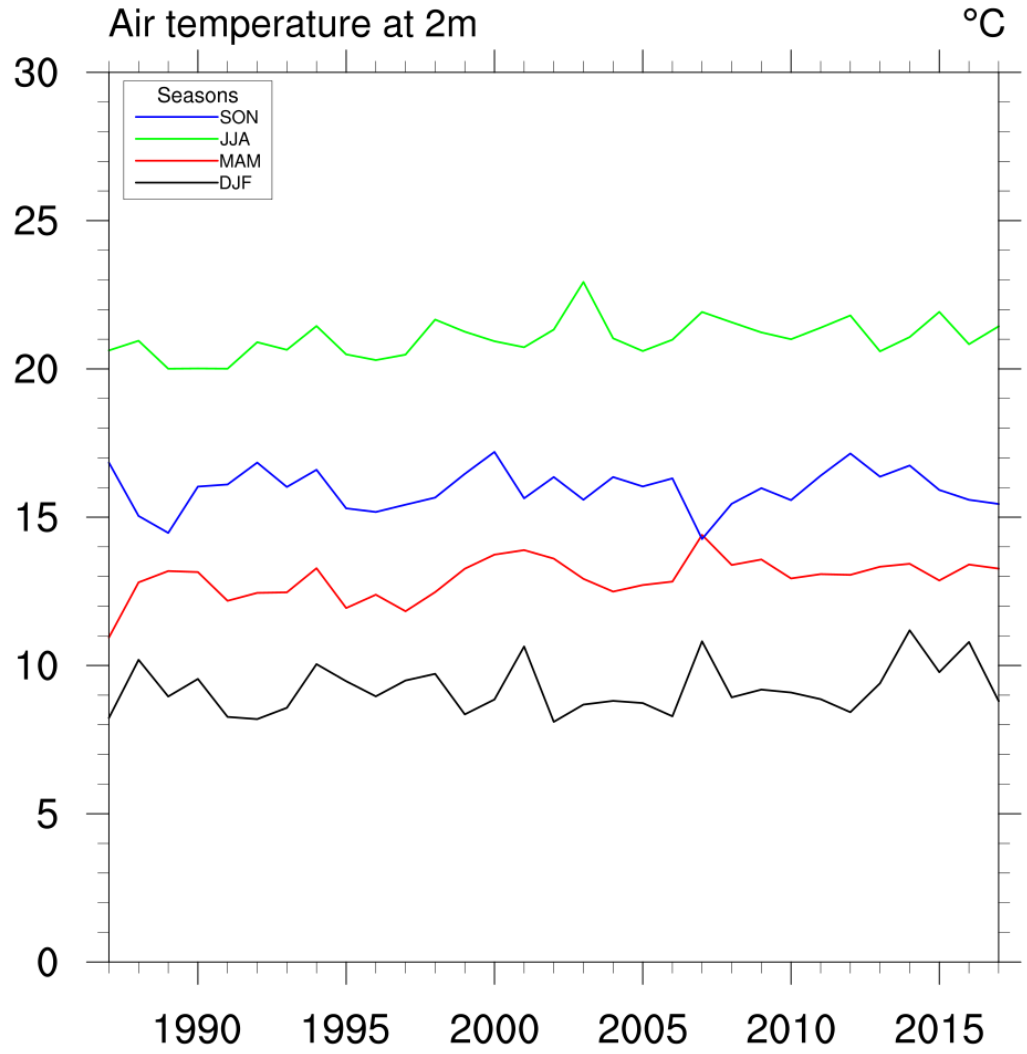

Figure 120. Seasonal air temperature at 2 m time series in the period 1987-2017 at the Vransko Lake site as simulated by the AdriSC modelling suite.

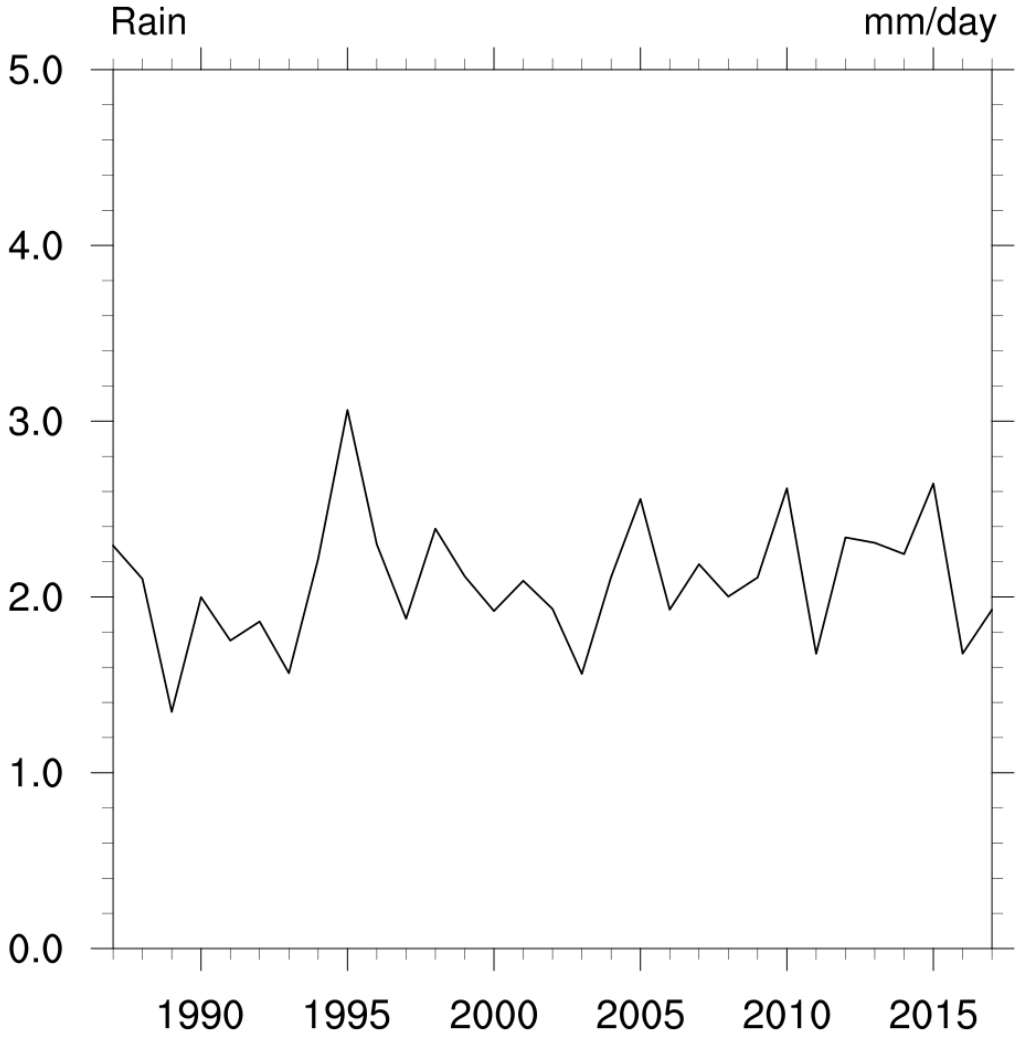

Figure 121. Annual precipitation time series in the period 1987-2017 at the Vransko Lake site as simulated by the AdriSC modelling suite.

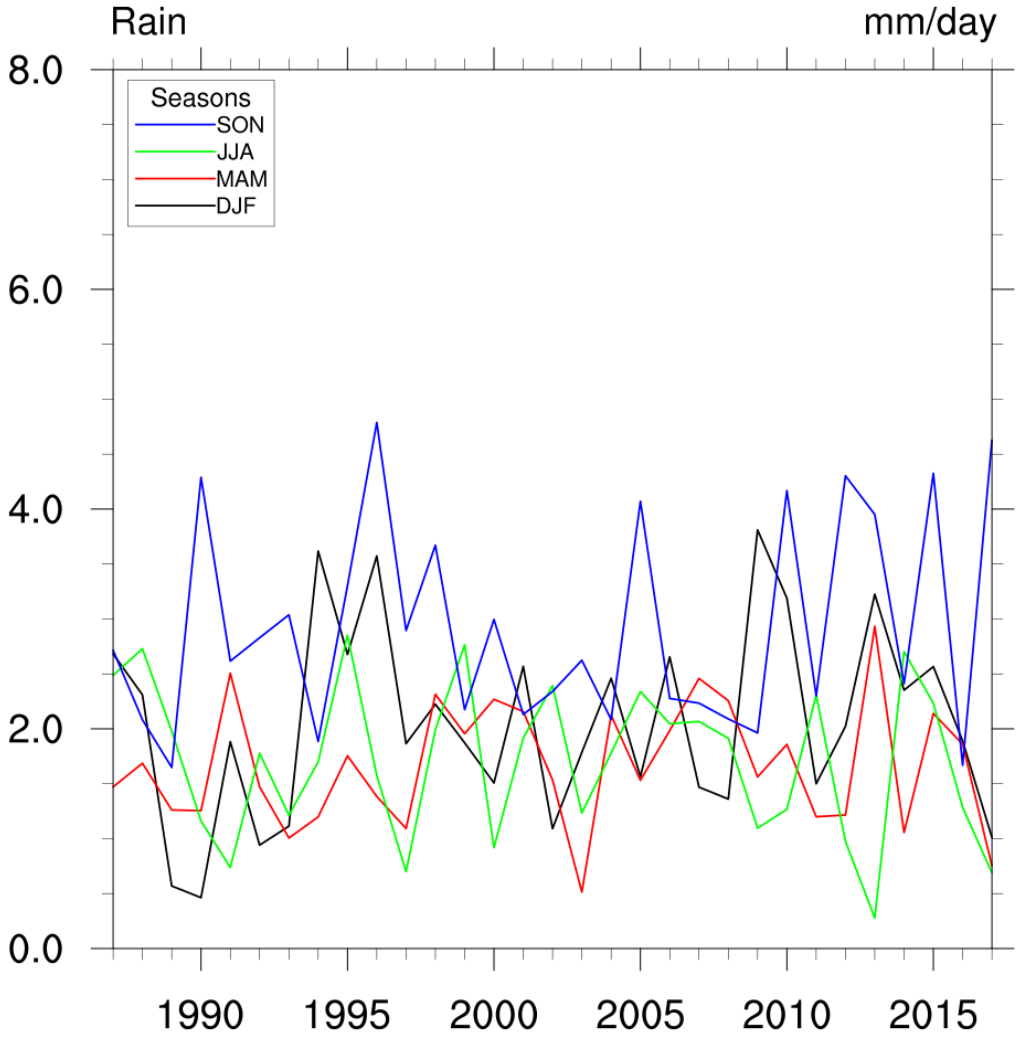

Figure 122. Seasonal precipitation rate time series in the period 1987-2017 at the Vransko Lake site as simulated by the AdriSC modelling suite.

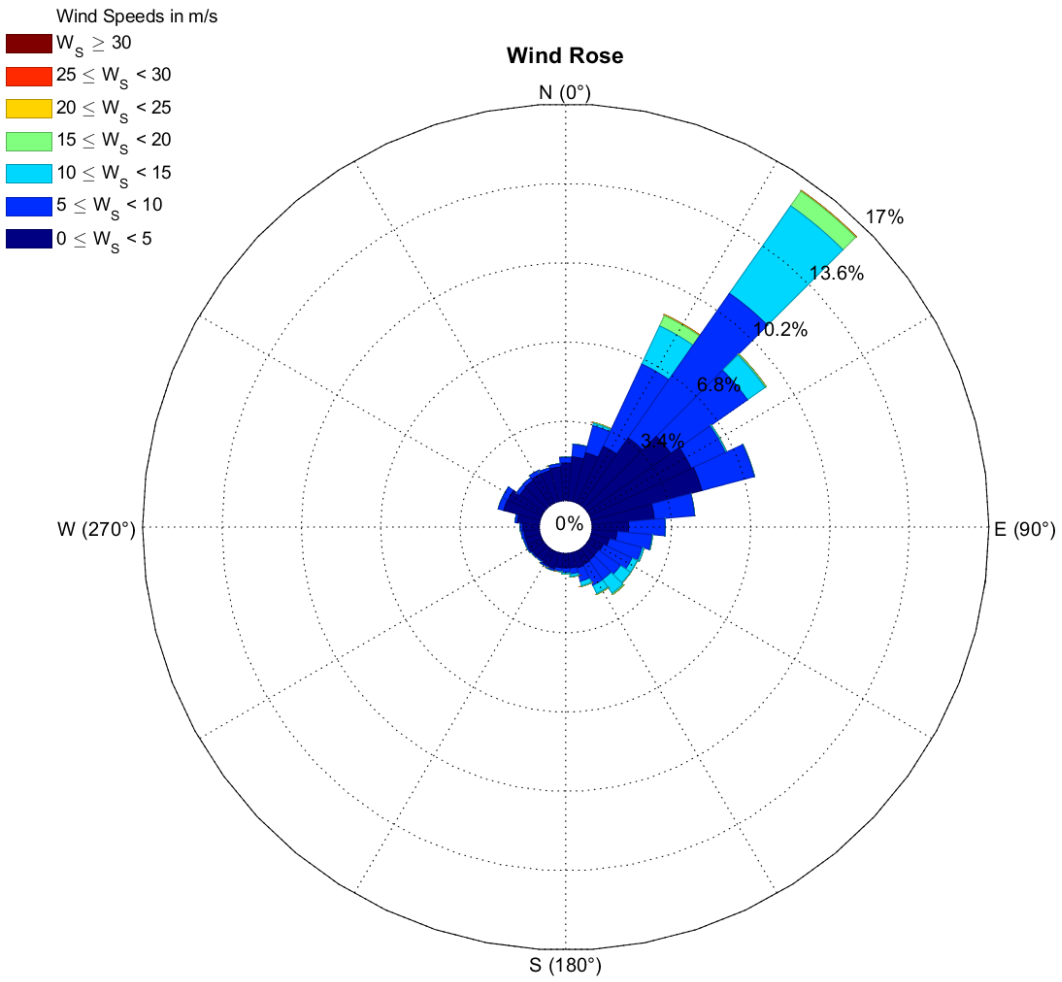

Figure 123. Wind rose at the Vransko Lake site as simulated by the AdriSC modelling suite (1987-2017).

4.3.2. Assessment of oceanic variables and processes

In the Adriatic Sea off the Vrana Lake site, the mean annual temperature (Fig. 124) has values rising from 17.0-17.5 °C at the beginning of the AdriSC simulation to 18.0-18.5 °C at the end of the AdriSC simulation. The positive trends are strongest in spring and autumn periods (Fig. 125). Sea surface salinity has strong interannual variability, ranging from 37.8 to 38.5, with lowest values in spring and highest in summer and autumn (Figs. 126-127).

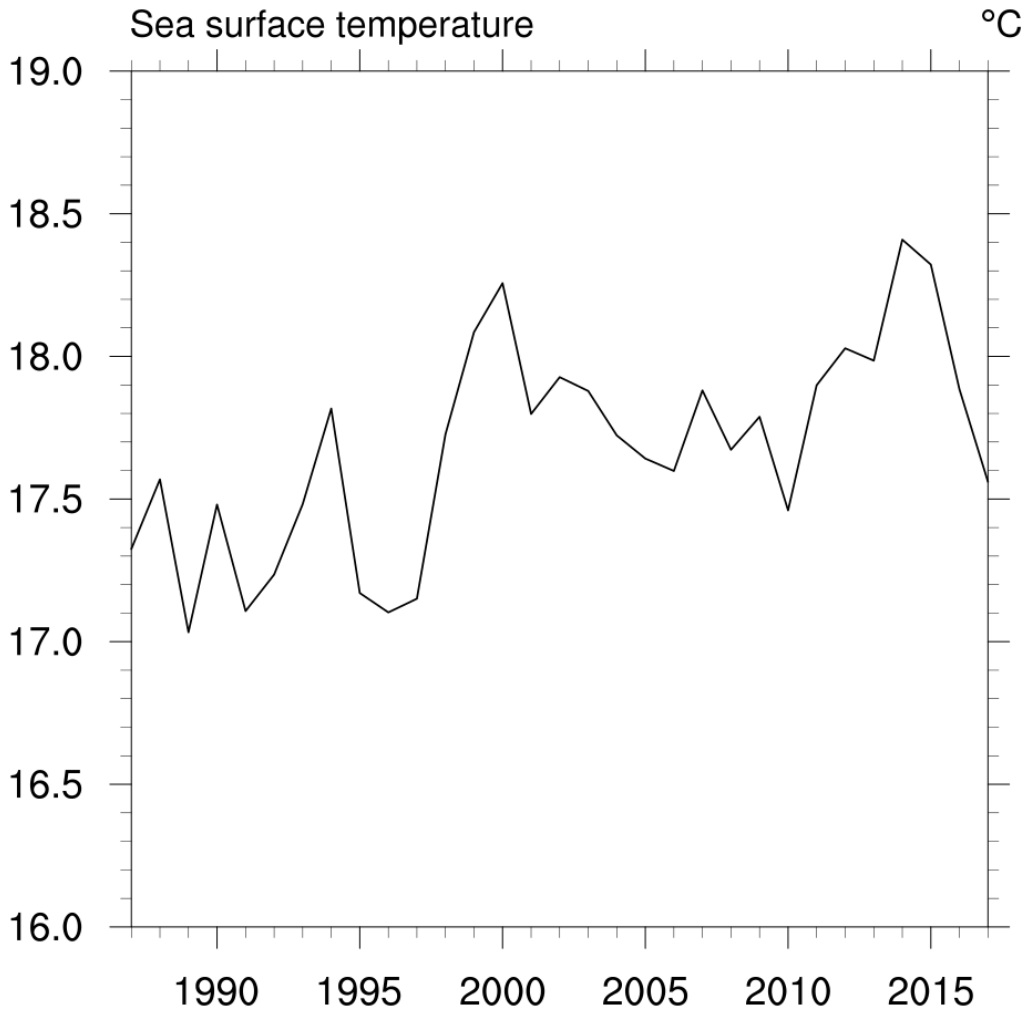

Figure 124. Annual sea surface temperature time series in the period 1987-2017 at the Vransko Lake site as simulated by the AdriSC modelling suite.

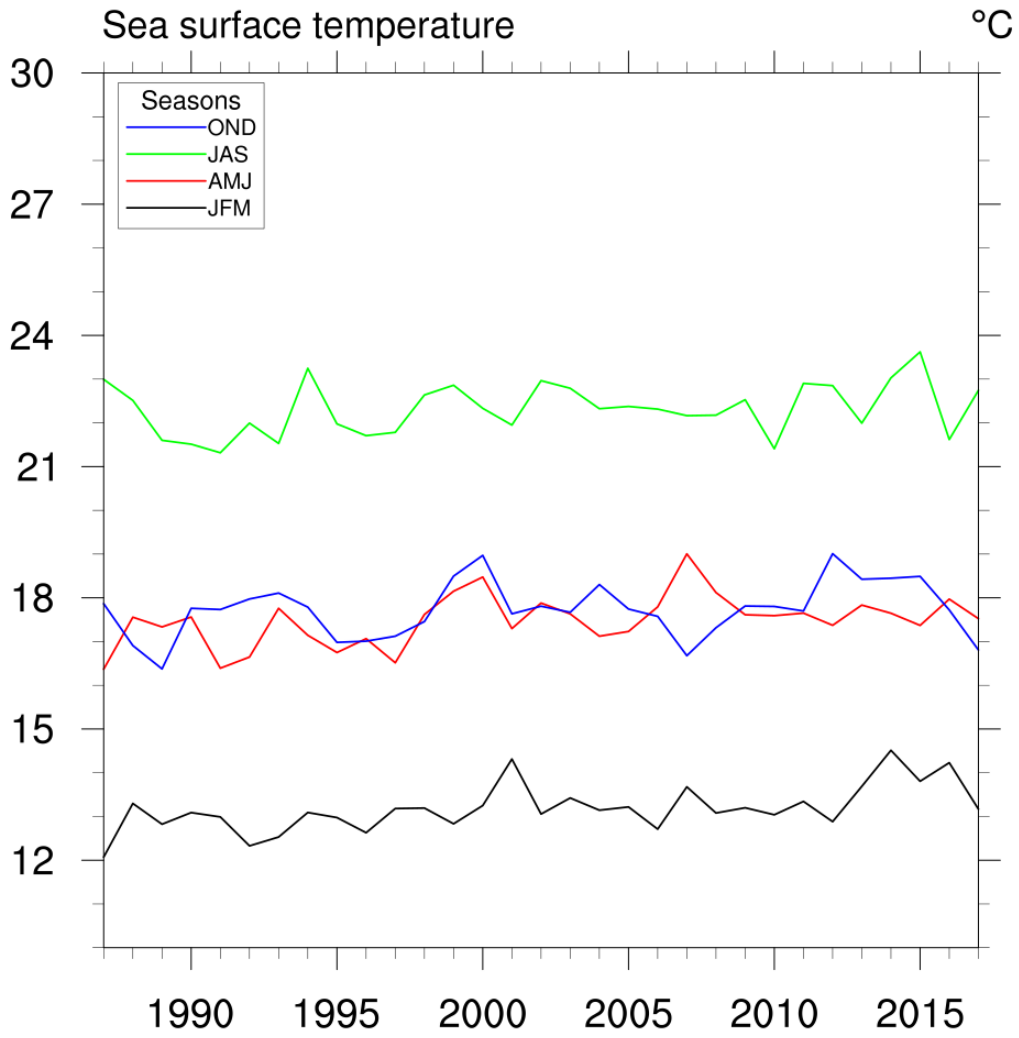

Figure 125. Seasonal sea surface temperature time series in the period 1987-2017 at the Vransko Lake site as simulated by the AdriSC modelling suite.

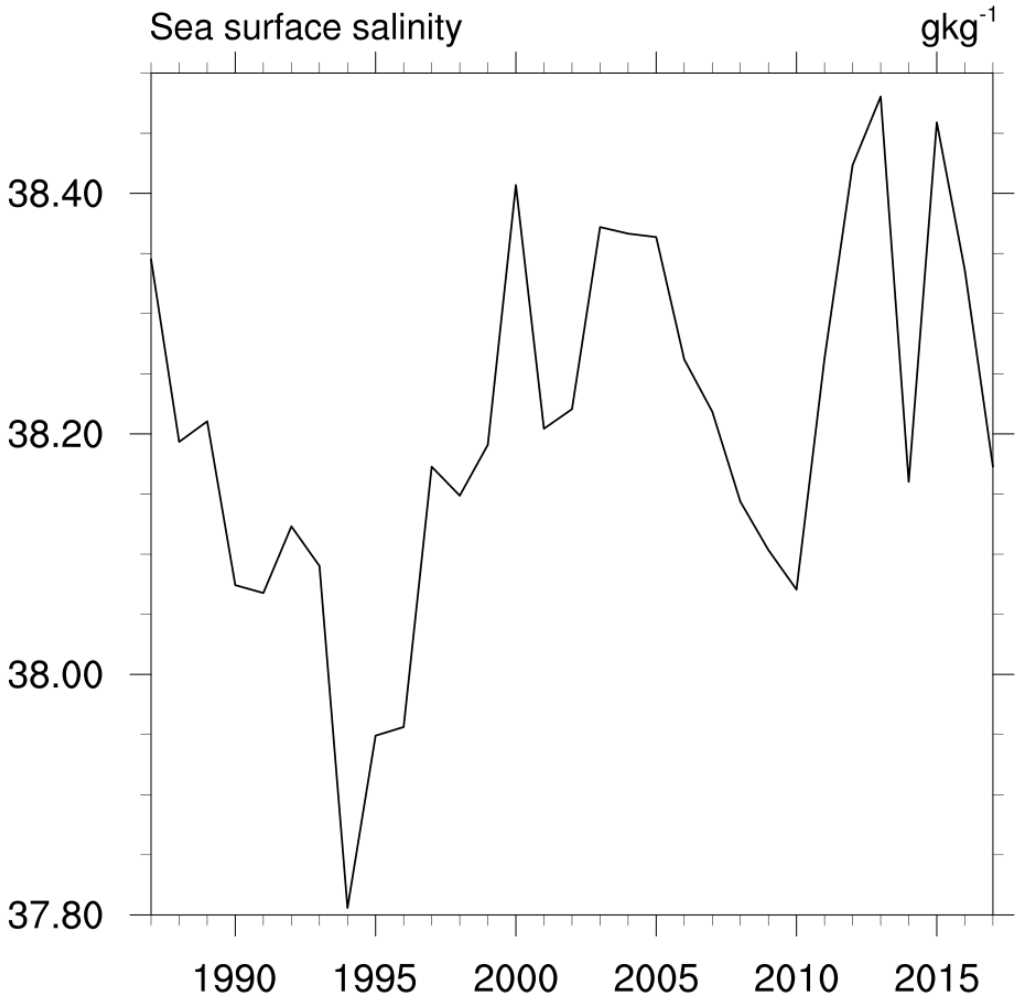

Figure 126. Annual surface salinity time series in the period 1987-2017 at the Vransko Lake site as simulated by the AdriSC modelling suite.

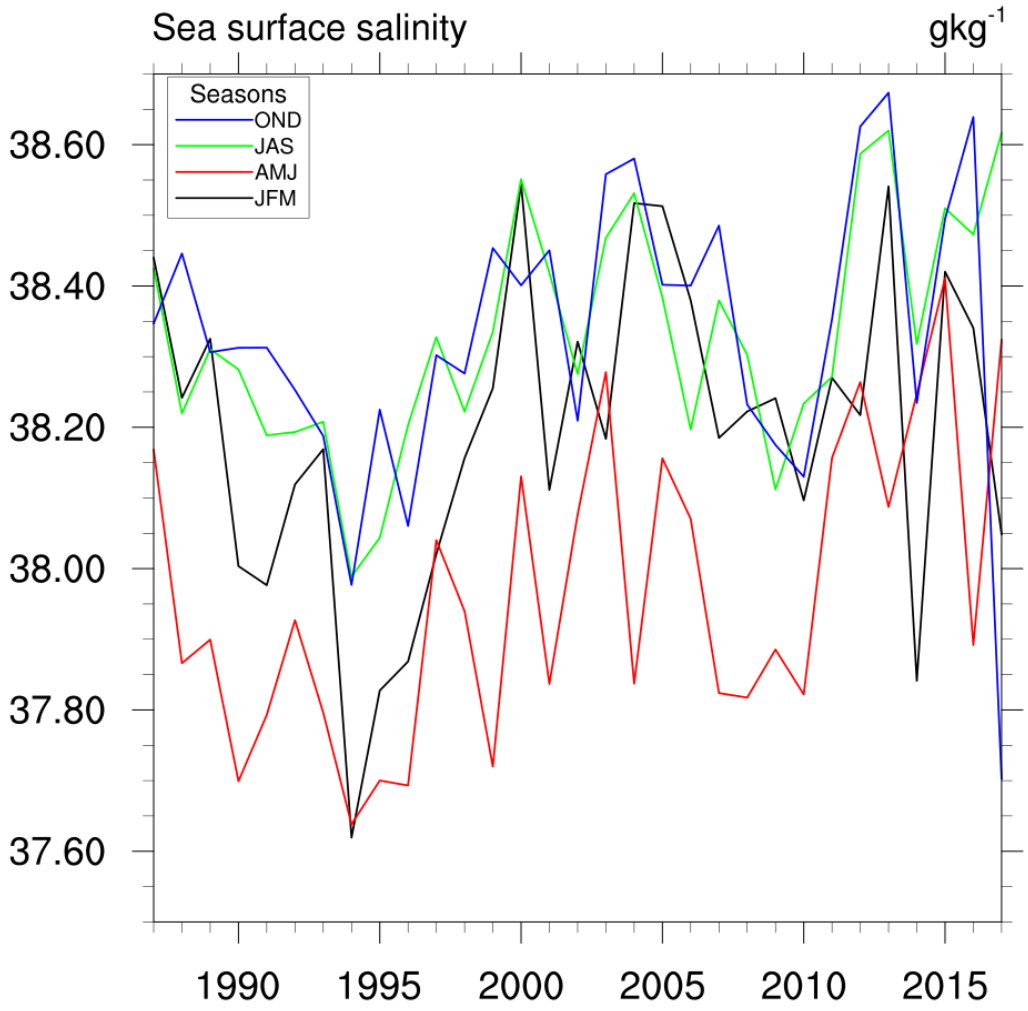

Figure 127. Seasonal surface salinity time series in the period 1987-2017 at the Vransko Lake site as simulated by the AdriSC modelling suite.

4.3.3. Assessment of hydrological variables and processes

The measurements of water levels in Vrana Lake has no substantial long-term trends, yet with a high interannual variability (Fig. 128). Water level can range for about 2.5 m, while the mean water level normally varies for a metre.

Water level is the highest in February (Fig. 129), while being the lowest in September. In September the water level is just about 10 cm higher than the adjacent sea level, while this difference is about a metre during late winter.

The water inflow to the lake is occurring at several places (Fig. 130), with highest rates in the main channel. All of the inflow is compensated by the outflow through the connecting channel with the sea (Prosika). Strong interannual variability of discharge is measured, peaking in 2010 and being lowest in 2007 and 2008.

As the water level of the lake is no much higher than of the sea, the sea may have an intrusion to the lake (Fig. 131). Although a strong variability in salt intrusions is measured, a strong salinization has been measured in the last ten years.

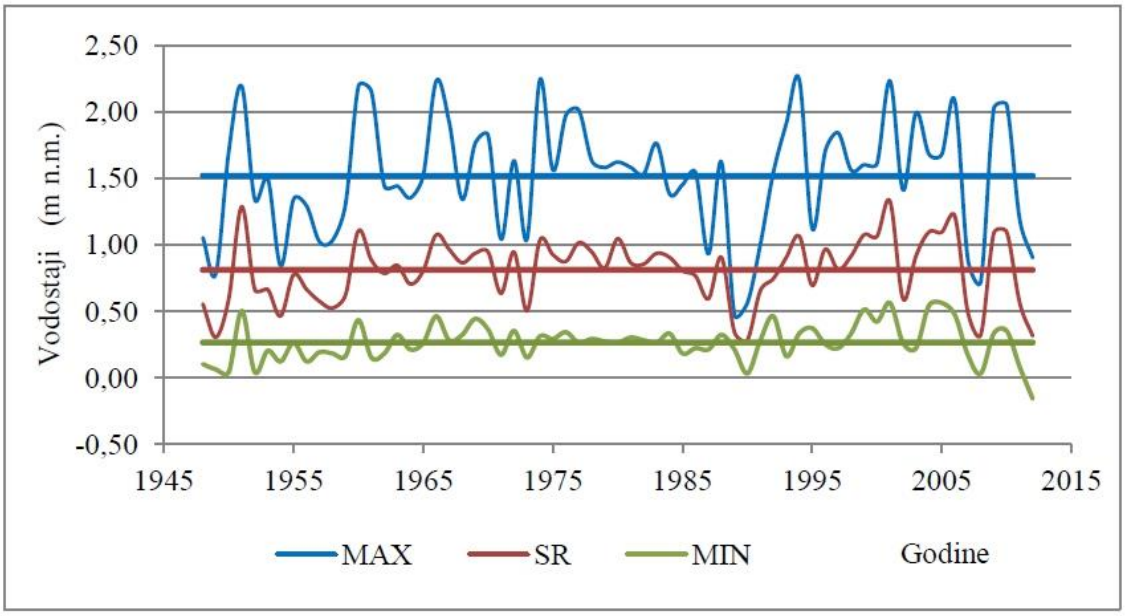

Figure 128. Maximum, mean and minimum water levels in Vrana Lake (after Rubinić, 2014).

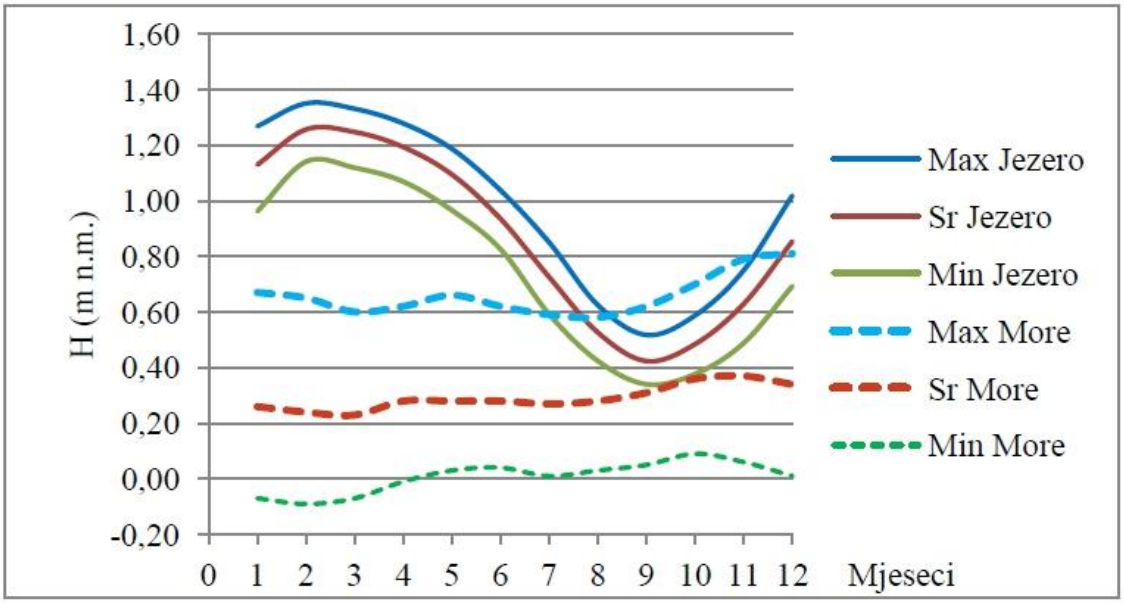

Figure 129. Seasonal course of maximum, mean and minimum water levels in Vrana Lake (jezero) and neighboring sea (more) (after Rubinić, 2014).

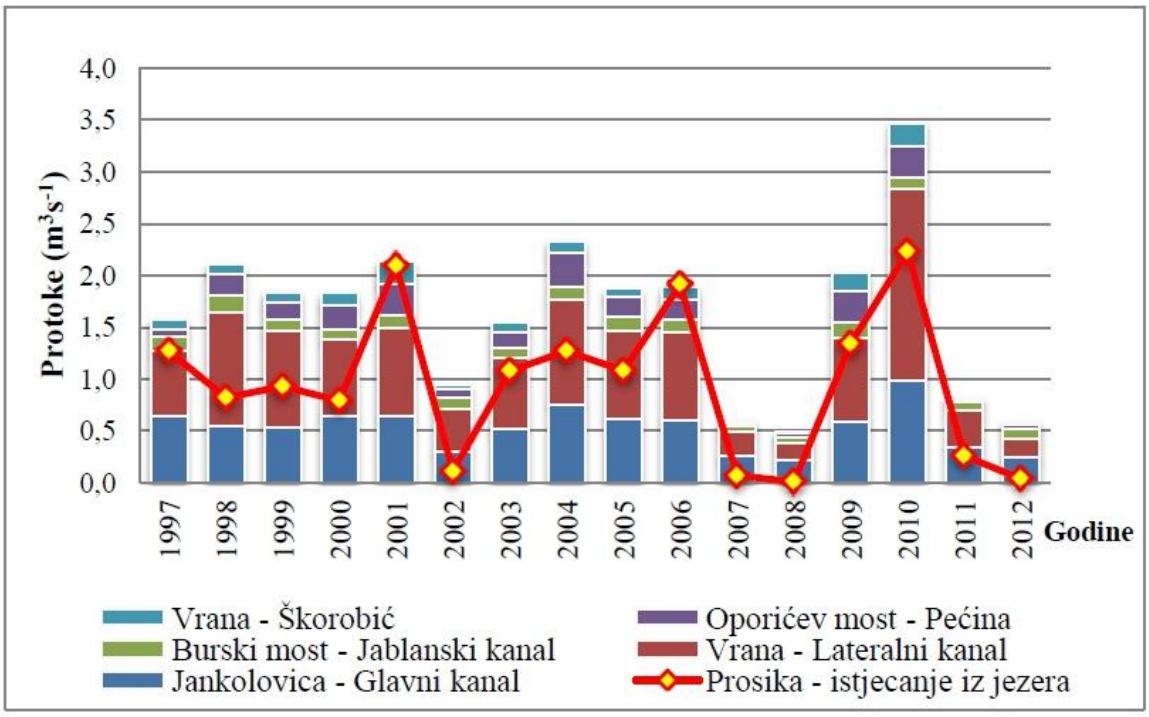

Figure 130. Annual discharge rates in Vrana Lake (after Rubinić, 2014).

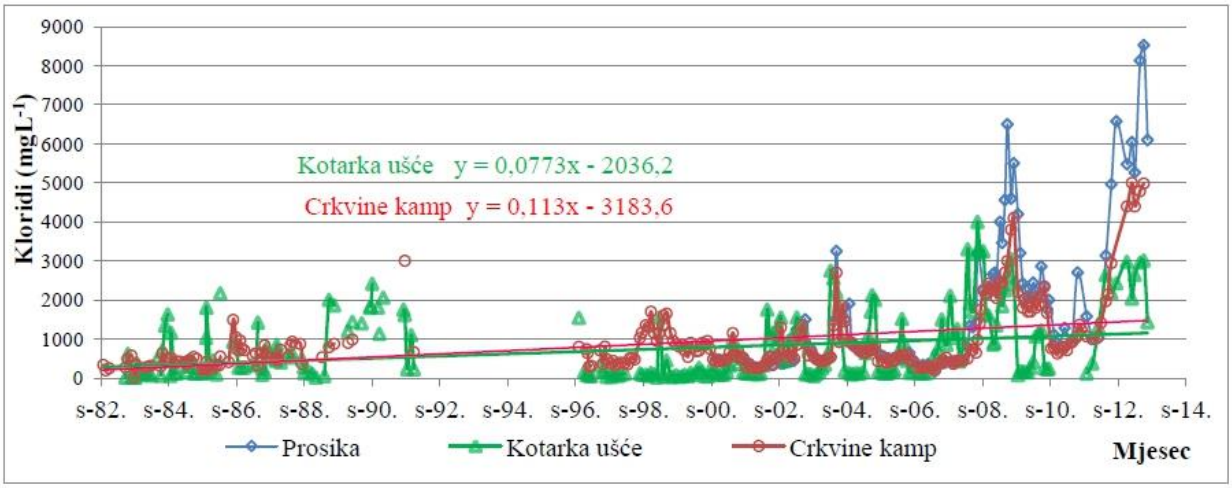

Figure 131. Concentration of chlorides in Vrana Lake (after Rubinić, 2014).

4.4. Jadro River

4.4.1. Assessment of atmospheric variables and processes

The annual time series of temperature at 2 m and precipitation are extracted for the area of Jadro River site from the AdriSC climate simulation (1987-2017). The analysis accompanies the fields the modelled atmospheric fields described in Section 2.3.

Annual values of temperature at 2 m range from 13.0 to 14.5 ^{o}C (Fig. 132), where the last value is reached in 2014. Clear temperature trend can be seen in the series, while annual temperatures can change for about 1 ^{o}C between years. The warming trend may be seen in all seasons (Fig. 133), while being lowest during winter. Mean temperatures range between 7 and 10 ^{o}C during winter, while summer mean temperatures span from 19 to 21 ^{o}C.

The precipitation rate (Fig. 134) is changing between 1 and 3 mm/day, i.e. between 400 and 1100 mm per year. The precipitation rate is maximal during autumn (Fig. 135), when it might reach 5 mm/day, while the minimum precipitation rate is achieved during summer, when it might go down to 0.5 mm/day, or about 50 mm per season.

The wind rose (Fig. 136) denotes the strongest winds from northeast, which are resembling bora conditions and the jet coming from Klis through a valley. Also, sirocco wind from southeast can blow strongly in the Jadro River site, although with lower frequency as somewhat protected by a mountainous area.

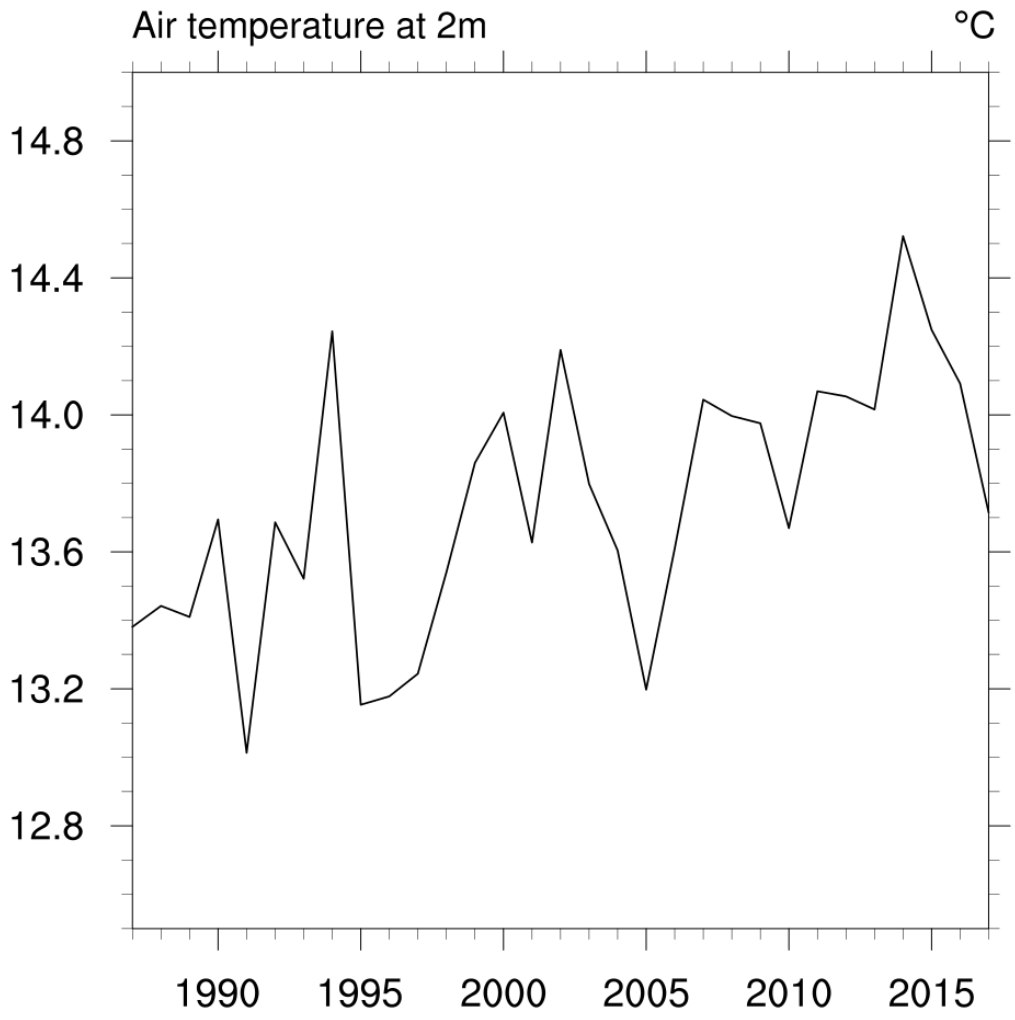

Figure 132. Annual air temperature at 2 m time series in the period 1987-2017 at the Jadro River site as simulated by the AdriSC modelling suite.

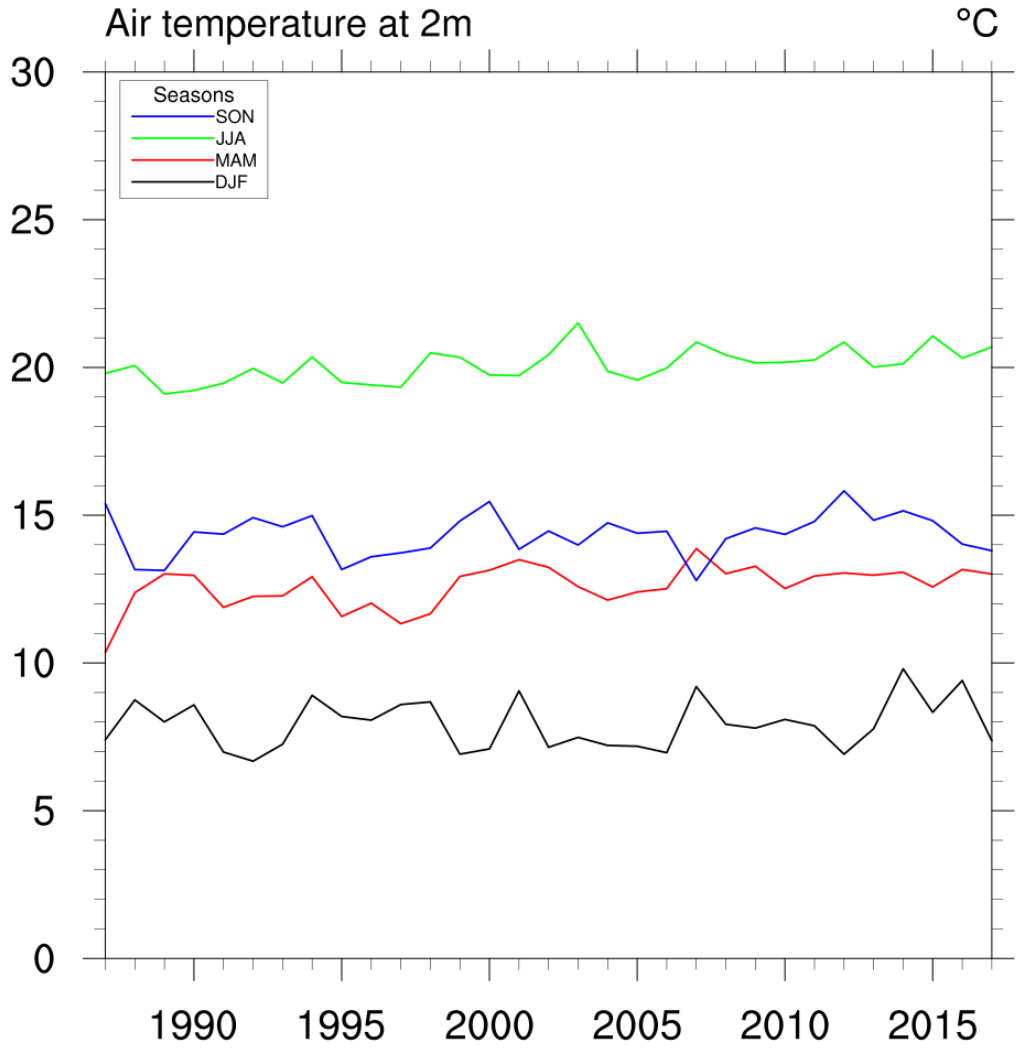

Figure 133. Seasonal air temperature at 2 m time series in the period 1987-2017 at the Jadro River site as simulated by the AdriSC modelling suite.

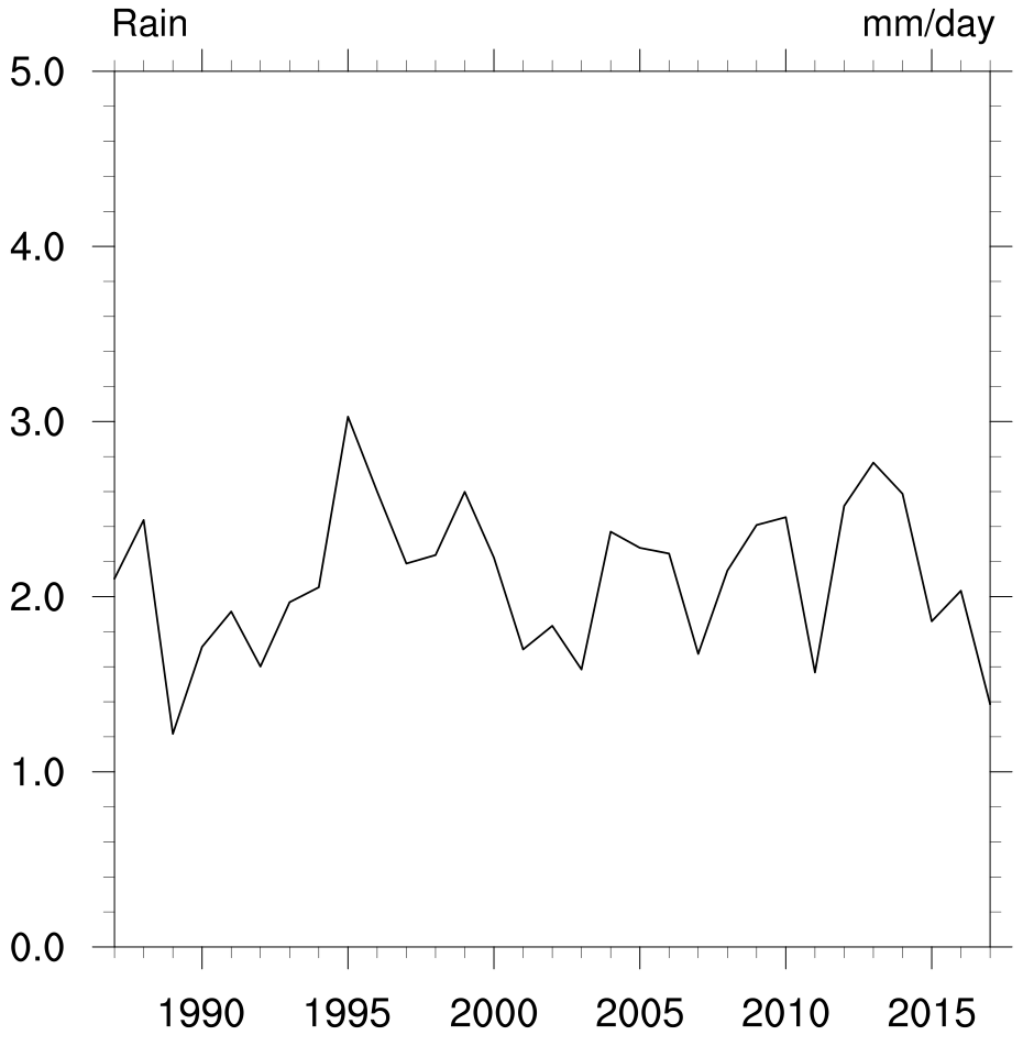

Figure 134. Annual precipitation time series in the period 1987-2017 at the Jadro River site as simulated by the AdriSC modelling suite.

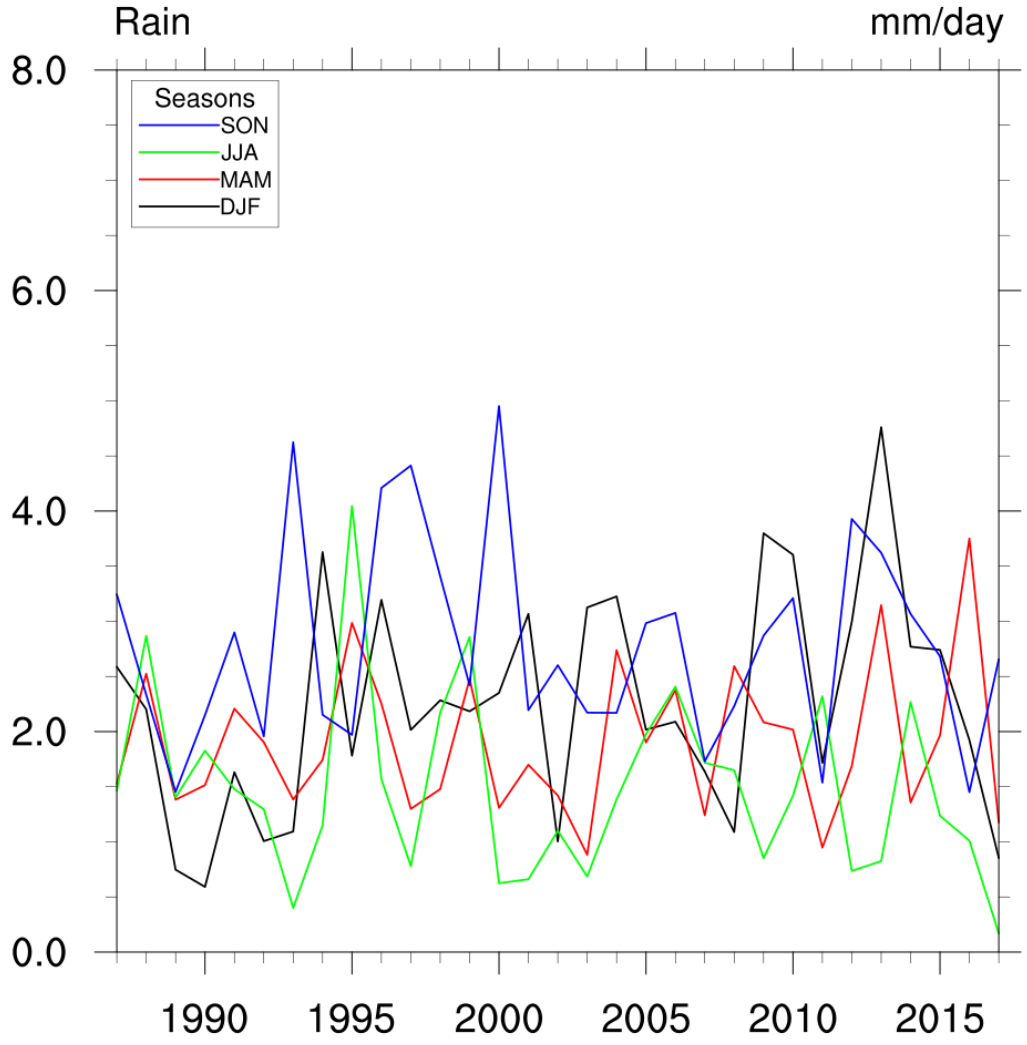

Figure 135. Seasonal precipitation rate time series in the period 1987-2017 at the Jadro River site as simulated by the AdriSC modelling suite.

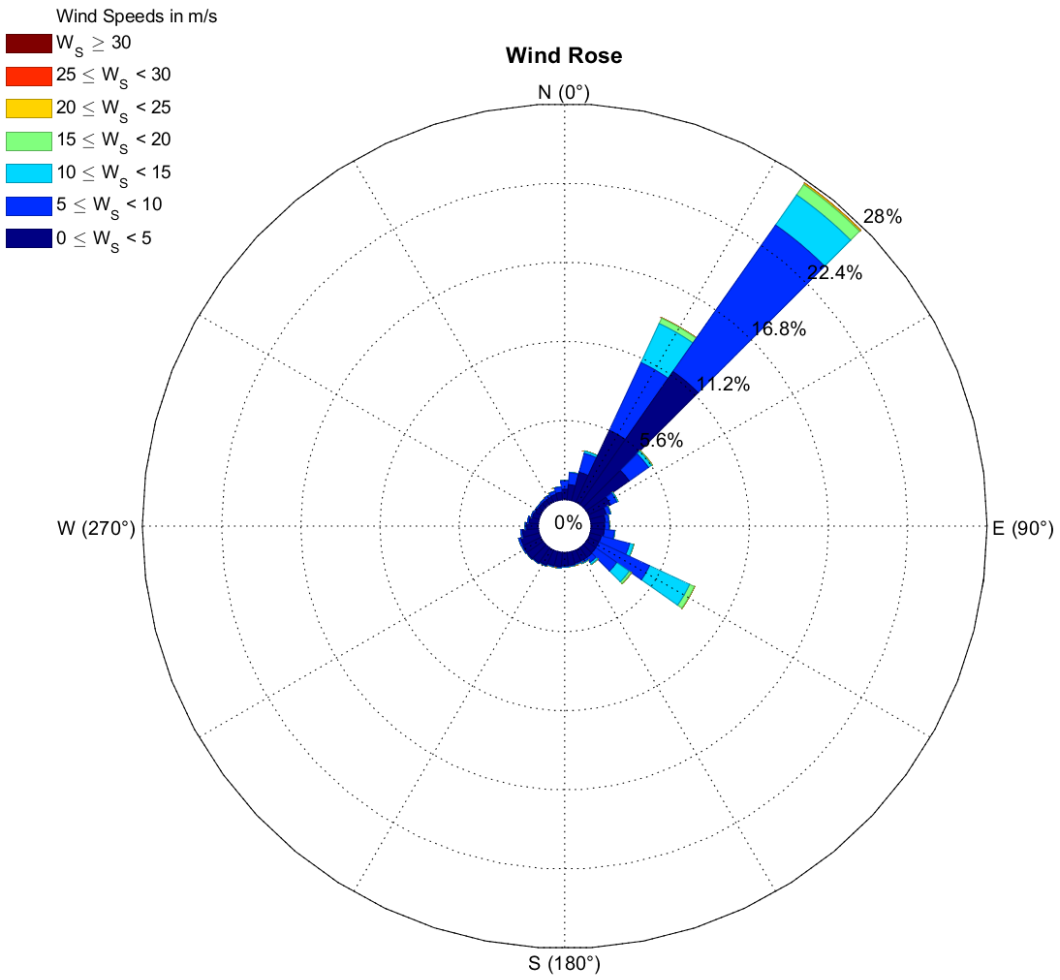

Figure 136. Wind rose at the Jadro River site as simulated by the AdriSC modelling suite (1987-2017).

4.4.2. Assessment of oceanic variables and processes

Off the Jadro River mouth, the mean annual temperature (Fig. 137) has values rising from 17.0 °C at the beginning of the AdriSC simulation to around 18.0 °C at the end of the AdriSC simulation. The positive trends are strong in all seasons (Fig. 138). Sea surface salinity has strong interannual variability, ranging from 37.2 to 37.7, with lowest values in spring and highest in summer (Figs. 139-140). Sea level constantly rose in the considered period (Fig. 141), yet with quite strong interannual variability and being the highest in autumn (Fig. 142).

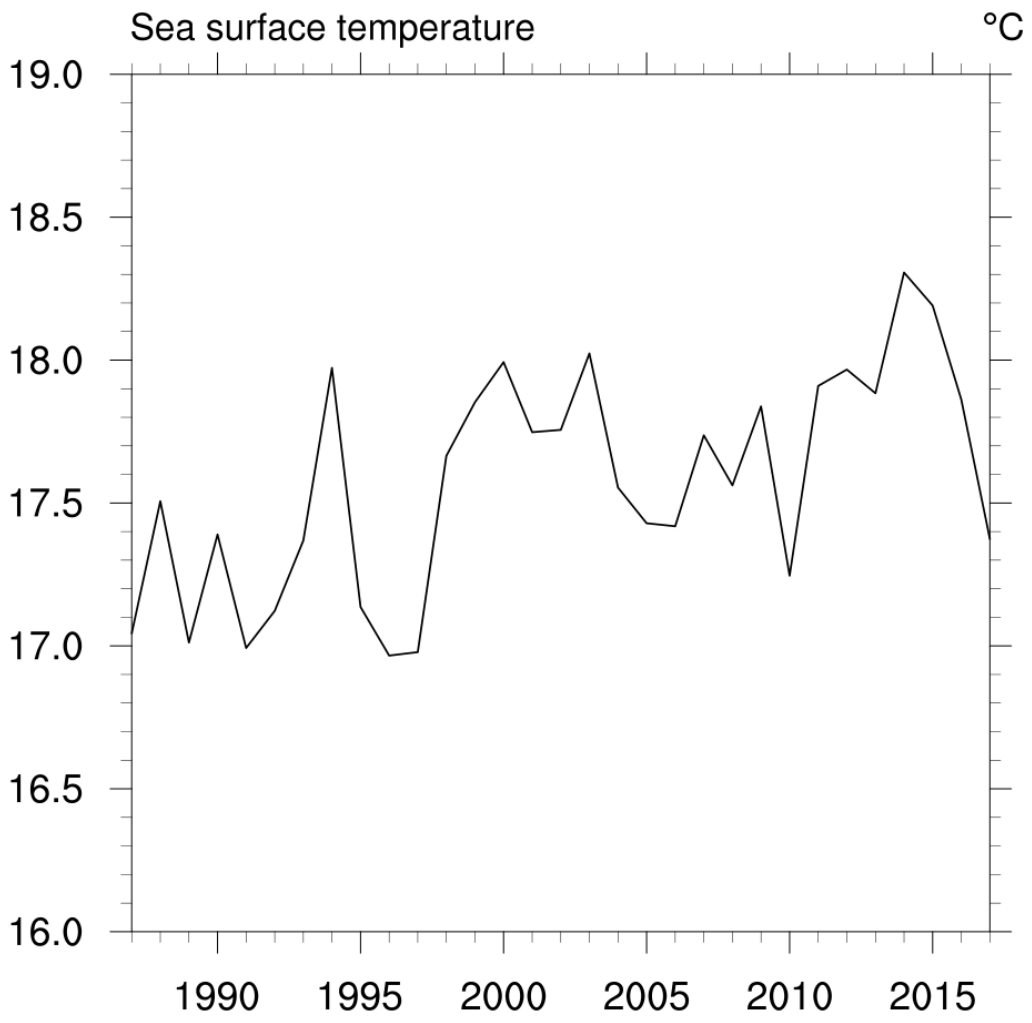

Figure 137. Annual sea surface temperature time series in the period 1987-2017 at the Jadro River site as simulated by the AdriSC modelling suite.

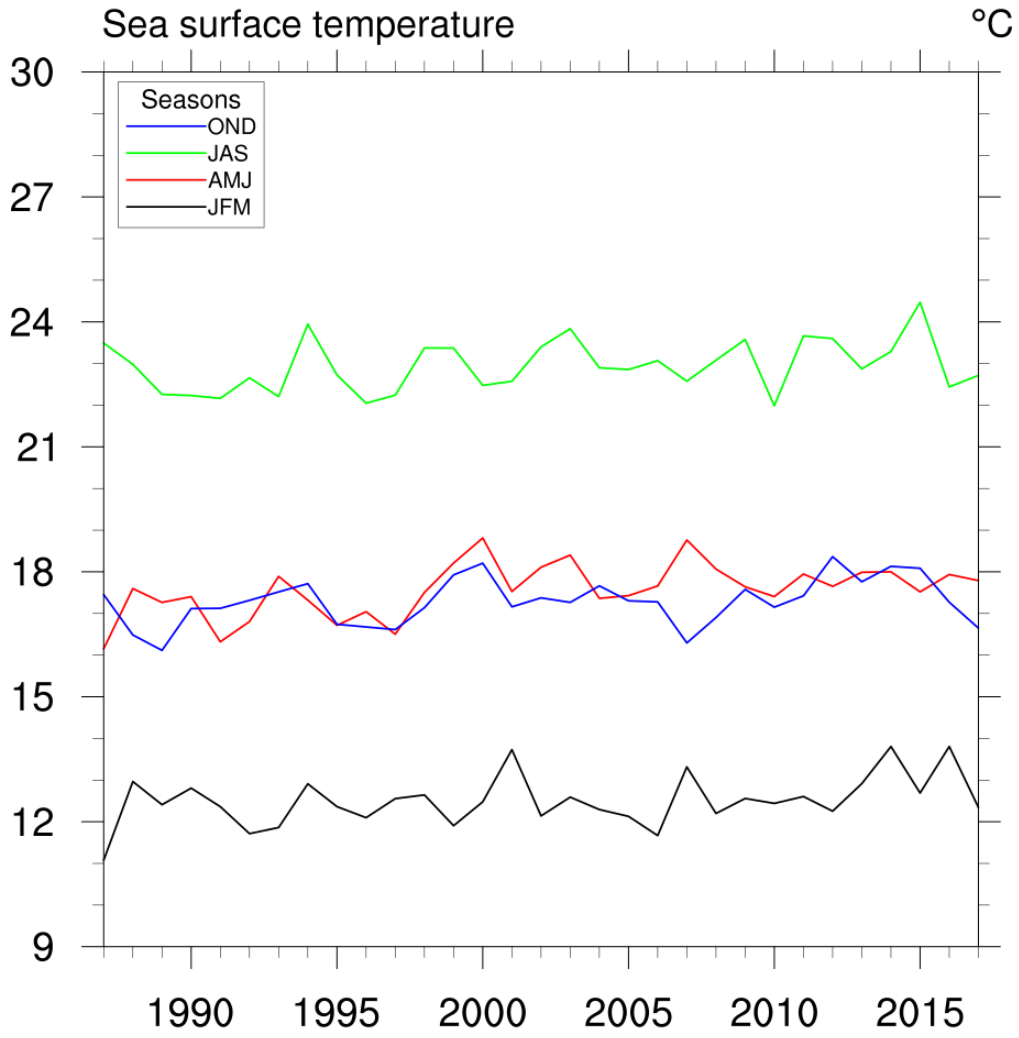

Figure 138. Seasonal sea surface temperature time series in the period 1987-2017 at the Jadro River site as simulated by the AdriSC modelling suite.

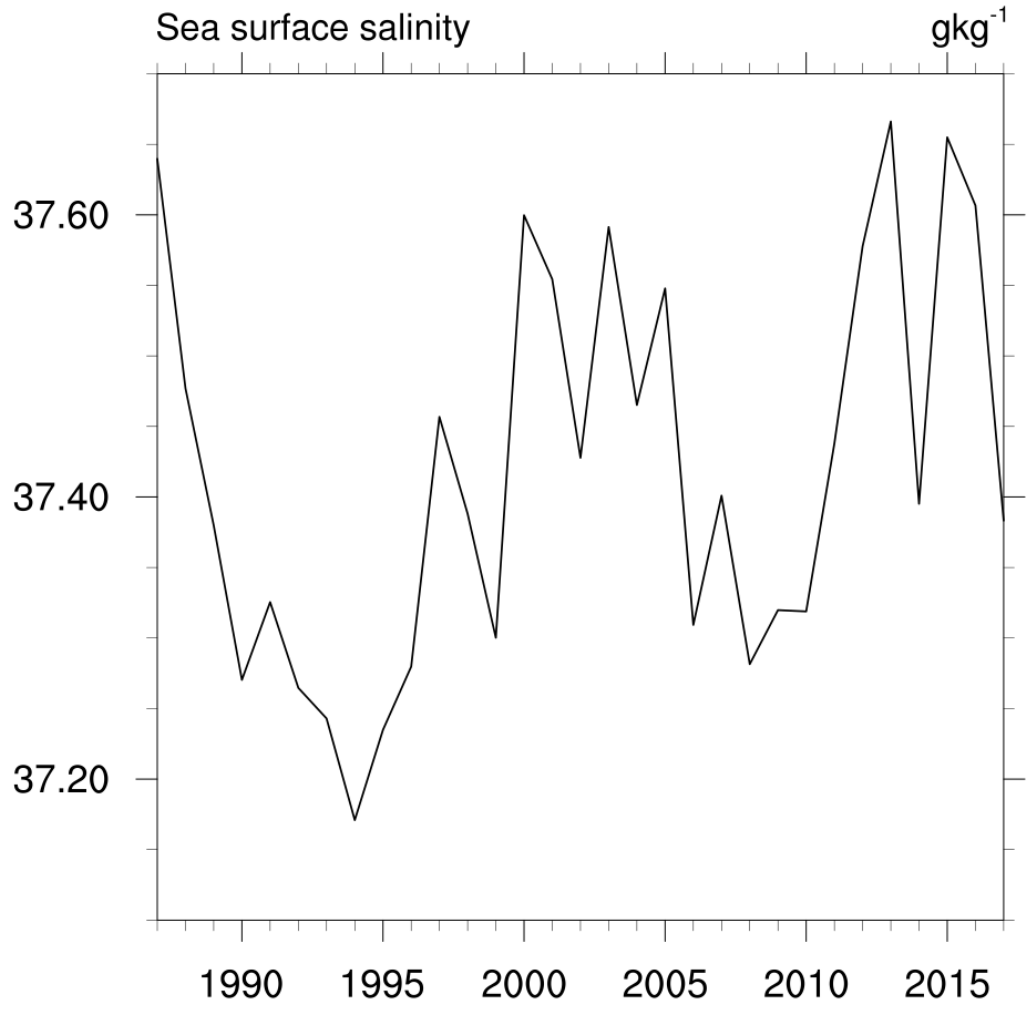

Figure 139. Annual surface salinity time series in the period 1987-2017 at the Jadro River site as simulated by the AdriSC modelling suite.

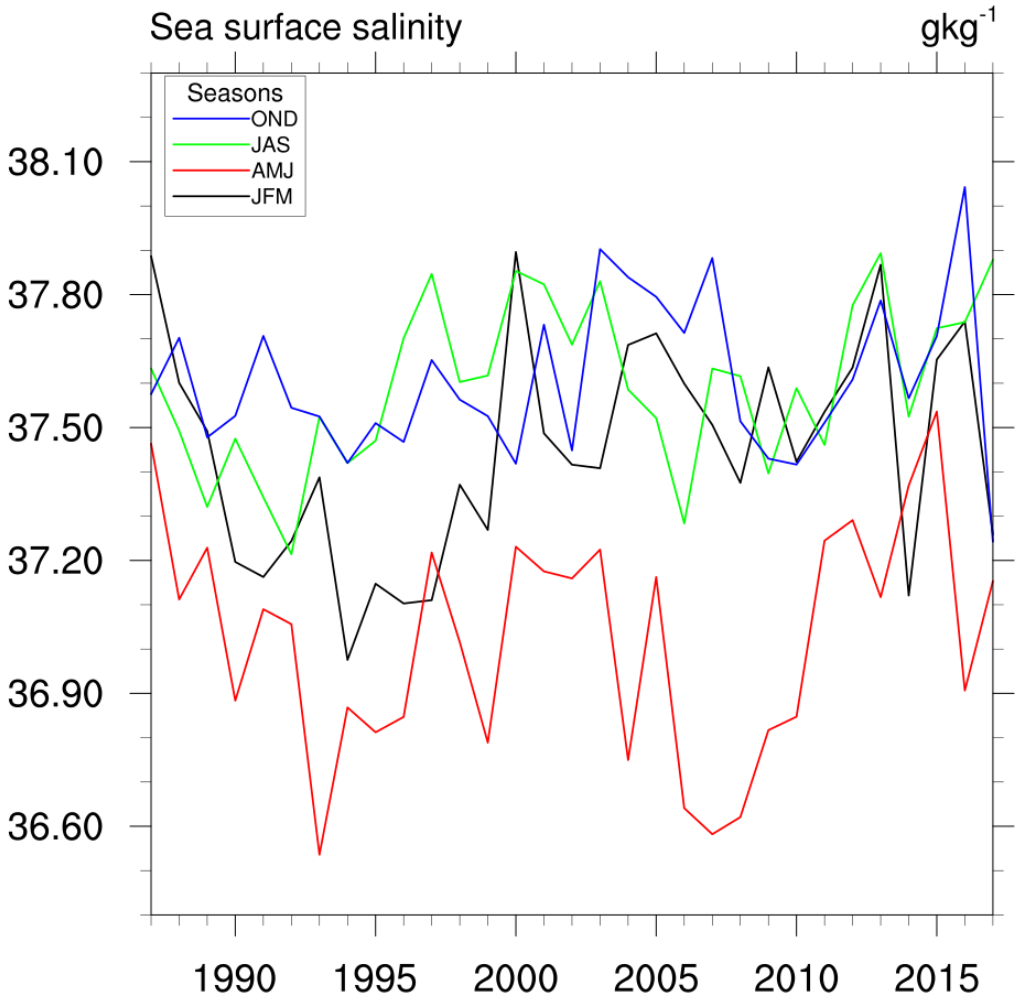

Figure 140. Seasonal surface salinity time series in the period 1987-2017 at the Jadro River site as simulated by the AdriSC modelling suite.

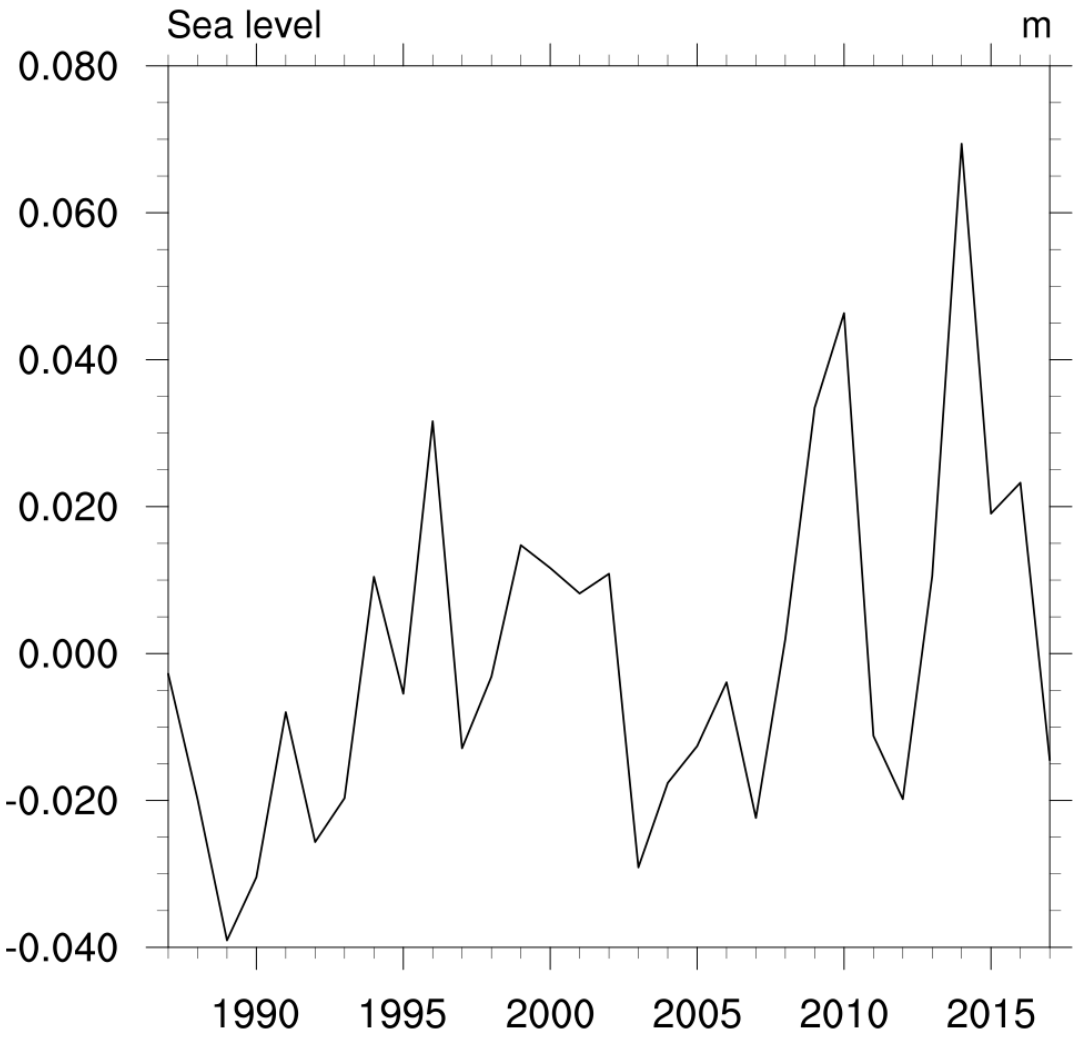

Figure 141. Annual sea surface height time series in the period 1987-2017 at the Jadro River site as simulated by the AdriSC modelling suite.

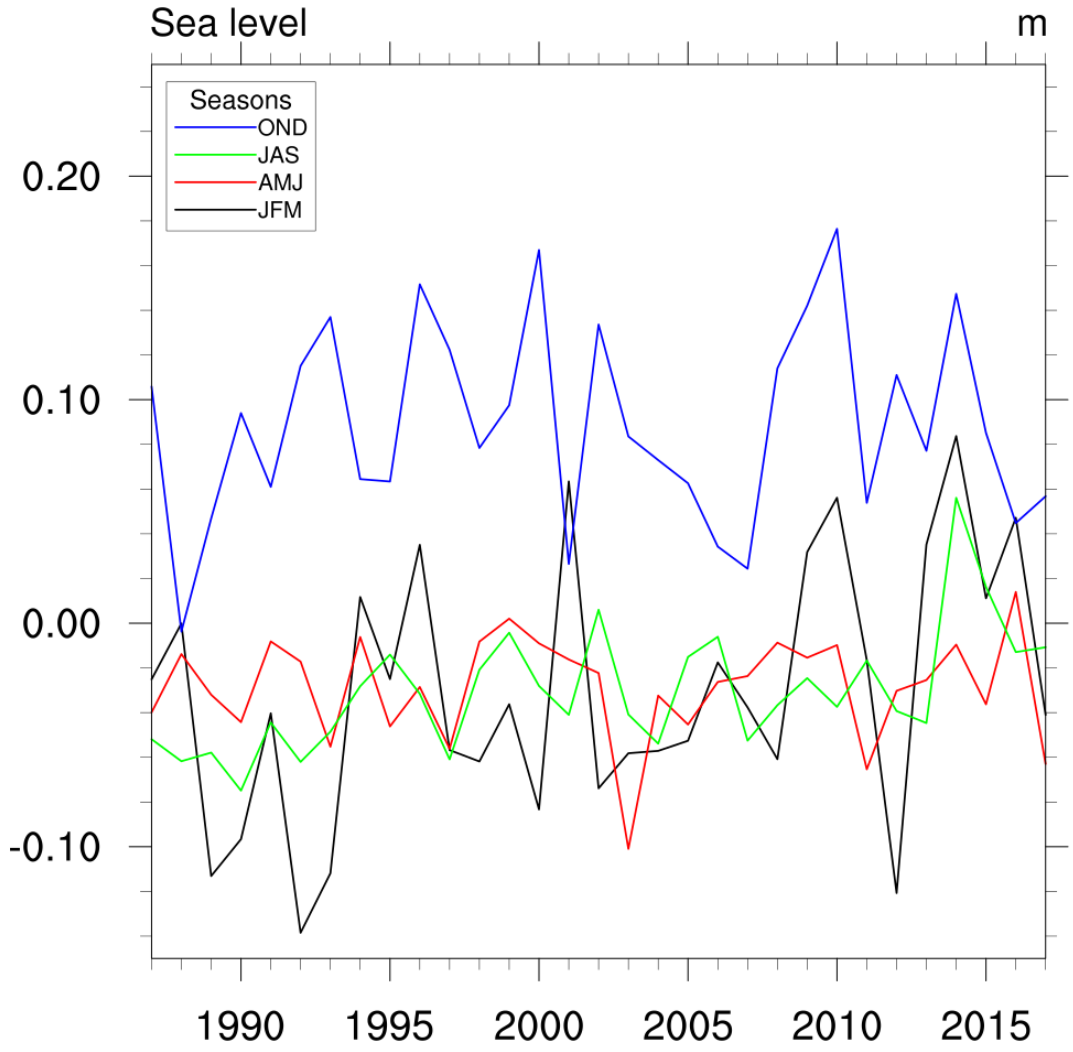

Figure 142. Seasonal sea surface height time series in the period 1987-2017 at the Jadro River site as simulated by the AdriSC modelling suite.

4.5. Neretva River

4.5.1. Assessment of atmospheric variables and processes

The annual time series of temperature at 2 m and precipitation are extracted for the area of Neretva River site from the AdriSC climate simulation (1987-2017). The analysis accompanies the fields the modelled atmospheric fields described in Section 2.3.

Annual values of temperature at 2 m range from 14.7 to 16.0 ^{o}C (Fig. 143), while interannual variability is lower than at other four pilot sites. Clear temperature trend can be seen in the series, while annual temperatures can change for about 1 ^{o}C between years. The warming trend may be seen in all seasons (Fig. 144), being the highest during summer and the lowest during winter. Mean temperatures range between 8.5 and 12 ^{o}C during winter, while summer mean temperatures span from 20.5 to 22.5 ^{o}C.

The precipitation rate (Fig. 145) is changing between 1 and 3 mm/day, i.e. between 400 and 1100 mm per year. The precipitation rate is maximal during autumn (Fig. 146), when it might reach 5 mm/day, while the minimum precipitation rate is achieved during summer, when it might go down to 0.5 mm/day, or about 50 mm per season.

The wind rose (Fig. 147) denotes the strongest winds from northeast, which are resembling bora conditions and the jet coming from Klis through a valley. Also, sirocco wind from southeast can blow strongly in the Jadro River site, although with lower frequency as somewhat protected by a mountainous area.

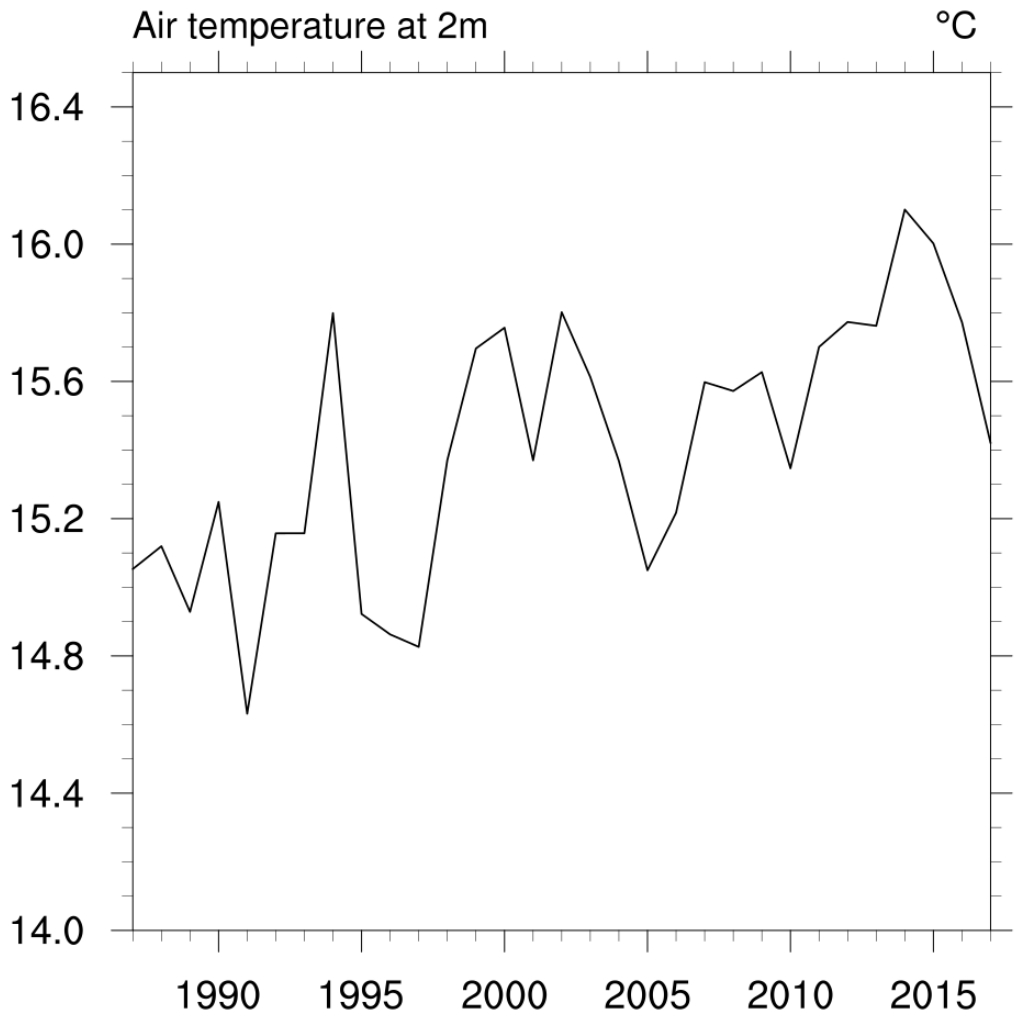

Figure 143. Annual air temperature at 2 m time series in the period 1987-2017 at the Neretva River site as simulated by the AdriSC modelling suite.

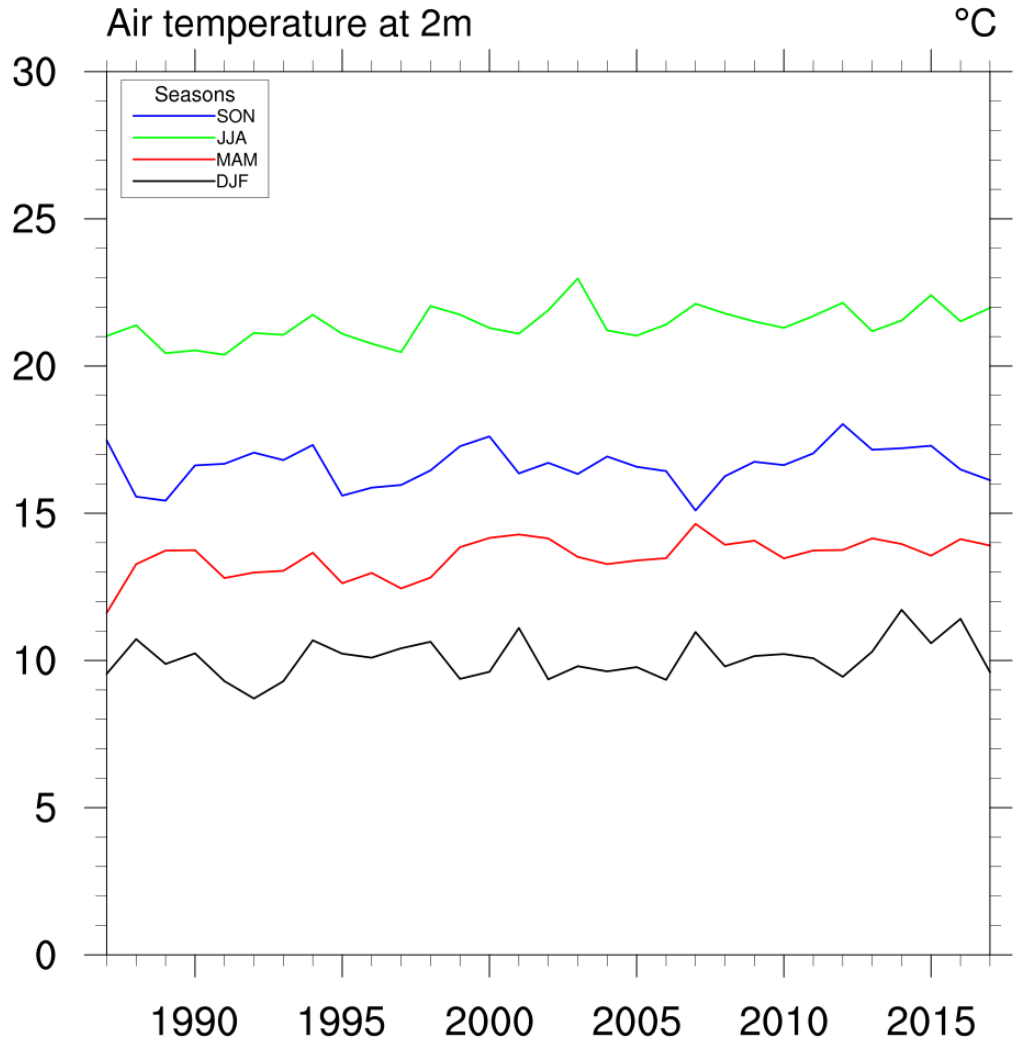

Figure 144. Seasonal air temperature at 2 m time series in the period 1987-2017 at the Neretva River site as simulated by the AdriSC modelling suite.

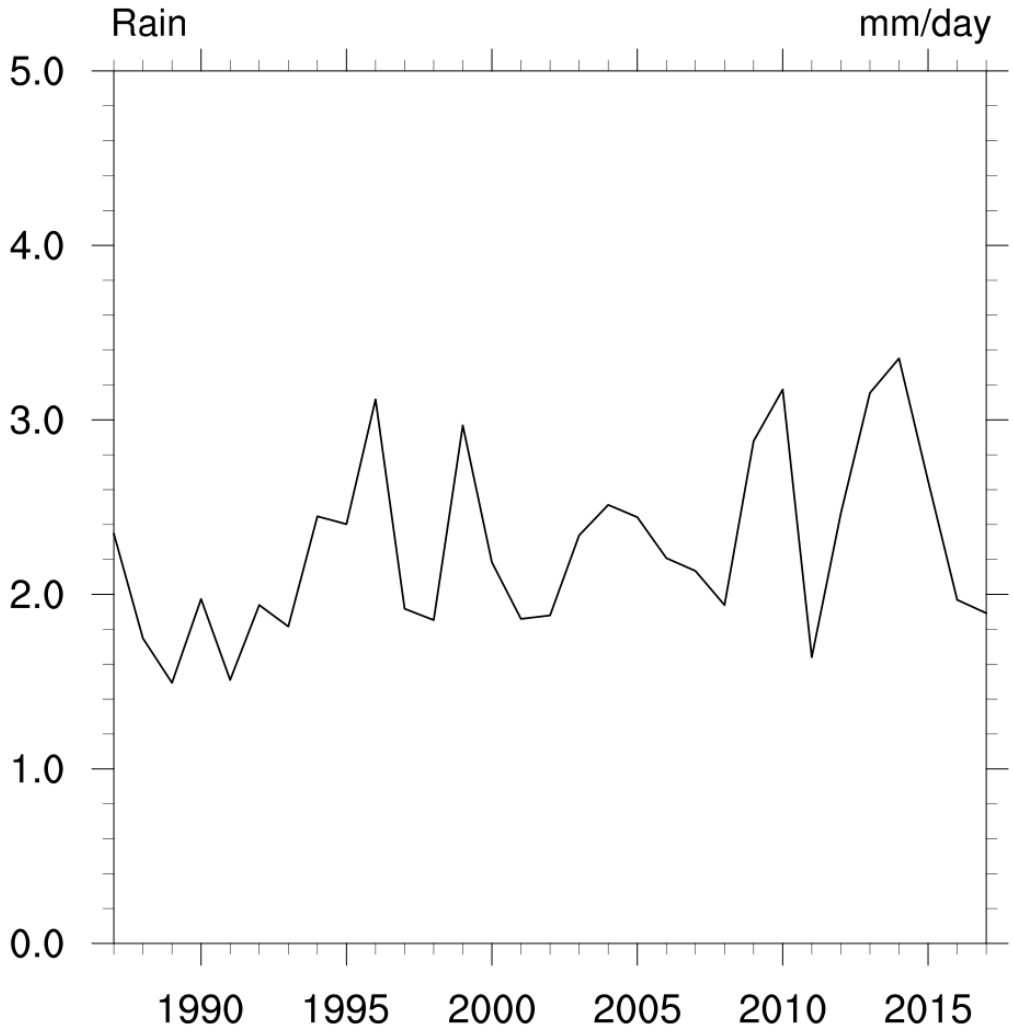

Figure 145. Annual precipitation time series in the period 1987-2017 at the Neretva River site as simulated by the AdriSC modelling suite.

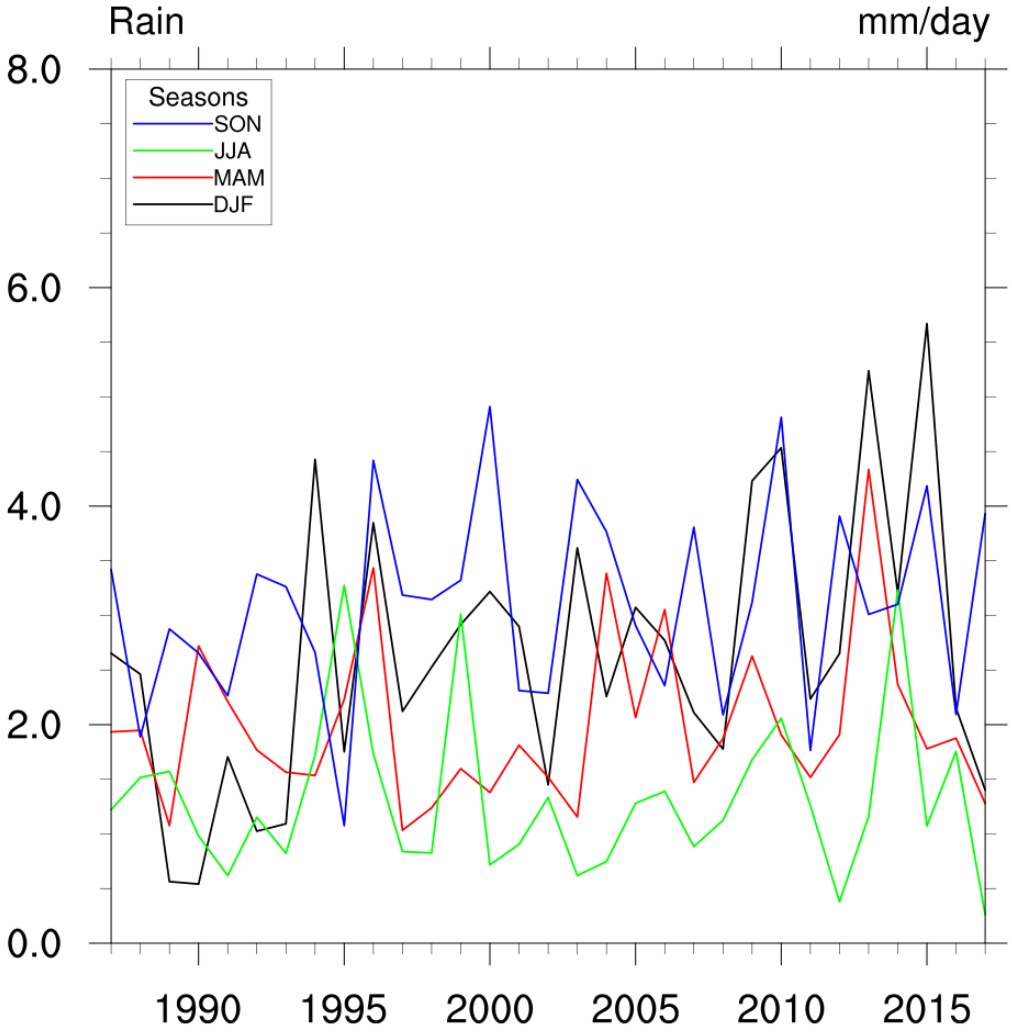

Figure 146. Seasonal precipitation rate time series in the period 1987-2017 at the Neretva River site as simulated by the AdriSC modelling suite.

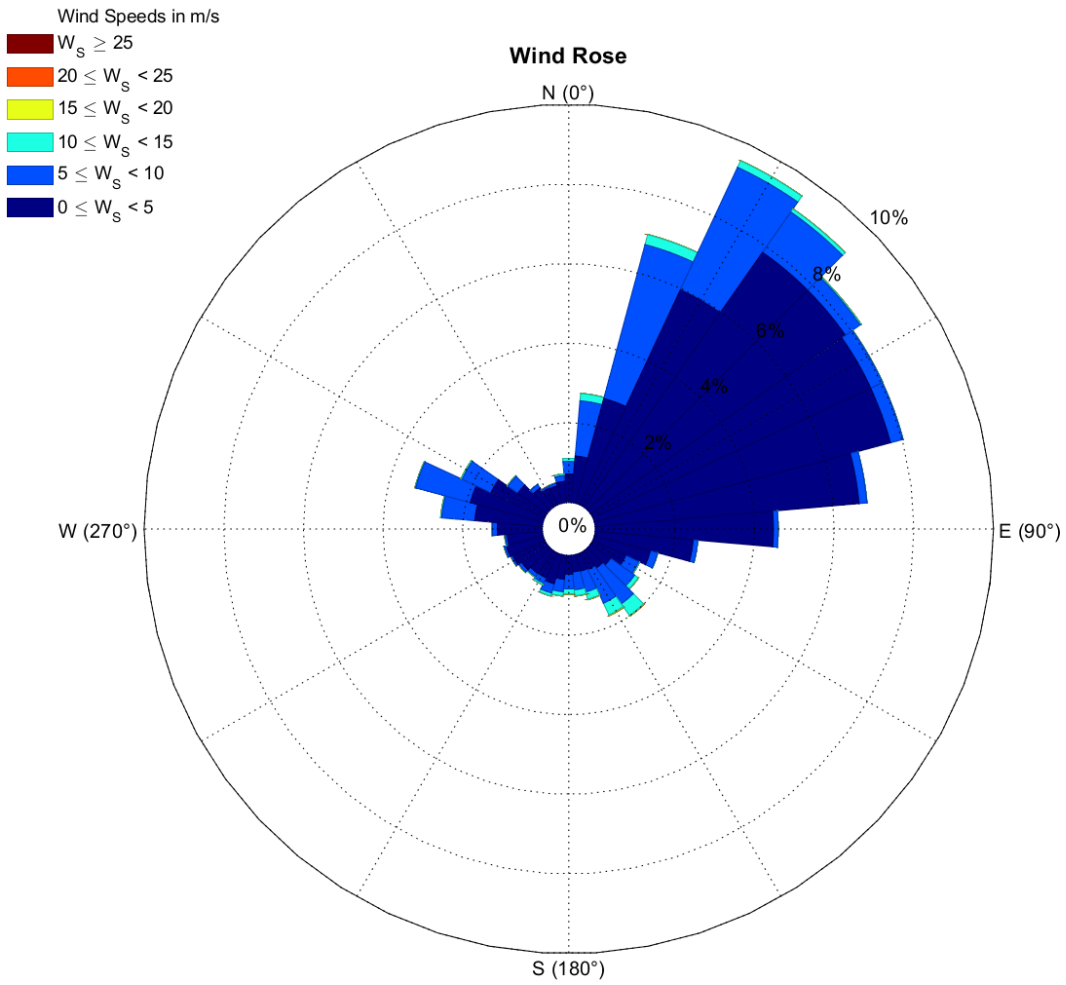

Figure 147. Wind rose at the Neretva River site as simulated by the AdriSC modelling suite (1987-2017).

4.5.2. Assessment of oceanic variables and processes

Off the Neretva River delta, the mean annual temperature (Fig. 148) has values rising from 18.5-19.0 °C at the beginning of the AdriSC simulation to around 19.5-20.0 °C at the end of the AdriSC simulation. The positive trends are strong in all seasons (Fig. 149). Sea surface salinity has strong interannual variability, ranging from 38.2 to 38.7, with lowest values in summer (Figs. 150-151). Sea level constantly rose in the considered period but having strong interannual variability (Fig. 152), yet with quite strong interannual variability and being the highest in autumn and then I summer (Fig. 153).

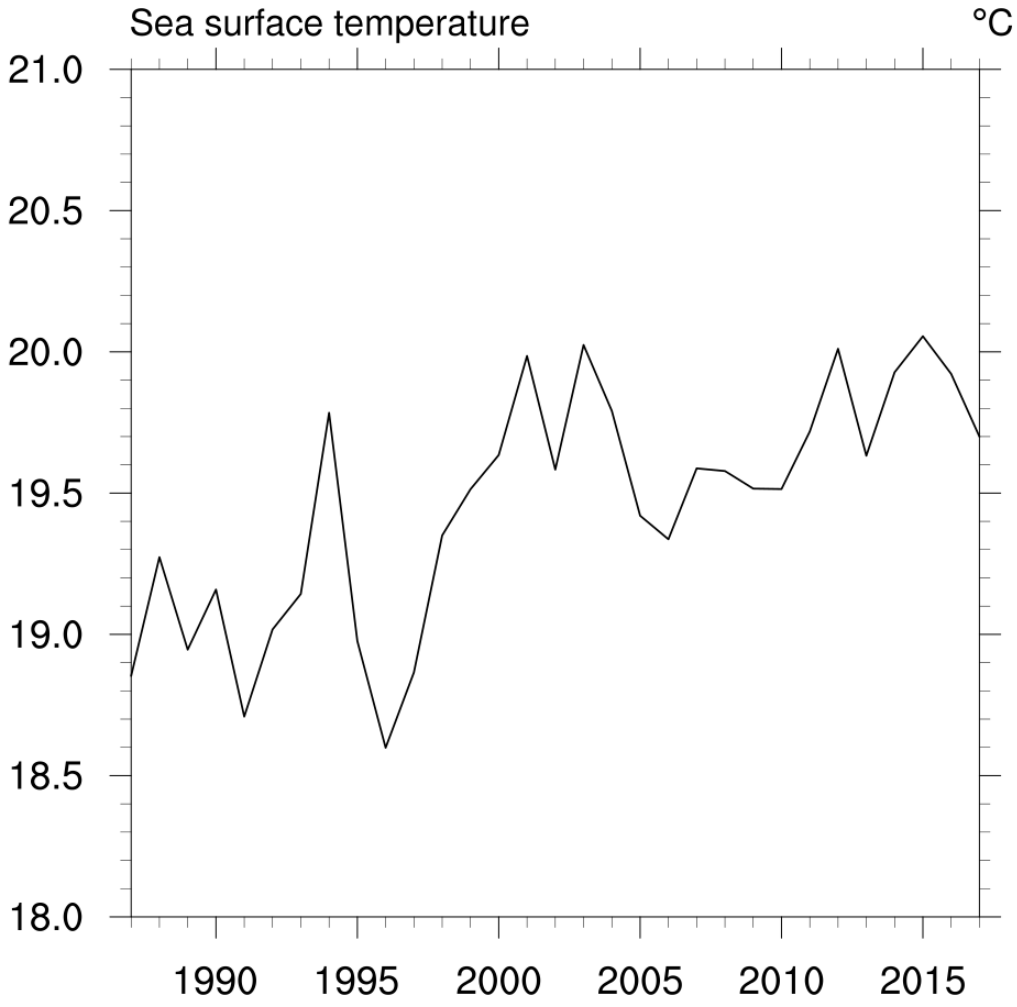

Figure 148. Annual sea surface temperature at the Neretva River site as simulated by the AdriSC modelling suite (1987-2017).

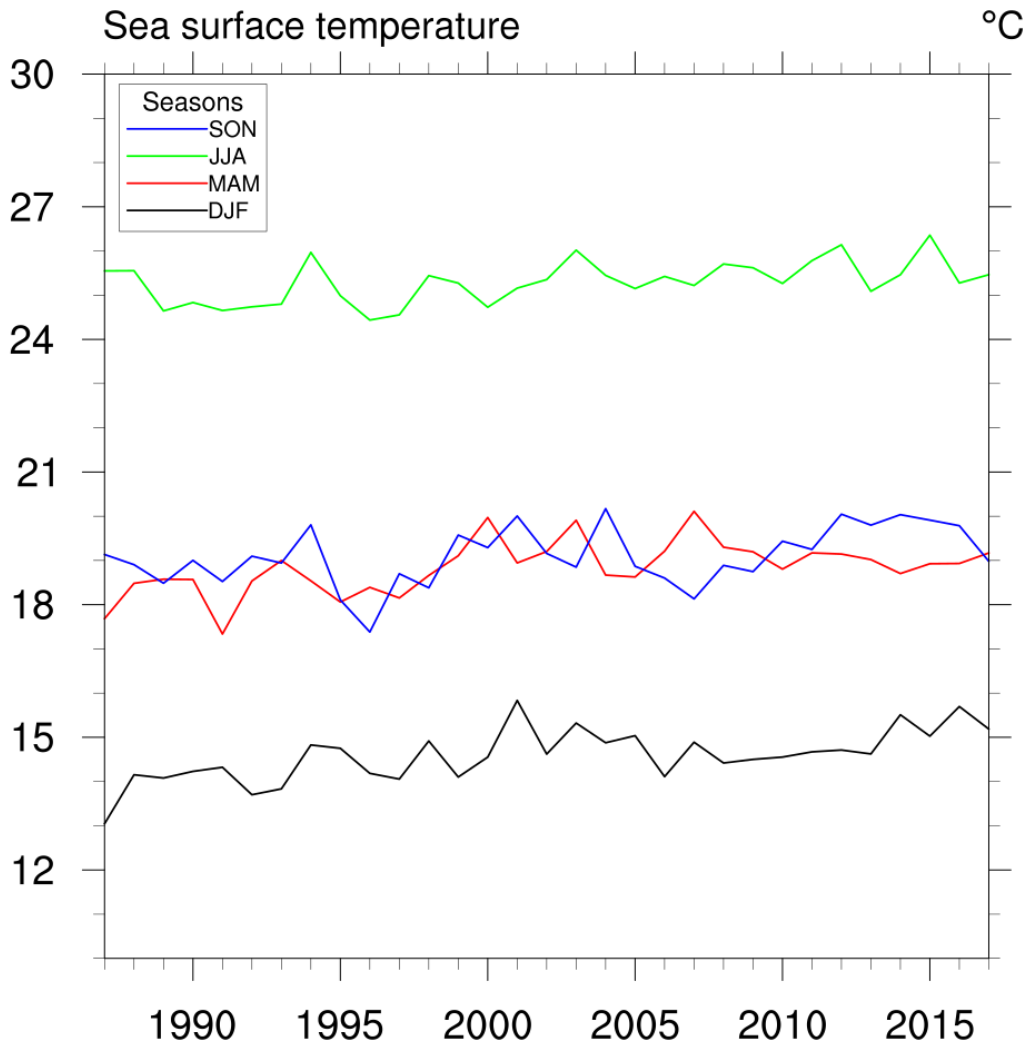

Figure 149. Seasonal sea surface temperature at the Neretva River site as simulated by the AdriSC modelling suite (1987-2017).

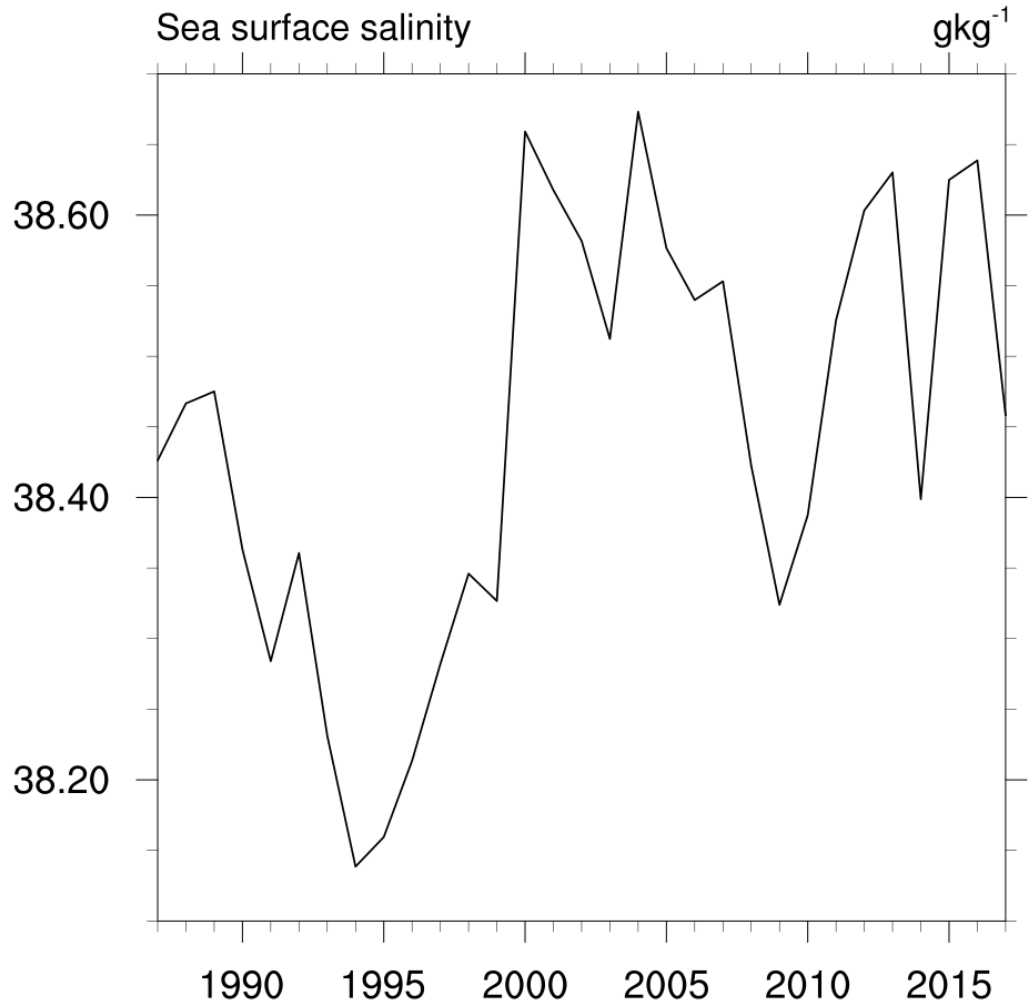

Figure 150. Annual surface salinity at the Neretva River site as simulated by the AdriSC modelling suite (1987-2017).

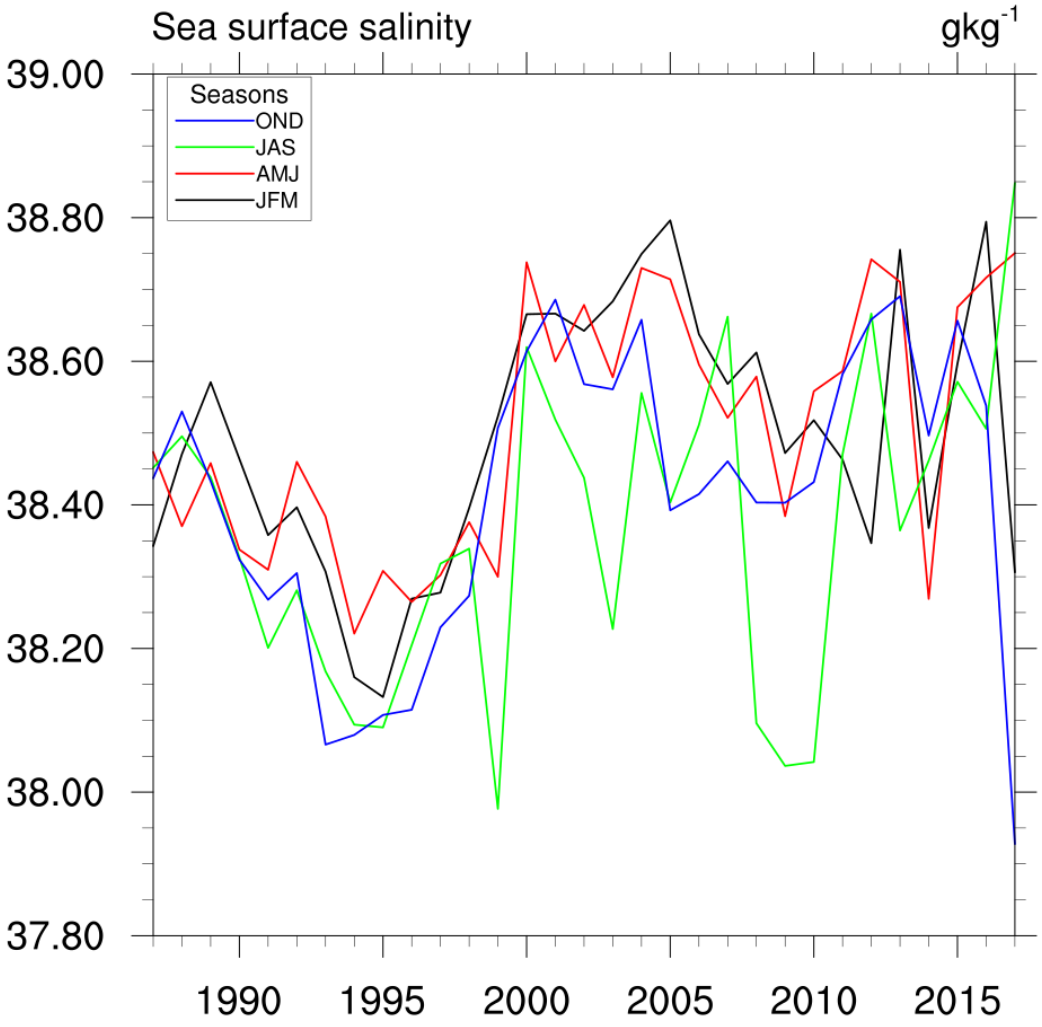

Figure 151. Seasonal surface salinity at the Neretva River site as simulated by the AdriSC modelling suite (1987-2017).

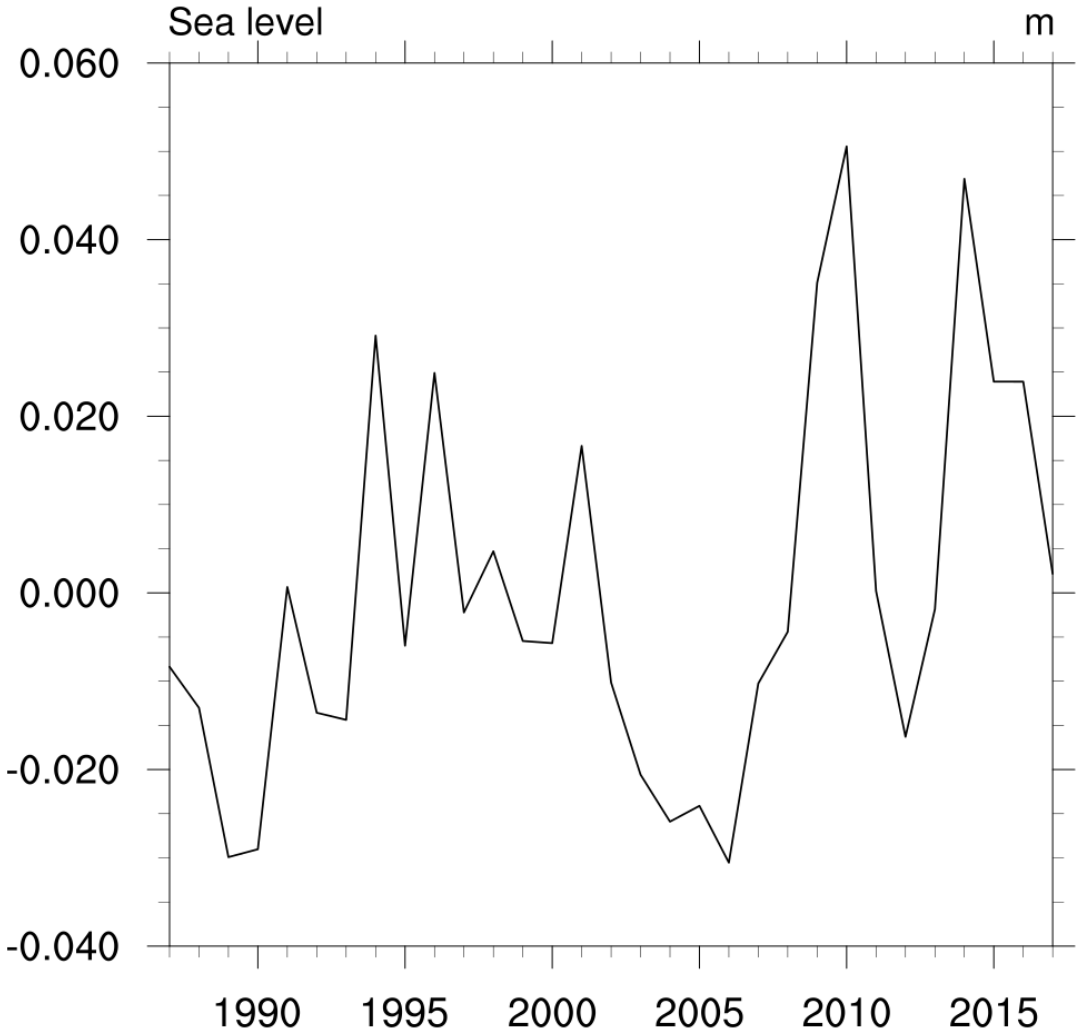

Figure 152. Annual sea surface height at the Neretva River site as simulated by the AdriSC modelling suite (1987-2017).

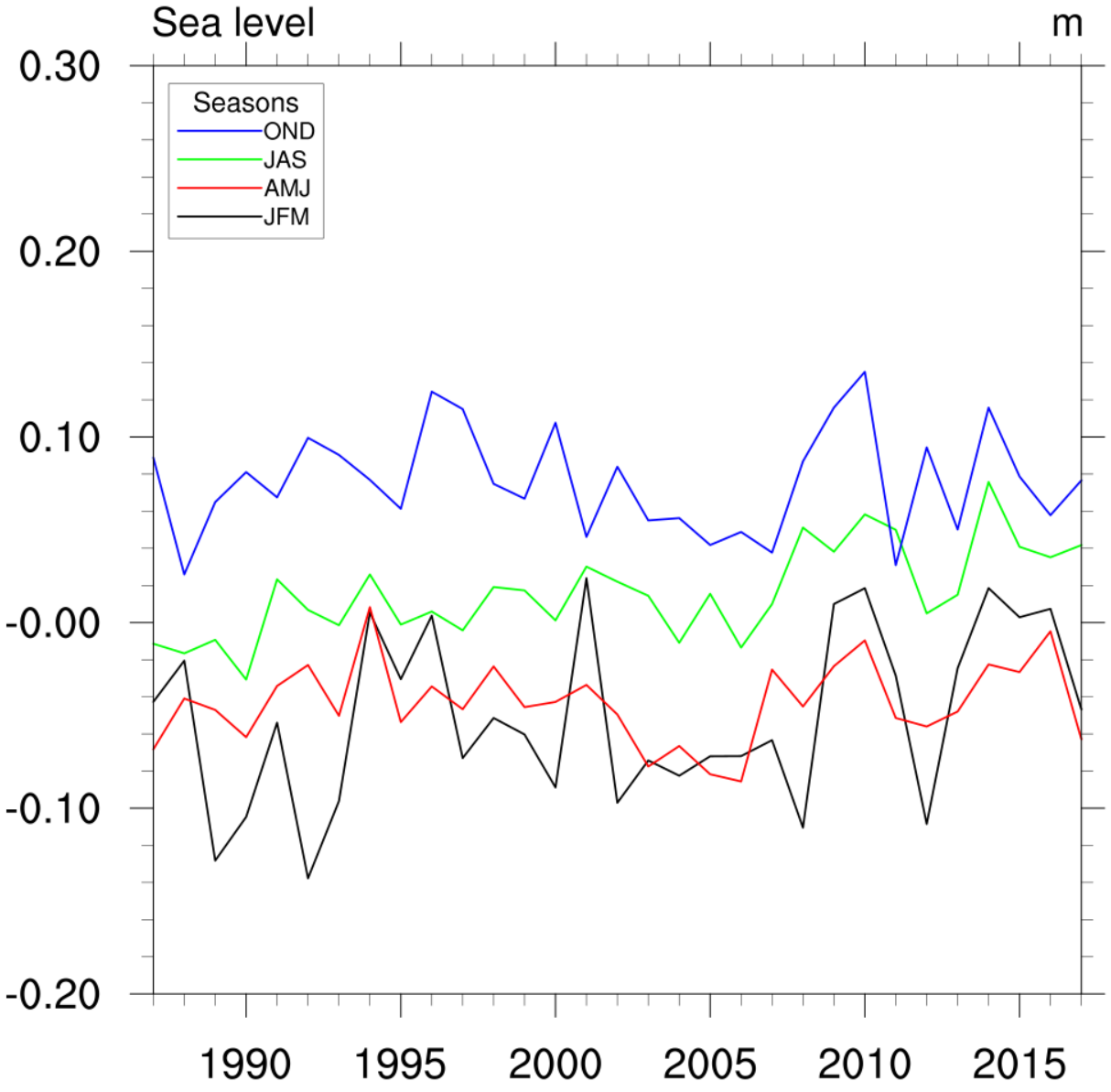

Figure 153. Seasonal sea surface height at the Neretva River site as simulated by the AdriSC modelling suite (1987-2017).

5. DATA SET ON PHYSICAL AND METEO-OCEANIC PROCESSES IN THE ADRIATIC SEA

A selection of the observational data and numerical model fields presented in this report is made publicly available as Deliverable 3.1.2, accessible from the Project Owncloud at the following link: https://owncloud.ve.ismar.cnr.it/owncloud/index.php/s/g4DVSdo58YTdgTK

6. SUMMARY AND CONCLUSIONS

This report contains an overview of present knowledge of climate changes in the Adriatic Sea, both in the atmospheric and in the ocean, by overviewing the scientific literature, analysing long-term in situ observations and presenting brand new results coming from the 31-year long atmosphere-ocean climate model. The analyses included both the Adriatic-wide climate and well as the climate of the five CHANGE WE CARE pilot sites.

Multi-decadal time series of measured data needed for climate studies are generally provided by long term model simulations (hindcasts). Valuable as they are, these estimates are necessarily affected by the approximations involved within the modelling process. However, the model allows to properly document spatial and temporal characteristics of both atmospheric and ocean processes. For the purpose of the Adriatic Sea climate assessment, we used the data coming from the AdriSC climate simulations and assesses trends and variability of variables in both the Adriatic and pilot sites. A warming trend might be seen in simulations, with high interannual variability in the atmosphere and interannual to decadal variability in the sea. The trends in the atmosphere differ between the seasons, being the largest in the summer, following the observations. Long-term observations also provides the following: (1) the decrease in precipitation in the most of the basin and in particular over the northern Italy, (3) a negative trend in freshwater budget in the Adriatic Sea, (3) an increase of annual number of dry days in the coastal Adriatic, (4) weakening of the Adriatic thermohaline circulation, i.e. lower water mass exchange between the Adriatic and the Ionian Seas, (5) strong increase in salinity, with the largest trend in coastal regions, (6) decrease in dissolved oxygen content in deep Adriatic layers, (7) acceleration of sea level rise in recent decades, and more.

On the contrary, multi-decadal observed time series are rare, but of course not exempt of problems. Local effects may prevent the identification of trends that are indeed present at large scale. Of course, where available for several decades, measured data are of great value for a number of reasons and can be valuable clues to delve further into the physics of the processes

of interest, especially if considering that waves, as an integrated product of the local climate, can provide related compact and meaningful information. Reliable multi-decadal time series of wind and wave data for climate studies are crucial for establishing climatology, analyzing trends, and estimating return values, hence for planning of long term sea operations. On a general scale and with global cover they are generally provided by long-term model simulations (hindcasts).

Also a critical approach to the single dataset analysis helps digging into the analysis of the physical processes of interest in order to get reliable long-term trends. The characterization of wind and wave conditions and storminess based on directional analysis for instance brings out a more detailed description of the different regimes, their associated meteorological conditions and their variation in time and geographical space (crossed sea conditions, distribution of energy on direction, etc.), with the possibility of widening the picture of the climate change processes in action.

Further, we can explore the long-term trends of the relevant partitions in order to assess the possible correlation between the local scale and the general climate and to use the measured data as long-term indicators of its evolution, thus helping the overall understanding of models capability to reproduce the physical processes in a climate change perspective.

The heterogeneity of regimes leading to waves along the bora direction is a likely explanation. In general, these results confirm the necessity of multiple analysis. Wave data, especially in relatively enclose zones, are capable to summarize in a compact information the complexity of the local meteorological situation. As a consequence, they are strongly related to the general large-scale meteorological and long-term climate patterns that determine the conditions in that basin. As such, where available, for a sufficiently long time, they are valuable to be exploited as a source of information.

7. REFERENCES

Branković, Č., Güttler, I., Patarčić, M., Srnec, L., 2010. Climate change impacts and adaptation measures - climate change scenario. In: Fifth National Communication of the Republic of Croatia under the United Nation Framework Convention on the Climate Change, Ministry of Environmental Protection, Physical Planning and Construction, 152-166, https://unfccc.int/resource/docs/natc/hrv_nc5.pdf

Branković, Č., Patarčić, M., Güttler, I., Srnec, L., 2012. Near-future climate change over Europe with focus on Croatia in an ensemble of regional climate model simulations. Climate Research, 52, 227-251.

Cozzi, S., Giani, M., 2011. River water and nutrient discharges in the Northern Adriatic Sea: Current importance and long term changes. Continental Shelf research, 31, 1881-1893.

Cushman-Roisin, B., Naimie, C. E., 2002. A 3d finite-element model of the Adriatic tides. J. Mar. Syst. 37, 279–297.

Dunić, N., 2019. Thermohaline properties and dynamical processes in the Adriatic Sea simulated with regional climate models, Ph.D. Thesis, University of Zagreb, Zagreb, 141 pp.

Eckholm, N., 1905. Sur la réduction du baromètre au niveau de la mer à employer pour les cartes synoptiques jounalières. Bureau Central Météorologique de Stockholm, Suéde. Centraltrykeriet, Stockholm, 9 pp.

Egbert, G.D. and Erofeeva, S.Y., 2002. Efficient inverse modeling of barotropic ocean tides, J. Atmos. Ocean. Tech., 19, 183 – 204.

Egbert, G. D., Bennett, A. F., Foreman, M. G. G., 1994. Topex/Poseidon tides estimated using a global inverse model, J. Geophys. Res., 99, 24,821 – 24,852.

Klein, B., Roether, W., Manca, B.B., Bregant, D., Beitzel, V., Kovačević, V., Luchetta, A., 1999. The large deep water transient in the Eastern Mediterranean. Deep-Sea Research I, 46, 371-414.

Krom, M. D., Kress, N., Brenner, S., 1991. Phosphorus limitation of primary productivity in the eastern Mediterranean Sea. Limnology and Oceanography, 36, 424-432.

Janeković, I., Mihanović, H., Vilibić, I., Tudor, M. (2014). Extreme cooling and dense water formation estimates in open and coastal regions of the Adriatic Sea during the winter of 2012. Journal of Geophysical Research, 119, 3200-3218, doi:10.1002/2014JC009865

Lalaurette F. 2002. Early detection of abnormal weather conditions using a probabilistic extreme forecast index. Q. J. R. Meteorol. Soc. 129: 3037–3057.

Laprise, R., 1992. The Euler Equations of motion with hydrostatic pressure as independent variable. Mon. Wea. Rev., 120, 197–207.

Larson, J., Jacob, R., Ong, E., 2005. The Model Coupling Toolkit: A New Fortran90 Toolkit for Building Multiphysics Parallel Coupled Models. The International Journal of High Performance Computing Applications, 19 (3), pp 277-292. doi:10.1177/1094342005056115

Lipizer, M., Partescano, E., Rabitti, A., Giorgetti, A., Crise, A., 2014. Qualified temperature, salinity and dissolved oxygen climatologies in a changing Adriatic Sea. Ocean Science, 10, 771–797.

Ljubenkov, I., 2015. Hydrodynamic modeling of stratified estuary: case study of the Jadro River (Croatia). Journal of Hydrology and Hydromechanics, 63(1), 29-37, doi: https://doi.org/10.1515/johh-2015-0001

Luettich, R.A., Birkhahn, R.H., Westerink, J.J., 1991. Application of ADCIRC-2DDI to Masonboro Inlet, North Carolina: A brief numerical modeling study. Contractors Report to the US Army Engineer Waterways Experiment Station, August, 1991.

Ludwig, W., E. Dumont, M. Meybeck, and S. Heussner, 2009. River discharges of water and nutrients to the Mediterranean Sea: Major drivers for ecosystem changes during past and future decades? Prog. Oceanogr., 80, 199–217, doi:10.1016/j.pocean.2009.02.001

Malačič, V. and Petelin, B., 2009. Climatic circulation in the Gulf of Trieste (northern Adriatic). J. Geophys. Res., 114, C07002, doi:10.1029/2008JC004904.

Pano, N. and Abdyli, B., 2002. Maximum floods and their regionalization on the Albanian hydrographic river network. International Conference on Flood Estimation. CHR. Report II, 17 Bern, Switzerland, pp.379-388.

Pano, N., Frasheri, A., Avdyli, B., 2010. The Climatic Change Impact in Water Potential Processe on the Albanian Hydrographic River Network. International Congress on Environmental Modelling and Software. 266. https://scholarsarchive.byu.edu/iemssconference/2010/all/266

Petroliagis and Pinson, 2012. Early indication of extreme winds utilising the Extreme Forecast Index. ECMWF Newsletter 132, Summer 2012, pp 13–19.

Philandras, C. M., Nastos, P. T., Kapsomenakis, J., Douvis, K. C., Tselioudis, G., Zerefos, C. S., 2011. Long term precipitation trends and variability within the Mediterranean region, Nat. Hazards Earth Syst. Sci., 11, 3235–3250

Pinardi, N., Allen, I., Demirov, E., De Mey, P., Korres, G., Lascaratos, A., Le Traon, P-Y., Maillard, C., Manzella, G. and Tziavos, C., 2003. The Mediterranean ocean Forecasting System: first phase of implementation (1998-2001). Annales Geophysicae, 21, 3-20, doi:10.5194/angeo-21-3-2003.

Pinardi, N. and Coppini, G., 2010. Operational oceanography in the Mediterranean Sea: the second stage of development. Ocean Science, 6, 263-267.

Pomaro, A., Cavaleri, L., Lionello, P., 2017. Climatology and trends of the Adriatic Sea wind waves: Analysis of a 37-year long instrumental data set. International Journal of Climatology.

Pomaro, A., Cavaleri, L., Papa, A., Lionello, P., 2018. Data Descriptor: 39 years of directional wave recorded data and relative problems, climatological implications and use. Scientific Data 5, 1{12.

Pomaro, A., Cavaleri, L., Papa, A. & Lionello, P., 2018. PANGAEA https://doi.org/10.1594/PANGAEA.885361.

Raicich, F., Colucci, R.R., 2019a. A near-surface sea temperature time series from Trieste, northern Adriatic Sea (1899-2015). Earth System Sciences Data, 11, 761-768, doi: 10.5194/essd-11-761-2019.

Raicich, F., Colucci, R.R., 2019b. Trieste 1899-2015 near-surface sea temperature. SEANOE, doi: 10.17882/58728.

Raicich, F., 2019. Sea level observations at Trieste, Molo Sartorio, Italy. SEANOE, doi: 10.17882/62758.

Rubinić, J., 2014. Water regime of Vransko lake in Dalmatia and climate impacts, Ph. D. Thesis, University of Rijeka, Rijeka.

Shchepetkin, A. F., and McWilliams, J.C., 2005. The regional oceanic modeling system: A split-explicit, free-surface, topography-following-coordinate ocean model. Ocean Modell., 9, 347–404.

Shchepetkin, A. F., and J. C. McWilliams, 2009. Correction and commentary for “Ocean forecasting in terrain-following coordinates: Formulation and skill assessment of the regional ocean modeling system” by Haidvogel et al., J. Comput. Phys., 227, pp. 3595–3624. J. Comput. Phys., 228, 8985–9000. doi:10.1016/j.jcp.2009.09.002

Skamarock, W. C., Klemp, J. B., Dudhia, J., Gill, D. O., Barker, D. M., Wang, W., Powers, J. G., 2005. A Description of the Advanced Research WRF Version 2. NCAR Technical Note NCAR/TN-468+STR, doi:10.5065/D6DZ069T.

Tonani M., A. Teruzzi, G. Korres, N. Pinardi, A. Crise, M. Adani, P. Oddo, S. Dobricic, C. Fratianni, M. Drudi, S. Salon, A. Grandi, G. Girardi, V. Lyubartsev and S. Marino, 2014. The Mediterranean Monitoring and Forecasting Centre, a component of the MyOcean system. Proceedings of the Sixth International Conference on EuroGOOS 4-6 October 2011, Sopot, Poland. Edited by H. Dahlin, N.C. Fleming and S. E. Petersson. First published 2014. Eurogoos Publication no. 30. ISBN 978-91-974828-9-9.

Toreti, A., Desiato, F., 2008. Temperature trend over Italy from 1961 to 2004. Theoretical and Applied Climatology, 91, 51-58.

Tsimplis, M.N., Baker, T.F., 2000. Sea level drop in the Mediterranean Sea: an indicator of deep water salinity and temperature changes? Geophys. Res. Lett., 27, 12 (doi: 10.1029/1999GL007004).

Tsonevsky, I., Richardson, D., 2012. Application of the new EFI products to a case of early snowfall in Central Europe. ECMWF Newsletter 133, Autumn 2012, p 4.

Vilibić, I., Matijević, S., Šepić, J., Kušpilić, G., 2012. Changes in the Adriatic oceanographic properties induced by the Eastern Mediterranean Transient. Biogeosciences, 9, 2085-2097.

Vilibić, I., Šepić, J., Proust, N., 2013. Weakening of thermohaline circulation in the Adriatic Sea. Climate Research, 55, 217–225.

Vörösmarty, C., Fakers, B., Tucker, B., 1996. River Discharge Database, Version 1.0 (RivDIS vLO), Volumes 0 through 6. A contribution to IHP-V Theme 1. Technical Documents Series. Technical report, UNESCO, Paris, France.

Warner, J.C., Armstrong, B., He, R., and Zambon, J.B., 2010. Development of a Coupled Ocean-Atmosphere-Wave-Sediment Transport (COAWST) modeling system: Ocean Modeling, v. 35, no. 3, p. 230-244.

Zerbini, S., Raicich, F., Prati, C.M., Bruni, S., Del Conte, S., Errico, M., Santi, E., 2017. Sea-level change in the northern Mediterranean Sea from long-period tide gauge time series. Earth Sci. Rev., 167, 72–87, doi: 10.1016/j.earscirev.2017.02.009.

Zsótér, E., 2006. Recent developments in extreme weather forecasting. ECMWF Newsletter 107, Spring 2006, pp 8–17.

Zsótér, E., Pappenberger, F. Richardson, D., 2014. Sensitivity of model climate to sampling configurations and the impact on the Extreme Forecast Index. Met. Apps. doi: 10.1002/met.1447